U.PORTO
FEUP FACULDADE DE ENGENHARIA
UNIVERSIDADE DO PORTO

Simultaneous treatment of gaseous and liquid streams containing organic compounds by Fenton's oxidation

Thesis presented to the

University of Porto

for the degree of

Doctor of Philosophy in Environmental Engineering

by

Vanessa Natalia de Lima

Supervisor: Prof. Dr. Luis Miguel Palma Madeira

Co-supervisor: Dra. Carmen Susana de Deus Rodrigues

lepabe
Laboratory for Process Engineering, Environment, Biotechnology and Energy

Department of Chemical Engineering

Faculty of Engineering

University of Porto

January, 2020

Abstract

In this thesis, it was intended to perform the proof-of-concept of the simultaneous treatment of gaseous and liquid effluents by the Fenton's reagent in a single multiphase reactor. For this purpose, two bubbling reactors were designed/adapted: a lab-scale bubble reactor (BR) and a bubble column reactor (BCR) with a capacity of 0.9 L and 9.0 L, respectively.

The study began with the evaluation of a model aromatic compound (hydroquinone) treatment, followed by a real liquid effluent, by the Fenton's process, intending to evaluate the performance of both reactors in the pollutant removal and mineralization of the organic matter present in the liquid phase. For the treatment of hydroquinone, the effect of the gas flow rate (Q_{gas}) and the height of the liquid phase (H_{liquid}) were evaluated, in addition to the classic Fenton's process parameters (concentrations of catalyst – $[Fe^{2+}]$ – and oxidant – $[H_2O_2]$ –, initial pH of the medium – $pH_{initial}$ – and reaction temperature – $T_{reaction}$); it has been observed that Q_{gas} and H_{liquid} did not influence the removal of the model compound neither the mineralization, which leads to conclude that no axial gradients exist within the column and, therefore, a good homogenization of the medium was ensured, not being necessary any additional stirring device to promote an efficient mixing.

The study of liquid effluents treatment proceeded with an industrial wastewater with high organic load (chemical oxygen demand – COD > 7000 mg O_2/L). Firstly, the BR was used to evaluate the influence of process variables, as well as the one related with the composition of the gas phase (air, N_2 or O_2) bubbled during the treatment. Mineralizations of ca. 50%, after 60 minutes, were reached using air and N_2 streams under the optimized conditions ($pH_{initial}$ = 4.6, $[H_2O_2]$ = 22.5 g/L, $[Fe^{2+}]$ = 0.75, T = 25 °C, Q_{gas} = 1 L/min, measured at room temperature and atmospheric pressure). A slight increase in the mineralization was observed using the O_2 stream (mineralization = 56%) under the same conditions. Additionally, the BR presented a similar behavior to that of a perfectly stirred reactor, since the mineralization achieved in that reactor typology was the same as that obtained in a batch reactor with magnetic stirring. Besides, the BR proved to be more advantageous in temperature control during the treatment, because this is an exothermic process (both organic matter oxidation and the Fenton's reaction itself). Finally, a scale-up for a BCR with a 10 times higher volumetric capacity was carried out, being found similar mineralization in both reactors.

At a later stage, the Fenton process was applied for the treatment of a volatile organic compound (VOC) – namely toluene – present in a gas stream, being absorbed and simultaneously oxidized in the liquid phase. A systematic parametric study was performed to assess the influence of temperature, oxidant and catalyst concentrations, and to optimize the process. The increase of temperature (from 25 to 40 ºC) favored the absorption of toluene in the water (process without reaction). However, during oxidation, toluene removal was reduced in the process at 40 ºC, demonstrating that temperature plays a key role in the oxidation dynamics of VOCs from gas streams. The increase in H_2O_2 concentration was found to be preponderant for the process, and an optimal Fe^{2+}

concentration was also determined. In all runs, an accumulation of organic matter in the liquid phase was observed (associated with the partial oxidation of toluene absorbed in the water), being reached a maximum value of 350 mg C/L under the optimized conditions: $[H_2O_2]$ = 20 mM, $[Fe^{2+}]$ = 2.5 mM, $pH_{initial}$ = 3.0, T = 25 °C, $C_{toluene}$ = 0.04 g/L, Q = 1.0 L/min – at room temperature and atmospheric pressure. In order to reduce the accumulated organic load after the treatment, a strategy of sequential gas-liquid treatment was adopted, in which intermediate steps of the liquid phase treatment were performed wherein the remaining catalyst dissolved in the solution has been used (i.e., with the addition of more oxidant only). This strategy made it possible to increase the efficiency of accumulated organic compounds removal (reduction of the dissolved organic carbon – DOC – of 43% in the final treatment stage). Finally, a scale-up for the BCR was carried out, being observed a reduction in the average toluene absorption rate (N), even though the toluene transfer has been satisfactory. In this reactor, the sequential treatment allowed to extend the gas-liquid treatment cycles, leading to the removal of more toluene and organic matter from the liquid effluent in a process that lasted almost 20 hours.

This thesis was concluded with the proof-of-concept of the simultaneous gas-liquid treatment by the Fenton's process. A gaseous toluene stream and the industrial wastewater were treated in the BR. At this stage, the effects of the aqueous matrix (water *vs.* effluent), the nature of the iron species that acts as catalyst (Fe^{2+} *vs*. Fe^{3+}), and the concentrations of organic matter in the liquid phase and toluene in the gas phase were evaluated. The gas-liquid mass transfer was affected by the nature of the aqueous phase matrix, being observed a reduction in the amount of toluene transferred per liter of solution, in the runs without reaction, when the liquid contains organic matter. However, the Fenton process was efficient in the treatment of both phases, increasing the absorption (against the blank run) and mineralizing the organic matter present in the liquid phase (25% of DOC reduction). Regardless of the iron species used, the mineralization degrees achieved were similar; however, the amount of toluene transferred per liter of solution was slightly lower when the Fenton-like process (H_2O_2 + Fe^{3+}) was applied. The increase of the feed toluene concentration led to a reduction in the gas treatment duration, and to a smaller apparent mineralization in the liquid phase, showing that the process needs to be optimized, depending on the nature and properties of the waste gas stream and liquid present in the reactor. Taking into account the high concentrations of organic matter in the treated liquid effluent, a sequential treatment cycle of the liquid phase was carried out, being found that this strategy allowed to mineralize more than 60% of the accumulated organic matter.

Keywords: Advanced oxidation processes. Fenton's process. Gas treatment. Effluent treatment. Bubbling reactor.

Resumo

Nesta tese pretendeu-se realizar a prova de conceito do tratamento simultâneo de efluentes gasosos e líquidos pelo reagente de Fenton num único reator multifásico. Para o efeito, foram projetados/adaptados dois reatores de borbulhamento: um reator à escala laboratorial (RB) e uma coluna (RCB) com capacidades de 0,9 L e 9,0 L, respetivamente.

O estudo foi iniciado com a avaliação do tratamento de um composto aromático modelo (hidroquinona), seguido por um efluente líquido real pelo processo Fenton, com o objetivo de avaliar o desempenho de ambos os reatores na remoção do poluente e mineralização da matéria orgânica presente na fase líquida. Para o tratamento da hidroquinona, avaliou-se o efeito do caudal de gás ($Q_{gás}$) e da altura da fase líquida (Hlíquido), para além dos clássicos parâmetros do processo Fenton (concentrações de catalisador – $[Fe^{2+}]$ – e oxidante – $[H_2O_2]$ –, pH inicial do meio – $pH_{inicial}$ – e temperatura reacional – $T_{reação}$); observou-se que $Q_{gás}$ e $H_{líquido}$ não influenciaram a remoção do composto modelo nem a mineralização, o que leva a concluir que não existiram gradientes axiais dentro da coluna e, portanto, garantiu-se uma boa homogenização do meio, não sendo necessário qualquer dispositivode agitação adicional para promover uma mistura eficiente.

O estudo de tratamento de efluentes líquidos prosseguiu com uma água residual industrial com elevada carga orgânica (carência química de oxigénio – CQO > 7000 mg O_2/L). Primeiramente, usou-se o RB para avaliar a influência das variáveis processuais, bem como da composição da fase gasosa (ar, N_2 ou O_2) borbulhada durante o tratamento. Alcançaram-se mineralizações de cerca de 50%, ao fim de 60 minutos, usando correntes de ar e N2 nas condições otimizadas ($pH_{inicial}$ = 4,6, $[H_2O_2]$ = 22,5 g/L, $[Fe^{2+}]$ = 0,75, T = 25 ºC, $Q_{gás}$= 1 L/min, medido à temperatura ambiente e pressão atmosférica). Foi observado um ligeiro aumento na mineralização usando a corrente de O2 (mineralização = 56%) nas mesmas condições. Adicionalmente, o RB apresentou um comportamento similar ao de um reator perfeitamente agitado, uma vez que a mineralização alcançada naquela tipologia de reator foi igual à obtida num reator descontínuo com agitação magnética. Além disso, o RB mostrou-se mais vantajoso no controlo da temperatura durante o tratamento, uma vez que se trata de um processo exotérmico (oxidação da matéria orgânica e a própria reação de Fenton). Finalmente, procedeu-se a um aumento de escala para o RCB com volume 10 vezes superior, tendo-se observado mineralização semelhante em ambos os reatores.

Numa fase posterior, procedeu-se à aplicação do processo Fenton para o tratamento de um composto orgânico volátil (COV) – nomeadamente tolueno – presente numa corrente gasosa, sendo absorvido e simultâneamente oxidado na fase líquida. Foi realizado um estudo paramétrico sistemático para avaliar a influência de temperatura, e concentratrações de oxidante e catalisador e otimizar o processo. O aumento da temperatura (de 25 para 40 ºC) favoreceu a absorção do tolueno na água (processo sem reação). Todavia, durante a oxidação a remoção de tolueno reduziu no processo a 40 ºC, demonstrando que a temperatura tem um papel fundamental na dinâmica da oxidação de COVs oriundos de correntes gasosas. O aumento da concentração de

H_2O_2 mostrou-se preponderante para o processo, tendo-se ainda determinado a existência de uma concentração ótima de Fe^{2+}. Em todos os ensaios observou uma acumulação de matéria orgânica na fase líquida (associada à oxidação parcial do tolueno absorvido na água), atingindo-se o valor máximo de 350 mg C/L nas condições otimizadas: $[H_2O_2]$ = 20 mM, $[Fe^{2+}]$ = 2,5 mM, $pH_{inicial}$ = 3,0, T = 25 ºC, $C_{tolueno}$ = 0,04 g/L, Q = 1,0 L/min – à temperatura ambiente e pressão atmosférica. Para reduzir a carga orgânica acumulada após o tratamento, adotou-se uma estratégia de tratamento sequencial gas-líquido, onde foram realizadas etapas intermédias de tratamento da fase líquida com utilização do catalisador remanescente dissolvido na solução (ou seja, com adição de mais oxidante apenas). Esta estratégia permitiu aumentar a eficiência de remoção dos compostos orgânicos acumulados (redução do carbono orgânico dissolvido – COD – de 43% na etapa final de tratamento). Finalmente, realizou-se um aumento de escala para o RCB, tendo-se observado uma redução na taxa média de absorção de tolueno (N), mesmo que a transferência do tolueno tenha sido satisfatória. Neste reator, o tratamento sequencial permitiu prolongar os ciclos de tratamento gas-líquido, levando à remoção de mais tolueno e de matéria orgânica do efluente líquido num processo que se extendeu por quase 20 horas.

Esta tese foi finalizada com a prova de conceito do tratamento simultâneo gas-líquido pelo processo Fenton. Tratou-se uma corrente de tolueno gasoso e o efluente industrial no BR. Nesta etapa, avaliaram-se os efeitos da matrix aquosa (água vs. efluente), da natureza da espécie de ferro que atua como catalisador (Fe^{2+} vs. Fe^{3+}), e da concentração de matéria orgânica na fase líquido e de tolueno na fase gasosa. A transferência de massa gás-liquido foi afetada pela natureza da matrix da fase aquosa, tendo-se obervado uma redução na quantidade de tolueno transferido por litro de solução, nos ensaios sem reação, quando o líquido contém matéria orgânica. Contudo, o processo Fenton foi eficiente no tratamento de ambas as fases, aumentando a absorção (face ao ensaio em branco) e mineralizando a matéria orgânica presente na fase líquida (redução do COD em 25%). Independentemente da espécie de ferro usada, as mineralizações alcançadas foram semelhantes; no entanto, a quantidade de tolueno transferido por litro de solução foi ligeiramente menor quando se aplicou o processo tipo-Fenton ($H_2O_2 + Fe^{3+}$). O aumento da concentração de tolueno na alimentação levou a uma redução no tempo de tratamento do gás, e a uma menor mineralização aparente na fase líquida, mostrando que o processo precisa ser otimizado consoante a natureza e propriedades da corrente gasosa e do efluente contido no reator. Tendo em conta as altas concentrações de matéria orgânica no efluente líquido tratado, procedeu-se a um ciclo de tratamento sequencial da fase líquida, tendo esta estatégia permitido mineralizar a matéria orgânica acumulada em mais de 60%.

Palavras-chave: Processos de oxidação avançados. Processo Fenton. Tratamento de gás. Tratamento de efluentes. Reator de borbulhamento.

Acknowledgments

Agradeço ao Professor Miguel Madeira e a Doutora Carmen Rodrigues pela disponibilidade para orientar este projeto. Por todo o esforço em ajudar a formular conceitos e processos, e encontrar alternativas dentro das possibilidades existentes. Dedico gratidão especial ao professor Madeira que aceitou-me como estudante estrangeira, e pelo esforço em corrigir minhas falhas diante das dificuldades encontradas, e ensinar-me sobre a necessidade de sermos rigorosos nas nossas atividades, de modo a conseguir as executar com excelência.

Agradeço aos técnicos superiores da FEUP os quais mostram-se sempre disponíveis. Especialmente deixo um agradecimento à Dra. Liliana Pereira pela atenção especial em grande parte das análises físico-químicas, e por responder muitas questões relativas ao trabalho analítico. Também agradeço à D. Maria do Céu, pela atenção nos momentos em que precisei tratar de análises, e pelo gentil empréstimo de equipamentos. Finalmente agradeço ao Eng. Luís Carlos Matos que esteve disponível para dar soluções aos problemas de engenharia e de aquisição de equipamentos.

Agradeço também aos investigadores do grupo de ambiente, supervisionados pelo Professor Miguel Madeira, pela presença e disponibilidade. Em especial agradeço ao Dr. Miguel Soria que contribuiu com respostas às minhas perguntas, e ajudou-me a pensar em soluções para executar processos e na manutenção de equipamentos. Agradeço ao trabalho dos jovens engenheiros Ricardo Borges e Emanuel Sampaio, que desempenharam algumas atividades durante este projeto. Agradeço ao Eng. Bruno Esteves que estive disponível em muitas situações para discutir resultados, e tornou o ambiente de trabalho no E203A silencioso e positivo. Também agradeço a Dra. Vanessa Guimarães que mesmo recém chegada ao grupo teve a disponibilidade de me auxiliar com conversas positivas, sinceras e acreditar no meu potencial nos últimos meses da escrita da tese. E, finalmente, aos demais colegas de laboratório, portugueses e estrangeiros, com os quais pude conviver, e em especial aqueles que ajudaram-me durante conversas científicas.

Agradeço também aos demais colegas da FEUP com os quais tive o prazer de conviver em situações distintas ao laboratório e conseguiram mostrar-me que a universidade pode oferecer muitas coisas além das horas trabalho científico. Em especial agradeço aos jovens estudantes com os quais estive a conviver durante o período que passei pela Engenharia Rádio. Fico grata por me incluírem no grupo, por fazerem sentir-me menos “estranha” longe do meu país, e especialmente agradeço ao Eng. Filipe Teixeira pela confiança e amizade, que levaram muitas horas extra de trabalho em diferentes momentos.

Agradeço adicionalmente a todos aqueles que estiveram presentes durante a minha formação, especialmente aos professores, muitos dos quais comecei a conviver logo na minha primeira iniciação científica em 2007, e que inspiraram-me a seguir o sonho de chegar ao doutorado. Especialmente agradeço à Dra. Arminda Saconi Messias, uma grande mulher que confiou na minha capacidade logo no começo desta jornada, e me

inspirou à seguir a investigação proporcionando os fundos para a minha formação como Engenheira Ambiental.

Deixo um também agradecimento as amizades que nasceram enquanto no Porto, e em especial àqueles que estiveram comigo nos momentos mais especiais e também nos mais difíceis:

Agradeço à Nutri. Natalia Canabrava, que tornou-se uma grande amiga, e foi como uma irmã neste quatro anos. Agradeço por ter sido minha confidente e parceira em diversos momentos, e por toda a sua compreensão e simpatia. Nossas conversas e seu suporte deram-me de fato ajuda para concluir esta etapa.

Agradeço ao Eng. Claver Pinheiro, um amigo que enfrentou junto comigo esses anos de doutorado e compreendeu as minhas dificuldades. Agradeço por me escutar e partilhar medos, anseios, dificuldades, para além da FEUP, mas também agradeço pelas boas risadas e excelente momentos, e por estender-me uma mão amiga nos momentos em que mais precisei.

Agradeço também Natália Leão, João Costa, Mariana Riccio, Laís Souza e José Bonifácio Sena, que estiveram disponíveis em muitos momentos especiais.

Finalmente agradeço ao Miguel Cunha, que tornou-se meu companheiro e amor. Alguém que fez o possível para que não deixar-me sozinha, e manteve um cuidado constante. Agradeço imensamente por todas as horas de dedicação, atenção e amor. Por cada lágrima, cada risada e também por toda a ajuda na etapa final da tese. Agradeço também por me permitir estar junto a sua família, especialmente por manter contato com seus pais e irmãos, um grupo de pessoas pelas quais nutro profundo respeito e carinho.

Agradeço também aos meus amigos de “casa”, tanto aqueles com quem mantive contatos, quanto aqueles que tornaram-se distantes, mas que nutriram sentimentos positivos, e tenho certeza que mantiveram-me no coração e nas suas orações. Em especial agradeço à:

À Eng. Renato Pereira, um dos meus grandes amigos, uma pessoas que sei que posso contar como nos dedos da mão. Agradeço por manter-se por perto, por aturar minhas conversas longas, por seu abraço acolhedor, pelo apoio e por mostra-se orgulhoso pelas minhas conquistas.

À Eng. Celso Lima com quem tive o prazer conviver durante meu mestrado, e que é um amigo de coração gigante e de alma maior ainda. Agradeço imenso por todo seu apoio nesses longos anos, e também por proporcionar o contato com a sua família a qual admiro imensamente, em especial por me permitir conhecer Nélia Lima e Roseana Pereira.

À Eng. Marcos Chaprão, um amigo desde a graduação, e que é um profissional que sinto imenso orgulho, e torço para que possamos trabalhar juntamente com soluções em Engenharia Ambiental.

Agradeço às pessoas da minha cidade que torcem por mim, que pensam em mim, e que mantiveram-me no coração. Não consigo mencionar todas, mas deixo meu

sentimento de gratidão à todos por acreditarem nas minhas capacidades, e por enviaram energias positivas.

Por fim, devido um agradecimento à minha família, e aos meus tios e primos, que mesmo longe sei que enviam boas energias e pensamentos positivos. Em especial agradeço:

À minha avó materna, Natalia Santos, que mesmo sem compreender a razão de me fez passar tantos anos longe do Brasil manteve-me em sua lembrança e nas suas orações diárias. Amo-a imensamente, e sua força inspira-me a ser mais forte. Grande parte do que sou deve-se aos seus ensinamentos.

Agradeço também ao meu irmão, Samuel Lima, que durante estes anos esteve junto à minha mãe, e agradeço todo o cuidado e por orgulhar-se de mim.

Agradeço ao meu pai, Luís Lima Sobrinho, que um dia considerou que a educação seria a chave para um nosso futuro, e para um crescimento social. Todo o seu investimento tornou-me capaz de enfrentar as adversidades da vida e ter a coragem de seguir mesmo sozinha.

E agradeço à minha mãe, Veronica Lima, a mulher que mais admiro neste mundo. Uma mulher doce, gentil e sensível, e que mesmo temerosa acreditou na minha capacidade de sozinha enfrentar todos os obstáculos dos anos em que estive vivendo longe como um passarinho livre. Sem sua presença, suporte, inspiração e apoio definitivamente não seria quem sou, e agradeço pelo orgulho que demonstra sentir.

Finalmente agradeço à Deus, por razões particulares...

I am grateful to Laboratory for Process Engineering, Environment, Biotechnology and Energy (LEPABE), and to the Doctoral Program of Environmental Engineering from the Faculty of Engineering of the University of Porto (FEUP). I thank the Brazilian National Council of Technological and Scientific Development (CNPq) for my PhD grant (Process 201859/2015-7), supported by national funds of the 'Ministério da Ciência, Tecnologia, Inovações e Comunicações' (MCTIC) from Brazil.

This work was financially supported by: Base Funding - UIDB/00511/2020 of the Laboratory for Process Engineering, Environment, Biotechnology and Energy – LEPABE - funded by national funds through the FCT/MCTES (PIDDAC), and by Project PTDC/EAM-AMB/29642/2017 - POCI-01-0145-FEDER-029642 - funded by FEDER funds through COMPETE2020 - Programa Operacional Competitividade e Internacionalização (POCI) and by national funds (PIDDAC) through FCT/MCTES.

Para minha mãe e avó, mulheres que me tornam mais forte...

Table of Contents

Abstract I
Resumo III
Acknowledgments V
List of Figures XV
List of Tables XIX
Abbreviations and Symbols XX

Part I: General Introduction & State of Art 1

Chapter 1. Introduction and Outline 3

1.1 Introduction and Motivation 3
1.2 References 6

Chapter 2. State of Art – Gaseous and Liquid Effluents Treatment in Bubble Column Reactors by Advanced Oxidation Processes 9

2.1 Introduction 10
2.2 Short overview of bubble columns reactors 11
2.3 Industrial applications of bubble columns and BCRs in the treatment of effluents 13
2.4 Advanced oxidation processes in BCRs 16
2.4.1 Mechanism of treatment of gas and/or liquid effluents by AOPs 18
2.4.2 Fenton 20
2.4.2.1 Influence of the temperature 24
2.4.2.2 Effect of the initial pH 25
2.4.2.3 Effect of the hydrogen peroxide concentration 27
2.4.2.4 Effect of the iron concentration 29
2.4.2.5 Influence of the gas flow rate 30
2.4.3 UV/H_2O_2 31
2.4.3.1 Effect of the hydrogen peroxide concentration 32
2.4.3.2 Effect of the UV lamp power 34
2.4.4 Photo-Fenton 35
2.4.4.1 Effect of the UV lamp power 36
2.4.5 Electro-Fenton 37
2.4.5.1 Effect of the materials used for making the electrodes 38
2.4.5.2 Effect of the pH 41
2.4.5.3 Effect of the operation mode 41
2.4.6 Ozonation 42
2.4.6.1 Effect of initial pH 49
2.4.6.2 Effect of ozone concentration and flow rate 51
2.4.6.3 Effect of UV light application 53

2.5 Future perspectives 53
2.6 Conclusions 55
2.7 References 56

Part II: Treatment of Liquid Effluents 67

Chapter 3. Application of Fenton's Process in a Bubble Column Reactor for Hydroquinone Degradation 69

3.1 Introduction 71
3.2 Material and methods 72
3.2.1 Chemicals 72
3.2.2 Fenton process in the BCR 73
3.2.3 Analytical methods 74
3.3 Results and discussion 74
3.3.1 Mixing process in the BCR 75
3.3.2 Effect of liquid height in the column 77
3.3.3 Effect of the iron dose 78
3.3.4 Influence of the initial hydrogen peroxide concentration 81
3.3.5 Influence of the temperature 81
3.3.6 Effect of the initial pH 82
3.3.7 Strategy to improve the mineralization 84
3.3.8 Reaction mechanism 85
3.3.9 Hydroquinone degradation in a real wastewater matrix 87
3.4 Conclusions 89
3.5 References 91

Chapter 4. Insights into Real Industrial Wastewater Treatment by Fenton's Oxidation in Gas Bubbling Reactors 95

4.1. Introduction 97
4.2 Material and methods 99
4.2.1 Real industrial wastewater 99
4.2.2 Reactors configuration 99
4.2.3 Experimental Procedure 100
4.2.3.1 Fenton's experiments 100
4.2.3.2 Processes assisted with radiation 100
4.2.4 Analytical methods 101
4.3 Results and discussion 101
4.3.1 Effect of reaction parameters 102
4.3.1.1 Effect of the oxidant dose 102
4.3.1.2 Effect of the catalyst dose 105
4.3.1.3 Effect of the initial pH 106
4.3.2 Influence of the reactor parameters 107

4.3.2.1 Influence of the air flow rate 107
4.3.2.2 Effect of the gas phase composition 108
4.3.2.3 Influence of the mixing mode 110
4.3.3 Scale-up to a bubble column reactor (BCR) 112
4.3.4 WW oxidation with UV-vis assisted processes 114
4.4 Conclusions 116
4.5 References 118

Part III: Waste Gas Treatment 125

Chapter 5. Sequential Gas-Liquid Treatment for Gaseous Toluene Degradation by Fenton's Oxidation in Bubble Reactors 127

5.1 Introduction 129
5.2 Material and methods 131
5.2.1 Simulated toluene gas stream 131
5.2.2 Bubbling reactors 131
5.2.3 Fenton process procedure and process efficiency indicators 133
5.2.4 Analytical Methods 134
5.3 Results and discussion 135
5.3.1. Parametric study in the lab-scale BR 135
5.3.1.1 Influence of the reaction's temperature 136
5.3.1.2 Effect of the ferrous ion dose 139
5.3.1.3 Effect of the oxidant dose 141
5.3.2 Sequential treatment of the gas stream containing toluene and liquid effluent produced 143
5.3.2.1 Sequential treatment in the lab-scale BR 143
5.3.2.2 Sequential treatment in a BCR 147
5.4 Conclusions 151
5.5 References 153

Chapter 6. Simultaneous Treatment of Toluene-Containing Waste Gas and Industrial Wastewater by the Fenton Process 159

6.1 Introduction 161
6.2 Material and methods 163
6.2.1 Contaminated gas stream 163
6.2.2 Real industrial effluent 164
6.2.3 Bubbling reactor and experimental procedure 164
6.2.4 Analytical methods 165
6.2.4.1 Gas phase analysis 165
6.2.4.2 Liquid effluent analysis 165
6.3. Results and discussion 166
6.3.1 Influence of the aqueous solution in the toluene absorption and oxidation 167

6.3.2 Influence of catalyst nature: Fenton's vs. Fenton-like's process 171
6.3.3 Effect of the organic matter load in the liquid phase 174
6.3.4 Effect of the inlet concentration of toluene 176
6.3.5 Strategy to increase the toluene removal and the mineralization 178
6.4 Conclusions 180
6.5 References 182

Part IV: Conclusions & Future Perspectives 189

Chapter 7. Final Conclusions and Future Work 191
7.1 Final conclusions 191
7.2 Future work 193

Appendixes 195
A1 Appendix for Chapter 3 196
A2 Appendix for Chapter 4 198

List of Figures

Chapter 1

Figure 1.1 Scheme of the bubbling devices (bubbling reactor – BR (a) and bubble column reactor – BCR (b)) designed for the experimental work along this PhD thesis. Legends: 1 – gas phase inlet, 2 – gas diffuser (a) / dispersive plate (b), 3 – gas phase outlet, 4 – liquid sampling port. 5

Chapter 2

Figure 2.1 Scheme of the main processes occurring in the gas and liquid phase for the degradation of volatile organic compounds (VOCs) present in the gas stream in a bubble column by the Fenton process (adapted from Handa *et al.* (2013)). 19

Figure 2.2 Effect of reaction temperature on NO removal efficiency (pH = 2, H_2O_2 = 0.75 mol/L and $FeSO_4$ = 0.05 mol/L) (adapted from Guo *et al.* (2011)) and on Hg^0 removal (O_2 = 6.0%, CO_2 = 12.0%, SO_2 = 1000 ppm, NO = 400 ppm, pH = 3.4, Fe^{2+} = 0.008 mol/L, Hg^0 inlet = 40 µg/m^3 and gas flow rate = 800 mL/min) (adapted from Liu *et al.* (2015)) by the Fenton reaction realized in a BCR. 25

Figure 2.3 Effect of the pH on methane removal (T = 25 ºC, Fe^{2+} = 2.0 mM and H_2O_2 = 80 mM and (adapted from Wei *et al.* (2012)), NO removal (T = 323 K, H_2O_2 = 0.75 mol/L and $FeSO_4$ = 0.05 mol/L (adapted from Guo *et al.* (2011)) and Hg^0 removal (O_2 concentration = 6.0%, CO_2 concentration = 12.0%, SO_2 = 1000 ppm; NO = 400 ppm; T = 55 °C; Fe^{2+} = 0.008 mol/L; Hg^0 inlet = 40 µg/m^3 and flue gas flow = 800 mL/min) (adapted from Liu *et al.* (2015)) by the Fenton reaction realized in a BCR. 27

Figure 2.4 Effect of H_2O_2 concentration on NO removal efficiency (T = 323 K, pH = 2 and $FeSO_4$ = 0.05 mol/L (adapted from Guo *et al.* (2011)) and Hg^0 removal (Hg^0 inlet = 40 µg/m^3, O_2 = 6.0 %, CO_2 = 12.0%, SO_2 = 1000 ppm, NO = 400 ppm, T = 55 °C, pH = 3.4 and gas flow rate = 800 mL/min) (adapted from Liu *et al.* (2015)) by the Fenton reaction realized in a BCR. 30

Figure 2.5 Effect of gas flow rate on Hg^0 removal efficiency by the Fenton process realized in a BCR (conditions: O_2 = 6.0%, CO_2 = 12.0%, SO_2 = 1000 ppm, NO = 400 ppm, T = 55 °C, pH = 3.4, Hg^0 inlet = 40 µg/m^3, Fe^{2+} = 0.008 mol/L) (adapted from Liu *et al.* (2015)). 31

Figure 2.6 Removal efficiencies of NO and SO_2 for different reaction systems. Conditions: UV lamp, 36 W; $[NO]_0$ = 407 ppm; $[SO_2]_0$ = 978 ppm; $[H_2O_2]_0$ = 2.0 mol/L (adapted from Liu *et al.* (2010)). 32

Figure 2.7 Removal efficiencies of NO and SO_2 under different H_2O_2 concentrations (a) and UV lamp powers (b) in the UV/H_2O_2 process (H_2O_2 concentration = 2.0 mol/L, NO = 419 ppm; and SO_2 = 948 ppm) (adapted from Liu *et al.* (2010)). 33

Figure 2.8 Effect of UV light intensity on the photo-Fenton degradation of toluene (maximum RE = maximum removal efficiency) and in the decomposition rate constant of H_2O_2 (k_{HP}) (toluene concentration = 0.25 mg/L, H_2O_2 = 400 mg/L, Fe_0 = 10 mg/L and pH_0 = 3.0) (adapted from Handa *et al.* (2013)). 37

Figure 2.9 Percentage removal of TOC for destruction of phenol by ozonation at different pHs (O_3 flow rate = 100 ml/min and phenol = 500 ppm) (adapted from Matheswaran and Moon (2009)). 50

Figure 2.10 Effect of ozone mass flow rate in the decolorization efficiency of AG25 dye (t = 3 min, dye concentration = 100 mg/L) (adapted from Kordkandi and Ashiri (2015)). 51

Figure 2.11 Effect of ozone flow rate on the removal of TOC (a) and phenol (b) with reaction time (phenol = 500 ppm and pH = 6) (adapted from Matheswaran and Moon (2009)). 52

Chapter 3

Figure 3.1 Schematic diagram of the bubble column reactor experimental set-up. 73

Figure 3.2 TOC removal over the reaction time for different: air flow rates (a) ([H_2O_2] = 500 mg/L; [Fe^{2+}] = 45 mg/L; T = 24 ºC; pH = 3.0; V = 7 L; H_3 = 0.5 m), and different sampling heights (b) ([H_2O_2] = 500 mg/L; [Fe^{2+}] = 45 mg/L; T = 24 ºC; pH = 3.0; V = 7 L; Q_{air} = 2.5 mL/min). 76

Figure 3.3 Hydrogen peroxide loss in blank runs with different volumes of liquid with the oxidant being added: by the top of the column (a) and in the lowest sampling point (H= 0.5 m) (b) ([H_2O_2] = 500 mg/L; T = 24 ºC; pH = 3.0; Q_{air} = 2.5 mL/min), and gas holdup for different volumes of liquid and air flow rates in the BCR (c). 78

Figure 3.4 TOC removal (a), pH over reaction time (b), H_2O_2 consumption and η_{H2O2} at 180 minutes of reaction (c) for different Fe^{2+} doses ([H_2O_2] = 500 mg/L; Q_{air} = 2.5 mL/min; T = 24 ºC; pH = 3.0; V = 5 L); TOC removal (d), pH over reaction time (e), H_2O_2 consumption and η_{H2O2} at 180 minutes of reaction (f) for different H_2O_2 concentrations ([Fe^{2+}] = 45 mg/L; Q_{air} = 2.5 mL/min; T = 24 ºC; pH = 3.0; V = 5 L). 80

Figure 3.5 Effect of temperature on TOC removal (a), pH over reaction time (b), H_2O_2 consumption and η_{H2O2} at 180 minutes of reaction (c) ([H_2O_2] = 500 mg/L; [Fe^{2+}] = 45 mg/L; Q_{air} = 2.5 mL/min; pH = 3.0; V = 5 L); and effect of initial pH on TOC removal (d), pH over reaction time (e), H_2O_2 consumption and η_{H2O2} at 180 minutes of reaction (e) ([H_2O_2] = 500 mg/L; [Fe^{2+}] = 45 mg/L; Q_{air} = 2.5 mL/min; T = 24 ºC; V = 5 L). 83

Figure 3.6 TOC removal (a) and H_2O_2 consumption and η_{H2O2} (b) during the reaction with single and gradual addition of the oxidant ([H_2O_2] = 500 mg/L; [Fe^{2+}] = 45 mg/L; pH = 3.0; Q_{air} = 2.5 mL/min; T = 24 ºC; V = 5 L). 85

Figure 3.7 Organic acids formation along reaction time: when oxidant was added totally in the beginning of the run (a) and was added H_2O_2 gradually (b) ([H_2O_2] = 500 mg/L; [Fe^{2+}] = 45 mg/L; pH = 3.0; Q_{air} = 2.5 mL/min; T = 24 ºC; V = 5 L). 86

Figure 3.8 Proposed reaction mechanism of hydroquinone degradation by the Fenton process. 87

Figure 3.9 Comparison of TOC removal in distilled water (HW solution) and wastewater spiked with HQ ([H_2O_2] = 500 mg/L; [Fe^{2+}] = 45 mg/L; pH = 3.0; Q_{air} = 2.5 mL/min; T = 24 ºC; V = 5 L). 88

Chapter 4

Figure 4.1 Influence of oxidant dose on the evolution of the DOC removal (a), reduction of pH (b), consumption of H_2O_2 (c), and temperature profile (d) along the oxidation process, and COD removal (e) after the WW treatment (*t* = 60 min) performed in the bubble reactor. Experimental conditions: [Fe^{2+}] = 0.75 g/L, pH = 4.6, V = 0.5 L, $T_{ref.}$ = 25 ºC, and Q_{air} = 1.0 L/min. 104

Figure 4.2 Effect of the catalyst dose (a) and initial pH (b) on the WW treatment (*t* = 60 min) performed in the bubble reactor. Experimental conditions: $[H_2O_2]_{a) \text{ and } b)}$ = 22.5 g/L, $[Fe^{2+}]_{b)}$ = 0.75 g/L, $pH_{a)}$ = 4.6, V = 0.5 L, $T_{ref.}$ = 25 ºC, and Q_{air} = 1.0 L/min. 106

Figure 4.3 Influence of the gas phase composition (air, N_2 or O_2) on the evolution of the DOC removal (a), reduction of pH (b), consumption of H_2O_2 (c), and temperature profile (d) along the oxidation process, and COD removal (e) after the WW treatment (*t* = 60 min) performed in the bubble reactor. Experimental conditions: [H_2O_2] = 22.50 g/L; [Fe^{2+}] = 0.75 g/L, pH = 4.6, V = 0.5 L, $T_{ref.}$ = 25 ºC, and Q_{gas} = 1.0 L/min. 109

Figure 4.4 Influence of the reactor configuration mixing mode on the evolution of the DOC removal (a), reduction of pH (b), consumption of H_2O_2 (c), and temperature profile (d) along the oxidation process, and COD removal (e) after the WW treatment (*t* = 60 min) performed in the bubble reactor with and without air bubbling. Experimental conditions:

[H_2O_2] = 22.50 g/L; [Fe^{2+}] = 0.75 g/L, pH = 4.6, V = 0.5 L, $T_{ref.}$ = 25 ºC, $Q_{air\ at\ BR}$ = 1.0 L/min or $V_{batch\ reactor}$ = 250 rpm..... 112

Figure 4.5 Evolution of the DOC removal (a), reduction of pH (b), consumption of H_2O_2 (c), and temperature profile (d) along the oxidation process, and COD removal (e) after the WW treatment (*t* = 60 min) performed in the bubble column and in the bubble column reactor. Experimental conditions: [H_2O_2] = 22.50 g/L; [Fe^{2+}] = 0.75 g/L, pH = 4.6, $V_{at\ BR}$ = 0.5 L, $V_{at\ BCR}$ = 4.0 L $T_{ref.}$ = 25 ºC, Q_{air} = 1.0 L/min..... 114

Figure 4.6 Evolution of the DOC removal (a) along the oxidation processes and COD removal (b) after the WW treatment (*t* = 60 min) performed using different AOPs (UV-vis, UV-vis/H_2O_2, Fenton, and photo-Fenton). Experimental conditions: [H_2O_2] = 22.50 g/L, [Fe^{2+}] = 0.75 g/L, I = 500 W/m^2, pH = 4.6, V = 0.5 L, $T_{ref.}$ = 25 ºC..... 115

Chapter 5

Figure 5.1 Scheme of the experimental set-up for the treatment of gaseous toluene by the Fenton's process (a), and details of the bubbling reactor (b) and bubble column reactor (c)..... 132

Figure 5.2 Influence of temperature in the toluene concentration at the outlet of the BR along the blank runs (without reagents) and Fenton's runs (a), and in the concentration of H_2O_2 (b), pH (c) and concentration of DOC (d) in the liquid phase along time. Experimental conditions: V = 0.5 L, pH_0 = 3.0, T = 25 ºC, and $Q_{toluene}$ = 1.0 L/min, $[H_2O_2]_{0\ when\ used}$ = 10 mM, and $[Fe^{2+}]_{0\ when\ used}$ = 2.5 mM..... 137

Figure 5.3 Effect of the catalyst dose in the toluene concentration at the outlet of the BR (a), and in the concentration of H_2O_2 (b), pH (c) and concentration of DOC (e) in the liquid phase along Fenton's reaction time. Experimental conditions: V = 0.5 L, pH_0 = 3.0, T = 25 ºC, $[H_2O_2]_0$ = 10 mM, and $Q_{toluene}$ = 1.0 L/min..... 140

Figure 5.4 Effect of the oxidant dose in the toluene concentration at the outlet of the BR (a), and in the concentration H_2O_2 (b), pH (c) and concentration of DOC (d) in the liquid phase during Fenton's reaction time. Experimental conditions: V = 0.5 L, pH_0 = 3.0, T = 25 ºC, $[Fe^{2+}]_0$ = 2.5 mM, and $Q_{toluene}$ = 1.0 L/min..... 142

Figure 5.5 Performance of the sequential gas-liquid treatment in the BR in terms of the toluene concentration at the outlet of the BR (a), and concentration of H_2O_2 (b) and DOC (c) along the Fenton process. Experimental conditions: V = 0.5 L, T = 25 ºC, pH_0 = 3.0, $[Fe^{2+}]_0$ = 2.5 mM, $[H_2O_2]_0$ = 20 mM, and $Q_{toluene/air}$ = 1.0 L/min..... 145

Figure 5.6 Performance of the sequential gas-liquid treatment in the BCR in terms of the toluene concentration at the outlet of the BCR (a), concentration of H_2O_2 (b), pH (c) and concentrations of DOC and COD (d) along the Fenton process time. Experimental conditions: V = 5.0 L, T = 25 ºC, $pH_{0,\ pH\ adjust\ steps}$ = 3.0, $[Fe^{2+}]_0$ = 2.5 mM, $[H_2O_2]_{0,\ oxidant\ dose\ steps}$ = 20 mM, and $Q_{toluene/air}$ = 1.0 L/min. 149

Chapter 6

Figure 6.1 Experimental set-up used for the simultaneous gas-liquid treatment in the bubbling reactor..... 163

Figure 6.2 Effect of the aqueous matrices (water vs. real effluent) in the toluene removal (a), toluene transferred (b), and DOC removal (c) along the blank (without Fenton's reagents) and Fenton's experiments carried out in the bubbling reactor. Experimental conditions: $V_{water\ or\ WW}$ = 0.5 L, pH_0 = 4.6, T = 25 ºC, $Q_{toluene}$ = 1.0 L/min, C_{in} = 0.040 g/L, [Fe^{2+}] = 0.75 g/L, [H_2O_2] = 22.5 g/L (Fe^{2+}:H_2O_2 = 0.033)..... 169

Figure 6.3 Effect of the catalysts nature in the toluene removal (a), toluene transferred (b), DOC removal (c), H_2O_2 consumption (d), pH reduction (e) and temperature profile (f) along the experiments performed for the simultaneous gas-liquid treatment.

Experimental conditions: V = 0.5 L, pH_0 = 4.6, T = 25 ºC, $Q_{toluene}$ = 1.0 L/min, C_{in} = 0.040 g/L, $Fe^{2+ \text{ or } 3+}$:H_2O_2 = 0.033. 172

Figure 6.4 Influence of the organic matter concentration in liquid phase in the toluene removal (a), toluene transferred (b) , DOC removal (c), H_2O_2 consumption (d), pH reduction (e) and temperature profile (f) along the experiments performed for the simultaneous gas-liquid treatment by the Fenton process. Experimental conditions: V = 0.5 L, T = 25 ºC, $Q_{toluene}$ = 1.0 L/min, C_{in} = 0.040 g/L, COD_0:H_2O_2 = 0.40 and Fe^{2+}:H_2O_2 = 0.033. 175

Figure 6.5 Effect of the inlet toluene concentration in the toluene removal (a), toluene transferred (b), DOC removal (c), H_2O_2 consumption (d), pH reduction (e) and temperature profile (f) along the experiments performed for the simultaneous gas-liquid treatment by the Fenton process. Experimental conditions: V = 0.5 L, T = 25 ºC, $Q_{toluene}$ = 1.0 L/min, COD_0:H_2O_2 = 0.40 and Fe^{2+}:H_2O_2 = 0.033. 177

Figure 6.6 Effect of the sequential treatment by Fenton's oxidation in the toluene removal (a), H_2O_2 consumption, DOC and pH reduction (b) in the gas and liquid treatment stages, and by-products concentrations and carbon balance at the end of each treatment stage (c). Experimental conditions: *Stage 1* – V = 0.5 L, DF_{WW} = 0.50, pH_0 = 4.4, T = 25 ºC, $Q_{toluene}$ = 1.0 L/min, C_{in} = 0.040 g/L, COD_0:H_2O_2 = 0.40 and Fe^{2+}:H_2O_2 = 0.033; *Stage 2* – pH_0 = 3.0 and H_2O_2 = 6.0 g/L. 179

Appendix A1

Figure A.1.1 Evolution of pH along reaction time (a) and H_2O_2 consumption and efficiency of its use at 120 minutes of reaction (b) for different air flow rates ([H_2O_2] = 500 mg/L; [Fe^{2+}] = 45 mg/L; T = 24 ºC; pH = 3.0; $V_{effluent}$ = 7 L; H_3 = 0.5 m); evolution of pH along reaction time (c) and H_2O_2 consumption and efficiency of its use at 120 minutes of reaction (d) for different sampling heights ([H_2O_2] = 500 mg/L; [Fe^{2+}] = 45 mg/L; T = 24 ºC; pH = 3.0; $V_{effluent}$ = 7 L; Q_{air} = 2.5 mL/min)..... 196

Figure A.1.2 TOC removal along reaction time for different volumes of effluent ([H_2O_2] = 500 mg/L; [Fe^{2+}] = 45 mg/L; T = 24 ºC; pH = 3.0; Q_{air} = 2.5 mL/min). 197

Appendix A2

Figure A.2.1 Effect of the catalyst dose in the DOC removal (a), reduction of the pH (b), consumption of H_2O_2 (c) and temperature profile (d) along Fenton oxidation in a bubbling reactor. Experimental conditions: [H_2O_2] = 22.50 g/L, pH = 4.6, V = 0.5 L, $T_{ref.}$ = 25 ºC, Q_{air} = 1.0 L/min. 198

Figure A.2.2 Effect of the initial pH in the DOC removal (a), reduction of the pH (b), consumption of H_2O_2 (c) and temperature profile (d) along Fenton oxidation in a bubbling reactor. Experimental conditions: [H_2O_2] = 22.50 g/L; [Fe^{2+}] = 0.75 g/L, V = 0.5 L, $T_{ref.}$ = 25 ºC, Q_{air} = 1.0 L/min. 199

Figure A.2.3 Influence of the air flow rate in the DOC removal (a), reduction of the pH (b), consumption of H_2O_2 (c) and temperature profile (d) along Fenton oxidation in a bubbling reactor. Experimental conditions: [H_2O_2] = 22.50 g/L; [Fe^{2+}] = 0.75 g/L, pH = 4.6, V = 0.5 L, $T_{ref.}$ = 25 ºC, Q_{air} = 1.0 L/min. 200

Figure A.2.4 Influence of the mixing mode on the temperature profile along Fenton's process blank runs (only water) performed with and without gas bubbling. Experimental conditions: [H_2O_2] = 22.50 g/L; [Fe^{2+}] = 0.75 g/L, pH = 4.6 (adjusted), V_{water} = 0.5 L, Tref. = 25 ºC, $Q_{air\ at\ BR}$ = 1.0 L/min or $V_{batch\ reactor}$= 250 rpm. 200

List of Tables

Chapter 2

Table 2.1 Oxidation potential of some chemical species (Legrini *et al.* 1993). 17

Table 2 2 Main advanced chemical oxidation processes (adapted from Poyatos *et al.* (2010)). 18

Table 2.3 Examples of applications of the Fenton process in the treatment of effluents in BCRs. 22

Table 2.4 Examples of applications of the electro-Fenton process in the treatment of effluents in BCRs. 39

Table 2.5 Examples of the application of ozonation in the treatment of wastewater in bubble column reactors. 44

Chapter 3

Table 3.1 Description of the real wastewater (WW) spiked with hydroquinone (100 mg/L) before and after the Fenton process application in the BCR. 89

Chapter 4

Table 4.1 Characteristics of the real industrial wastewater before and after the Fenton and photo-Fenton processes under optimal conditions (removal efficiencies are shown between brackets). 102

Chapter 5

Table 5.1 Experimental conditions, process duration, average toluene absorption rate, and amount of toluene transferred after all experiments of the parametric study in the lab-scale bubbling reactor. 139

Table 5.2 Gas treatment stages indicators, and characterization of the liquid effluent (and its treatment efficiency) along the sequential gas-liquid treatment in the bubbling reactor. 146

Table 5.3 Gas treatment stages indicators, and characterization of the liquid effluent (and its treatment efficiency) along the sequential gas-liquid treatment in the bubbling column reactor. 151

Chapter 6

Table 6.1 Characterization of the real effluent and after dilution to ca. ½ (dilution factor, DF_{ww}, of 0.50) and ¼ (dilution factor, DF_{ww}, of 0.25). 167

Table 6.2 Average absorption rate after overall process for each experiment processed using water and the effluent. 170

Appendix A1

Table A.1.1 Level of the liquid and liquid aerated in the BCR used. 197

Abbreviations and Symbols

Abbreviations

AG25	anthraquinone acid
AOP	advanced oxidation process
BCR	bubble column reactor
BOD	biological oxygen demand
BR	bubble reactor
BTEX	benzene, toluene, ethylbenzene and xylene
COD	chemical oxygen demand
CR	congo red
DCM	dichloromethane
DEA	diethanolamine
DNT	dinitrotoluene
DOC	dissolved organic carbon
GC	gas chromatography
HPLC	high performance liquid chromatography
HQ	hydroquinone
IC50	half maximal inhibitory concentration
MB	methylene blue
MDEA	mixture of monoethanolamine and diethanolamine
MEA	Monoethanolamine
NTU	nephelometric turbidity units
PNP	*p*-nitrophenol
RH	organic species/organic matter
TOC	total organic carbon
TSS	total suspended solids
TNT	2,4,6-trinitrotoluene
UV	ultraviolet radiation
UV-C	ultraviolet radiation C
VOC	volatile organic carbon
VSS	volatile suspended solids
WW	wastewater
WWTP	wastewater treatment plant

Greek letters

η_{H2O2}	efficiency of H_2O_2 use
ε_g	gas holdup

Notations and Symbols

CO_2	carbon dioxide
D (m)	diameter
eV	electronvolt
f_{H2O2}	factor relative to the stoichiometric H_2O_2 required to the organic matter oxidation
Fe^{3+}	ferric ion
Fe^{2+}	ferrous ion
$FeSO_4.7H_2O$	ferrous sulfate heptahydrate
Q (L/min)	gas flow rate
K_La (s^{-1})	gas-liquid mass transfer coefficient
H (m)	height
H_2O_2	hydrogen peroxide
$C_6H_6O_2$	Hydroquinone
$HO^{\bullet}$	hydroxyl radical
C_{in} (g/L)	inlet concentration
N_2	nitrogen
C_{out} (g/L)	outlet concentration
O_2	oxygen
t (s)	reaction time
T_{ref} (ºC)	reference temperature
rpm	revolutions per minute
N (mol/L.s)	average absorption rate
NaOH	sodium hydroxide
Na_2SO_3	sodium sulphite
k'	specific oxygen uptake rate
H_2SO_4	sulfuric acid
UV-vis	ultraviolet visible spectrum
UV	ultraviolet spectrum
V (L)	volume

Part I: General Introduction & State of Art

This part presents the motivation, outline and objectives of this Ph.D. thesis, as well as the state of art concerning the application of bubble column reactors for the treatment of liquid and gaseous effluents by advanced oxidation processes.

Chapter 1. Introduction and Outline

1.1 Introduction and Motivation

This thesis addresses the treatment of gas and liquid effluents, a very relevant topic nowadays. The aim of the study was to perform the proof-of-concept of a novel technology for the simultaneous treatment of organic gaseous and liquid effluents by an advanced oxidation process (AOP), namely the Fenton's process, in the same multiphase reactor; this constitutes a recent thematic, scarcely reported in the literature.

The Fenton process is, in short, a destructive chemical advanced oxidation process (AOP) that was developed by H.J.H. Fenton in the late 19th century during the oxidation of an organic acid (i.e., tartaric acid) using an iron salt as catalyst (Fenton 1894). The process is typically carried out in aqueous solution, making use of hydrogen peroxide (H_2O_2) and a catalyst (usually an iron species) to yield the hydroxyl radical ($HO^{\bullet}$), a chemical species with a very high oxidation potential and the core of many AOPs (Gligorovski *et al.* 2015). The generation of this oxidizing species has, therefore, the objective of performing the degradation/mineralization of organic species present in the effluents (Walling 1975; Barb *et al.* 1951b; 1949; 1951a) – a more detailed description of the process is given in Chapter 2.

The application of the Fenton's process has been exhaustively studied for the degradation and treatment of several model pollutants and/or real wastewater (Pliego *et al.* 2015; Oturan and Aaron 2014; Babuponnusami and Muthukumar 2014; Huang *et al.* 2017; Zhang *et al.* 2019; Thakur and Chauhan 2018), with the objective of reducing the risks associated with their discharge into the environment. The advantages of this AOP include the use of environmentally friendly reagents (Oturan and Aaron 2014), simple operation, moderated conditions of temperature (Bautista *et al.* 2008; Babuponnusami and Muthukumar 2014; Pliego *et al.* 2015; Oturan and Aaron 2014) and operation at atmospheric pressure, besides not requiring the application of external sources of energy, such as radiation, for the generation of the oxidizing species. Therefore, the process has an enormous interest in applications at wastewater treatment plants (WWTPs). On the other hand, in the last years, the interest in the application of this process for the treatment of gaseous effluents has increased (as reported in Chapter 2); however, little studies have been focussed on this topic for application towards organic compounds abatement, therefore opening a door for new researches and developments.

The application of Fenton's reagent for the treatment of gaseous effluents requires particular attention, especially focused on the choice of the reactor typology, once the Fenton process is carried out in the liquid phase. So, firstly it is necessary to perform the transfer of the pollutant from the gas stream to a liquid phase where the oxidation of the pollutant(s) occurs. This issue boosted the research to find an adequate device capable of providing the transfer of the contaminant from the gas phase to an aqueous matrix containing the Fenton's reagent. Thus, taking into account previous researches in this topic (Tokumura *et al.* 2013; Handa *et al.* 2013; Tokumura *et al.* 2012), the bubbling reactor (BR) was selected as the core device to perform the simultaneous absorption and Fenton oxidation, due to its high capacity to promote the mass (and heat transfer) (Kantarci *et al.* 2005; Bai 2010; Rollbusch *et al.* 2015; Kováts *et al.* 2017). Other advantages of this reactor configuration are listed in Chapter 2.

Although gas treatment in BRs has been previously reported for other AOPs (as reported in Chapter 2), this thesis emerged with the new perspectives for the treatment of volatile organic compounds (VOCs) by the homogenous Fenton's process, namely considering the effect in the aqueous matrix where by-products are accumulated. So, for this research, two BRs were designed: i) a smaller (0.9 L-capacity) acrylic lab-scale bubbling reactor (BR) (upon adapting an existing batch reactor to operate with a gas diffuser and gas inlet and outlet sampling ports – Fig. 1.1a) and ii) a 9 L-capacity acrylic bubble column reactor (BCR) – similar to others reported in the literature - Fig. 1.1b (Tokumura *et al.* 2013; Handa *et al.* 2013; Tokumura *et al.* 2012).

Firstly, two studies were performed for the treatment of a model compound (hydroquinone) and a real wastewater in both reactors, i.e., addressing only the liquid phase oxidation, being the gas used merely to promote an efficient mixing (and heat management); these works are reported in Chapters 3 and 4. After this, the treatment of a gaseous effluent containing toluene (a VOC selected as a model compound) was studied, being the results obtained presented and discussed in Chapter 5. Finally, the simultaneous treatment of a toluene-containing gaseous stream and the real effluent (from a Portuguese chemical industry) was carried out. For these approaches, Fenton's reagents were dosed *in situ* (in the water or effluent present in the BR), while the gas stream was continuously bubbled inside the reactor in a semi-continuous process. The proof-of-concept of the novel process for simultaneous gas-liquid treatment by this AOP is reported in Chapter 6.

Finally, Chapter 7 summarizes the main conclusions obtained along this Ph.D. work, while also providing some perspectives/suggestions for future work.

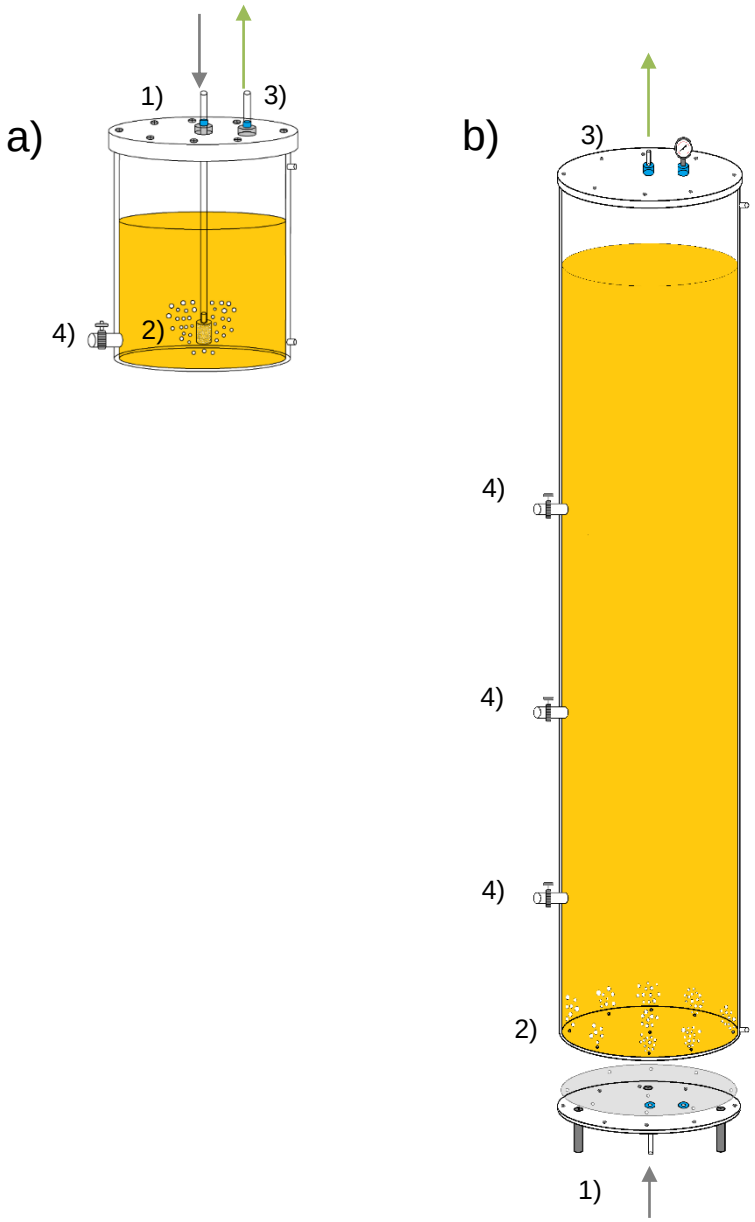

Figure 1.1 Scheme of the bubbling devices (bubbling reactor – BR (a) and bubble column reactor – BCR (b)) designed for the experimental work along this PhD thesis. Legends: 1 – gas phase inlet, 2 – gas diffuser (a) / dispersive plate (b), 3 – gas phase outlet, 4 – liquid sampling port.

1.2 References

Babuponnusami, A., and K. Muthukumar. 2014. 'A Review on Fenton and Improvements to the Fenton Process for Wastewater Treatment'. *Journal of Environmental Chemical Engineering* 2 (1): 557–72.

Bai, Wei. 2010. *Experimental and Numerical Investigation of Bubble Column Reactors*. Eindhoven: Technische Universiteit Eindhoven.

Barb, W. G., J. H. Baxendale, P. George, and K. R. Hargrave. 1951a. 'Reactions of Ferrous and Ferric Ions with Hydrogen Peroxide. Part I.—The Ferrous Ion Reaction'. *Trans. Faraday Soc.* 47 (0): 462–500.

Barb, W. G., J. H. Baxendale, P. George, and K. R. Hargrave. 1951b. 'Reactions of Ferrous and Ferric Ions with Hydrogen Peroxide. Part II.—The Ferric Ion Reaction'. *Trans. Faraday Soc.* 47 (0): 591–616.

Barb, W. G., J. H. Baxendale, Philip George, and K. R. Hargrave. 1949. 'Reactions of Ferrous and Ferric Ions with Hydrogen Peroxide'. *Nature* 163 (4148): 692–94.

Bautista, P., A. F. Mohedano, J. A. Casas, J. A. Zazo, and Juanjo J. Rodriguez. 2008. 'An Overview of the Application of Fenton Oxidation to Industrial Wastewaters Treatment'. *Journal of Chemical Technology and Biotechnology* 83 (10): 1323–38.

Fenton, H.J.H. 1894. 'LXXIII.—Oxidation of Tartaric Acid in Presence of Iron'. *Journal of the Chemical Society, Transactions* 65: 899–910.

Gligorovski, S., R. Strekowski, S. Barbati, and D. Vione. 2015. 'Environmental Implications of Hydroxyl Radicals (•OH)'. *Chemical Reviews* 115 (24): 13051–92.

Handa, M., Y. Lee, M. Shibusawa, M. Tokumura, and Y. Kawase. 2013. 'Removal of VOCs in Waste Gas by the Photo-Fenton Reaction: Effects of Dosage of Fenton Reagents on Degradation of Toluene Gas in a Bubble Column'. *Journal of Chemical Technology and Biotechnology* 88 (1): 88–97.

Huang, D., C. Hu, G. Zeng, M. Cheng, P. Xu, X. Gong, R. Wang, and W. Xue. 2017. 'Combination of Fenton Processes and Biotreatment for Wastewater Treatment and Soil Remediation'. *Science of the Total Environment* 574: 1599–1610.

Kantarci, N., F. Borak, and K. O. Ulgen. 2005. 'Bubble Column Reactors'. *Process Biochemistry*.

Kováts, P., D. Thévenin, and K. Zähringer. 2017. 'Investigation of Mass Transfer and Hydrodynamics in a Model Bubble Column'. *Chemical Engineering and Technology*

40 (8): 1434–44.

Nunes, T., C. Poceiro, M. Evtyugina, M. Duarte, C. Borrego, and M. Lopes. 2013. 'Mapping Anthropogenic and Natural Volatile Organic Compounds around Estarreja Chemical Industrial Complex'. In *WIT Transactions on Ecology and the Environment*, 174:55–64.

Oturan, M. A., and J. J. Aaron. 2014. 'Advanced Oxidation Processes in Water/Wastewater Treatment: Principles and Applications. A Review'. *Critical Reviews in Environmental Science and Technology* 44 (23): 2577–2641.

Pliego, G., J.A. Zazo, P. Garcia-Muñoz, M. Munoz, J.A. Casas, and J.J. Rodriguez. 2015. 'Trends in the Intensification of the Fenton Process for Wastewater Treatment: An Overview'. *Critical Reviews in Environmental Science and Technology* 45 (24): 2611–92.

Rollbusch, P., M. Bothe, M. Becker, M. Ludwig, M. Grünewald, M. Schlüter, and R. Franke. 2015. 'Bubble Columns Operated under Industrially Relevant Conditions – Current Understanding of Design Parameters'. *Chemical Engineering Science* 126: 660–78.

Thakur, S., and M. S. Chauhan. 2018. 'Treatment of Dye Wastewater from Textile Industry by Electrocoagulation and Fenton Oxidation: A Review', 117–29.

Tokumura, M., M. Shibusawa, and Y. Kawase. 2013. 'Dynamic Simulation of Degradation of Toluene in Waste Gas by the Photo-Fenton Reaction in a Bubble Column'. *Chemical Engineering Science* 100: 212–24.

Tokumura, M., Y. Wada, Y. Usami, T. Yamaki, A. Mizukoshi, M. Noguchi, and Y. Yanagisawa. 2012. 'Method of Removal of Volatile Organic Compounds by Using Wet Scrubber Coupled with Photo-Fenton Reaction - Preventing Emission of by-Products'. *Chemosphere* 89 (10): 1238–42.

Walling, C. 1975. 'Fenton's Reagent Revisited'. *Accounts of Chemical Research* 8 (4): 125–31.

Zhang, M. H., H. Dong, L. Zhao, D. X. Wang, and D. Meng. 2019. 'A Review on Fenton Process for Organic Wastewater Treatment Based on Optimization Perspective'. *Science of the Total Environment* 670: 110–21.

Chapter 2. State of Art – Gaseous and Liquid Effluents Treatment in Bubble Column Reactors by Advanced Oxidation Processes

Abstract: *This review aims to provide insight and highlight recent research trends about the treatment of gaseous and liquid effluents by advanced oxidation processes (AOPs) in bubble column reactors (BCRs), which has become an important technology to ensure efficient degradation of different types of pollutants. UV/H_2O_2, Fenton, and photo-Fenton processes have been applied in BCRs for pollutants removal from gas streams, namely containing NO, Hg^0, SO_2, and VOCs. In such a case, degradation is carried out in the liquid phase, while bubbling promotes an efficient mass transfer of the contaminants from the gas to the liquid before oxidation. This reactor configuration was however also used to remove pollutants present in liquid effluents by Fenton, electro-Fenton, as well as ozonation, which has been extensively studied; for that reason, only a summary view of BCRs application in ozonation is presented. In this case, a good mass transfer of the oxidant (O_3), present in the gas stream, is required before oxidation in the polluted liquid phase. In this review, the main features that should be taken into account in the application of different homogeneous AOPs in BCRs are addressed. The effects of determining factors like temperature, pH, oxidant, and catalyst dose or radiation power are also analyzed, with some relevant illustrative examples.*

The contents of this chapter were adapted from: Lima, V. N., Rodrigues, C. S., Borges, R. A., and Madeira, L. M. (2018). *Gaseous and liquid effluents treatment in bubble column reactors by advanced oxidation processes: A review*. **Critical Reviews in Environmental Science and Technology**, 48(16-18), 949-996.

2.1 Introduction

The treatment processes, for gas and liquid streams, are constantly changing and evolving, so that every year more investigations are conducted in order to find ways to carry out them more efficiently, in different types of reactors and different types of processes (Shi *et al.* 2017). Among the available devices, the bubble column reactors (BCRs) have recently received considerable attention for providing new ways of treating different pollutants, present in different phases (Handa *et al.* 2013; Tokumura *et al.* 2013).

A BCR is basically, and more commonly, a vertical cylindrical vessel containing a liquid in which the gaseous phase is injected (Kantarci *et al.* 2005; Pourtousi *et al.* 2014). In general, BCR operation is simple and is based in the feeding of a gaseous stream in the bottom of the column through a gas disperser, which may be a single-nozzle gas sparger or a diffuser plate with multiple orifices (Heijnen and Van't Riet 1984; Sarrafi *et al.* 1999). Then, the gas rises and forms the bubbles that contact with the liquid phase. During their movement the gas bubbles may promote an efficient mixing of the liquid phase, while occurring mass (and eventually heat) transfer among the two-phases (De Jesus *et al.*, 2017; Deckwer *et al.* 1974; Deckwer 1979; Heijnen and Van't Riet 1984; Shah *et al.*, 1982).

Bubble columns and BCRs are widely used in the chemical, petrochemical and biochemical industries, namely in chemical processes involving reactions such as oxidation, hydrogenation and polymerization, in industrial processes such as absorption and fermentation, and in the chemical and biological treatment of gas and water (Jhawar and Prakash 2012; Shah *et al.* 1982). The main reason for the use of bubble columns in these industries is due to their easiness in operation and maintenance; moreover, mass and heat transfer are better controlled and more effective (Kantarci *et al.* 2005). Further, the non-existence of moving parts makes BCRs advantageous and lowers the operating and maintenance costs when compared to other types of reactors commonly used in industry (Furusaki *et al.* 2002).

In recent years, several authors have studied and developed dynamic simulation models for processes performed in bubble columns. Many have evaluated the optimum characteristics as the right height and diameter of the column or still the characteristics of the bubbles formed by different types of gas dispersers. Kantarci *et al.* (2005) reviewed and described several works on BCRs and their characteristics, and addressed industrially relevant aspects like design and fluid dynamics, focusing especially in the reactors used in bioprocesses. More recently, Pourtousi *et al.* (2014) described the effect

of interfacial forces and turbulence models on predicting flow pattern inside the bubble column, while Rollbusch *et al.* (2015) analyzed recent works that describe the most important conditions for bubbling columns operation in industrial processes, namely their hydrodynamics at elevated pressures.

Besides research related to the BCRs transport phenomena, internal dynamics and construction, many authors have recently used bubble columns for effluent treatment. In this sense researchers applied biological, physical and chemical processes in bubble columns and BCRs for the treatment of different types of effluents, namely gaseous and liquid. Among the chemical processes, a technology used in effluents treatment has to be highlighted: the Advanced Oxidation Processes (AOPs). Such processes are, in short, a set of chemical treatment procedures designed to remove contaminants from water and wastewater by oxidation making use of the highly oxidative hydroxyl radicals ($HO^{\bullet}$). A diversity of AOPs is available, as detailed below, which use different oxidants (e.g. ozone (O_3) or hydrogen peroxide (H_2O_2)), with or without catalysts (that are dissolved or not in the liquid-phase), with or without external radiation, etc. Herein, we will focus our attention only in two-phase (liquid-gas) processes.

The application of AOPs in two-phase bubble columns was investigated by some authors (Handa *et al.* 2013; Lan *et al.* 2008; Lima *et al.* 2017; Nidheesh and Gandhimathi 2012; Rodrigues *et al.* 2018; Tokumura *et al.* 2013), mostly in the past ten years, aiming assessing the feasibility of the treatment of waste gases and liquids. Particular attention has been directed towards homogeneous AOPs like the Fenton, UV/H_2O_2, photo-Fenton, electro-Fenton and ozonation, which will be addressed in this review. Before that, a short reference is made to the main characteristics of bubble columns and important aspects like their hydrodynamics.

2.2 Short overview of bubble columns reactors

The BCRs have been designed to meet different processes demands, mostly in chemical industries. In some cases, the applicability of these reactor configurations has a stronger dependence on the constructive characteristics of the column than on the reactions been carried out therein. Therefore, different aspects should be taken into consideration when designing and using BCRs. Simple design characteristics such as the type of gas disperser, the height-to-diameter ratio of the column, and even the type of liquid/gas to be used are important features for the successful application of such technology. Some authors have been studying the effects of different operating conditions on mass transfer, reaction kinetics and column hydrodynamics for different types of applications

of bubble columns in various industrial sectors. Some merely illustrative examples are given herein below, to show how diverse are the possible applications of these devices (Besagni and Inzoli 2016; Cheng *et al.* 2013; Gómez-Díaz and Navaza 2016; Lee *et al.* 2015; McClure *et al.* 2016; Plevan *et al.* 2015; Pourtousi *et al.* 2015; Stacy *et al.* 2014; Yavorskyy *et al.* 2012).

Regarding the design of BCRs, it is worth stressing that chemical bubble column reactors normally operate with a height/diameter ratio of at least 5, but in biochemical applications this value typically varies from 2 to 5 (Degaleesan *et al.* 2001). The height/diameter ratio will be quite important when performing column scale-up for industrial applications. The operation mode is another main aspect to consider; it may occur in continuous mode, in other words, the liquid and the gas phase are continuously fed, or in semi-batch mode, if the gas is fed continuously and the liquid phase is steady (Kantarci *et al.* 2005). In continuous mode, the gas is ascending, while the fluid movement can be upward (co-current) or downward (counter-current); however, the superficial liquid velocity must be much lower than the superficial gas velocity (Pino *et al.* 1992). It is noteworthy that most of the researches using BCRs to treat gaseous effluents by oxidation processes (which will be discussed in further detail in section 2.4) were performed in the semi-batch mode.

The bubbles formation is a crucial aspect to have in mind; it has direct correlation with the superficial gas velocity (regulated by gas flow rate, which directly affects also the residence time) (Kantarci *et al.* 2005), but also with the type of orifice sparger (or gas diffuser), being that their size is regulated by the hole diameter (generally in the range of 0.5 to 6 mm (Kulkarni and Joshi 2011)). In the literature is reported the formation of larger bubbles when increasing the hole diameter in the dispersive plate, this way enhancing the surface tension they are subjected to (Leonard *et al.* 2015). In fact, the control of the disperser opening area is extremely important for industrial bubble columns, as the presence of small bubbles is preferred for providing higher mass transfer values (Behkish *et al.* 2002; Fukuma *et al.* 1987; Krishna and Van Baten 2003; Leonard *et al.* 2015).

The properties of the liquid phase are also crucial as they will influence the process performed in the bubble column. Particularly, the viscosity of the medium affects the gas-liquid mass transfer coefficient (k_La); the mass transfer decreases with the increase of the liquid viscosity, as high viscosities provide lower gas-liquid surface areas (Kulkarni and Joshi 2011). Further, the temperature of the liquid phase also has a direct influence on the gas holdup (increasing with the raise of temperature) and, consequently, on the mass transfer (Kantarci *et al.* 2005).

Some features of the BCRs are responsible for their performance and affect the k_La, as well as the gas holdup (ε). There are several studies addressing specifically the mass transfer in bubble columns with correlations to predict k_La (Akita and Yoshida 1973; Kang *et al.* 1999; Lee *et al.* 2015; Öztürk *et al.* 1987; Shah *et al.* 1982) and, consequently, the oxygen transfer rate (OTR) in biological process (which directly depends of k_La).

The operating conditions are also an issue to consider in BCRs, namely the total operating pressure. This type of reactor may be operated at atmospheric pressure or above, and several studies have concluded that the operating pressure has a significant effect on the k_La and on the bubbles size (Behkish *et al.* 2002; Dewes *et al.* 1995; Wilkinson *et al.* 1994). However, most of the studies reported in the section 2.4 did not report system pressure.

All the previously mentioned factors should be taken into account in the scale-up of BCRs for the application of chemical processes, such as AOPs. Along this review are presented and discussed the more recent researches using BCRs to treat effluents by such oxidative processes at lab scale. However, it is worth mentioning some examples of the use of bubble columns and BCRs for effluents treatment by other processes, particularly at industrial scale (as briefly discussed in the next section).

2.3 Industrial applications of bubble columns and BCRs in the treatment of effluents

Bubble columns (used in non-reactive conditions) and BCRs (used under reactive conditions) have been employed in different industrial processes for gas and liquid effluents treatment (some of them involving three-phases systems), which include absorption, adsorption, membrane and biofilters, biological processes, among others (Kennes and Veiga 2013). Although this is not the focus of the present review, a few examples, at industrial scale, are provided below.

In the case of gas treatment, removal of SO_2, an important atmospheric contaminant, was realized in a bubble column scrubber through desulfurization – an absorption process in water (Meikap *et al.* 2002). In this example, the flue gas is fed from the column bottom (gas flow rate of 1.20-5.46 x 10^{-3} Nm^3/s) and the liquid (flow rate of 34.48-175 x 10^{-6} m^3/s) from the top. It was observed a gradually increase of the SO_2 removal in tests with increasing gas velocities, for constant liquid flow rate; this occurs because the increase in gas velocity promotes more turbulence in the gas-liquid interface. In other tests the increase of the liquid flow rate was responsible for an increased interfacial

contact area between the gas bubbles and the water, which favored the SO_2 removal (due to increased mass transfer). This study highlights the fact that the process, realized in a bubble column, can be operated either continuously in counter-current mode (gas injected into the bottom and liquid from the top), or in a discontinuous mode, only with the gas internal movement (Meikap *et al.* 2002).

Several companies around the world have developed solutions for the chemical industries through the design of packed columns for the treatment of inorganic gases (Tri-Mer Corporation 2013) and organic compounds (Clean Gas Systems 2010). Among the advantages of this device can be highlighted the low pressure drop in the system, besides the possibility of low costs of maintenance and operation. The packed bubble column is a device designed with a fixed structure of packing (containing for instance absorbents, catalysts or simply inert materials) inside the BCR (Bai 2010; Zehner and Kraume 2000). In these devices, the absorptive process normally occurs with the contact between the packing and the liquid phase in continuous mode while the gas is injected in the system being dispersed through the packaging channels (Molga and Westerterp 1997). This technology was used to remove carbon dioxide (CO_2) from a solution containing diethanolamine (DEA) and ethylene glycol by Molga and Westerterp (1997), showing the applicability of such three-phases device.

Carbon dioxide also been very often removed from gaseous effluents in simple bubble columns, particularly through chemical absorption in DEA and monoethanolamine (MEA); N-methyldiethanolamine (MDEA) has also been used (Navaza *et al.* 2009). In this process, the CO_2 present in the gas phase is fed into the column by the bottom (via glass capillaries – generating small bubbles). The authors assessed the effect of the gas flow rate and MDEA concentration in CO_2 removal. The increase of the MDEA concentration in the liquid phase is responsible for the increase of the global CO_2 removal. The process investigated in this study demonstrates a practical application of the BCR in environmental processes for pollutants abatement in gas emission.

Another interesting example is a hybrid process making use of a bubble column bioreactor with one biofilter, both integrated in the same device. This process was realized by Abtahi *et al.* (2014) and Naddafi *et al.* (2016) for dichloromethane (DCM) removal from waste gas streams. The hybrid system contains a bubble column bioreactor (1st step, bottom of the unit) followed by a biofilter (2nt step, in the top) working in an up flow mode; while in the bubble column bioreactor the microorganisms are present in suspension, in the biofilter they are immobilized. It was assessed the efficiency of each process individually and of the hybrid integrated unit. The treatment was carried out feeding the gas (with DCM) stream by an air diffuser placed in the column

bottom. It was concluded that the use of the bubble column in such bioprocess is an excellent way to add oxygen to aerobic systems favouring the oxygen transfer rate. However, in this example the bubble column remains as a co-adjuvant in the process, since the treatment/degradation does not happen only in the column, but also in the biofilter.

Studies based in bubble columns or BCRs at industrial scale were also realized by some authors. In the 1990's, Adkins *et al.* (1996) evaluated the effects of the internal pressure in the hydrodynamic conditions of one bubble column of 3 m high, 0.48 m of diameter and wall thickness of 12.7 mm. In this system, the air is fed from the bottom with the gas sparger in the form of a ring with 0.15 m of diameter (with 12 holes – Ø = 3.18 mm). The maximum pressure for this device is 34 kPa (5 psi) and the gas velocity is 0.40 m/s. The relatively large dimensions of this column demonstrate its industrial applicability, so that large volumes/flow rates can be treated.

More recently, some research institutes performed studies in BCRs of large scale. In Spain, a novel photobioreactor composed of one bubble column with an injection system based in an air-lift was conceived for the processing of large amounts of biomass to produce biodiesel by microalgae (Abtahi *et al.* 2014; Navaza *et al.* 2009). This structure, placed in an external area in direct contact with sun light, is a transparent cylinder (for optimization of the light transmission) with CO_2 injection (responsible for algae development). In Canada, another research group has assembled two bubble columns of large dimensions. One reactor is made of Plexiglass, operating in co-current upward with different liquid phases (different viscosities), having 2.7 m x 0.292 m, height and diameter, and with injection of the gas being performed by a plate distributor with 94 holes (Ø = 1 mm), operating at ambient temperature and pressure. The other unit was conceived for high pressure (up to 3 MPa) and temperature (up to 800 ºC) operation for hydrodynamic studies under industrial conditions, with 4.8 m x 0.152 m, height and diameter, the gas being fed into the bottom through a plate gas distributor (Process Engineering Advanced Research Lab 2017).

Although few data are available in the open literature on large-scale applications of BCRs to treat effluents, it is obvious that advances in this area are necessary, and these always start with laboratory research. Despite the few examples briefly cited in this section, we believe that BCRs deserve further attention, particularly for implementing Advanced Oxidation Processes. In the open literature are reported some studies being carried recently focusing on BCRs, mostly in laboratory scale, to treat effluents by AOPs. Such works will be described with more detail along the next section.

2.4 Advanced oxidation processes in BCRs

Classic effluent treatment processes, namely physical-chemical process (such as filtration or coagulation-flocculation) and biological process, are not enough to generate water with acceptable levels of pollutants, particularly when charges of contaminants are too high or contain toxic substances, respectively (Lafi and Al-Qodah 2006; Legrini et al 1993; Mantzavinos and Psillakis 2004). Hence, other treatments become necessary to achieve this goal, as is the case of advanced oxidation processes (AOPs), which are recommended when pollutants have a high chemical stability and/or low biodegradability (Poyatos *et al.* 2010). Regardless of the AOP chosen, they all have in common the fact of generating and taking advantage of the formed hydroxyl radical, which after fluorine is the species with higher oxidation potential (Table 2.1).

These radicals are highly reactive, non-selective and attack most organic molecules, originating CO_2, H_2O and inorganic ions, or at least transform the organic pollutant compounds into less toxic products (Rosenfeldt *et al.* 2007; Skoumal *et al.* 2006). There are several possibilities for the reactions between the hydroxyl radical and the organics species (RH), which include radical addition, hydrogen abstraction and/or transfer of electrons, as detailed in Eqs. 2.1-2.3, respectively (Legrini *et al.* 1993).

$$HO^{\bullet} + RH \rightarrow RH_2O \quad (2.1)$$

$$HO^{\bullet} + RH \rightarrow R^{\bullet} + H_2O \quad (2.2)$$

$$HO^{\bullet} + RH \rightarrow RH^{\bullet} + HO^{-} \quad (2.3)$$

There is a large number of AOPs available. Many of them use a combination of oxidizing agents (e.g. H_2O_2 and/or O_3) with or without catalysts (e.g. metal ions) and radiation (ultraviolet and/or visible). In the homogeneous process (main focus of this review), the catalyst is present/dissolved in solution, thereby forming a single phase, while in heterogeneous processes the catalyst is in a distinct phase (often the solid one). In Table 2.2 are shortly described some of the most popular AOPs.

The evolution of the application of AOPs for effluents treatment in the last years was towards the improvement of technologies, preparation and use of new catalysts, selection of new reactor configurations and coupled processes. Some reviews were carried out presenting current research trends about different AOPs for water/wastewater treatment. For instance, Moreira *et al.* (2017) performed a review of the electrochemical oxidation processes applied to synthetic and real wastewaters, while Oturan and Aaron (2014) assessed the principles and applications of AOPs. Clarizia *et al.* (2017) evaluated studies about the application of the homogeneous photo-Fenton

process at near neutral pH, while He and Zhou (2017) addressed the performance of the electro-Fenton process. Boczkaj and Fernandes (2017) performed a review about the application of AOPs at basic pH conditions. Garcia-Segura *et al.* (2016) evaluated recent studies about the fluidized-bed Fenton process. Regarding the use of the new catalysts, Bokare and Choi (2014) performed a review of Fenton-like systems using non-ferrous Fenton catalysts, while Pouran *et al.* (2014) addressed heterogeneous Fenton reactions with modified iron oxides. Finally, Pliego *et al.* (2015) performed an overview about the trends in the intensification of the Fenton process to treat wastewater. Other researchers evaluated coupled processes for wastewater treatment, namely AOPs with biological treatments (Ayed *et al.* 2017; Oller *et al.* 2011), cavitation with Fenton process (Bagal and Gogate 2014) and hybrid processes (Gogate and Pandit 2004).

Table 2.1 Oxidation potential of some chemical species (Legrini *et al.* 1993).

Species	Redox potential (eV)
Fluorine	3.03
Hydroxyl radical	2.80
Atomic oxygen	2.42
Ozone	2.07
Hydrogen peroxide	1.78
Hydroperoxyl radical	1.70
Permanganate	1.68
Chlorine	1.36
Bromine	1.09
Iodine	0.54

As stated above, the treatment of effluents in bubble columns can occur through various processes among which stands out the absorption (Hsueh *et al.* 2010), the biological (Lee *et al.* 2015), and the AOPs. In the physical absorption process, it only occurs the mass transfer of contaminants from the gas to the liquid phase, being necessary to subsequently treat this stream. Therefore, the absorption ends up not promoting the actual degradation of the pollutants. On the other hand, biological processes are not feasible for non-biodegradable or toxic substances. Accordingly, the use of the bubble columns with AOPs has emerged to solve these problems; the contaminants present in the gas are absorbed in the liquid wherein are subsequently removed by oxidation reactions.

Table 2.2 Main advanced chemical oxidation processes (adapted from Poyatos *et al.* (2010)).

Type	Energy Source	Process
Homogeneous	Yes	O_3/UV
		H_2O_2/UV
		O_3/H_2O_2/UV
		H_2O_2/Fe^{2+}/UV (Photo-Fenton)
		O_3/Ultra sounds
		Electro-Fenton
	No	O_3/H_2O_2
		O_3 in an alkaline medium
		H_2O_2/Fe^{2+} (Fenton)
Heterogeneous	Yes	Heterogeneous Photocatalysis (Catalyst/UV)
		Photocatalytic Ozonation (Catalyst/UV/O_3)
	No	Catalytic Ozonation (Catalyst/O_3)
		Fenton (Supported catalyst/H_2O_2)

Regarding the application of AOPs in bubble columns, some works have emerged recently since the 2000s. Fenton and photo-Fenton processes have been mostly applied for gaseous effluents, while electro-Fenton and ozonation were studied to treat different types of compounds in liquid effluents; some of these processes are described below, in sections 2.4.2 to 2.4.6.

2.4.1 Mechanism of treatment of gas and/or liquid effluents by AOPs

Before addressing each of the AOPs that have been integrated with BCRs, in this section is shortly described the mechanism, i.e., the operation mode, for the cases wherein the target pollutants are present in gas or liquid streams.

The degradation of pollutants present in gas streams through AOPs in column reactors involves a gas-liquid mass transfer with chemical reaction(s) involving hydroxyl radicals occurring simultaneously, as illustrated in Fig. 2.1 for the particular case of the dark Fenton process.

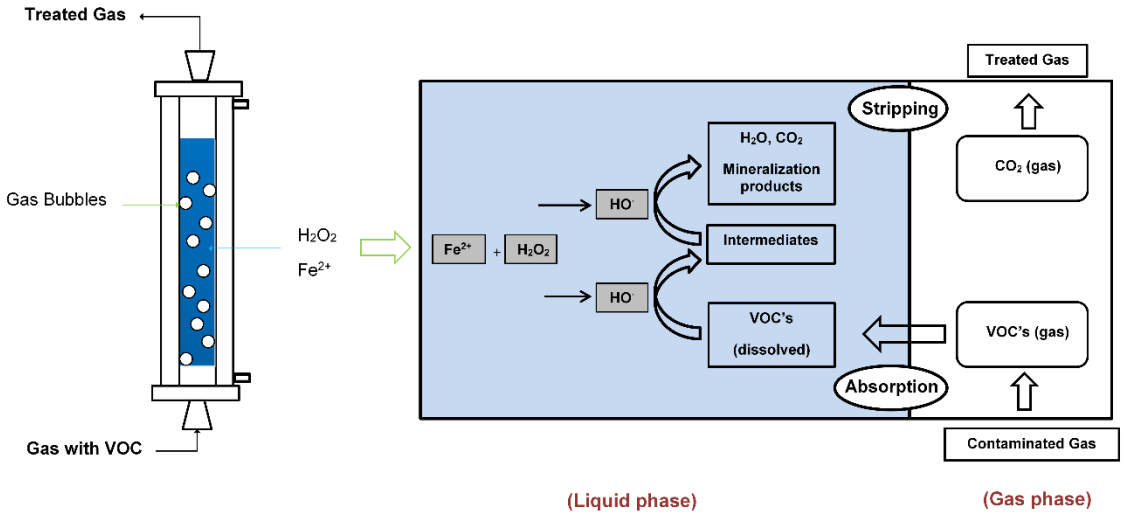

Figure 2.1 Scheme of the main processes occurring in the gas and liquid phase for the degradation of volatile organic compounds (VOCs) present in the gas stream in a bubble column by the Fenton process (adapted from Handa *et al.* (2013)).

As detailed in Fig. 2.1, this process involves the following steps (exemplified for a gas stream contaminated with volatile organic compounds - VOCs) (Handa *et al.* 2013):

1. Transfer of the pollutants (VOCs in this case) from the gas stream to the liquid phase, where oxidation will occur;
2. Generation of the hydroxyl radicals in the liquid phase by a particular AOP (in this case the Fenton process is illustrated, making use of a H_2O_2/Fe^{2+} mixture);
3. Oxidation of the pollutants by the hydroxyl radicals in the liquid phase. This oxidation will decrease the concentration of pollutant (VOCs) in the liquid phase, thus increasing the driving force for mass transfer (stage 1).

On the other hand, in the treatment of liquid effluents in BCRs by AOPs the pollutants will be degraded in the same phase where they are initially present (the liquid), and so it is the oxidant, which is often present in the gas stream (e.g. ozone), the species that has to be transferred. In general, the mechanism of ozonation is very similar to that described previously for the degradation of pollutants present in gas effluents; the particularity is that now is ozone (the oxidant) that is transferred for the liquid phase where it oxidizes the pollutants. There are however some examples integrating BCRs and AOPs where the role of the gas streams is the simple homogenization and mixing of the liquid phase (Wonders *et al.* 2006); the bubbling in such works allows to obtain a good homogenization inside the BCR, similar to that of perfectly stirred reactors without resorting to mechanical agitation (Rodrigues *et al.* 2018).

2.4.2 Fenton

It is commonly accepted that this AOP started with the work of Henry Fenton, by the end of the 19th century, who described the activation of the H_2O_2 molecule by iron (II) salts to oxidize tartaric acid (Fenton 1894). Since then the number of works related to the Fenton process for the treatment of contaminated effluents has grown tremendously, particularly in the recent years. It is known that H_2O_2, when compared with other oxidizing agents, is cheap, safe, easy to handle and does not imply a threat to the environment since it is easily (self)degraded into water and oxygen, while iron is also cheap and safe for the environment (Pignatello *et al.* 2006). Moreover, the process can be carried out at moderate conditions of temperature and pressure (close to room temperature and atmospheric pressure). These aspects make the Fenton process attractive. The Fenton reaction mechanism proposed by Barb *et al.* (1949, 1951a, 1951b) and Walling (1975), in the absence of an organic compound, comprises the following reactions:

$$Fe^{2+}+H_2O_2 \rightarrow Fe^{3+}+HO^{\bullet}+OH^{-} \quad (2.4)$$

$$Fe^{3+}+H_2O_2 \rightarrow Fe^{2+}+HO_2^{\bullet}+H^{+} \quad (2.5)$$

$$HO^{\bullet}+Fe^{2+} \rightarrow Fe^{3+}+OH^{-} \quad (2.6)$$

$$HO^{\bullet}+H_2O_2 \rightarrow H_2O+HO_2^{\bullet} \quad (2.7)$$

$$Fe^{2+}+HO_2^{\bullet}+H^{+} \rightarrow Fe^{3+}+H_2O_2 \quad (2.8)$$

$$Fe^{3+}+HO_2^{\bullet} \rightarrow Fe^{2+}+ H^{+}+O_2 \quad (2.9)$$

$$HO_2^{\bullet}+ HO_2^{\bullet} \rightarrow H_2O_2 +O_2 \quad (2.10)$$

Also according to Pignatello *et al.* (2006), the Fenton process takes place by a cyclic set of equations (2.4-2.10). The desired oxidant is the hydroxyl radical formed in reaction 4, by combining a Fe (II) salt with H_2O_2. At the same time, the regeneration of Fe(II) occurs through Eq. 2.5, with the formation of hydroperoxyl radicals which have however a much smaller oxidation power than the hydroxyl species – Table 2.1 (Legrini *et al.* 1993). This reaction is much slower than the previous one, and therefore may be the limiting step of the process. It is worth noting that the hydroxyl radical might be sequestered by excess of Fe(II) and/or H_2O_2, as described by Eqs. 2.6 and 2.7, respectively. There are however further parallel equations as shown, for instance, in Eqs. 2.8-2.10 (Mantzavinos and Psillakis 2004), which lead in practice to the requirement of optimizing doses of oxidant and catalyst for each particular case, as detailed below.

Table 2.3 shows some examples of studies where application of the Fenton process was carried out in a bubble column, to treat either gas or liquid effluents. Different reactors, with slightly different dimensions, have been employed. The range of operating conditions change from one study to another, depending also on the effluent to treat, and hence the performance also differs, as summarized in Table 2.3. It is noteworthy that, although these studies were performed in BCRs, the authors did not focus on technical parameters of the columns, bubble size or gas retention, which play an important role in the efficiency of the treatment.

The Fenton process is influenced by some basic operation conditions such as pH, temperature, gas flow rate and concentration of iron and hydrogen peroxide. Their effects will be illustrated in the following sections, with some examples.

Table 2.3 Examples of applications of the Fenton process in the treatment of effluents in BCRs.

Effluent/Compound	Reactor characteristics	Operation conditions	Removals (%)	Ref.
Gas phase				
$Hg^o/SO_2/NO$	Model = bubbling reactor Diameter (m) = 0.09 Length (m) =0.4	pH = 1.1-11.2 T (ºC) = 25-75 H_2O_2 conc. (mol/L) = 0.0-1.2 Iron conc. (mol/L) = 0.00-015 Gas flow rate (L/min) =0.4-2.0	Simultaneous removal: Hg^o = 100 SO_2 = 100 NO = 83.6	(Liu *et al.* 2015a)
Methane	Model: self-designed bubbling reactor Diameter and height: not specified	pH = 1-5 T (ºC) = 25 H_2O_2 conc. (mM) = 5-120 Iron conc. (mM) = 0.25-2.5 Gas flow rate (L/min): 10	Methane = 25	(Wei *et al.* 2012)
NO	Lab-scale bubbling reactor with mechanical stirring Diameter (m) = 0.10 Height (m) = 0.15	pH = 2-6 T (K) = 298-343 [$FeSO_4$] (mol/L) = 0.05 H_2O_2 conc. (mol/L) = 0.5-1.5 NO conc. (ppm) = 250-1000 Gas flow rate (L/min) = 2	NO = 75	(Guo *et al.* 2011)

Effluent/Compound	Reactor characteristics	Operation conditions	Removals (%)	Ref.
Liquid phase				
Hydroquinone	Model: bubble column reactor Diameter (m) = 0.098 Height (m) = 1.40	pH = 3-7 T (ºC) = 15-70 $V_{internal}$ (L) = 5-9 H_2O_2 conc. (g/L) = 0-1.5 Iron conc. (mg/L) = 0-120 Air flow rate (mL/min) = 1.0-5.0	TOC = 55.9 hydroquinone = 100	(Lima *et al.* 2017)
p-nitrophenol	Model: bubble column reactor Diameter (m) = 0.098 Height (m) = 1.40	pH = 3-7 T (ºC) = 22-24 H_2O_2 conc. (g/L) = 0.4-2.0 Iron conc. (mg/L) = 40-120 Air flow rate (mL/min) = 1.0-5.0	TOC = 75.1 *p*-nitrophenol = 100	(Rodrigues *et al.* 2018)

2.4.2.1 Influence of the temperature

The temperature is a parameter that must be considered in the Fenton reaction in any type of reactor. However, as it occurs with several operating variables, it should be carefully selected. In fact, if by one hand increased temperatures favor the acceleration of both radicals generation and organics attack (as kinetic constants increase exponentially with temperature – Arrhenius equation), on the other hand, when the reaction proceeds at too high temperatures (higher than 50 ºC), the thermal decomposition of H_2O_2 into H_2O and O_2 occurs (Williams 1928), and thereby the H_2O_2 available in solution is decreased (Guo *et al.* 2011; Samet *et al.* 2012). Therefore, it is very common to find an optimum temperature (a range between 25 and 50 ºC has been commonly reported) for Fenton oxidation, although values change from work to work.

Guo *et al.* (2011) evaluated the effect of temperature on the removal of NO (Fig. 2.2) by the Fenton reaction in a BCR. It was observed that increasing the reaction temperature beyond 320 K (47 °C) the removal efficiency reached, in pseudo-steady state, fell from over 65% to below 55%. The authors argue that this behavior must be related with the hydrogen peroxide decomposition at higher temperatures, which is unfavorable for the oxidation process. The NO removal by oxidation was reported in the literature as being responsible for the formation of by-products (or intermediates) such as nitrogen oxides (NOx) (Sousa *et al.* 2013), which are quite dangerous to the environment (US EPA, 1999). For that reason, Guo *et al.* (2011) measured the concentration of NOx in the effluent discharged, so as to evaluate their possible formation during the oxidative process, which should be avoided.

Liu *et al.* (2015a) also evaluated the influence of temperature on the Fenton reaction for the removal of elementary mercury (Hg^0) in flue gas. The elementary mercury is an anthropogenic compound formed in different chemical industrial process and is reported to be toxic for the human health (US EPA, 2012). In the work of Liu *et al.* (2015a) a BCR with small dimensions (0.09 x 0.4 m, diameter and length) was employed, working with temperatures in the range between 298 K (25 ºC) and 348 K (75 °C). They noticed that for temperatures higher than 323 K (50 ºC) the Hg^0 removal efficiency decays, independently of the H_2O_2 concentration applied, although the drop is not that sharp, as can be seen in Fig. 2.2. The authors have used the same device for the simultaneous elimination of several species by the Fenton process, reaching efficiencies as high as 100% for SO_2, 100% for Hg^0 and 83.6% for NO, under optimal conditions – cf. Table 2.3.

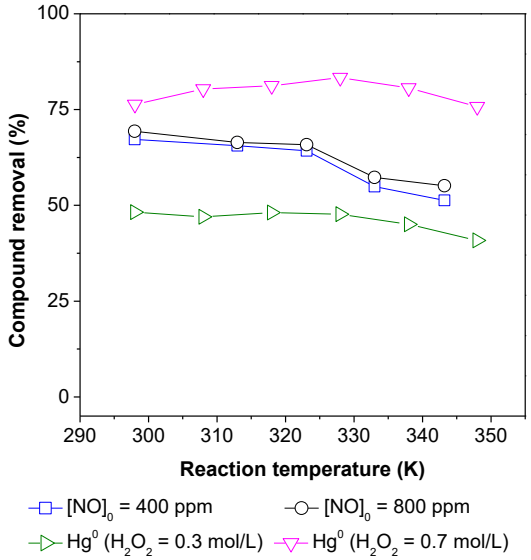

Figure 2.2 Effect of reaction temperature on NO removal efficiency (pH = 2, H_2O_2 = 0.75 mol/L and $FeSO_4$ = 0.05 mol/L) (adapted from Guo *et al.* (2011)) and on Hg^0 removal (O_2 = 6.0%, CO_2 = 12.0%, SO_2 = 1000 ppm, NO = 400 ppm, pH = 3.4, Fe^{2+} = 0.008 mol/L, Hg^0 inlet = 40 μg/m^3 and gas flow rate = 800 mL/min) (adapted from Liu *et al.* (2015a)) by the Fenton reaction realized in a BCR.

The effect of the temperature reported above for treating gas streams was similar to that observed when treating a simulated liquid effluent containing hydroquinone by the Fenton process in a BCR (Lima *et al.* 2017). Lima *et al.* (2017) evaluated the influence of this parameter in the range of 15 to 70 ºC and reached the maximum total organic carbon (TOC) removal (nearly 45%) for T = 24 ºC (room temperature). The increase of the temperature above this value was responsible for decreasing the TOC removal due to the hydrogen peroxide decomposition, which was experimentally checked by the authors.

It is worth highlighting that the effect of the temperature was only investigated in the target compound(s) removal. However, it is important to evaluate the influence of this parameter in the mass transfer (i.e. in the OTR - OTR = k_La (C*-C), that depends directly from k_La and indirectly from the temperature, which affects the dissolved oxygen saturated concentration - C*) and in bubbles formation, a topic that was not yet reported in the literature for the integration of AOPs in BCRs.

2.4.2.2 Effect of the initial pH

When carrying out the Fenton reaction in a BCR for the removal of NO present in flue gas, Guo *et al.* (2011) studied the effects of different parameters in the reaction.

Regarding the effect of the pH, it was decided to study this parameter in the range of 2-6; Fig. 2.3 shows the NO removal at different pHs for two different inlet concentrations of the target compound. The greater removal of NO was obtained at pH 2 in both cases; for pH below this value the efficiency of the Fenton process decreases since the large quantities of H^+ in solution promotes the formation of $H_3O_2^+$ and the regeneration of Fe^{2+} (through reaction between Fe^{3+} and H_2O_2 - cf. Eq. (2.5)) is partly inhibited; as a direct consequence, the hydroxyl radical concentration falls (Guo *et al.* 2011; Pignatello *et al.* 2006). On the other hand, at the maximum pH studied (pH = 6) the removal of NO in both concentrations (400 and 800 ppm) was below 60%. At pH above 3 occurs the formation of iron colloidal oxides and iron precipitates as $Fe(OH)_3$, therefore decreasing the amount of catalyst available in solution; moreover, hydrogen peroxide is less stable, being decomposed into water and oxygen, all the factors being responsible for diminishing the formation of hydroxyl radicals and inherently process performance (Handa *et al.* 2013; Pignatello *et al.* 2006).

In another study, Liu *et al.* (2015a) evaluated the removal efficiency of Hg^0, present in flue gas, through the Fenton reaction at different H_2O_2 concentrations and at different pH values (from 1.1 to 11.1), also shown in Fig. 2.3. In this study it was observed a sharp decay of Hg^0 removal when the reaction was processed above pH 5-6. The authors indicate that H_2O_2 in alkaline solutions tends to hydrolyze the HO_2^- which reduces the H_2O_2 concentration available for the oxidation reactions. For the hydrogen peroxide concentrations tested, the difference between the removal efficiencies between pH 1.1-5.1 was low, which would indicate that pH 2-3 is not always the optimum, and this will depend on other operating conditions. Indeed, Wei *et al.* (2012) studied the methane degradation and the optimum pH found was 2.5, as shown in Fig. 2.3, pointing for the scavenging of hydroxyl radicals in acid conditions.

The pH effect was also assessed for treating two distinct liquid effluents (containing *p*-nitrophenol (Rodrigues *et al.* 2018) and hydroquinone (Lima *et al.*, 2017)) and the better mineralization of both compounds was always obtained for an initial pH of 3 (~49 and ~39% for *p*-nitrophenol and hydroquinone effluents, respectively), which decreases along the oxidation process. Rodrigues *et al.* (2018), after optimizing the experimental conditions, propose a strategy to improve the mineralization, which consisted of readjusting the pH to the optimum value (pH = 3) during the reaction, achieving an increase in the mineralization efficiency of ~49 to ~63%, thus showing the importance of this parameter in the Fenton reaction.

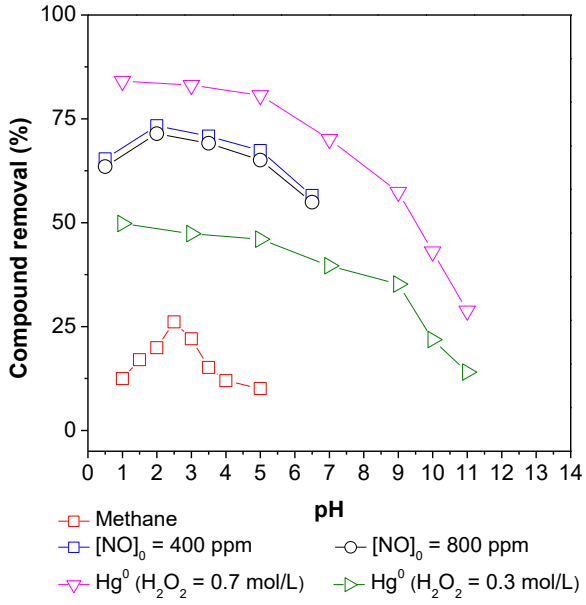

Figure 2.3 Effect of the pH on methane removal (T = 25 ºC, Fe^{2+} = 2.0 mM and H_2O_2 = 80 mM and (adapted from Wei *et al.* (2012)), NO removal (T = 323 K, H_2O_2 = 0.75 mol/L and $FeSO_4$ = 0.05 mol/L (adapted from Guo *et al.* (2011)) and Hg^0 removal (O_2 concentration = 6.0%, CO_2 concentration = 12.0%, SO_2 = 1000 ppm; NO = 400 ppm; T = 55 °C; Fe^{2+} = 0.008 mol/L; Hg^0 inlet = 40 µg/m^3 and flue gas flow = 800 mL/min) (adapted from Liu *et al.* (2015a)) by the Fenton reaction realized in a BCR.

Notwithstanding in these studies the pH influence in the mass transfer coefficient was not studied, it is a crucial parameter to take into account as proven in the study developed by Ferreira *et al.* (2013).

2.4.2.3 Effect of the hydrogen peroxide concentration

One of the most important parameters in the Fenton process is the concentration of oxidant (H_2O_2) (Handa *et al.* 2013). An increase in the H_2O_2 dose has a positive influence on the formation of hydroxyl radicals, but above a certain concentration, which may be in the range of mM or up to M (depending on the characteristics and concentration of the pollutant(s)/effluent to be treated, and remaining operating conditions), the opposite effect may be noticed; this is commonly attributed to the scavenging of radicals by the H_2O_2 present in excess (Eq. 2.7), thereby decreasing the amount of available hydroxyl radicals to oxidize the target pollutant(s) (Liu *et al.* 2015a; Zhan *et al.* 2013). This can be observed in Fig. 2.4, which again summarizes results obtained by different authors, with different pollutants. For instance, in the work developed by Guo *et al.* (2011), who evaluated the effect of H_2O_2 concentration in the range of 0.5-1.5 mol/L in NO removal. The increase of the reagent dose favored the removal of NO till a hydrogen peroxide concentration of 1.3 mol/L. For this concentration the authors obtained the highest NO

removal (~70%), but when the hydrogen peroxide concentration was increased to 1.5 mol/L, the removal fall to about nearly 50%, regardless the NO concentrations employed (400 or 800 ppm).

Liu *et al.* (2015a) evaluated the effect of the H_2O_2 concentration in the range of 0 to 1.2 mol/L for Hg^0 removal present in flue gas, by Fenton oxidation (Fig. 2.4). The authors carried out two runs with different catalyst doses (0.002 and 0.008 mol/L of $FeSO_4$); in both experiments the removal increases with the oxidant concentration, being noticed that after a certain oxidant dose, this increase becomes less pronounced. The hydrogen peroxide scavenging effect in this case was not noticed, what would possibly require the use of higher H_2O_2 concentrations. Nevertheless, it seems that there is a scavenging due to the excess of catalyst, as discussed in the following section. In fact, in the run performed with 0.002 mol/L of $FeSO_4$ a better performance was reached, being that more than 90% of Hg^0 was removed when the maximum H_2O_2 concentration (1.2 mol/L) was used.

Apart from these, other examples that illustrate the importance of the careful selection of the oxidant dose for each particular situation can be found in the literature. For instance, Wei *et al.* studied the methane (present in coal-mine gas) removal and reached an optimum H_2O_2 concentration at 100 mM (Wei *et al.* 2012). The Fenton process also was investigated by Liu *et al.* (2017) in a continuous-flow aeration container for benzene oxidation. The procedure realized promotes the mass transfer between benzene (a volatile organic compound) and the Fenton solution (liquid phase). One important aspect addressed in this study is the regular dosing of the hydrogen peroxide (either intermittently or continuously) along with the pollutant gas supply in the container to ensure the maximum presence of the hydroxyl radicals. Otherwise, H_2O_2 would be rapidly eliminated during the treatment of the continuous-flow VOCs waste-gas.

Regarding the treatment of liquid effluents, it is worth mentioning two further examples where the effect of the oxidant dose in the *p*-nitrophenol (Rodrigues *et al.*, 2018) and hydroquinone (Lima *et al.* 2017) degradation was assessed. Again, an optimum H_2O_2 concentration was found in both cases. Moreover, and as in the research of Liu *et al.* (2017), a gradual dosing of the oxidant (along the reaction time) was employed to improve the efficiency of the hydrogen peroxide use. The effect of bubbling in the hydrogen peroxide stripping was observed by Lima *et al.* (2017), but it was concluded that this effect was not pronounced and did not seem to affect the oxidation process. Other authors used H_2O_2 for oxidation in BCRs, but the effect of its loss was in most cases not investigated.

2.4.2.4 Effect of the iron concentration

The increase of the Fe^{2+} concentration in the reaction medium will be beneficial for the Fenton reaction, as more iron will be available in the solution to catalyze the process. However, an excess of available ferrous ions may inhibit the process because these ions can capture hydroxyl radicals, as shown in Eqs. (2.6, 2.8-2.9) (Zhan *et al.* 2013). Such scavenging effect was reported above, in the example provided in Fig. 2.4; the authors worked with different concentrations of iron (0.002 and 0.008 mol/L) and different concentrations of H_2O_2 (from 0.0 to 1.2 mol/L) in the removal of Hg^0 present in a gas stream. It is worth noting that the Hg^0 removal efficiency was higher in the runs with smaller iron concentration whatever the hydrogen peroxide dose in the range tested (see Fig. 2.4). Wei *et al.* (2012) studied the influence of catalyst dose in range of 0.25 to 2.5 mM and achieved an optimal iron dose of 2.0 mM for the removal of methane (~25 %).

The reduction of the iron concentration (or iron use) is quite important because one major disadvantage of the Fenton process is the generation of iron sludge (that must withdraw at the process end by precipitation and clarification). Still, in case of the BCR, an excess of this sludge can promote the clogging of the gas diffuser. However, the use of heterogeneous matrices (i.e., solid supports like zeolites, activated carbons, clays, etc.) where the catalyst can be supported without being leached into the solution is another strategy that has been extensively studied in recent years to avoid the formation of sludge and loss of catalyst. Nevertheless, application to BCRs has not yet been reported, being a topic worth of studying.

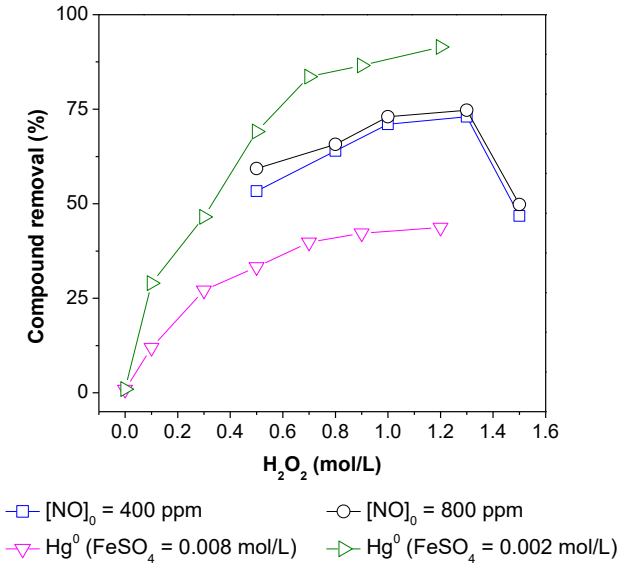

Figure 2.4 Effect of H_2O_2 concentration on NO removal efficiency (T = 323 K, pH = 2 and $FeSO_4$ = 0.05 mol/L (adapted from Guo *et al.* (2011)) and Hg^0 removal (Hg^0 inlet = 40 µg/m^3, O_2 = 6.0 %, CO_2 = 12.0%, SO_2 = 1000 ppm, NO = 400 ppm, T = 55 °C, pH = 3.4 and gas flow rate = 800 mL/min) (adapted from Liu *et al.* (2015b)) by the Fenton reaction realized in a BCR.

2.4.2.5 Influence of the gas flow rate

The gas flow rate has also an important effect in the compounds removal, because the increase of the gas flow rate decreases the residence time of the bubbles in the liquid phase, and consequently decreases the mass transfer of pollutants from one phase to the other. This factor was observed in the study of Liu *et al.* (2015b) where the gas flow rate was changed from 0.4 to 2.0 L/min, decreasing the Hgº removal, whatever the H_2O_2 initial concentration (see Fig. 2.5). The authors report that by increasing the gas flow rate the gas bubbles movement is faster, not favoring the gas-liquid contact. However, it is also reasonable to consider that stripping of the oxidant from the liquid phase could occur at high gas flow rates.

The number of studies dealing with the treatment of gas streams where the effect of the gas flow was taken into account is quite limited. This is a topic that could to be further exploited considering that it affects the bubbles size and the gas holdup, and inherently the process efficiency. Another aspect to be taken into account could be the properties of the liquid that influences the bubbles size, as mentioned above.

The effect of this parameter was however assessed in a couple of preliminary studies wherein the pollutant was present in the liquid phase, being the air stream used to simple promote the mixing of the liquid phase. It was found that the mixing was effective for all gas (air) flow rates evaluated - superficial velocities of nearly 40 to 200 m/s, pointing for

a good mixing efficiency in the BCR (Lima *et al.* 2017; Rodrigues *et al.* 2018). As previously discussed, the bubbling affected the hydrogen peroxide present in the medium and promoted stripping of nearly 40% of the oxidant. This fact did not compromise the hydroquinone degradation (which was 100%) (Lima *et al.* 2017).

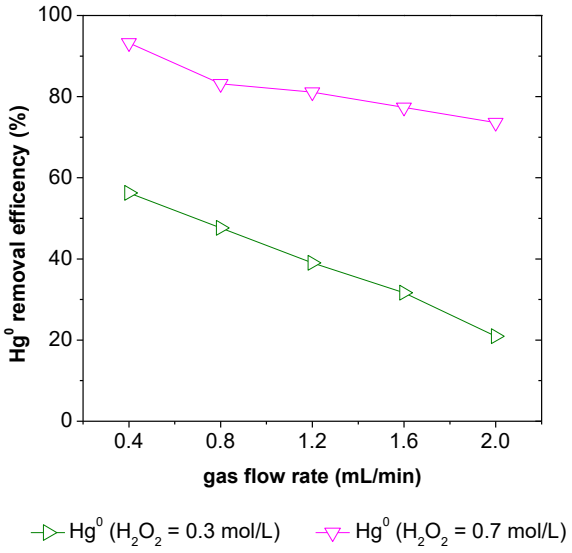

Figure 2.5 Effect of gas flow rate on Hg^0 removal efficiency by the Fenton process realized in a BCR (conditions: O_2 = 6.0%, CO_2 = 12.0%, SO_2 = 1000 ppm, NO = 400 ppm, T = 55 °C, pH = 3.4, Hg^0 inlet = 40 μg/m^3, Fe^{2+} = 0.008 mol/L) (adapted from Liu *et al.* (2015a)).

2.4.3 UV/H_2O_2

The use of UV (ultraviolet) radiation associated with hydrogen peroxide is described by various authors as an effective AOP to degrade some organic compounds. In this process the degradation of the organics can occur by direct photolysis, by the direct action of the oxidant (to a small extent although), or through reactions with hydroxyl radicals produced by the photolytic dissociation of the H_2O_2 molecules (Eq. 2.11) with radiation at λ < 300 nm (Hernandez 2002; Muruganandham *et al.* 2014).

$$H_2O_2 + hv \longrightarrow 2HO^{\bullet} \qquad (2.11)$$

This process was recently applied in a BCR for coal-fired flue gas treatment. Liu *et al.* (2010) studied the simultaneous removal of NO and SO_2 from a gas stream comprised by NO + SO_2 + O_2 + N_2 in a laboratory scale bubble reactor (0.40 m height and internal diameter 0.08 m). The simultaneous removal of these species is very important, because SO_2 and NO_2 are found together in atmospheric emissions. In the Liu *et al.* (2010) study the liquid stream (600 mL), containing H_2O_2 solution, was added to the BCR and then,

with the UV lamps turned on, the gas stream was added to the reactor continuously at a flow rate of 500 mL/min. The temperature of 298 K and pH 3.2 were kept constant in all experiments. Runs were carried out with three different reaction systems (UV, H_2O_2, UV/H_2O_2); results are shown in Fig. 2.6 as a function of time. The SO_2 removal efficiency was 100% in the three situations, while the efficiency of NO removal was strongly affected by the type of process used. Through photolysis (only UV light), the removal of NO was only about 3%, but increased up to 11% when the authors used hydrogen peroxide. This oxidant is known to have a low oxidation potential as compared with the hydroxyl radicals (Table 2.1) that are generated in the presence of hydrogen peroxide and radiation (Eq. 2.11). So, NO removal efficiency reached 72% in the UV/H_2O_2 system (Liu *et al.* 2010) – Fig. 2.6.

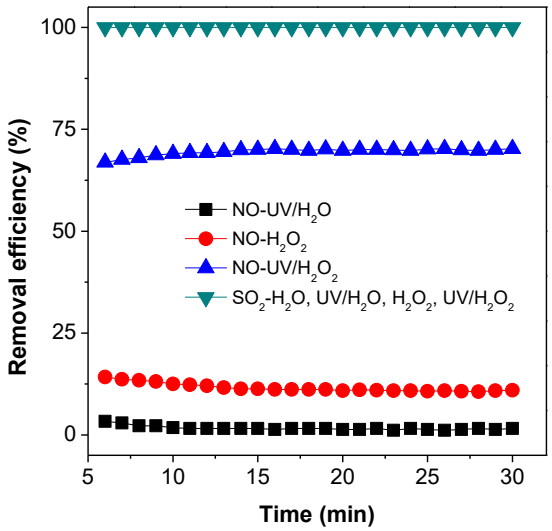

Figure 2.6 Removal efficiencies of NO and SO_2 for different reaction systems. Conditions: UV lamp = 36 W; $[NO]_0$ = 407 ppm; $[SO_2]_0$ = 978 ppm; $[H_2O_2]_0$ = 2.0 mol/L (adapted from Liu *et al.* (2010)).

This AOP is affected by several variables, and the effect of the most important are detailed in the next sections while providing a few examples in BCRs.

2.4.3.1 Effect of the hydrogen peroxide concentration

The hydrogen peroxide concentration is an important regulator of the UV/ H_2O_2 process as occurs in the Fenton reaction. In the study performed by Liu *et al.* (2010), the NO removal efficiency increased with the H_2O_2 concentrations till 1.5 mol/L and remained

nearly unchanged for a higher oxidant dose, while the SO_2 removal was always 100%, as can be seen in Fig. 2.7a.

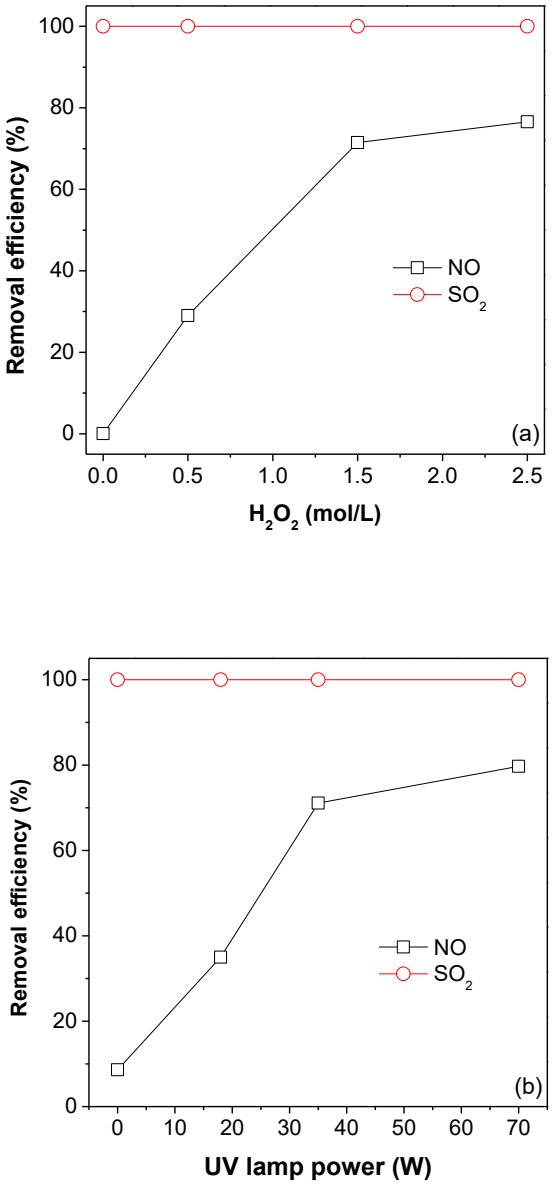

Figure 2.7 Removal efficiencies of NO and SO_2 under different H_2O_2 concentrations (a) and UV lamp powers (b) in the UV/H_2O_2 process (H_2O_2 concentration = 2.0 mol/L, NO = 419 ppm; and SO_2 = 948 ppm) (adapted from Liu *et al.* (2010)).

It is known that as a releasing agent of hydroxyl radicals, H_2O_2 plays a key role in this photochemical process. The effect of H_2O_2 concentration on the NO removal efficiency can be explained by the following reasons. Within a certain range, increasing the H_2O_2 concentration improves the yield of $HO^{\bullet}$ free radicals, as illustrated in Eq. (2.11), increasing the NO removal efficiency. However, when exceeding a certain value, further

increase of H_2O_2 concentration may cause side reactions, like the one shown in Eq. (2.7). So, the H_2O_2 is also the etchant of OH free radicals besides the releasing agent. The oxidation potential of the HO_2 free radicals (1.70 eV – Table 2.1) produced by this side reaction is much smaller than that of OH free radicals (2.80 eV – Table 2.1). Therefore, further increase of H_2O_2 concentration only has a slight impact on the NO removal efficiency.

2.4.3.2 Effect of the UV lamp power

Apart from the radiation type, the power also strongly influences the radiation-assisted H_2O_2 process since the energy generated accelerates the formation of hydroxyl radicals, which are responsible for oxidation of the compounds. However, this depends on the target compound, and operating conditions. In the study accomplished by Liu *et al.* (2010) the authors operated with a 36W UV lamp and as a result obtained a SO_2 (present in the gas phase) removal independent of the lamp power (Fig. 2.7b). In this case, even with the lamp off, 100% removal of the compound occurred (as a result of the mere addition of H_2O_2). However, for NO the lamp power interfered with the removal efficiency. With the lamp off, the NO removal was ~10.8% and the efficiency gradually increased up to the value of 72.5% with the 36 W. From 36 W to 70 W, the efficiency increased less significantly.

Under UV light irradiation, H_2O_2 releases $HO^{\bullet}$ free radicals as described by Eq. (2.11), which, due to their high redox potential, have strong oxidation ability to remove NO by oxidation. Therefore, compared with the reaction system without UV light, the addition of UV light can greatly enhance NO removal. Furthermore, the photochemical reaction yield is proportional to the UV irradiation intensity (which is also proportional to UV lamp power), meaning that increasing UV lamp power can improve the energy density per unit in solution, producing more effective photons, and finally generate more ·OH free radicals (Liu *et al.* 2010). Therefore, the NO removal efficiency increased with the increase of UV lamp power. Nevertheless, when the UV lamp power exceeds a certain value, several side reactions, such as Eqs. (2.7) and (2.12), may be also caused in solution, leading to a great loss of ·OH free radicals. So, further increase of UV lamp power only has a little impact on NO removal efficiency (Liu *et al.* 2010).

$$HO^{\bullet}+HO^{\bullet}\rightarrow H_2O_2 \qquad (2.12)$$

There is a notorious amount of work regarding the UV/H_2O_2 application in liquids effluent treatment. However, the studies applied to treat gaseous streams and particularly in BCRs are still reduced.

2.4.4 Photo-Fenton

The photo-Fenton process is an improvement of the dark Fenton one by using UV-visible radiation. Thus, this AOP is faster and enables reducing the consumption of reagents as the hydroxyl radicals generation occurs by three different mechanisms: i) the decomposition of hydrogen peroxide with the Fe^{2+} catalyst – Fenton reaction (Eq. 2.4); ii) the incidence of ultraviolet radiation, with $\lambda < 360\text{-}365$ nm, decomposes the hydrogen peroxide into hydroxyl radicals (Eq. 2.11) (Galvez and Rodriguez, 2003) and iii) by using radiation with wavelengths in the range $290 < \lambda < 410$ nm (Sun and Pignatello 1993) there is the additional production of $HO^{\bullet}$ radicals upon Fe^{2+} regeneration either by Eq. 2.13 or by photolysis of iron (III) hydroxides (Eq. 2.14). Finally, it is worth mention in the overall mechanism the Eq. 2.15 bellow, which still refers to Fe^{2+} regeneration by photolysis of complexes formed between the organic compounds (or their intermediates) with Fe^{3+} (Galvez and Rodriguez 2003; Huang *et al.* 2008). The improved regeneration of Fe^{2+} species by several reactions is therefore another reason for the faster rate of the photo-Fenton process as compared to the dark one, where catalyst regeneration is commonly rate-limiting.

$$Fe^{3+}+H_2O+h\nu \rightarrow Fe^{2+}+HO^{\bullet}+H^{+} \quad (2.13)$$

$$Fe(OH)^{2+}+h\nu \rightarrow Fe^{2+}+HO^{\bullet} \quad (2.14)$$

$$[Fe(RCO_2]^{2+}+h\nu \rightarrow Fe^{2+} \quad (2.15)$$

The application of this AOP in a BCR has been employed in two reactor configurations: with the lamps being arranged externally to the reactor (Handa *et al.* 2013) or axially (internally) (Liu *et al.* 2015).

Handa *et al.* (2013) evaluated the toluene removal from a waste gas stream comprised of air and toluene in a medium-sized bubble column (1.40 m high and diameter of 0.098 m) by the photo-Fenton process using 3 UV lamps with 40 W each, emitting at 352 nm and arranged externally to the reactor. The process was conducted in semi-batch mode; the liquid portion, with a volume of about 7 L containing water and Fenton reagents, was added to the column and was operated in a batch way, while the gas stream containing air and toluene was added continuously to the column at a flow rate of 5 L/min. The values of temperature and toluene inlet concentration were kept constant at 298 K and 0.25 g/m^3, respectively. The authors found that the photo-Fenton reaction in the liquid-phase improved the overall toluene absorption rate by increasing the driving force for mass transfer; as a result, the removal of toluene from exhaust gas was enhanced (up to > 90%).

Just like in the Fenton reaction, operating conditions are essential for reaching good results on pollutants removal through photo-Fenton systems. Accordingly, the pH of the medium, the reaction temperature, the gas flow rate and the concentration of reactants (Fe^{2+} and H_2O_2) should always be taken into consideration, as well at the intensity of UV/vis radiation applied. The effects of the first variables were described above, in the Fenton section, while the effect of the radiation intensity in a BCR is exemplified herein below.

2.4.4.1 Effect of the UV lamp power

It is known that in the photo-Fenton process the UV light irradiation accelerates the iron redox cycle, which increases the degradation efficiency of pollutants through oxidation. In the study performed by Handa *et al.* (2013) it can be observed the effect of UV light intensity on the toluene degradation (present in the waste gas stream) in a BCR coupled with UV lamps. In this study, Handa *et al.* (2013) evaluated the degradation of 0.25 mg/L toluene at room temperature, at pH 3.0 with a concentration of 400 mg/L H_2O_2 and 10 mg/L of iron. For the tests it was chosen to vary the number of UV lamps connected during the reaction to assess the effect of increased UV irradiation intensity. It can be seen in Fig.2.8 that in the test where none of the lamps was turned on (simulating the dark Fenton reaction) the removal efficiency reached was 53%. However, by applying the radiation from only one lamp (40 W) it was obtained a removal of over 80% and this result was even (although slightly) improved by further increasing the amount of available radiation (2 and 3 lamps), reaching more than 90% removal of toluene. According to Handa *et al.* (2013), this result suggests that the iron redox cycle or generation of $HO^{\bullet}$ radicals occurred especially in the Fenton reaction stage. However, it was noted that the rate of the Fenton reaction (without UV lamps connected) is slower compared to the photo-Fenton reaction, as the reduction of iron (II) to iron (III) is accelerated in the presence of the lamps.

Tokumura *et al.* (2013) also applied the photo-Fenton process for the degradation of toluene present in waste gas in a bubble column. These authors evaluated the toluene degradation, the formation and degradation of intermediate compounds (benzaldehyde, p-cresol and acetic acid) and concluded that toluene degradation was around 93%. The authors present a dynamic model for the chemical-absorption process, which is able to satisfactorily predict the unsteady- and steady-state performance of the BCR. The authors consider the effect of several important variables (such as Fe dosage, hydrogen peroxide concentration and toluene concentration in the gas supply) but the effects of

solution pH and light intensity were not accounted. However, the effect of these parameters should be also taken into account for optimizing the process efficiency, whereby more studies are required.

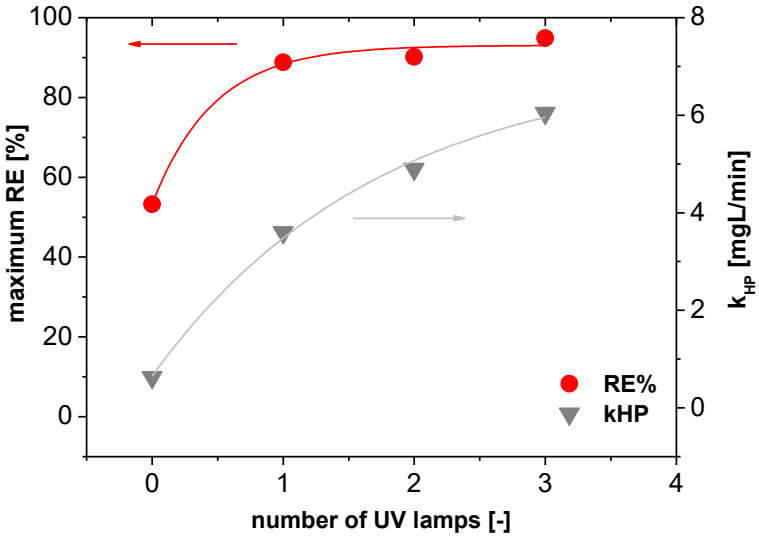

Figure 2.8 Effect of UV light intensity on the photo-Fenton degradation of toluene (maximum RE = maximum removal efficiency) and in the decomposition rate constant of H_2O_2 (k_{HP}) (toluene concentration = 0.25 mg/L, H_2O_2 = 400 mg/L, Fe_0 = 10 mg/L and pH_0 = 3.0) (adapted from Handa *et al.* (2013)).

2.4.5 Electro-Fenton

The electro-Fenton (E-Fenton) process is a technology that is based in the anodic and indirect electro-oxidation of the pollutants. Thus, the column structure must be adapted to contain a cathode and an anode. The mineralization of the compounds by the E-Fenton process occurs by three ways: i) by direct electro transfer reaction (Babuponnusami and Muthukumar 2014), ii) by the hydroxyl radicals formed on the electrode surface (Eq. 2.16) (Babuponnusami and Muthukumar 2014) and iii) by the hydroxyl radicals formed by the Fenton reaction (Eq. 2.4).

$$H_2O \rightarrow HO^{\bullet} + H^+ + e^- \qquad (2.16)$$

Other reactions occur at the same time, namely the electro-regeneration of Fe^{2+} through the reduction of ferric ions on the cathode (Eq. 2.17) and the electro-generation of hydrogen peroxide (Eq. 2.18) by supplying O_2 (or air) into the water (or liquid stream) (Brillas *et al.* 2009). In the application of the E-Fenton's reaction to treat a liquid stream in a BCR the oxygen, necessary for the electro-generation of the oxidant, is continuously

fed by the bottom of the column (Nidheesh and Gandhimathi 2015a). This continuous feeding also allows to promote stirring and mixing of the liquid.

$$Fe^{3+}+e^{-}\rightarrow Fe^{2+} \quad (2.17)$$

$$O_2+2H^{+}+2e^{-}\rightarrow H_2O_2 \quad (2.18)$$

Like the Fenton or photo-Fenton, the E-Fenton process was not extensively studied in BCRs; some examples are shown in Table 2.4. A few studies were reported in the literature that assessed the treatability of real textile wastewater (Nidheesh and Gandhimathi 2015b), an effluent containing Rhodamine B (Nidheesh and Gandhimathi 2015a), and Lissamine Green and Azure B (Rosales *et al.*, 2009) dyes. It is also worth highlighting one study about the E-Fenton applied in a hybrid process with bioremediation for the degradation of green table olive wastewater (Kyriacou *et al.* 2005), showing the importance of this technology in coupled processes. Still in this perspective, Díez *et al.* (2017) assessed the E-Fenton process effect in the removal of two pesticides (pyrimethanil and pirimicarb) and in the treatment of real winery wastewater in a sequential two-column electro-Fenton/photolytic reactor.

Like in other AOPs, previously discussed, the efficiency of the liquid effluent treatment by the E-Fenton process is governed by several parameters. Below is addressed the effect of some of them, namely the materials used for making the electrodes, the pH and the operation mode.

2.4.5.1 Effect of the materials used for making the electrodes

Differently of the other AOPs, the E-Fenton has a major dependence on the type of material used for making the electrodes. These materials are entirely responsible for the efficiency of the surface reactions; in addition, they have an important contribution in the total costs of the process once the materials commonly required are very expensive. Rosales *et al.* (2009) studied the effect of the materials (stainless steel, graphite, platinum, PbO_2, titanium compounds, boron doped diamond, and ceramics) used for making the electrodes in the discoloration of the Lissamine Green B, Methyl Orange, Reactive Black 5 and Fuchsin Acid dyes. The results obtained by the authors show that the materials selected have an important effect in the reaction time; for example, >99% of Lissamine Green B dye removal was reached after 10 or 40 h of E-Fenton reaction (see conditions in Table 2.4) when using electrode bars made of graphite or stainless steel, respectively. These reaction times were very long, which potentially makes the treatment process expensive due to a high energy consumption.

Table 2.4 Examples of applications of the electro-Fenton process in the treatment of effluents in BCRs.

Effluent/Compound	Reactor characteristics	Operation conditions	Removals (%)	Ref.
Dyes (Lissamine Green, Reactive Black 5 and Methyl Orange)	Model: glass cylindrical reactor Diameter and height: not specified Anode (mm) = 270 Cathode (mm) = 30	pH = 2-5 Voltage (V) = 15 Iron (mg/L) = 150 Air flow rate (L/min) = 1 Residence time (h) = 21	Lissamine Green = 80 Reactive Black 5 = 60 Methyl Orange = 80	(Rosales *et al.* 2009)
Pesticides (pyrimethanil and pirimicarb) and winery wastewater	Model: sequential two-column reactor (hybrid-process with UV-LED radiation) Anode area (m^2) = 0.0018 Cathode area (m^2) = 0.0024 LED Lamp (W) = 40	pH = 2 Voltage (V) = 5 Iron (mg/L) = 75 Air flow rate (L/min) = 0.5	Pesticides = 97 Winery wastewater: TOC = 67 COD = 77 IC_{50} = 76.5	(Díez *et al.* 2017)
Rhodamine B	Model: bubble column reactor Height (m) = 0.4 Diameter (m) = 0.104 Anode area (m^2) = 0.0080 Cathode area (m^2) = 0.01	pH = 3 Voltage (V) = 2-4 Iron (mg/L) = 2.5-5 Air flow rate (mL/min) = 5-15	Rhodamine B = 98	(Nidheesh and Gandhimathi 2015a)

Effluent/Compound	Reactor characteristics	Operation conditions	Removals (%)	Ref.
Textile wastewater	Model: bubble column reactor Diameter and height: not specified Anode area (m^2) = 0.008 Cathode area (m^2) = 0.01	pH = 2-4 Voltage (V) = 5 Iron (mg/L) = 2.5-7.5 Air Flow rate (mL/min) = 10	COD = 37 Color = 67.7	(Nidheesh and Gandhimathi 2015b)
Acid Orange 7 dye	Model: bubble column micro-reactor Diameter and height: not specified Anode and cathode: not specified	T (ºC) = 25 pH = 3 H_2O_2 con. (mM) = 0.5-0.6 Air flow rate (L/min) = 0.35 Water flow rate (mL/min) = 0.1 Current (A/m^2) = 10-500 Voltage (V) = 2.1-2.5	Color = 100 COD = ~80	(Scialdone *et al.* 2013)

The overall cost of the process increases with the reaction time, since the cost of energy is increased with the process duration; so, it is important to select electrodes with materials that allow high efficiencies to be obtained in short times. However, the initial investment needs to be also carefully accounted. Nidheesh and Gandhimathi (2015b) quantified the cost associated to the price of energy, electrode material (graphite plate) and catalyst (ferric chloride) and obtained 2.13 US$/g of COD (chemical oxygen demand) removed (for the removal of 400 mg/L of COD from textile wastewater), being an expensive treatment process.

2.4.5.2 Effect of the pH

Like in the Fenton process the pH has an important influence in the E-Fenton process, with slight differences. This effect was assessed in the study of Rosales *et al.* (2009) that evaluated its influence in the pH range of 2-5. The dye removal was better using pH = 2, with nearly 40% of the discoloration. For higher pH the authors observed a decrease in the removal being more accentuated until pH 4; at this pH the removal reached was only ~10 % after the 120 minutes of reaction. This decrease of the process efficiency is explained by the precipitation of iron (in the form of Fe^{3+}), consequently reducing the amount of dissolved iron available in the effluent to catalyze the process.

In the E-Fenton system proposed the authors advise the use of pH < 3 to improve the discoloration because the ferrous iron is continuously regenerated via reduction of Fe^{3+} in the cathode (Eq. 2.17).

2.4.5.3 Effect of the operation mode

Rosales *et al.* (2009) also evaluated in their work the possibility of operating the E-Fenton bubble reactor in continuous mode, using different liquid flow rates (that correspond to residence times of 5.5, 16 and 21 h) during Lissamine Green B, Methyl Orange and Reactive Black 5 removal. The authors concluded, from tracer experiments, that the hydrodynamic behavior of the BCR is such as an ideal continuous stirred tank reactor (CSTR). The discoloration of the dyes increased with the residence time. For Lissamine Green B and Methyl Orange a similar degree of degradation was reached (nearly 80% of discoloration in the run with 21 h of residence time). On the other hand, for Reactive Black 5 dye the removal obtained was lower (60%), for the same residence time.

2.4.6 Ozonation

The decomposition of ozone in aqueous solution has been studied by many researchers, being known that it generates $HO^{\bullet}$ species, especially when initiated with HO^- (Eqs. 2.19-2.25):

$$O_3+HO^-\rightarrow O_2+HO_2^- \quad (2.19)$$

$$HO_2^-+O_3\rightarrow O_3^{\bullet-}+HO_2^{\bullet} \quad (2.20)$$

$$HO_2^{\bullet}\leftrightarrow O_2^{\bullet-}+H^+ \quad (2.21)$$

$$O_2^{\bullet-}+O_3\rightarrow O_3^{\bullet-}+O_2 \quad (2.22)$$

$$O_3^{\bullet-}+H^+\leftrightarrow HO_3^{\bullet} \quad (2.23)$$

$$HO_3^{\bullet}\rightarrow HO^{\bullet}+O_2 \quad (2.24)$$

$$O_3+HO^{\bullet}\leftrightarrow O_2+HO_2^{\bullet} \quad (2.25)$$

Ozonation is considered an excellent form of effluents pre-treatment. For example, through this oxidation process, the organic compounds are converted into aldehydes, ketones or carboxylic acids (biodegradable forms) (Mondal and Bhagchandani 2016), the biological treatment being implemented downstream. Moreover, this technique can be coupled to other AOPs.

During the process, O_3 is transferred from the injected gas into the liquid phase (containing the pollutants to be degraded). In this process, in which the BCR operates more commonly in semi-batch mode, the gas-liquid contact occurs very often in an efficient manner, so that bubbles are dispersed in the liquid and end up favoring the mass transfer of ozone to this phase (Matheswaran and Moon 2009).

In this AOP, both ozone and $HO^{\bullet}$ species are present, but with different importance in the degradation of the compounds. Ozone is a very selective oxidant, while the $HO^{\bullet}$ radicals readily react with most contaminants in water (Von Gunten 2003). The later have also a higher oxidation potential than molecular ozone (Table 2.1). Depending on the type of compound with which ozone reacts, this reaction (that occurs in aqueous phase) can be classified in two ways: direct reaction (ozone reacts with the pollutant in its molecular state) and indirect reaction (the hydroxyl radical formation occurs through ozone decomposition and this radical is responsible for pollutants degradation) (Kordkandi and Ashiri 2015).

Advantages of using ozone in wastewater treatment are mostly related with the high selectivity of this molecule towards complex matrices such as mixed effluents, which

makes the application of this technology feasible for different types of effluents. Table 2.5 provides a summary of some ozonation studies carried out in BCRs. Some other examples are briefly addressed below.

Suh and Mohseni (2004) studied the relationship between biodegradability enhancement and oxidation of 1,4-dioxane using ozone and hydrogen peroxide in a laboratory scale BCR (1.60 x 0.10 m, height and diameter, respectively). One should note that the ozone injected in the reactor is produced in an ozone generator coupled to an O_2 generator. The ozone is injected into the reactor by the bottom of the column and the exhausted gas is captured at the top. In this particular experimental apparatus there is the recirculation of the liquid to be treated, which generates the necessity of an internal pressure control system. With the combination of oxidants, ozone and hydrogen peroxide, the authors were able to eliminate 1,4-dioxane and to enhance the biodegradability of dioxane-contaminated water.

BCRs have been used with O_3 for the treatment of different types of dyes, namely textile dyes. Turhan and Turgut (2009) studied the effect of many factors, such as initial pH of the dye solution, dye concentration, O_3 concentration and flow rate, in the decolorization of the direct dye Sirius Blue SBRR. Turhan *et al.* (2012) used a batch bubble column for textile dye (basic dye Methylene Blue, MB) treatment and obtained a COD reduction of more than 64% and complete MB dye degradation under basic conditions (pH 12) in 12 min.

Recently, Khuntia *et al.* (2016) used catalytic ozonation with Fe (II), Fe (III), Mn (II) and Cu (II) ions in a microbubble reactor operated in semi-batch mode for dyes degradation. In this study, the metal ions increased the decolorization efficiency of the azo dye, Congo Red (CR); the performance of the metal catalyst on the decolorization followed the order Fe(III) < Fe(II) < Mn(II) < Cu(II). It was evaluated the contribution of the hydroxyl radical, and it was obtained a total organic carbon (TOC) removal of 90% for 30-40 minutes of the O_3 reaction.

Other aromatic compounds were treated by ozonation combined with others AOPs (or oxidants) in BCRs. For instance, Monteagudo *et al.* (2005) studied the oxidation, by photo-Fenton-assisted ozonation, of p-coumaric acid, reaching a performance of 77% with the UV/Fenton/O_3 system, far better than with simple ozonation (4% only).

Table 2.5 Examples of the application of ozonation in the treatment of wastewater in bubble column reactors.

Effluent/Compound	Reactor characteristics	Operation conditions	Removals (%)	Ref.
1,4-dioxane	Model = bubble column reactor (with liquid recycle) Diameter (m) = 1.6 Height (m) = 0.1	pH = 5.8-11 T (ºC) = 20-25 H_2O_2 conc. (mg/L) = 0-120 O_3:H_2O_2 ratio (mol/mol) = 0-0.6 Liquid recycle flow rate (L/min) = 1	75	(Suh and Mohseni, 2004)
Acid anthraquinone	Model = semibatch bubble column Lab scale OzoMatic ozone generator	pH = 7.3 T (ºC) = 23 Dye conc. (mg/L) = 50-100 Ozone mass flow (g/h) = 0.32-1. 6	70	(Kordkandi and Ashiri, 2015)
Alkyl xanthates	Model = semi-batch bubble column reactor (with water recycle) Diameter (mm) = 700 Height (mm) = 45 Low-pressure Hg lamp	pH = 10 T (ºC) = 25 Alkyl xanthates conc. (mg/L) = 160 Ozone gas flow (L/min) = 0.4-3.0 Ozone mass flow (mg/min) = 14.7-125.9	97 (O_3) and 100 (O_3/UV)	(Fu *et al.*, 2015)
Azo dyes (Acid Red 27 and Orange II)	Model = ozonation column Diameter (m) = 0.15 Height (m) = 0.57 Ozone generator	pH (Orange II) = 5.0-9.0 pH (Acid Red 27) = 7.5 T (ºC) = 23.5 Gas flow rate (L/min) = 3.3 Gas velocity (m/h) = 11.3	98 (for both dyes)	(Silva *et al.*, 2009)

Effluent/Compound	Reactor characteristics	Operation conditions	Removals (%)	Ref.
Cork-processing water	Model = semi-batch bubble column reactor Diameter (m) = 0.1 Height (m) = 1	pH = 6.45 Ozone/oxygen mixture flow rate (L/min) = 1-5.4 Ozone range (mg/min) = 15-120 Water recycle (L/min) = 1	TOC and COD = 90	(Lan *et al.*, 2008)
Cyanide	Model = conventional bubble column reactor (counter-current flow regimen) Diameter (m) = 0.094 Height (m) = 2.4 Hole diameter (m) = 0.09 (porous plate) Oxidizing gas (oxygen–ozone mixture)	pH = 11 T (ºC) = 24 Gas velocity (mc/s) = 0.12 Liquid velocity (cm/s) = 1.32 Ozone conc. (mg/L) = 43-160	93	(Barriga-Ordonez *et al.*, 2006)
Drinking water	Model = bubble column reactor Diameter (mm) = 454 Height (mm) = 3550 Single pipe (gas distributor) Hole diameter (mm) = 6	T (ºC) = 20 Gas flow rate (m^3/s) = $1.04x10^{-4}$ Liquid flow rate (m^3/s) = 5.36×10^{-3} Ozone conc. (kg/m^3) = 0.148	100	(Muroyama *et al.*, 2005)
Dye	Model = microbubble generator (MBG) Diameter and height: not specified Corona discharge ozonator	pH = 3-9 Metal conc. (mM) = 0.2-1.0 Ozone range (mg/s) = 0-3 Ozone flow rate (mL/s) = 8-80	Dye = 100 TOC = 90	(Khuntia *et al.*, 2016)

Effluent/Compound	Reactor characteristics	Operation conditions	Removals (%)	Ref.
Olive mill wastewaters	Model = semi-batch cylindrical bubble column reactor Diameter (m) = 0.102 Height (m) = 1.84 Ozone generator	pH = 4.8 Ozone conc. (mg/L) = 10-70 Ozone flow rate (L/min) = 2	Decolorization = >80 Phenol = >80 COD = 10-60	(Karageorgos *et al.*, 2006)
Phenol wastewater	Model = bubble column reactor (counter current flow mode) Diameter (mm) = 75 Height (mm) = 300 Ozone generator	pH = 1.0-9.0 T (ºC) = 25 Phenol conc. (ppm) = 100-1000 Ozone flow rate (mL/min) = 25-250	Phenol = 100 TOC = 52	(Matheswaran and Moon, 2009)
p-Nitrophenol	Model = bubble column reactor Diameter (m) = 2.05 Height (m) = 0.11 Ozone generator	T (ºC) = 20 Pressure (kPa) = 101.325 Gas velocity (m/s) = 0.0164 Flow rate (cm^3/min) = 350-400 Ozone concentration (mol/dm^3) = 5.13×10^{-5} – 1.46×10^{-4}	100	(Kuosa *et al.*, 2007)
Pulp mill effluent	Model = semi batch bubble column reactor Diameter (m) = 0.1 Height (m) = 2 Ozone generator	pH = 4.5-11 Ozone conc. (mg/mL) = 0-0.8 Ozone flow rate (mL/min) = 185-280	TOC = 50	(Bijan and Mohseni, 2005)

Effluent/Compound	Reactor characteristics	Operation conditions	Removals (%)	Ref.
Reactive Orange 122	Model = electrochemical ozone reactor Diameter and height: not specified	pH = 4.5 and 12.0 T (ºC) = 30 Ozone flow rate (g/h) = 0.25	TOC ≥ 70	(Santana *et al.*, 2009)
Tannery effluent	Model = bubble column reactor Diameter (m) = 0.085 Height (m) = 1.25 Lab-scale ozone generator	pH = 3-12 Ozone flow rate (g/h) = 3	Color = 98 COD = 34.9	(Srinivasan *et al.*, 2012)
Sirius Blue SBRR dye	Model = bubble column reactor Diameter (m) = 0.05 Height (m) = 1.10 Fischer 502 ozone generator	pH = 2-12 T (ºC) = 20 Dye conc. (mg/L) = 100-800 Ozone conc. (g/m^3) = 4-24 Ozone flow rate (L/h) = 120	Color = 91.2	(Turhan and Turgut, 2009)
Methylene Blue dye	Model = glass bubble column reactor Diameter (m) = 0.05 Height (m) = 1.10 Fischer 502 ozone generator	pH = 2-12 T (ºC) = 20 Dye conc. (mg/L) = 50–600 Ozone conc. (g/m^3) = 4.2-24 Ozone flow rate (L/h) = 120	COD = 65 Dye = 100	(Turhan *et al.*, 2012)
Textile wastewater	Model: bubble column contactor with ultrasound Diameter (m) = 0.10	pH = 3.7-10.2 Ozone dosage (g/h) = 2.4-9 Ultrasound (W) = 500-1000	Color = 98	(Grande *et al.*, 2017)

Effluent/Compound	Reactor characteristics	Operation conditions	Removals (%)	Ref.
	Height (m) = 3.50 Counter-current flow (gas-liquid)	Ozone flow rate (L/h) = 100		
Winery wastewater	Model: semi-batch bubble-column reactor Diameter (m) = 0.1 Height (m) = 1 quartz UV-lamp tube	pH = 4-10 COD:H_2O_2 ratio (w/w) = 1-4 Water recirculation flow rate (L/min) = 1 Ozone flow rate (L/min) = 3.6	TOC = 88 (t = 300 min)	(Lucas *et al.*, 2010)

In order to use ozone at an industrial scale it is necessary to take into account the energy cost involved in its production. Matheswaran and Moon (2009) warn about its production cost. Therefore, alternative techniques coupled to ozonation should be considered as they can help reducing the consumption of O_3, thus favoring increased oxidation of organics at smaller costs.

Among the various forms of application of ozone in effluent treatment, the photolysis of dissolved ozone should be highlighted since it generates directly hydroxyl radicals through the following reactions (Eq. 2.26 and 2.27) (Legrini *et al.* 1993; Lucas *et al.* 2010):

$$H_2O+O_3+h\nu \rightarrow O_2+H_2O_2 \quad (2.26)$$

$$H_2O_2+2O_3 \rightarrow 3O_2+2HO^{\bullet} \quad (2.27)$$

In this process, the liquid, saturated with ozone, is irradiated with ultraviolet light (Guittonneau *et al.* 1990), which results in the generation of hydroxyl radicals in the medium.

Some factors must be taken into account when using ozonation in bubble columns for effluents treatment. These factors eventually limit the operational issues and the reactions involved in the oxidative process. Following some of these factors are briefly presented.

2.4.6.1 Effect of initial pH

The pH has a different effect in the ozonation as compared to other AOPs that are based in the use of H_2O_2 for wastewater treatment (such as the Fenton's one). In the Fenton process, the optimal range of pH is in the acidic range; in the ozonation, at very acidic conditions (pH = 2) it is observed the slow decomposition of O_3 for formation of $HO^{\bullet}$ species, which raises under reactions conditions of higher pH (Buffle *et al.* 2006). However, in strong alkaline medium (pH > 10) the efficiency of the process decays due to the decomposition of the hydroxyl radicals formed in the liquid medium (Kang *et al.* 2008).

Matheswaran and Moon (2009) studied the effect of pH in the ozonation of phenol wastewater in a bubble column (in counter current flow mode) with recirculation, and the results are shown in Fig. 2.9. In this study, the authors evaluated the effect of initial pH (1-9) on the TOC removal for a phenol-containing solution (500 ppm) and with ozone flow rate of 100 mL/min. A positive effect of increasing pH (alkalinization trend) has been

observed in the TOC removal in the conditions of the study. In comparison with the assay under the same conditions at pHs = 1-6, there was an increase in TOC removal at pH = 9, where removal at the end of 4 hours was over 70%, in line with the comment made above. In fact, unlike what happens in the Fenton reaction, where the H_2O_2 tends to decompose in an alkaline pH, the molecule of ozone does not suffer from this effect. On the contrary, the process is improved for basic conditions as can be anticipated from the mechanism illustrated in Eqs. 2.19-2.25.

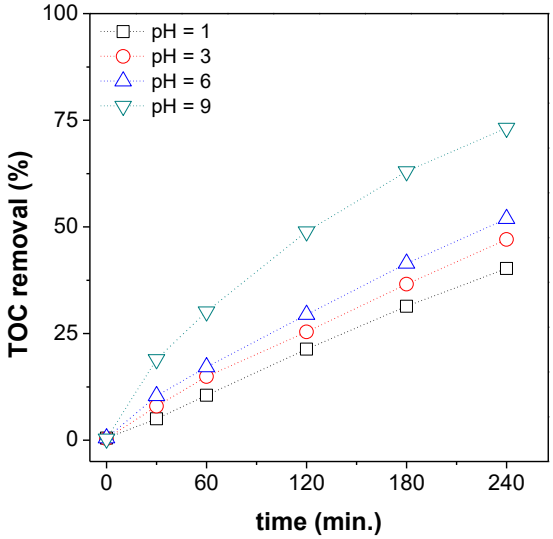

Figure 2.9 Percentage removal of TOC for destruction of phenol by ozonation at different pHs (O_3 flow rate = 100 mL/min and phenol = 500 ppm) (adapted from Matheswaran and Moon (2009)).

Lucas *et al.* (2010) studied the oxidation of winery wastewater and evaluated the influence of the initial pH (in the range 4-10) on the ozonation of the effluents after 300 minutes of reaction. The results point to the same conclusion as in the study by Matheswaran and Moon (2009), because at higher pH (pH = 10) the TOC removal percentage increased.

Turhan and Turgut (2009) evaluated the effect of the initial pH (2-12) in their study about the ozonation of a direct dye (Sirius Blue SBRR) and came to a similar conclusion. It was observed that the decolorization time decreased with increasing initial pH, changing from about 24 minutes at pH 2 to about 12 minutes at pH 12, representing a decrease of ca. 50% in the reaction time, which is characterized as an operational and energetic gain. It is also noteworthy that the decolorization time was only slightly reduced between pH 10 and 12. This indicates that a very strong alkalization of the medium is not required.

2.4.6.2 Effect of ozone concentration and flow rate

Kordkandi and Ashiri (2015) studied the oxidation of anthraquinone acid (AG25) using ozone and assessed the effect of the increased ozone flow rate (from 0.32 to 1.4 g/h) on the degradation of AG25 (initial concentration of 100 mg/L). The results are shown in Fig. 2.10, illustrating the values of color removal percentage (decolorization efficiencies) versus applied O_3 flow rate (g/h). It is possible to observe an increase in the decolorization efficiency values with the increase of O_3 flow rate, which were higher than 70% for the highest O_3 flow rate studied (1.4 g/h). The authors suggest that with increasing flow rate in the reactor more O_3 bubbles are formed favoring the mass-transfer to the liquid solution. This ultimately facilitates the chemical oxidation of the AG25 dye (Kordkandi and Ashiri 2015). Thus, control of oxidant flow injected into the column must be taken into consideration, of course having the opposite effect as compared with the case where the pollutant and oxidant are in opposite phases (cf. Fig. 2.5).

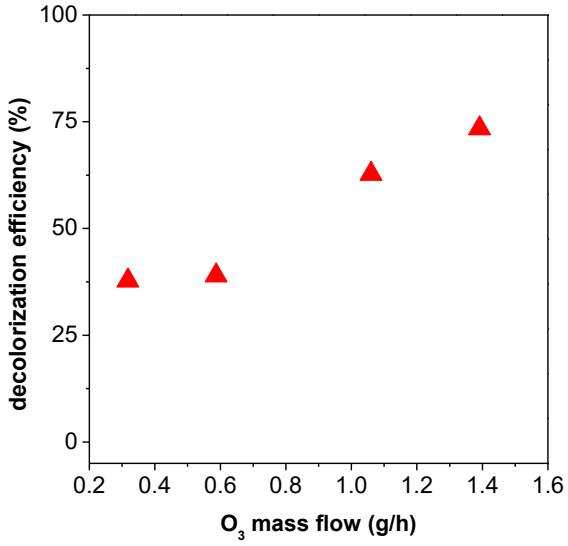

Figure 2.10 Effect of ozone mass flow rate in the decolorization efficiency of AG25 dye (t = 3 min, dye concentration = 100 mg/L) (adapted from Kordkandi and Ashiri (2015)).

Matheswaran and Moon (2009) investigated the effect of ozone flow rate in the oxidation of phenol in a bubble column. By working with a phenol concentration of 500 ppm and pH = 6, these authors evaluated different O_3 flow rates (25-250 mL/min) as shown in Fig. 2.11. As expected, it was observed that a higher ozone flow rate favors the TOC and the

phenol removal rate during the reaction. The TOC removal after 4 hours of reaction varied from about 5% in the test with 25 mL/min to a value near 70% in the test with 250 mL/min of ozone flow rate (Fig. 2.11a). The same trend is found for phenol removal, which was complete in 2 hours of reaction for the flow rate of 250 mL/min (Fig. 2.11b), meaning that the oxidation of phenol was effective in the conditions studied.

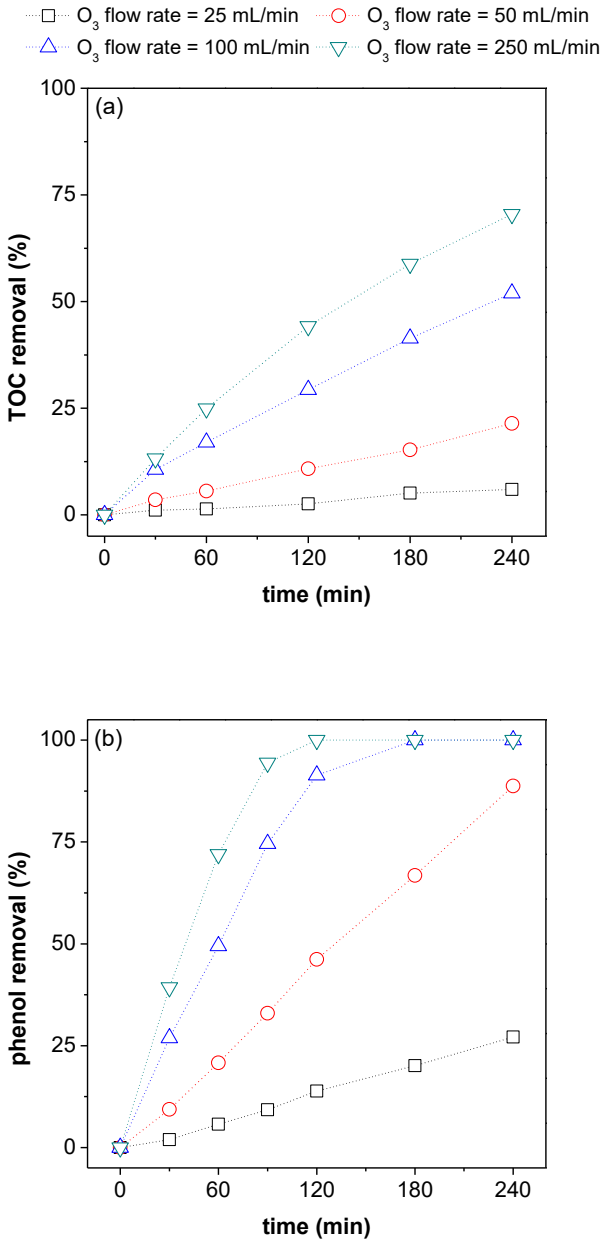

Figure 2.11 Effect of ozone flow rate on the removal of TOC (a) and phenol (b) with reaction time (phenol = 500 ppm and pH = 6) (adapted from Matheswaran and Moon (2009)).

The knowledge acquired from the amount of studies applying the ozonation process in liquid effluents treatment in BCRs shows the need to evaluate the effect of gas flow rate

on the process efficiency. Nevertheless, the studies previously discussed do not normally evaluate the effect on the hydrodynamics a topic that also deserves further attention by the community working in this thematic. Moreover, it would be convenient to have more info enabling fast estimates of the mass transfer, to see if it is rate-limiting. In such circumstances, one should act and improve the mass transfer itself, to improve overall process efficiency.

2.4.6.3 Effect of UV light application

As in the UV/H_2O_2 and photo-Fenton processes, ozone can be combined with UV radiation to improve the removal of the recalcitrant compounds present in the effluents. Below are provided a couple of examples.

Lucas *et al.* (2010) studied the treatment of a winery effluent by ozonation with a hybrid processes (O_3/UV and O_3/UV/H_2O_2) and compared with O_3 per se and UV light only in a pilot-scale BCR (operation conditions are described in Table 2.5). The treatment performances were analyzed in terms of reducing the COD. It was found that the direct photolytic action of UV-C radiation (200 to 280 nm) on the compounds dissolved in the winery wastewater was insignificant. Ozonation reduced the initial COD by 12% and the combination of UV-C radiation and ozonation removed 21% of COD, after 180 min of reaction. Such improved performance can be attributed to the generated hydroxyl radicals, as described in Eq.2.26 and 2.27. However, the combination of ozone, with hydrogen peroxide and UV radiation facilitates the treatment of the effluent by reducing further the COD (35% after 3 hours of reaction).

Still regarding the application of O_3/UV, Chen *et al.* (2007) achieved, using this process, 94% of mineralization during dinitrotoluene (DNT) isomers and 2,4,6-trinitrotoluene (TNT) degradation. According to these authors, the use of the UV lamp (96 W), with 3.8 g/h of O_3, improved the efficiency of the process (it was reached 76.4% of TOC removal). This demonstrates that some of these coupled technologies can provide excellent results and should be seen as complementary, although for every case different strategies have to be considered.

2.5 Future perspectives

The treatment of gaseous and liquid streams by AOPs in BCRs was reported in this review. A gap found in the main studies reported in the open literature about this topic is the lack of analysis focused on the assessment of the hydrodynamic and other aspects

closely related with the bubble column itself and the effect it may have in the process efficiency. So, it is strongly recommend to assess the influence of issues like the bubble size, gas holdup, the regime of operation, the gas (and/or liquid) flow rate and their effects in the mass transfer coefficient, and consequently how they impact the efficiency of the treatment process. Such information can be obtained experimentally and/or estimated using correlations available. Moreover, CFD tools have been applied successfully in many bubble column systems and may be useful to improve and better understand BCRs as well.

The application of processes with UV radiation (e.g. photo-Fenton and UV/H_2O_2) discussed in this review show the feasibility of their use in BCRs. Particularly, they revealed to be effective and an alternative to consider as compared to more conventional ones employed in gaseous effluents treatment (e.g. absorption), because instead of a simple transfer of the pollutants from one phase (gas) to another (liquid), their destruction is carried out. However, future studies in this topic will have to be directed towards the reduction of treatment costs, a crucial factor for their industrial application. This cost reduction can be achieved using solar radiation, a technology already used in the treatment of liquid effluents in a conventional reactor (Klavarioti *et al.* 2009).

In general, the studies presented in this review have reported degradation of pollutants by AOPs in BCRs operating in the semi-bath mode (with feeding of the liquid phase in discontinuous mode and of the gas phase in continuous mode). However, for industrial application it is mandatory to design and operate bubble columns working in continuous mode (with continuous feeding of both streams), meeting the demand of the process with the generation of decontaminated liquid and/or gas streams. In this perspective, it is not difficult to conceive alternative strategies for operating new reactors, which must be tested and subsequently optimized. For instance, a continuous Fenton-based BCR to treat simultaneously gas and liquid streams, or an ozone-fed unit to treat pollutants present in gas and liquid streams. In the perspective of process integration, these units could provide several advantages in industrial applications, due to the utilization of only one device, therefore shortening the number of process units. After proof of the concept at lab scale, their scale-up should be considered.

Another aspect that was already addressed above and that deserves to be further explored in future works is the integration of BCRs with structured catalytic systems (e.g., use of Fenton catalysts supported over monolithics structures, similar to those used, although scarcely, in ozonation).

2.6 Conclusions

The technical choices to accomplish an AOP in any reactor (and particularly in a BCR) should be based on the knowledge regarding the influence of the operational parameters like temperature, pH, doses of chemicals, flow rate, nature and intensity of external radiation (if used), etc. This review summarizes the most important ones, for different systems.

Fenton, photo-Fenton and UV/H_2O_2 are mostly used in BCRs in the treatment of pollutants present in the gas phase with the oxidation reactions occurring in the aqueous phase, indicating that the mass transfer process between the gas (bubbles) and the liquid should be efficient enough. However, it would still be important to evaluate the effect of the bubble size, gas holdup and gas velocity, e.g., as a strategy for optimizing and extrapolating these processes to industrial scale.

Another process addressed to treat liquid effluents in BCRs was E-Fenton; however, this technology has not yet been exhaustively studied. Nevertheless, the studies reported were enough to prove the efficiency of this AOP when performed in a BCR, although a lot research has yet to be carried out with other pollutants/effluents to optimize the treatment process, and to assess the hydrodynamic factors of the column in the treatment efficiency.

For effluents containing organic compounds in liquid phase, the more commonly applied AOP is based on ozonation, a well-known technique that has presented excellent results, due also to the efficiency of ozone mass transfer between the two phases. Moreover, this is a process already consolidated.

The studies reported in the literature show in general good and promising performances of the AOPs when performed in BCRs. Although some aspects still need to be better comprehended and explored (as detailed in the previous section), it is expectable that these technologies can in the short term be scaled-up from lab- or pilot-scale to the industrial one.

2.7 References

Abtahi, M., K. Naddafi, A. Mesdaghinia, K. Yaghmaeian, R. Nabizadeh, N. Jaafarzadeh, N. Rastkari, S. Nazmara, and R. Saeedi. 2014. 'Removal of Dichloromethane from Waste Gas Streams Using a Hybrid Bubble Column/Biofilter Bioreactor'. *Journal of Environmental Health Science and Engineering* 12 (1): 1–7.

Adkins, D.R., K.A. Schollenberger, T.J. O'Hern, and J.R. Torczynski. 1996. 'Pressure Effects on Bubble-Comumn Flow Characteristics'. In *National Heat Transfer Conference, Instrumentation an Measurements Symposium*, 1–15.

Akita, K., and F. Yoshida. 1973. 'Gas Holdup and Volumetric Mass Transfer Coefficient in Bubble Columns. Effects of Liquid Properties'. *Industrial & Engineering Chemistry Process Design and Development* 12 (1): 76–80.

Ayed, L., N. Asses, N. Chammem, N. B. Othman, and M. Hamdi. 2017. 'Advanced Oxidation Process and Biological Treatments for Table Olive Processing Wastewaters: Constraints and a Novel Approach to Integrated Recycling Process: A Review'. *Biodegradation* 28 (2–3): 125–38.

Babuponnusami, A., and K. Muthukumar. 2014. 'A Review on Fenton and Improvements to the Fenton Process for Wastewater Treatment'. *Journal of Environmental Chemical Engineering* 2 (1): 557–72.

Bagal, M. V., and P. R. Gogate. 2014. 'Ultrasonics Sonochemistry Wastewater Treatment Using Hybrid Treatment Schemes Based on Cavitation and Fenton Chemistry : A Review'. *Ultrasonics - Sonochemistry* 21 (1): 1–14.

Barb, W. G., J. H. Baxendale, P. George, and K. R. Hargrave. 1951a. 'Reactions of Ferrous and Ferric Ions with Hydrogen Peroxide. Part II.—The Ferric Ion Reaction'. *Trans. Faraday Soc.* 47 (0): 591–616.

Barb, W. G., J. H. Baxendale, P. George, and K. R. Hargrave.. 1951b. 'Reactions of Ferrous and Ferric Ions with Hydrogen Peroxide. Part II. - The Ferric Ion Reaction'. *Trans. Faraday Soc.* 47 (0): 591–616.

Barriga-Ordonez, F., F. Nava-Alonso, and A. Uribe-Salas. 2006. 'Cyanide Oxidation by Ozone in a Steady-State Flow Bubble Column'. *Minerals Engineering* 19 (2): 117–22.

Behkish, A., Z. Men, J. R. Inga, and B. I. Morsi. 2002. 'Mass Transfer Characteristics in a Large-Scale Slurry Bubble Column Reactor with Organic Liquid Mixtures'. *Chemical Engineering Science* 57 (16): 3307-3324.

Besagni, G., and F. Inzoli. 2016. 'Influence of Internals on Counter-Current Bubble Column Hydrodynamics: Holdup, Flow Regime Transition and Local Flow Properties'. *Chemical Engineering Science* 145 (May): 162–80.

Bijan, L., and M. Mohseni. 2005. 'Integrated Ozone and Biotreatment of Pulp Mill Effluent and Changes in Biodegradability and Molecular Weight Distribution of Organic Compounds'. *Water Research* 39 (16): 3763–72.

Boczkaj, G., and A. Fernandes. 2017. 'Wastewater Treatment by Means of Advanced Oxidation Processes at Basic PH Conditions: A Review'. *Chemical Engineering Journal* 320 (July): 608–33.

Bokare, A. D., and W. Choi. 2014. 'Review of Iron-Free Fenton-like Systems for Activating H2O2 in Advanced Oxidation Processes'. *Journal of Hazardous Materials* 275 (June): 121–35.

Brillas, E., I. Sirés, and M. A. Oturan. 2009. 'Electro-Fenton Process and Related Electrochemical Technologies Based on Fenton's Reaction Chemistry'. *Chemical Reviews* 109 (12): 6570–6631.

Chen, W, C Juan, and K Wei. 2007. 'Decomposition of Dinitrotoluene Isomers and 2,4,6-Trinitrotoluene in Spent Acid from Toluene Nitration Process by Ozonation and Photo-Ozonation'. *Journal of Hazardous Materials* 147 (1–2): 97–104.

Cheng, L., T. Li, T.C. Keener, and J.Y. Lee. 2013. 'A Mass Transfer Model of Absorption of Carbon Dioxide in a Bubble Column Reactor by Using Magnesium Hydroxide Slurry'. *International Journal of Greenhouse Gas Control* 17 (September): 240–49.

Clarizia, L., D. Russo, I. Di Somma, R. Marotta, and R. Andreozzi. 2017. 'Homogeneous Photo-Fenton Processes at near Neutral PH: A Review'. *Applied Catalysis B: Environmental* 209 (July): 358–71.

Degaleesan, S., M. Dudukovic, and Y. Pan. 2001. 'Experimental Study of Gas-Induced Liquid-Flow Structures in Bubble Columns'. *AIChE Journal* 47 (9): 1913–31.

Dewes, I., A. Kuksal, and A. Schumpe. 1995. 'Gas-Density Effect on Mass-Transfer in 3-Phase Sparged Reactors'. *Chemical Engineering Research & Design* 73 (6): 697–700.

Díez, A. M., M. A. Sanromán, and M. Pazos. 2017. 'Sequential Two-Column Electro-Fenton-Photolytic Reactor for the Treatment of Winery Wastewater'. *Environmental Science and Pollution Research* 24: 1137–1151.

Fenton, H.J.H. 1894. 'LXXIII.—Oxidation of Tartaric Acid in Presence of Iron'. *Journal of*

the Chemical Society, Transactions 65: 899–910.

Ferreira, A., P. Cardoso, J. A. Teixeira, and F. Rocha. 2013. 'PH Influence on Oxygen Mass Transfer Coefficient in a Bubble Column. Individual Characterization of KL and A'. *Chemical Engineering Science* 100: 145–52.

Fu, P., J. Feng, T. Yang, and H. Yang. 2015. 'Comparison of Alkyl Xanthates Degradation in Aqueous Solution by the O3 and UV/O3 Processes: Efficiency, Mineralization and Ozone Utilization'. *Minerals Engineering* 81 (October): 128–34.

Fukuma, M., K. Muroyama, and A. Yasunishi. 1987. 'Properties of Bubble Swarn in a Slurry Bubble Column'. *Journal of Chemical Engineering of Japan* 20 (1): 28–33.

Furusaki, S., J. Garside, and L. S. Fan. 2002. *The Expanding World of Chemical Engineering*. Edited by S. Furusaki, J. Garside, and L. S. Fan. Second. New York: Taylor & Francis.

Galvez, J.B., and S.M. Rodriguez. 2003. *Solar Detoxification*. Paris: UNESCO.

Garcia-Segura, S., L. M. Bellotindos, Y.-H. Huang, E. B., and M.-C. Lu. 2016. 'Fluidized-Bed Fenton Process as Alternative Wastewater Treatment Technology—A Review'. *Journal of the Taiwan Institute of Chemical Engineers* 67 (October): 211–25.

Gogate, P. R., and A. B. Pandit. 2004. 'A Review of Imperative Technologies for Wastewater Treatment II: Hybrid Methods'. *Advances in Environmental Research* 8 (3–4): 553–97.

Gómez-Díaz, D., and J.M. Navaza. 2016. 'CO2 Continuous Removal Using Ion Exchange as Regeneration Process'. *Fuel* 180 (September): 27–33.

Grande, G. A., G. Rovero, S. Sicardi, and M. Giansetti. 2017. 'Degradation of Residual Dyes in Textile Wastewater by Ozone: Comparison between Mixed and Bubble Column Reactors'. *Canadian Journal of Chemical Engineering* 95 (2): 297–306.

Guittonneau, S., J. De Laat, J.P. Duguet, C. Bonnel, and M. Doré. 1990. 'Oxidation of Parachloronitrobenzene in Dilute Aqueous Solution by O_3 + UV and H_2O_2 + UV: A Comparative Study'. *Ozone: Science & Engineering* 12 (1): 73–94.

Gunten, U. V. 2003. 'Ozonation of Drinking Water: Part I. Oxidation Kinetics and Product Formation'. *Water Research* 37 (7): 1443–67.

Guo, R. T., W. G. Pan, X. B. Zhang, J. X. Ren, Q. Jin, H. J. Xu, and J. Wu. 2011. 'Removal of NO by Using Fenton Reagent Solution in a Lab-Scale Bubbling Reactor'. *Fuel* 90 (11): 3295–98.

Handa, M., Y. Lee, M. Shibusawa, M. Tokumura, and Y. Kawase. 2013. 'Removal of VOCs in Waste Gas by the Photo-Fenton Reaction: Effects of Dosage of Fenton Reagents on Degradation of Toluene Gas in a Bubble Column'. *Journal of Chemical Technology & Biotechnology* 88 (1): 88–97.

He, H., and Z. Zhou. 2017. 'Electro-Fenton Process for Water and Wastewater Treatment'. *Critical Reviews in Environmental Science and Technology*.

Hernandez, R., M. Zappi, J. Colucci, and R. Jones. 2002. 'Comparing the Performance of Various Advanced Oxidation Processes for Treatment of Acetone Contaminated Water'. *Journal of Hazardous Materials* 92 (1): 33–50.

Hsueh, H.T., C.L. Hsiao, and H. Chu. 2010. 'Removal of CO2 from Flue Gas with Ammonia Solution in a Packed Tower'. *Environmental Engineering and Management Journal* 20: 1–7.

Huang, Y.-H., Y.-F. Huang, P.-S. Chang, and C.-Y. Chen. 2008. 'Comparative Study of Oxidation of Dye-Reactive Black B by Different Advanced Oxidation Processes: Fenton, Electro-Fenton and Photo-Fenton'. *Journal of Hazardous Materials* 154 (1–3): 655–62.

Jesus, S. S. De, J. M. Neto, and R. M. Filho. 2017. 'Hydrodynamics and Mass Transfer in Bubble Column, Conventional Airlift, Stirred Airlift and Stirred Tank Bioreactors, Using Viscous Fluid: A Comparative Study'. *Biochemical Engineering Journal* 118 (February): 70–81.

Jhawar, A. K., and A. Prakash. 2012. 'Heat Transfer in a Slurry Bubble Column Reactor: A Critical Overview'. *Industrial & Engineering Chemistry Research* 51 (4): 1464–73.

Kang, Y., Y.J. Cho, K.J. Woo, and S.D. Kim. 1999. 'Diagnosis of Bubble Distribution and Mass Transfer in Pressurized Bubble Columns with Viscous Liquid Medium'. *Chemical Engineering Science* 54 (21): 4887–93.

Kantarci, N., F. Borak, and K. O. Ulgen. 2005. 'Bubble Column Reactors'. *Process Biochemistry* 40 (7): 2263–83.

Karageorgos, P., A. Coz, M. Charalabaki, N. Kalogerakis, N. P. Xekoukoulotakis, and D. Mantzavinos. 2006. 'Ozonation of Weathered Olive Mill Wastewaters'. *Journal of Chemical Technology and Biotechnology* 81 (9): 1570–1576.

Katoh, S., J. I. Horiuchi, and F Yoshida. 2015. *Biochemical Engineering: A Textbook for Engineers, Chemists and Biologists*. Edited by S. Katoh, J. I. Horiuchi, and F Yoshida. Second. Weinheim, Germany: John Wiley & Sons.

Kennes, C, and MC Veiga. 2013. *Bioreactors for Waste Gas Treatment*. Edited by C Kennes and MC Veiga. Vol. 4. Springer Science & Business Media.

Khuntia, S., S. K. Majumder, and P. Ghosh. 2016. 'Catalytic Ozonation of Dye in a Microbubble System: Hydroxyl Radical Contribution and Effect of Salt'. *Journal of Environmental Chemical Engineering* 4 (2): 2250–58.

Klavarioti, M., D. Mantzavinos, and D. Kassinos. 2009. 'Removal of Residual Pharmaceuticals from Aqueous Systems by Advanced Oxidation Processes'. *Environment International* 35 (2): 402–17.

Kordkandi, S. A., and R. Ashiri. 2015. 'Modeling and Kinetics Study of Acid Anthraquinone Oxidation Using Ozone: Energy Consumption Analysis'. *Clean Technologies and Environmental Policy* 17 (8): 2431–2439.

Krishna, R., and J. M. Van Baten. 2003. 'Mass Transfer in Bubble Columns'. *Catalysis Today* 79–80 (April): 67–75.

Kulkarni, A. V., and J. B. Joshi. 2011. 'Design and Selection of Sparger for Bubble Column Reactor. Part I: Performance of Different Spargers'. *Chemical Engineering Research and Design* 89 (10): 1972–85.

Kuosa, M., A. Laari, A. Solonen, H. Haario, and J. Kallas. 2007. 'Estimation of Multicomponent Reaction Kinetics of *p*-Nitrophenol Ozonation in a Bubble Column'. *Industrial & Engineering Chemistry Research* 46 (19): 6235–6243.

Kyriacou, A., K. E. Lasaridi, M. Kotsou, C. Balis, and G. Pilidis. 2005. 'Combined Bioremediation and Advanced Oxidation of Green Table Olive Processing Wastewater'. *Process Biochemistry* 40 (3–4): 1401–8.

Lafi, W. K., and Z. Al-Qodah. 2006. 'Combined Advanced Oxidation and Biological Treatment Processes for the Removal of Pesticides from Aqueous Solutions'. *Journal of Hazardous Materials* 137 (1): 489–97.

Lan, B. Yan, R. Nigmatullin, and G. L. Puma. 2008. 'Ozonation Kinetics of Cork-Processing Water in a Bubble Column Reactor'. *Water Research* 42 (10–11): 2473–82.

Lee, J., M. Yasin, S. Park, I.S. Chang, K.S. Ha, E.Y. Lee, J. Lee, and C. Kim. 2015. 'Gas-Liquid Mass Transfer Coefficient of Methane in Bubble Column Reactor'. *Korean Journal of Chemical Engineering* 32 (6): 1060–1063.

Legrini, O., E. Oliveros, and A.M. Braun. 1993. 'Photochemical Processes for Water Treatment'. *Chemical Reviews* 93 (2): 671–98.

Leonard, C., J.-H. Ferrasse, O. Boutin, S. Lefevre, and A. Viand. 2015. 'Bubble Column Reactors for High Pressures and High Temperatures Operation'. *Chemical Engineering Research and Design* 100 (August): 391–421.

Lima, V. N., C. S.D. Rodrigues, and L. M. Madeira. 2018. 'Application of the Fenton's Process in a Bubble Column Reactor for Hydroquinone Degradation'. *Environmental Science and Pollution Research* 25 (35): 34851–62.

Liu, G., H. Huang, R. Xie, Q. Feng, R. Fang, Y. Shu, Y. Zhan, X. Ye, and C. Zhong. 2017. 'Enhanced Degradation of Gaseous Benzene by a Fenton Reaction'. *RSC Adv.* 7 (1): 71–76.

Liu, Y. X., J. Zhang, and Y. Yin. 2015b. 'Removal of Hg^0 from Flue Gas Using Two Homogeneous Photo-Fenton-like Reactions'. *AIChE Journal* 61 (4): 1322–33.

Liu, Y., Y. Wang, Q. Wang, J. Pan, Y. Zhang, J. Zhou, and J. Zhang. 2015a. 'A Study on Removal of Elemental Mercury in Flue Gas Using Fenton Solution'. *Journal of Hazardous Materials* 292 (July): 164–72.

Liu, Y., J. Zhang, C. Sheng, Y. Zhang, and L. Zhao. 2010. 'Simultaneous Removal of NO and SO2 from Coal-Fired Flue Gas by UV/H_2O_2 Advanced Oxidation Process'. *Chemical Engineering Journal* 162 (3): 1006–11.

Lucas, M. S., J. A. Peres, and G. L. Puma. 2010. 'Treatment of Winery Wastewater by Ozone-Based Advanced Oxidation Processes (O_3, O_3/UV and O_3/UV/H_2O_2) in a Pilot-Scale Bubble Column Reactor and Process Economics'. *Separation and Purification Technology* 72 (3): 235–41.

Mantzavinos, D., and E. Psillakis. 2004. 'Enhancement of Biodegradability of Industrial Wastewaters by Chemical Oxidation Pre-Treatment'. *Journal of Chemical Technology and Biotechnology* 79 (5): 431–54.

Matheswaran, M., and Il S. Moon. 2009. 'Influence Parameters in the Ozonation of Phenol Wastewater Treatment Using Bubble Column Reactor under Continuous Circulation'. *Journal of Industrial and Engineering Chemistry* 15 (3): 287–92.

McClure, D. D., J. M. Kavanagh, D. F. Fletcher, and G. W. Barton. 2016. 'Characterizing Bubble Column Bioreactor Performance Using Computational Fluid Dynamics'. *Chemical Engineering Science* 144 (April): 58–74.

Meikap, B. C., G. Kundu, and M. N. Biswas. 2002. 'Modeling of a Novel Multi-Stage Bubble Column Scrubber for Flue Gas Desulfurization'. *Chemical Engineering Journal* 86 (3): 331–42.

Mondal, S., and C. G. Bhagchandani. 2016. 'Textile Waste Water Treatment by Advanced Oxidation Processes'. *International Journal on Advances in Engineering Technology and Science* 2 (1).

Monteagudo, J.M., M. Carmona, and A. Durán. 2005. 'Photo-Fenton-Assisted Ozonation of p-Coumaric Acid in Aqueous Solution'. *Chemosphere* 60 (8): 1103–10.

Moreira, F. C., R. A.R. Boaventura, E. Brillas, and V. J.P. Vilar. 2017. 'Electrochemical Advanced Oxidation Processes: A Review on Their Application to Synthetic and Real Wastewaters'. *Applied Catalysis B: Environmental* 202 (March): 217–61.

Muroyama, K., M. Yamasaki, M. Shimizu, E. Shibutani, and T. Tsuji. 2005. 'Modeling and Scale-up Simulation of U-Tube Ozone Oxidation Reactor for Treating Drinking Water'. *Chemical Engineering Science* 60 (22): 6360–70.

Muruganandham, M., R. P. S. Suri, Sh. Jafari, M. Sillanpää, Gang-Juan Lee, J. J. Wu, and M. Swaminathan. 2014. 'Recent Developments in Homogeneous Advanced Oxidation Processes for Water and Wastewater Treatment'. *International Journal of Photoenergy* 2014: 1–21.

Naddafi, K., A. Mesdaghinia, M. Abtahi, K. Yaghmaeian, R. Nabizadeh, N. Jaafarzadeh, N. Rastkari, R. Saeedi, and S. Nazmara. 2016. 'Removal of Dichloromethane from Waste Glasstreams Using a Hybrid Bubble Column/ Bioreactor: Effect of Empty Bed Retention Time and Kinetic of Biofiltration'. *Journal of Air Pollution and Health* 1 (2): 51–60.

Navaza, J. M., D. Gómez-Díaz, and M. D. La Rubia. 2009. 'Removal Process of CO_2 Using MDEA Aqueous Solutions in a Bubble Column Reactor'. *Chemical Engineering Journal* 146 (2): 184–88.

Nidheesh, P. V., and R. Gandhimathi. 2015a. 'Textile Wastewater Treatment by Electro-Fenton Process in Batch and Continuous Modes'. *Journal of Hazardous, Toxic, and Radioactive Waste* 19 (3): 04014038.

Nidheesh, P. V., and R. Gandhimathi. 2015b. 'Electro Fenton Oxidation for the Removal of Rhodamine B from Aqueous Solution in a Bubble Column Reactor under Continuous Mode'. *Desalination and Water Treatment* 55 (1): 263–71.

Oller, I., S. Malato, and J.A. Sánchez-Pérez. 2011. 'Combination of Advanced Oxidation Processes and Biological Treatments for Wastewater Decontamination—A Review'. *Science of The Total Environment* 409 (20): 4141–66.

Oturan, M. A., and J. J. Aaron. 2014. 'Advanced Oxidation Processes in Water/Wastewater Treatment: Principles and Applications. A Review'. *Critical*

Reviews in Environmental Science and Technology 44 (23): 2577–2641.

Öztürk, S. S., A. Schumpe, and W. D. Deckwer. 1987. 'Organic Liquids in a Bubble Column: Holdups and Mass Transfer Coefficients'. *AIChE Journal* 33 (9): 1473–80.

Pignatello, J.J., E. Oliveros, and A. MacKay. 2006. 'Advanced Oxidation Processes for Organic Contaminant Destruction Based on the Fenton Reaction and Related Chemistry'. *Critical Reviews in Environmental Science and Technology* 26 (1): 1–84.

Pino, L.Z., R.B. Solari, S. Siquier, L. A. Estevez, M.M. Yepez, and A.E. Saez. 1992. 'Effect of Operating Conditions on Gas Holdup in Slurry Bubble Columns with a Foaming Liquid'. *Chemical Engineering Communications* 177 (1): 367–82.

Plevan, M., T. Geißler, A. Abánades, K. Mehravaran, R.K. Rathnam, C. Rubbia, D. Salmieri, L. Stoppel, S. Stückrad, and Th. Wetzel. 2015. 'Thermal Cracking of Methane in a Liquid Metal Bubble Column Reactor: Experiments and Kinetic Analysis'. *International Journal of Hydrogen Energy* 40 (25): 8020–33.

Pliego, G., J.A. Zazo, P. Garcia-Muñoz, M. Munoz, J.A. Casas, and J.J. Rodriguez. 2015. 'Trends in the Intensification of the Fenton Process for Wastewater Treatment: An Overview'. *Critical Reviews in Environmental Science and Technology* 45 (24): 2611–92.

Pouran, S. R., A. A. A. Raman, and W. M. A. W. Daud. 2014. 'Review on the Application of Modified Iron Oxides as Heterogeneous Catalysts in Fenton Reactions'. *Journal of Cleaner Production* 64 (February): 24–35.

Pourtousi, M., P. Ganesan, and J.N. Sahu. 2015. 'Effect of Bubble Diameter Size on Prediction of Flow Pattern in Euler–Euler Simulation of Homogeneous Bubble Column Regime'. *Measurement* 76 (December): 255–70.

Pourtousi, M., J.N. Sahu, and P. Ganesan. 2014. 'Effect of Interfacial Forces and Turbulence Models on Predicting Flow Pattern inside the Bubble Column'. *Chemical Engineering and Processing: Process Intensification* 75 (January): 38–47.

Poyatos, J.M., M.M. Muñio, M.C. Almecija, J.C. Torres, E. Hontoria, and F. Osorio. 2010. 'Advanced Oxidation Processes for Wastewater Treatment: State of the Art'. *Water, Air, and Soil Pollution* 205: 187–204.

Process Engineering Advanced Research Lab. 2017. 'Hydrodynamics Modelling and Catalytic Reactions of Multiphase Reactors at Extreme Conditions'. Polytechnique Montréal. 2017.

Rodrigues, C. S.D., R. A.C. Borges, V. N. Lima, and L. M. Madeira. 2018. '*p*-Nitrophenol Degradation by Fenton's Oxidation in a Bubble Column Reactor'. *Journal of Environmental Management* 206: 774–85.

Rollbusch, P., M. Bothe, M. Becker, M. Ludwig, M. Grünewald, M. Schlüter, and R. Franke. 2015. 'Bubble Columns Operated under Industrially Relevant Conditions – Current Understanding of Design Parameters'. *Chemical Engineering Science* 126: 660–78.

Rosales, E., M. Pazos, M. A. Longo, and M. A. Sanromán. 2009. 'Electro-Fenton Decoloration of Dyes in a Continuous Reactor: A Promising Technology in Colored Wastewater Treatment'. *Chemical Engineering Journal* 155 (1–2): 62–67.

Rosenfeldt, E., P. Chen, S. Kullman, and K. Linden. 2007. 'Destruction of Estrogenic Activity in Water Using UV Advanced Oxidation'. *Science of The Total Environment* 377 (1): 105–13.

Samet, Y., E. Hmani, and R. Abdelhédi. 2012. 'Fenton and Solar Photo-Fenton Processes for the Removal of Chlorpyrifos Insecticide in Wastewater'. *Water SA* 38 (4): 537–42.

Santana, M. H.P., L. M. Da Silva, A. C. Freitas, J. F.C. Boodts, K. C. Fernandes, and L. A. De Faria. 2009. 'Application of Electrochemically Generated Ozone to the Discoloration and Degradation of Solutions Containing the Dye Reactive Orange 122'. *Journal of Hazardous Materials* 164 (1): 10–17.

Scialdone, O, A Galia, and S Sabatino. 2013. 'Electro-Generation of H2O2 and Abatement of Organic Pollutant in Water by an Electro-Fenton Process in a Microfluidic Reactor'. *Electrochemistry Communications* 26: 45–47.

Shah, Y. T., B. G. Kelkar, S. P. Godbole, and W.-D. Deckwer. 1982. 'Design Parameters Estimations for Bubble Column Reactors'. *AIChE Journal* 28 (3): 353–379.

Shi, W., N. Yang, and X. Yang. 2017. 'A Kinetic Inlet Model for CFD Simulation of Large-Scale Bubble Columns'. *Chemical Engineering Science* 158 (February): 108–16.

Silva, A. C., J. S. Pic, G. L. Sant'Anna, and M. Dezotti. 2009. 'Ozonation of Azo Dyes (Orange II and Acid Red 27) in Saline Media'. *Journal of Hazardous Materials* 169 (1–3): 965–71.

Skoumal, M., P.-L. Cabot, F. Centellas, C. Arias, R. M. Rodríguez, J. A. Garrido, and E. Brillas. 2006. 'Mineralization of Paracetamol by Ozonation Catalyzed with Fe^{2+}, Cu^{2+} and UVA Light'. *Applied Catalysis B: Environmental* 66 (3–4): 228–40.

Sousa, J., M. F. R. Pereira, and J. L. Figueiredo. 2013. 'Modified Activated Carbon as Catalyst for NO Oxidation'. *Fuel Processing Technology* 106: 727–33.

Srinivasan, S.V., G.P.S. Mary, C. Kalyanaraman, P.S. Sureshkumar, K.S Balakameswari, R. Suthantharajan, and E. Ravindranath. 2012. 'Combined Advanced Oxidation and Biological Treatment of Tannery Effluent'. *Clean Technologies and Environmental Policy* 14 (2): 251–256.

Stacy, C. J., C. A. Melick, and R. A. Cairncross. 2014. 'Esterification of Free Fatty Acids to Fatty Acid Alkyl Esters in a Bubble Column Reactor for Use as Biodiesel'. *Fuel Processing Technology* 124 (February): 1–18.

Suh, J. H., and M. Mohseni. 2004. 'A Study on the Relationship between Biodegradability Enhancement and Oxidation of 1,4-Dioxane Using Ozone and Hydrogen Peroxide'. *Water Research* 38 (10): 2596–2604.

Sun, Y., and J.J. Pignatello. 1993. 'Photochemical Reactions Involved in the Total Mineralization of 2,4-D by Fe3+/H2O2/UV'. *Environmental Science & Technology* 27 (2): 304–10.

Tokumura, M., M. Shibusawa, and Y. Kawase. 2013. 'Dynamic Simulation of Degradation of Toluene in Waste Gas by the Photo-Fenton Reaction in a Bubble Column'. *Chemical Engineering Science* 100: 212–24.

Turhan, K., I. Durukan, S. A. Ozturkcan, and Z. Turgut. 2012. 'Decolorization of Textile Basic Dye in Aqueous Solution by Ozone'. *Dyes and Pigments* 92 (3): 897–901.

Turhan, K., and Z. Turgut. 2009. 'Decolorization of Direct Dye in Textile Wastewater by Ozonization in a Semi-Batch Bubble Column Reactor'. *Desalination* 242 (1–3): 256–63.

US EPA. 1999. 'Nitrogen Oxides (NOx), Why and How They Are Controlled'. *Epa-456/F-99-006R*, no. November: 48.

US EPA. 2012. 'Mercury and Air Toxics Standards (MATS)'. *U.S. Environmental Protection Agency*.

Walling, C. 1975. 'Fenton's Reagent Revisited'. *Accounts of Chemical Research* 8 (4): 125–31.

Wei, J., B. Yu, J. Yang, and J. Dai. 2012. 'Feasibility Study of Decomposing Methane with Hydroxyl Radicals'. *Safety Science* 50 (4): 873–77.

Wilkinson, P. M., H. Haringa, and L. L. Van Dierendonck. 1994. 'Mass Transfer and Bubble Size in a Bubble Column under Pressure'. *Chemical Engineering Science*

49 (9): 1417–27.

Wonders, A. G., H. W. J. Jenkins, L. R. Partin, W. S. Strasser, and M. De Vreede. 2006. Optimized liquid-phase oxidation in a bubble column reactor. EP 1 786 555 B1, issued 2006.

Yavorskyy, A., O. Shvydkiv, C. Limburg, K. Nolan, Y. M. C. Delauré, and M.Oelgemöller. 2012. 'Photooxygenations in a Bubble Column Reactor'. *Green Chemistry* 14 (4): 888.

Zhan, F., C. Li, G. Zeng, S. Tao, Y. Xiao, X. Zhang, L. Zhao, J. Zhang, and J. Ma. 2013. 'Experimental Study on Oxidation of Elemental Mercury by UV/Fenton System'. *Chemical Engineering Journal* 232 (October): 81–88.

Part II: Treatment of Liquid Effluents

This part presents the experimental data relative to the treatment of liquid effluents by the Fenton's process carried out inside bubbling reactors. The contents were separated in two chapters, which report the treatment of a model compound (hydroquinone) and a real wastewater.

Chapter 3. Application of Fenton's Process in a Bubble Column Reactor for Hydroquinone Degradation

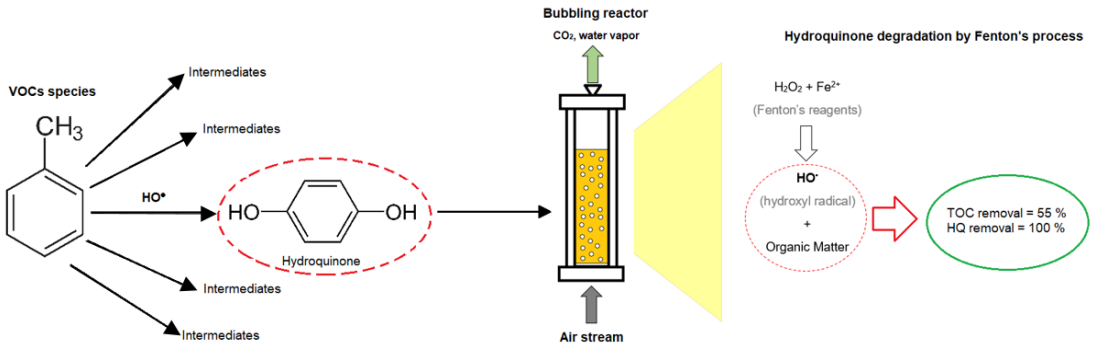

- Bubble column reactor (BCR) was used to perform Fenton oxidation;
- Hydroquinone (HQ) is totally degraded by Fenton's reaction in less than 5 min;
- Total organic carbon (TOC) that remains in solution is due to carboxylic acids formed during the reaction;
- Fenton oxidation in a BCR is promising for HQ degradation and considerable mineralization was reached.

The contents of this chapter were adapted from: Lima, V. N., Rodrigues, C. S., and Madeira, L. M. (2018). *Application of the Fenton's process in a bubble column reactor for hydroquinone degradation*. **Environmental Science and Pollution Research**, 25(35), 34851-34862.

Abstract: *The aim of this study was to assess the degradation and mineralization of hydroquinone (HQ) by the Fenton's process in a bubble column reactor (BCR). The effect of the main operating variables, namely, air flow rate, effluent volume, hydrogen peroxide (H_2O_2) concentration, catalyst (Fe^{2+}) dose, initial pH, and temperature, were assessed. For all air flow rates tested, no concentration gradients along the column were noticed, evidencing that a good mixing was reached in the BCR. For the best conditions tested ($[H_2O_2]$ = 500 mg/L, $[Fe^{2+}]$ = 45 mg/L, T = 24 °C, Q_{air} = 2.5 mL/min, pH = 3.0, and V = 5 L), complete HQ degradation was reached, with ~ 39% of total organic carbon (TOC) removal, and an efficiency of the oxidant use—η_{H2O2}— of 0.39 (ratio between TOC removed per H_2O_2 consumed normalized by the theoretical stoichiometric value); moreover, a non-toxic effluent was generated. Under these conditions, the intermediates and final oxidation compounds identified and quantified were a few carboxylic acids, namely, maleic, pyruvic, and oxalic. As a strategy to improve the TOC removal, a gradual dosage of the optimal H_2O_2 concentration was implemented, being obtained ~ 55% of mineralization (with complete HQ degradation). Finally, the matrix effect was evaluated, for which a real wastewater was spiked with 100 mg/L of HQ; no reduction in terms of HQ degradation and mineralization was observed compared to the solution in distilled water.*

3.1 Introduction

The bubble column reactor (BCR) is an important reactor configuration for the chemical industry (Stacy *et al.* 2014; Salehi *et al.* 2014; Nanou *et al.* 2017). Its use has increased in the recent years (Rollbusch *et al.* 2015) because it is an attractive alternative to other reactor configurations (for example, the continuous stirred tank reactors – CSTRs) since the agitation (responsible for internal mixing) is promoted by the bubbling of gas in the liquid (Wonders *et al.* 2006); so, it does not require any mechanical stirrers/moving parts. Moreover, through an efficient interaction between the two-phase (liquid and gas) and an efficient mass (and/or heat) transfer is reached (Silva *et al.* 2015).

In environmental applications, the BCR has been used for wastewater and/or gaseous effluents treatment, with its application being useful to promote a better interaction among the reagents and the pollutants (that may be present in the liquid or gas phase) during the reaction process. This reactor configuration has been used for the treatment of liquid effluents by advanced oxidation processes (AOPs), namely through ozonation and H_2O_2-based processes, assisted or not by radiation (Lucas *et al.* 2010), as well as by the electro-Fenton process (Nidheesh and Gandhimathi 2015). For gas streams containing volatile organic compounds (VOCs), treatment by the photo-Fenton reaction in a BCR has also been implemented (Handa *et al.* 2013; Tokumura *et al.* 2013).

The application of AOPs for effluents' treatment has been increasing year after year (Clarizia *et al.* 2017). The Fenton reaction, an important AOP, deserves particular attention because it can be operated under moderate temperature and pressure conditions, making use of environmentally friendly reagents. It is based in the hydroxyl radicals ($HO^{\bullet}$) formation by H_2O_2 decomposition catalyzed by Fe^{2+} ions (Eq. 3.1) in acid medium. Among several other reactions, it is worth mentioning the regeneration of the catalyst by reaction between Fe^{2+} and H_2O_2 (Eq. 3.2) and the oxidation of the organic compounds by $HO^{\bullet}$ with formation of intermediate species (Eq. 3.3) that can be subsequently oxidized and ultimately mineralized into CO_2 and H_2O (Walling 1975).

$$Fe^{2+}+H_2O_2 \rightarrow Fe^{3+}+HO^{\bullet}+OH^{-} \quad (3.1)$$

$$Fe^{3+}+H_2O_2 \rightarrow Fe^{2+}+HO_2^{\bullet}+H^{+} \quad (3.2)$$

$$HO^{\bullet}+RH \rightarrow H_2O+\text{intermediates} \quad (3.3)$$

The application of the Fenton process in a BCR may be of high interest. One variation of this process (the photo-Fenton) was studied for degradation of VOCs that inherently need to be transferred from the gas to the liquid phase where oxidation proceeds (Handa *et al.* 2013; Tokumura *et al.* 2013). The formation of the gas bubbles in the

column promotes a better contact between both phases. This way, the pollutants are transferred from the gas to the liquid (the latter containing the Fenton reagents, i.e. H_2O_2 and catalyst) where the organic compounds degradation and mineralization occurs, further accelerating the mass transfer process – as their concentration in the liquid decreases, the driving force for mass transfer is increased (Handa *et al.* 2013). However, and up to the authors' knowledge, such technology has never been implemented for pollutants present in the liquid phase.

In this study it was evaluated the hydroquinone (HQ) degradation by the homogeneous Fenton process in a BCR. This organic was selected as model compound because it is used in some important industries for the production of rubbers, dyes, pesticides, plastics, pharmaceuticals, and cosmetics (Chang *et al.* 2009). In addition, it is reported as an intermediate compound formed during the oxidation of benzene (Ito *et al.* 1988), and phenol (Lominchar *et al.* 2017). In literature it is reported the HQ degradation by oxidation using an inorganic catalyst - δ-MnO_2 (Chang *et al.* 2009) and by a combination of photochemical oxidation and electrocoagulation processes (Akyol *et al.* 2015); however, no studies were made that applied the Fenton process for its degradation.

The application of the Fenton process for HQ degradation in a BCR is addressed herein. In this reactor configuration the HQ is present in the same phase where the Fenton reaction occurs (the liquid one); therefore, the bubbling of air promotes the mixing and stirring. The aim of this study was to evaluate the efficiency and optimize the Fenton process, identify and quantify the intermediate compounds formed, and evaluate the matrix effect using a real wastewater. Such preliminary work is the first step for subsequent integration of both gas and liquid (real) effluents treatment in the same device.

3.2 Material and methods

3.2.1 Chemicals

In this study hydroquinone ($C_6H_6O_2$, from Sigma-Aldrich) was used as model compound. The hydrogen peroxide (30% w/v), ferrous sulfate ($FeSO_4 \cdot 7H_2O$), sodium sulfite (Na_2SO_3), sodium hydroxide (NaOH), methanol (98%) and sulfuric acid (H_2SO_4 97-98%) were purchased from Panreac. Hydroquinone (99%), 4-benzoquinone (99%) and the organic acids - maleic, pyruvic, and oxalic (99%), were reagent grade, purchased from Sigma-Aldrich.

3.2.2 Fenton process in the BCR

The Fenton process was carried out in a BCR with the total capacity of ~10 L (1.40 m of height and 9.8 cm of internal diameter). In the bottom the column has a gas dispersive plate with 9 holes (0.5 mm of diameter). The double wall column is connected to a thermostatic bath (Polystat CC1) for maintaining the temperature constant inside the reactor, when required (i.e., in the runs performed with temperature control). The air is feed to the column through an Aqua medic, Mistral 2000 pump, being the flow rate controlled (in the range of 1 to 5 mL/min; measured at ambient temperature and atmospheric pressure) by two rotameters (Ohmega FL-2015). In Fig. 3.1 is presented a schematic of the experimental set-up, being worth noticing the existence of three sampling points along the column at different heights (0.5, 0.7 and 0.9 m from the bottom).

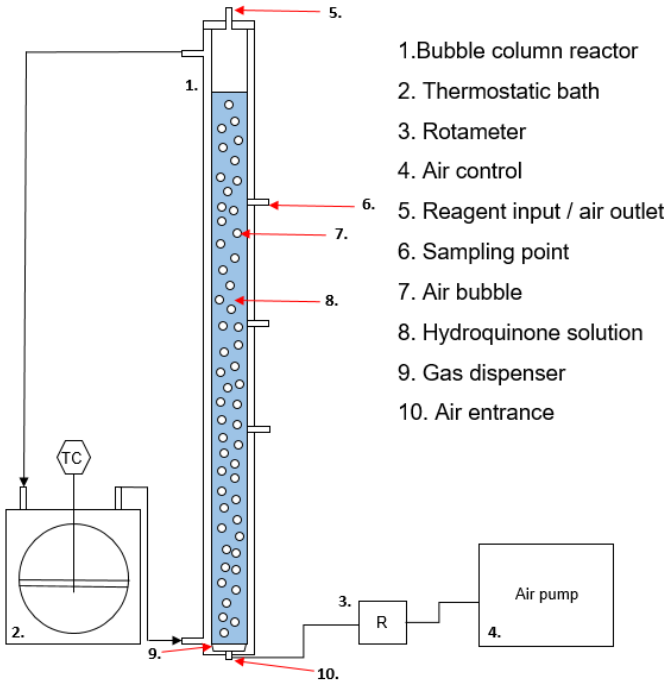

Figure 3.1 Schematic diagram of the bubble column reactor experimental set-up.

The experiments were carried out with 5-9 L of HQ solution, with a concentration of 100 mg/L; this concentration was selected based on literature information about the level of HQ in industrial effluents (Suresh 2015); after stabilization of the temperature, the pH was adjusted with 1 M H_2SO_4 to the desired value. Then, the catalyst ($FeSO_4.7H_2O$) was added and subsequently the H_2O_2 solution, being this instant the one at which the reaction started, i.e., time zero of reaction coincides with the addition of the oxidant.

At given times samples were collected for measuring the residual H_2O_2 concentration (which was done immediately), as well as the HQ concentration and TOC after stopping the homogeneous reaction in the sampling vials; this was done with excess of Na_2SO_3 (which instantaneously consumes any residual H_2O_2), or by raising the pH to ±7.0 using 1 M NaOH for the other parameters described in the following section.

3.2.3 Analytical methods

The total organic carbon (TOC) measurement was performed according to the method 5310 D (APHA 1988) using a TOC-L analyzer from Shimadzu. For determination of the residual H_2O_2, at the end of the reaction, the method developed by Sellers (1980) was adopted, which consists in measuring the absorbance that results from the reaction between the remaining H_2O_2 and oxalate titanium, at a wavelength of 400 nm, in a HEλIOS γ spectrophotometer (from Thermo Electron Corporation).

The toxicity of the effluent was evaluated by inhibition of *Vibrio fischeri* in accordance to the standard DIN/EN/ISO 11348-3 (Standardization 2005), i.e., assessing the bioluminescence after contact times (between the samples and the bacteria) of 5, 15 and 30 minutes, at 15 ºC, in a Microtox ModernWater model 500 unit.

The HQ and carboxylic acids were identified and quantified by high-performance liquid chromatography (HPLC) - Hitachi Elite LaChrom from VWR apparatus – equipped with a diode array detector. Firstly, the samples were filtered through a 0.2 µm PES filter. For HQ analysis, 20 µL of sample was injected for identification at 280 nm; the mobile phase was composed of pure methanol and water (90/10 %, v/v) with a flow rate of 0.75 mL/min, the separation being performed at 35 ºC using a Purospher STAR RP-18 column (5 mm, 250 x 4.0 mm). For analysis of the carboxylic acids (oxalic, maleic and pyruvic acid), it was injected 15 µL of sample and the identification was carried out at 210 nm; the mobile phase was composed of a 2.5 mM H_2SO_4 solution with a flow rate of 0.17 mL/min, and the separation was performed at 25 ºC using a Rezex ROA-Organic Acid H+ (8%) column (250 x 46 mm), from Phenomenex.

3.3 Results and discussion

The hydroquinone solution used had the following characteristics: natural pH of 5.2, a TOC content of 71.2 mgC/L and provided a complete (100%) inhibition towards *Vibrio fischeri*.

A blank run was firstly carried out by bubbling air into the HQ solution (without adding any other chemicals). It was found that the concentration of this compound remained unchanged (HQ removal was less than 1% after 120 minutes), and so it can be concluded that the stripping of HQ does not occur under the conditions used (T = 24 ºC; Q_{air} = 1.0 mL/min; pH = 3.0) neither the oxygen itself has any oxidation effect.

3.3.1 Mixing process in the BCR

The mixing in the reactor has an important role in the efficiency of the treatment process, as is responsible for promoting a uniform contact between reagents and the effluent. In a BCR, efficient mixing can be reached by the movement of the gas bubbles in the liquid phase.

In this study, the air was feed through the bottom of the BCR by using a gas dispersive plate, and the bubbles formed were uniform. The dispersion bubble process (bubbling) is responsible for the turbulence inside the reactor (Heijnen and Van't Riet 1984), which is believed to provide conditions similar to a perfectly stirred reactor. To assess the efficiency of mixing inside the reactor, the effect of the air flow rate (Q_{air}) was studied by changing this variable (1.0, 2.5 and 5.0 mL/min; measured at ambient temperature and atmospheric pressure) while collecting samples at different heights (H) along the column (0.5, 0.7 and 0.9 m). In these runs it was used a H_2O_2 concentration of 500 mg/L, slightly above the stoichiometric value for total HQ mineralization (401.4 mgC/L, calculated according to Eq. 3.4).

$$C_6H_6O_2+13H_2O_2 \rightarrow 6CO_2+16H_2O \quad (3.4)$$

Fig. 3.2a shows the TOC removal during the reaction for different air flow rates tested, being the samples taken at the lowest sampling point shown in Fig. 3.1 (H_3 = 0.5 m). It can be seen that mineralization was similar for the three air flow rates tested, with a maximum reduction of 27.0% after two hours of the Fenton reaction. The same tendency was observed for different sampling heights at constant air flow rate (see Fig. 3.2b). It is worth noting that the HQ degradation was complete in all these runs.

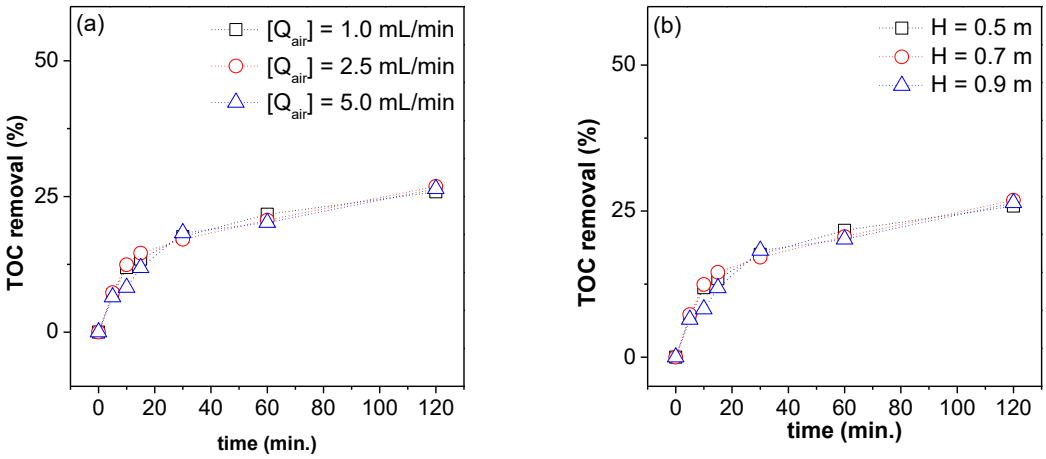

Figure 3.2 TOC removal over the reaction time for different: air flow rates (a) ([H_2O_2] = 500 mg/L; [Fe^{2+}] = 45 mg/L; T = 24 ºC; pH = 3.0; V = 7 L; H_3 = 0.5 m), and different sampling heights (b) ([H_2O_2] = 500 mg/L; [Fe^{2+}] = 45 mg/L; T = 24 ºC; pH = 3.0; V = 7 L; Q_{air} = 2.5 mL/min).

The evolution of the pH was also quite similar in all the experiments, as well as the efficiency of the H_2O_2 use (η_{H2O2}), calculated according to Eq. 3.5 (see results in the Appendix section – Fig. A.1.1). In this way, it can be concluded that a good mixing (homogenization) was reached and no axial gradients should exist within the column, thus demonstrating a good applicability of this reactor configuration for the Fenton reaction.

$$\eta_{H2O2} = \left(\frac{TOC_0 - TOC_{final}}{H_2O_{2_0} - H_2O_{2_{final}}}\right) / f_{H2O2} \quad (3.5)$$

where:

η_{H2O2} = efficiency of H_2O_2 use.

TOC_0 = TOC in the initial instant of the reaction (t = 0), mg/L.

TOC_{final} = TOC in the end of the reaction, mg/L.

$H_2O_{2\,0}$ = H_2O_2 concentration in the initial instant of the reaction (t = 0), mg/L.

$H_2O_{2\,final}$ = H_2O_2 concentration in the end of the reaction, mg/L.

f_{H2O2} = Factor relative to the stoichiometric H_2O_2 required for the HQ mineralization (calculated by Eq. 3.6 based in Eq. 3.4).

$$f_{H2O2} = \frac{6*MM_C}{13*MM_{H2O2}} = \frac{6*12(\frac{g}{mol})}{13*34\,(\frac{g}{mol})} = 0.163 \quad (3.6)$$

MM_i = molar mass of species i.

3.3.2 Effect of liquid height in the column

To evaluate the effect of the liquid height three runs were carried out in which this variable was changed (by using 5, 7 and 9 L of the HQ solution). The HQ removal was again 100% for all volumes tested in only 5 minutes of reaction, however the mineralization decreased with increased volume of solution put in the reactor (see results in the Appendix section A.1.1. – Fig. A.1.2).

Considering that a good homogenization was found inside the column, as was demonstrated in the previous section, H_2O_2 loss by stripping was evaluated, in three blank runs, where the oxidant (500 mg/L of H_2O_2) was inserted by the top of the BCR and then air was bubbled (Q_{air} = 2.5 mL/min) for different liquid volumes. In Fig. 3.3a are presented the results obtained; it can be seen that a considerable loss of H_2O_2 was reached (32-35%) in the first 5 minutes, which slightly increased with time afterwards (40-42% after 120 minutes); however, this loss was independent of the liquid volume put into the BCR.

The way H_2O_2 is added into the column, made through the top in Fig. 3.3a, could be the problem for such a level of stripping, and so three additional runs were performed where the oxidant was injected through the lowest sampling point (H = 0.5 m), in the same conditions. The results obtained (Fig. 3.3b) permit to observe almost no effect in the H_2O_2 concentration that remained in solution because it was reached a similar loss (30-31% and 42-44% after 5 and 120 minutes, respectively). Again, the stripping of oxidant occurred, but this effect is not too pronounced (and does not seem to affect the oxidation process, as detailed below). Other authors used H_2O_2 for oxidation in BCR, but the effect of its loss was not investigated.

Sasaki *et al.* (2016) evaluated the effect of the liquid height (water) in the gas (air) holdup (ε_g) in a cylindrical bubble column reactor and observed that the increase of the height of liquid was responsible for the decrease of the gas holdup. The gas holdup was measured under the conditions used in our work (see the procedure described in the Appendix section A.1.1 and data in Table A.1.2), and the results are shown in Fig 3.3c. It is observed an increase of the gas holdup with the rise of the gas flow rate for all volumes of water initially loaded in the column, as reported by Yan *et al.* (2016) in a study about the BTEX removal by UV-Fenton in a BCR. Moreover, the increase of the liquid height was responsible for a decrease in ε_g, as found by Sasaki *et al.* (2016). Although not affecting the H_2O_2 loss, such phenomena can interfere in the oxidation process, namely in the complex reaction mechanism and/or CO_2 (ultimate oxidation species) stripping (in line with the results shown in Fig. A.1.2).

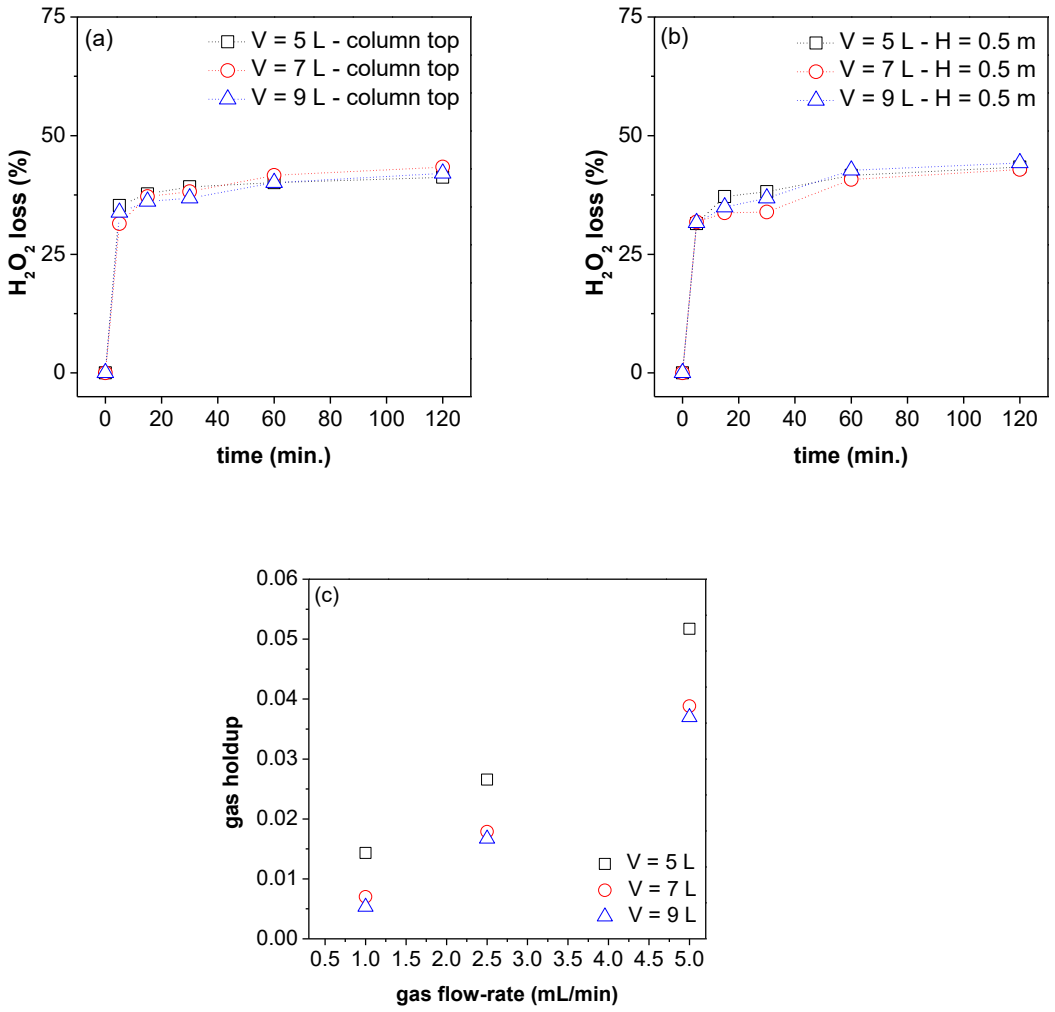

Figure 3.3 Hydrogen peroxide loss in blank runs with different volumes of liquid with the oxidant being added: by the top of the column (a) and in the lowest sampling point (H= 0.5 m) (b) ([H_2O_2] = 500 mg/L; T = 24 ºC; pH = 3.0; Q_{air} = 2.5 mL/min), and gas holdup for different volumes of liquid and air flow rates in the BCR (c).

3.3.3 Effect of the iron dose

The iron (Fe^{2+}) concentration has an important role in the Fenton process once it is the catalyst that promotes the decomposition of the H_2O_2 molecule to form the $HO^{\bullet}$ species – see Eq. 3.1 – (Walling 1975). Its effect was evaluated in the range of 0 to 120 mg/L. In these runs it was used the same H_2O_2 concentration of the previous tests but the reaction time was increased to 3 h to assess the possibility of further increasing organics mineralization.

Again, total HQ degradation was obtained in all runs (except when no Fe^{2+} was used). In Fig. 3.4a it can be seen that the mineralization increased with the Fe^{2+} dose until 45

mg/L and decreased when using higher Fe^{2+} concentrations. For the optimal dose the maximum removal achieved was 39.9% after 180 minutes of reaction (Fig. 3.4a) with a rapid mineralization in the first few minutes (more than 30% of the TOC was removed in 15 min.). The existence of an optimal Fe^{2+} dose can be explained by the scavenging of the hydroxyl radicals when excess of such ions are present in solution, as described in Eq. 3.7 (Walling 1975).

$$Fe^{2+} + HO^{\bullet} \rightarrow Fe^{3+} + OH^{-} \quad (3.7)$$

The pH decreased along the reactions (Fig. 3.4b) and for all runs the evolution of pH during the reaction was similar, except when no Fe^{2+} was used. This decrease of pH along the reaction is due to the formation of H^+ by reaction between ferric species Fe^{3+} and H_2O_2 (Eq. 3.2) (Oliveira *et al.* 2014) and to the formation of short chain organic acids. The H_2O_2 consumption was 100% for all runs in which iron was used, but the efficiency of oxidant use was superior in the run with 45 mg/L of Fe^{2+} (η_{H2O2} = 0.37) (Fig. 3.4c).

Regarding the toxicity, only for the smaller dose of catalyst (30 mg/L) the final effluent showed some inhibition of *Vibrio fischeri*, however it decreased from 100% (for the initial HQ solution) to 19.3% after reaction, which is associated with the formation of organic compounds that are less toxic. For all the other runs, the final effluent was not toxic towards the bacteria.

The use of the H_2O_2 alone – 500 mg/L – (without the presence of iron – $[Fe^{2+}]$ = 0 mg/L) only provided ~15% of TOC (Fig. 3.4a) and 60% of HQ removal; a very slight decrease in the pH was observed (Fig. 3.4b) and only 45% of the oxidant was consumed with an efficiency of use of 0.34 (see Fig. 3.4c) after 3 hours of reaction. The much lower performance and efficiency is due to the low oxidation potential of H_2O_2 as compared with the hydroxyl radicals. Despite the low performance reached, this result is important because the H_2O_2 consumption was 45%, showing that during the oxidation reaction the H_2O_2 quickly oxidizes the HQ not being lost by stripping as occurred in the blank tests (Fig. 3.3a). In this run the HQ concentration present at the end of the reaction (~40 mg/L) showed to be harmful in the toxicity test (100% of *Vibrio fischeri* inhibition).

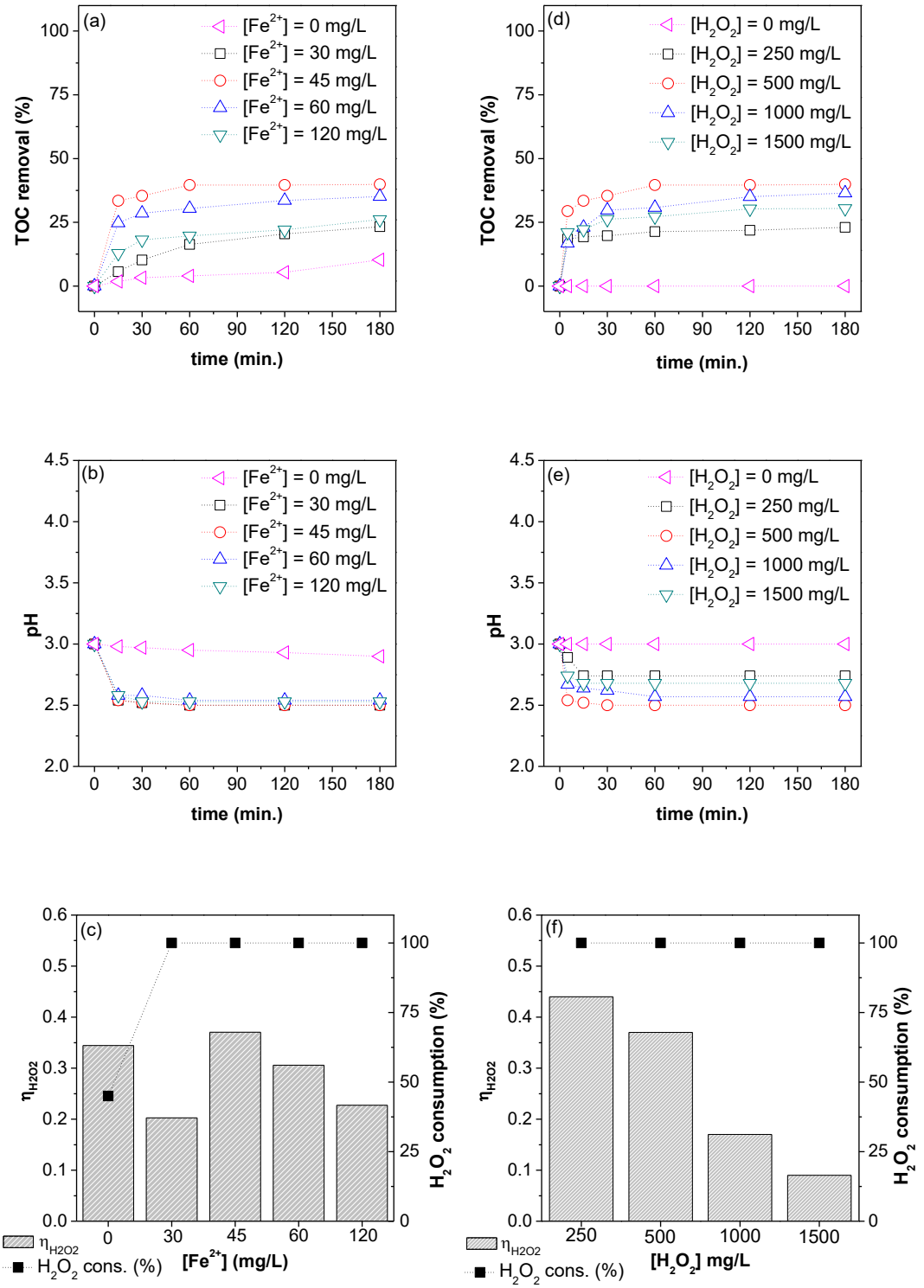

Figure 3.4 TOC removal (a), pH over reaction time (b), H_2O_2 consumption and η_{H2O2} at 180 minutes of reaction (c) for different Fe^{2+} doses ($[H_2O_2]$ = 500 mg/L; Q_{air} = 2.5 mL/min; T = 24 ºC; pH = 3.0; V = 5 L); TOC removal (d), pH over reaction time (e), H_2O_2 consumption and η_{H2O2} at 180 minutes of reaction (f) for different H_2O_2 concentrations ($[Fe^{2+}]$ = 45 mg/L; Q_{air} = 2.5 mL/min; T = 24 ºC; pH = 3.0; V = 5 L).

3.3.4 Influence of the initial hydrogen peroxide concentration

To assess the effect of the H_2O_2 concentration, runs with different oxidant concentrations (between 0 to 1500 mg/L) were carried out, fixing the other conditions as follows: $pH_{initial}$ = 3, Q_{air} = 2.5 mL/min, V = 5 L, T = 24 ºC and $[Fe^{2+}]$ = 45 mg/L.

The use of Fe^{2+} alone - 45 mg/L - (run where $[H_2O_2]$ = 0 mg/L) did not provide any removal of organic compounds and the pH of the solution was constant throughout the experiment (see Figs. 3.4d-e); moreover, the toxicity of the final effluent was similar (96-99%) to that obtained for the initial HQ solution.

The HQ degradation was complete for all H_2O_2 concentrations tested and the mineralization increased with the oxidant concentration until 500 mg/L (slightly above the stoichiometric value of 400 mg/L necessary to completely mineralize the HQ solution), with ~39 % of TOC removal (Fig. 3.4d) after 3 h. The acidification of the medium along the reaction was again observed (Fig. 3.4e), which was more accentuated for the optimum peroxide dose, indicating that the reaction was more efficient and more carboxylic acids were formed.

For all concentrations of oxidant tested it was reached 100% of H_2O_2 consumption, but using higher oxidant doses did not result in an increase in the efficiency. By the contrary, the η_{H2O2}, shown in Fig. 3.4f, decreased; this indicated that the consumption of more H_2O_2 was not used efficiently in the mineralization of organic compounds. However, the toxicity of the produced effluent was null for all oxidant concentrations tested.

The existence of an optimum H_2O_2 concentration in the Fenton's process was also observed by other authors (Kang *et al.* 2002a, b; Pérez *et al.* 2002; Thakur and Chauhan 2016) and is explained by the scavenging of hydroxyl radicals by H_2O_2 in excess, generating $HO_2^{\bullet}$ species (Eq. 3.8) with a lower oxidation potential (Walling 1975).

$$HO^{\bullet} + H_2O_2 \rightarrow H_2O + HO^{\bullet}_2 \qquad (3.8)$$

3.3.5 Influence of the temperature

The influence of the temperature was also assessed and for that this parameter was varied in the range of 15 to 70 ºC. For the minimum temperature (T = 15 ºC) the reduction of organic compounds was lower, being only reached ~14 % of mineralization after 3 hours of Fenton's reaction (see Fig. 3.5a). The removal increased with the temperature up to a value close to the room temperature (24 ºC) and decreased for runs with higher temperatures, particularly at 70 ºC. The same tendency was observed for the pH

evolution during the reaction, i.e., the run at room temperature showed a greater decrease in the pH (see Fig. 3.5b).

This trend is justified, on one hand, by the fact that the kinetics of the reactions increase with the temperature according to Arrhenius's law, which leads to a greater hydroxyl radicals generation and, consequently, to a higher mineralization; but, on the other hand, increased temperatures can improve the thermal decomposition of H_2O_2 into O_2 and H_2O, particularly for values equal or above 50 ºC (Ramirez *et al.* 2007; Duarte *et al.* 2013); consequently, less amounts of hydroxyl radicals are formed, inhibiting the oxidation of organic matter.

The oxidant was completely consumed in all the runs at all temperatures tested (Fig. 3.5c), which did not corresponded to an improvement of TOC removal (Fig. 3.5a); consequently, the efficiency of oxidant use decreased for temperatures higher than 24 ºC (Fig. 3.5c).

Again, total degradation of HQ was reached. The toxicity of the effluent, as quantified by the inhibition of *Vibrio fischeri*, decreased from 100% to 3.3% after the Fenton reaction at 15 °C but was 0.0% for all other temperatures tested.

3.3.6 Effect of the initial pH

The initial pH of the effluent is a determinant variable in the Fenton process. So, in this study, it was evaluated its effect in the HQ degradation and mineralization in the range of 3 to 7. The natural pH of the effluent (5.2) was considered as an alternative to reduce the cost of the acid consumption in the pre-acidification stage. The results obtained show that the TOC removal increased for more acidic conditions (see Fig. 3.5d). For an initial pH of 5.2 it was observed a very slight decrease as compared to pH 3.0 (39% to 35% after 180 min, which is however more notorious in short reaction times), while the efficiency of the process decays significantly when using pH 7.0 (18.1% for 180 minutes of reaction). Regarding the pH evolution, it is possible to see from Fig. 3.5e that its reduction is much more pronounced in the first five minutes of reaction, with a less pronounced decrease until 120 minutes of reaction, remaining nearly constant afterwards.

Several studies point for the pH of 3.0 as being the optimal for the Fenton reaction (Lucas and Peres 2006; Rodrigues *et al.* 2009) because for values of pH > 4 dissolution of Fe^{2+} species decreases, with inherent precipitation.

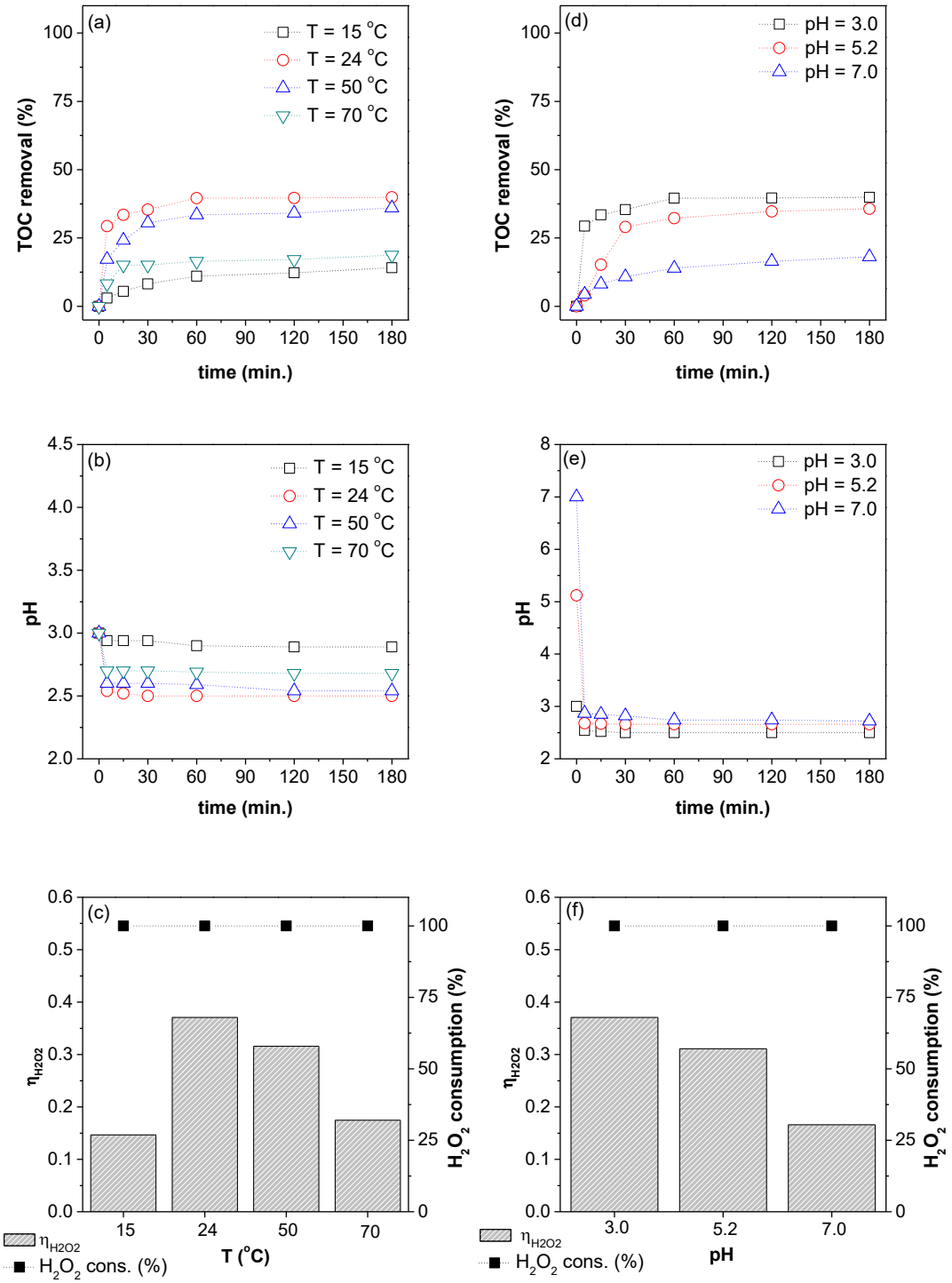

Figure 3.5 Effect of temperature on TOC removal (a), pH over reaction time (b), H_2O_2 consumption and η_{H2O2} at 180 minutes of reaction (c) ([H_2O_2] = 500 mg/L; [Fe^{2+}] = 45 mg/L; Q_{air} = 2.5 mL/min; pH = 3.0; V = 5 L); and effect of initial pH on TOC removal (d), pH over reaction time (e), H_2O_2 consumption and η_{H2O2} at 180 minutes of reaction (e) ([H_2O_2] = 500 mg/L; [Fe^{2+}] = 45 mg/L; Q_{air} = 2.5 mL/min; T = 24 ºC; V = 5 L).

The H_2O_2 consumption was total for all pH values tested; however, the efficiency of the oxidant use was not very different for pH of 3.0 and 5.2 (η_{H2O2} = 0.37 and η_{H2O2} = 0.31,

respectively), but a significant decreased was observed for pH 7.0, with $\eta_{H2O2} = 0.17$ (see Fig. 3.5f), as a consequence of the reduction in the mineralization. For all pH values tested the removal of HQ was 100% in only 5 minutes of reaction and the toxicity of the final effluent was null.

3.3.7 Strategy to improve the mineralization

Aiming to improve the TOC removal, one run was carried under the best conditions found up to now ($pH_{initial} = 3.0$, T = 24 ºC, $[Fe^{2+}] = 45$ mg/L, $[H_2O_2] = 500$ mg/L, $Q_{air} = 2.5$ mL/min and V = 5 L), but the oxidant was added gradually along the first hour of the reaction (41.7 mg/L of H_2O_2 were added every 5 minutes, in 12 divided doses). This strategy was adopted because this way it is anticipated to reduce the undesired parallel reactions ("scavenging" of hydroxyl radicals) and to realize a better use of the oxidant during the Fenton reaction.

The TOC removal in the run with gradual addition of the oxidant was lower in the first minutes of reaction (until 60 minutes) as compared to the reaction in which the used H_2O_2 was added once, at the start of the run (Fig. 3.6a), because in the first case the reaction kinetics is slowed down (smaller concentration of the reactant). However, the TOC removal increases afterwards, till ~55 %, indicating that the partitioned addition of H_2O_2 increases the efficiency of the process. Fig. 3.6b shows that only after 120 min the oxidant was completely consumed, promoting an increase of over 30% in the efficiency of oxidant use (after 3 h, one reached: $\eta_{H2O2\ (single\ addition)} = 0.37$ vs. $\eta_{H2O2\ (gradual\ addition)} = 0.49$).

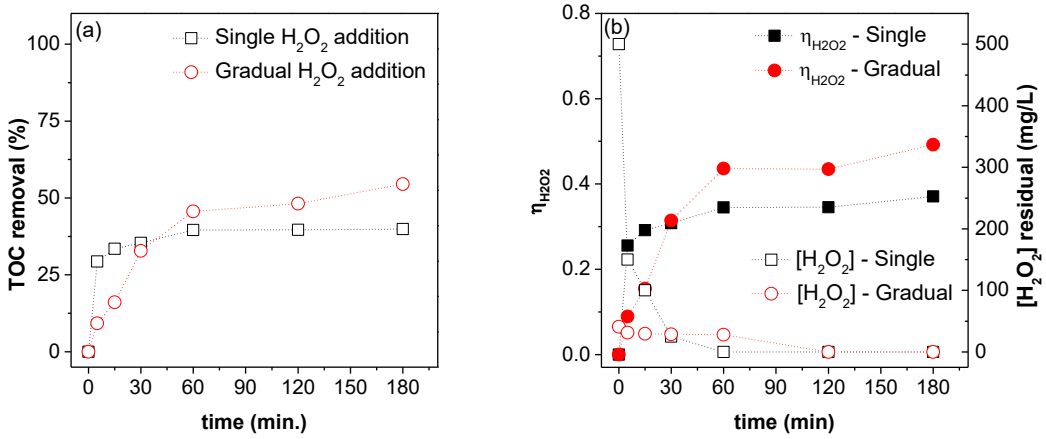

Figure 3.6 TOC removal (a) and H_2O_2 consumption and η_{H2O2} (b) during the reaction with single and gradual addition of the oxidant ($[H_2O_2]$ = 500 mg/L; $[Fe^{2+}]$ = 45 mg/L; pH = 3.0; Q_{air} = 2.5 mL/min; T = 24 ºC; V = 5 L).

3.3.8 Reaction mechanism

Given that HQ was completely removed, but it was only reached ~39% of mineralization (with the single addition of H_2O_2), the presence of intermediate or refractory compounds (namely carboxylic acids, because they are commonly the last compounds formed in oxidation processes) was evaluated in the run under the best operating conditions. In the literature it is reported the formation of 4-benzoquinone (Owsik and Kolarz 2004; Beheshti and McIntosh 2007) and carboxylic acids, namely maleic, fumaric, oxalic, propionic, glyoxylic, acetic and formic acid (Suzuki *et al.* 2015), during HQ oxidation. In this run 4-benzoquinone was not detected, possibly because this intermediate is easily oxidized by the hydroxyl radicals formed in the Fenton reaction.

Three carboxylic acids were identified (maleic, pyruvic and oxalic acid) (Fig. 3.7a). In the first five minutes of reaction maleic acid was identified (~0.30 mM), while for longer reaction times its presence was not found, possibly because it was oxidized to oxalic acid. At 15 minutes the presence of pyruvic acid was identified (~0.01 mM), apart from oxalic acid (~2.3 mM). For longer reaction times the concentration of pyruvic acid was null, while oxalic acid continuously increased up to 180 minutes (till ~2.64 mM). Oxalic acid remained in solution because it is the last carboxylic acid formed and known to be difficult to oxidize. Again, HQ was completely degraded in the first 5 minutes.

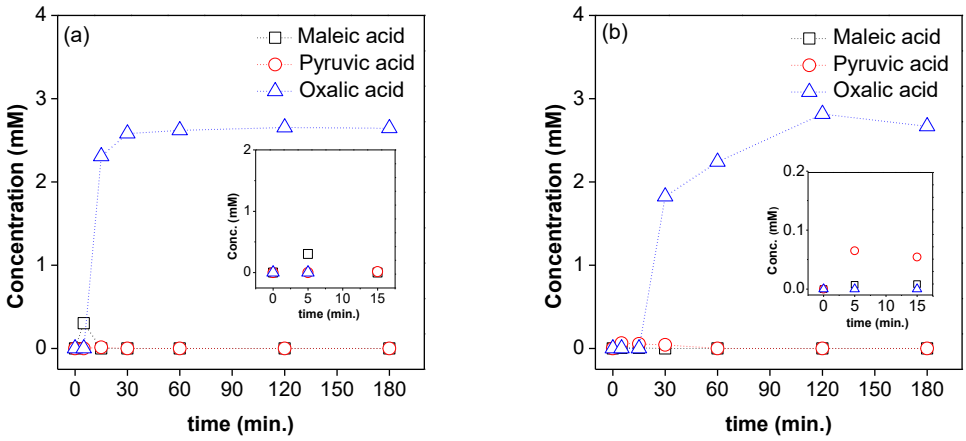

Figure 3.7 Organic acids formation along reaction time: when oxidant was added totally in the beginning of the run (a) and was added H_2O_2 gradually (b) ([H_2O_2] = 500 mg/L; [Fe^{2+}] = 45 mg/L; pH = 3.0; Q_{air} = 2.5 mL/min; T = 24 ºC; V = 5 L).

In the run where the oxidant was added gradually every 5 minutes up to 55 minutes reaction time, HQ removal was also 100 % in the first 5 minutes (even with the low H_2O_2 dose employed up to this time, i.e. [H_2O_2] = ~41 mg/L). The compounds identified were again maleic, pyruvic and oxalic acid (Fig. 3.7b). After five minutes it was identified the presence in solution of maleic acid (<0.01 mM) that remained in solution until 15 minutes with nearly the same concentration, and pyruvic acid (~0.06 mM) that remained in solution until 60 minutes (< 0.01 mM). For a reaction time of 30 minutes the formation of oxalic acid was observed (~1.8 mM), which concentration increased during the reaction until 120 minutes, and then a slight decrease was observed (~2.6 mM after 180 minutes of reaction). The concentration of this compound at the end of the reaction was very similar to that observed when the H_2O_2 was added totally at the beginning of the run. The different patterns observed in Figs. 3.7a) and b) is mostly related with the fact that in the latter the oxidant is added gradually, so at the early stages of the process reaction kinetics is slowed down. Therefore, formation of oxalic acid, for instance, is noticed at longer reaction times. Based on these results, and those reported in the literature (Suzuki *et al.* 2015), a reaction mechanism is proposed, as summarized in Fig. 3.8.

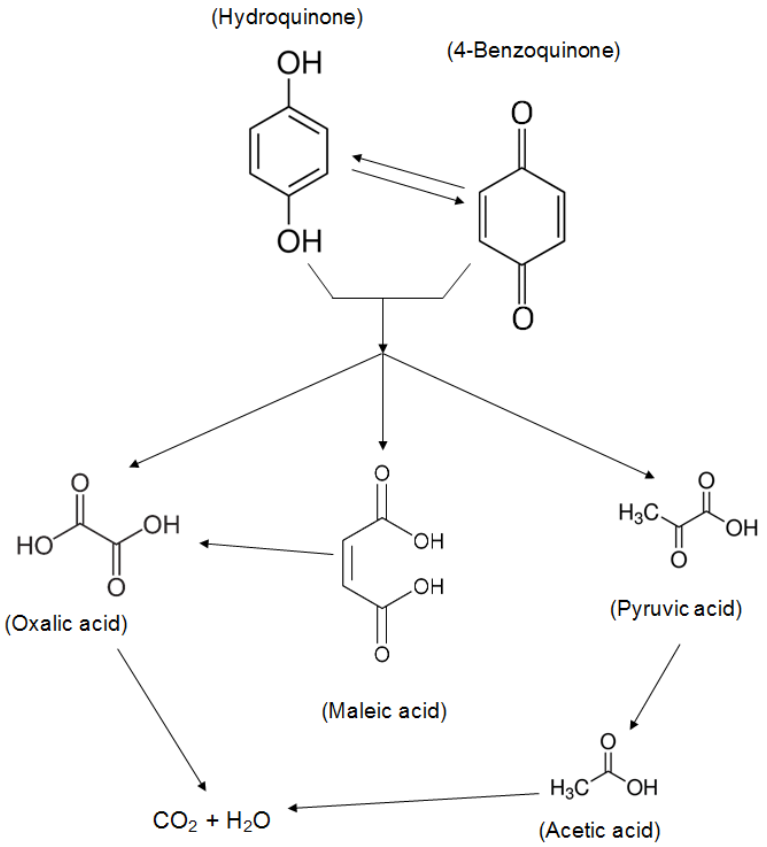

Figure 3.8 Proposed reaction mechanism of hydroquinone degradation by the Fenton process.

3.3.9 Hydroquinone degradation in a real wastewater matrix

The effect of the matrix was evaluated using a domestic effluent collected after the secondary treatment in a wastewater treatment plant, located in the northern region of Portugal, and spiked with 100 mg/L of HQ. Firstly, the wastewater containing the model compound was characterized and the results are presented in Table 3.1; it is worth noting that the TOC was 25% higher as compared to the HQ solution (88.9 mg/L for the real effluent and 71.2 mg/L for the HQ solution). The optimal conditions obtained for treating the HQ solution, for which a mineralization degree of ~40% was reached, were employed in the Fenton oxidation of the spiked wastewater. As occurs with the HQ solution, the compound was totally degraded in the first 5 minutes of reaction and there was a rapid TOC removal in the first 30 minutes of reaction (Fig. 3.9). After this time the TOC removal increased very slowly, being achieved a mineralization after 180 minutes of reaction of ~56%, which was slightly higher than that reached in the HQ solution. Such difference can be attributed to the organic matter present in the real effluent, which should be completely mineralized by the hydroxyl radicals. In fact, such assumption, together with the hypothesis of reaching the same level of HQ mineralization of 40% as in the synthetic solution, would account for an overall TOC reduction of 52%, which is

very similar to the experimental one. Therefore, the higher TOC reduction is simply due to the organic load already present in the real wastewater.

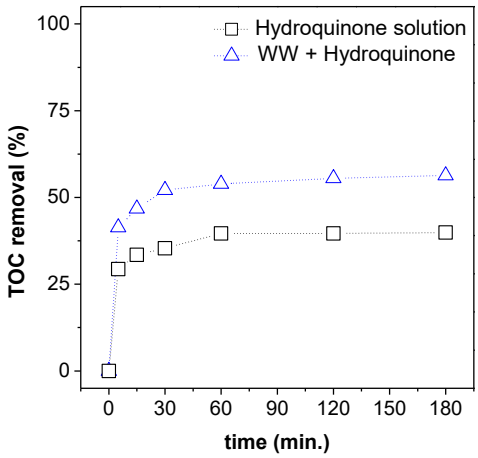

Figure 3.9 Comparison of TOC removal in distilled water (HW solution) and wastewater spiked with HQ ($[H_2O_2]$ = 500 mg/L; $[Fe^{2+}]$ = 45 mg/L; pH = 3.0; Q_{air} = 2.5 mL/min; T = 24 ºC; V = 5 L).

The wastewater spiked with HQ was characterized after three hours of treatment using the Fenton reagent in the BCR and the results are shown in Table 3.1. The COD reduction was ~59% (from 308.7 mg/L to 127.8 mg/L, before and after Fenton treatment, respectively). A small reduction of nutrients was observed: ~ 4% for total phosphorus and total nitrogen and ~2% for ammoniacal nitrogen. It was also observed a reduction of the solids in 11% for VSS and 18% for TSS and, consequently, a reduction of the turbidity (ca. 13%) was noticed. A nontoxic effluent was generated as regards the inhibition of *Vibrio fischeri*, which decayed from 100% before treatment to 0.0% after treatment.

Taking into account the good performance achieved by the Fenton process in the BCR for treating a domestic wastewater containing HQ, our future work will be focused on the treatability of real wastewaters and in the treatment of gas and liquid effluents simultaneously in the same device.

Table 3.1 Description of the real wastewater (WW) spiked with hydroquinone (100 mg/L) before and after the Fenton process application in the BCR.

Parameter	Real WW matrix	Real WW after Fenton	Removal (%)
pH	7.60	7.02*	---
TOC (mg C/L)	88.9	39.2	55.9
Turbidity (NTU)	30	26	13.3
COD (mg O_2/L)	308.7	127.8	58.6
TSS (mg/L)	22	18	18.2
VSS (mg/L)	18	16	11.1
Total phosphorus (mg/L)	13.22	12.72	3.8
Total nitrogen (mgN/L)	12.14	11.68	3.8
Ammoniacal nitrogen (mgN/L)	1.04	1.02	1.9
Nitrite (mgN/L)	0.007	0.006	14.3
Nitrate (mgN/L)	<0.18	< 0.18	---
Vibrio fischeri innibition (%)	100.00	0.00	---

*after neutralization.

3.4 Conclusions

The HQ degradation by the Fenton's process was studied in a bubble column reactor. A parametric study was carried out, allowing to conclude that: i) the air flow rate did not influence the HQ and TOC removal and promotes an efficient mixing and homogenization inside the column, ii) the bubbling promotes the stripping of some of the H_2O_2, although this effect is not strong enough and does not seem to affect the oxidation process, which radical reactions are considerably fast, and iii) the application of the Fenton reagent was efficient in the removal of this compound in the BCR (100% in the first minutes of reaction), providing a considerable mineralization degree (~39 %) under the best conditions employed.

The strategy of adding the oxidant (H_2O_2) gradually increased significantly the TOC removal (~55%) and the efficiency of oxidant use (from 0.37 when the oxidant is added once, in the beginning of reaction, to 0.49 with gradual addition). In both cases, the toxicity of the final effluent towards *Vibrio fischeri* was null, while the raw effluent completely inhibited the bacteria. Organic acids (maleic, pyruvic and oxalic) were identified in a run with HQ solution and the reaction mechanism was proposed.

Finally, it was found that the change of the matrix, i.e., using real wastewater instead of distilled water, did not influence the Fenton process because it was reached total HQ degradation and a similar mineralization.

3.5 References

Akyol, A., O. T. Can, and M. Bayramoglu. 2015. 'Treatment of Hydroquinone by Photochemical Oxidation and Electrocoagulation Combined Process'. *Journal of Water Process Engineering* 8: 45–54.

APHA, WEF A. 1988. 'Standard Methods for the Examination of Water and Wastewater'. In *Water Pollution Control Federation*, edited by American Public Health Association. Washington DC,: American Water Works Association.

Beheshti, N., and A. C. McIntosh. 2007. *A Biomimetic Study of the Explosive Discharge of the Bombardier Beetle*. *International Journal of Design and Nature*. Vol. 1.

Chang, S.W.C., H.L. Chen, M.C. Wang, and K. Seshaiah. 2009. 'Oxidative Degradation and Associated Mineralization of Catechol, Hydroquinone and Resorcinol Catalyzed by Birnessite'. *Chemosphere* 74 (8): 1125–33.

Clarizia, L., D. Russo, I. Di Somma, R. Marotta, and R. Andreozzi. 2017. 'Homogeneous Photo-Fenton Processes at near Neutral PH: A Review'. *Applied Catalysis B: Environmental* 209 (July): 358–71.

Duarte, F., V. Morais, F.J. Maldonado-Hódar, and L. M. Madeira. 2013. 'Treatment of Textile Effluents by the Heterogeneous Fenton Process in a Continuous Packed-Bed Reactor Using Fe/Activated Carbon as Catalyst'. *Chemical Engineering Journal* 232: 34–41.

Heijnen, J.J., and K. Van't Riet. 1984. 'Mass Transfer, Mixing and Heat Transfer Phenomena in Low Viscosity Bubble Column Reactors'. *The Chemical Engineering Journal* 28 (2): B21–42.

ISO. 2005. 'Water Quality - Determination of the Inhibitory Effect of Water Method, Samples on the Light Emission of Vibrio Fischeri (Luminescent Bacteria Test) - Part 3: Using Freeze-Dried Bacteria'. In . International Organization for Standardzation.

Ito, S., A. Kunai, H. Okada, and K. Sasaki. 1988. 'Direct Conversion of Benzene to Hydroquinone. Cooperative Action of Copper(I) Ion and Dioxygen'. *The Journal of Organic Chemistry* 53 (2): 296–300.

Kang, N., D. S. Lee, and J. Yoon. 2002. 'Kinetic Modeling of Fenton Oxidation of Phenol and Monochlorophenols'. *Chemosphere* 47 (9): 915–24.

Kang, S.-F., C.-H. Liao, and M.-C. Chen. 2002. 'Pre-Oxidation and Coagulation of Textile Wastewater by the Fenton Process'. *Chemosphere* 46 (6): 923–28.

Lominchar, M. A., S. Rodríguez, D. Lorenzo, N. Santos, A. Romero, and A. Santos. 2017. 'Activated Persulfate by NZVI, H_2O_2 and NaOH in Phenol Abatement and Development of a Kinetic Model for Alkaline Activation'. *Environmental Technology*, February, 1–32.

Lucas, M. S., and J. A. Peres. 2006. 'Decolorization of the Azo Dye Reactive Black 5 by Fenton and Photo-Fenton Oxidation'. *Dyes and Pigments* 71 (3): 236–44.

Lucas, M. S., J. A. Peres, and G. L. Puma. 2010. 'Treatment of Winery Wastewater by Ozone-Based Advanced Oxidation Processes (O_3, O_3/UV and O_3/UV/H_2O_2) in a Pilot-Scale Bubble Column Reactor and Process Economics'. *Separation and Purification Technology* 72 (3): 235–41.

Nanou, K., T. Roukas, E. Papadakis, and P. Kotzekidou. 2017. 'Carotene Production from Waste Cooking Oil by Blakeslea Trispora in a Bubble Column Reactor: The Role of Oxidative Stress'. *Engineering in Life Sciences*, 1–22.

Nidheesh, P.V., and R. Gandhimathi. 2015. 'Electro Fenton Oxidation for the Removal of Rhodamine B from Aqueous Solution in a Bubble Column Reactor under Continuous Mode'. *Desalination and Water Treatment* 55 (1): 263–71.

Oliveira, C., K. Gruskevica, T. Juhna, K. Tihomirova, A. Alves, and L. M. Madeira. 2014. 'Removal of Paraquat Pesticide with Fenton Reaction in a Pilot Scale Water System'. *Drinking Water Engineering and Science* 7: 11–21.

Owsik, I. A., and B. N. Kolarz. 2004. 'The Catalytic Oxidation of Hydroquinone: Influence of Surface Properties of Polymeric Catalysts with Aminoguanidyl Ligand on Catalytic Properties'. *Catalysis Today* 91–92 (July): 199–204.

Pérez, M., F. Torrades, X. Domènech, and J. Peral. 2002. 'Fenton and Photo-Fenton Oxidation of Textile Effluents'. *Water Research* 36 (11): 2703–10.

Ramirez, J. H., C. A. Costa, L. M. Madeira, G. Mata, M. A. Vicente, M.L. Rojas-Cervantes, A.J. López-Peinado, and R.M. Martín-Aranda. 2007. 'Fenton-like Oxidation of Orange II Solutions Using Heterogeneous Catalysts Based on Saponite Clay'. *Applied Catalysis B: Environmental* 71 (1): 44–56.

Rodrigues, C. S.D., L.M. Madeira, and R. A.R. Boaventura. 2009. 'Optimization of the Azo Dye Procion Red H-EXL Degradation by Fenton's Reagent Using Experimental Design'. *Journal of Hazardous Materials* 164 (2–3): 987–94.

Rollbusch, P., M. Bothe, M. Becker, M. Ludwig, M. Grünewald, M. Schlüter, and R. Franke. 2015. 'Bubble Columns Operated under Industrially Relevant Conditions – Current Understanding of Design Parameters'. *Chemical Engineering Science* 126:

660–78.

Salehi, K., S.M. Jokar, J. Shariati, M. Bahmani, M.A. Sedghamiz, and M.R. Rahimpour. 2014. 'Enhancement of CO Conversion in a Novel Slurry Bubble Column Reactor for Methanol Synthesis'. *Journal of Natural Gas Science and Engineering* 21 (November): 170–83.

Sasaki, S., K. Hayashi, and A. Tomiyama. 2016. 'Effects of Liquid Height on Gas Holdup in Air – Water Bubble Column'. *Experimental Thermal and Fluid Sicience* 72 (April): 67–74.

Sellers, R. M. 1980. 'Spectrophotometric Determination of Hydrogen Peroxide Using Potassium Titanium (IV) Oxalate'. *Analyst* 105 (1255): 950–54.

Silva, C.R., M.N. Esperança, A.J.G. Cruz, L.F. Moura, and A.C. Badino. 2015. 'Stripping of Ethanol with CO_2 in Bubble Columns: Effects of Operating Conditions and Modeling'. *Chemical Engineering Research and Design* 102 (October): 150–60.

Stacy, C. J., C. A. Melick, and R. A. Cairncross. 2014. 'Esterification of Free Fatty Acids to Fatty Acid Alkyl Esters in a Bubble Column Reactor for Use as Biodiesel'. *Fuel Processing Technology* 124 (February): 1–18.

Suresh, S. 2015. 'Biodegradation of Hydroquinone Using Sequential Batch Reactor : A Preliminary Study of Industrial Effluent'. *Research Journal of Chemistry and Environment* 15 (February): 48–56.

Suzuki, H., S. Araki, and H. Yamamoto. 2015. 'Evaluation of Advanced Oxidation Processes (AOP) Using O_3, UV, and TiO_2 for the Degradation of Phenol in Water'. *Journal of Water Process Engineering* 7: 54–60.

Thakur, S., and M. S. Chauhan. 2016. 'Removal of Malachite Green Dye from Aqueous Solution by Fenton Oxidation'. *International Research Journal of Engineering and Technology* 3 (7): 254–59.

Tokumura, M., M. Shibusawa, and Y. Kawase. 2013. 'Dynamic Simulation of Degradation of Toluene in Waste Gas by the Photo-Fenton Reaction in a Bubble Column'. *Chemical Engineering Science* 100 (August): 212–24.

Walling, C. 1975. 'Fenton's Reagent Revisited'. *Accounts of Chemical Research* 8 (4): 125–31.

Wonders, A. G., H. W. J. Jenkins, L. R. Partin, W. S. Strasser, and M. De Vreede. 2006. Optimized liquid-phase oxidation in a bubble column reactor. EP 1 786 555 B1, issued 2006.

Yan, L., J. Liu, Z. Feng, and P. Zhao. 2016. 'Continuous Degradation of BTEX in Landfill Gas by the UV-Fenton Reaction'. *RSC Adv.* 6 (2): 1452–59.

Chapter 4. Insights into Real Industrial Wastewater Treatment by Fenton's Oxidation in Gas Bubbling Reactors

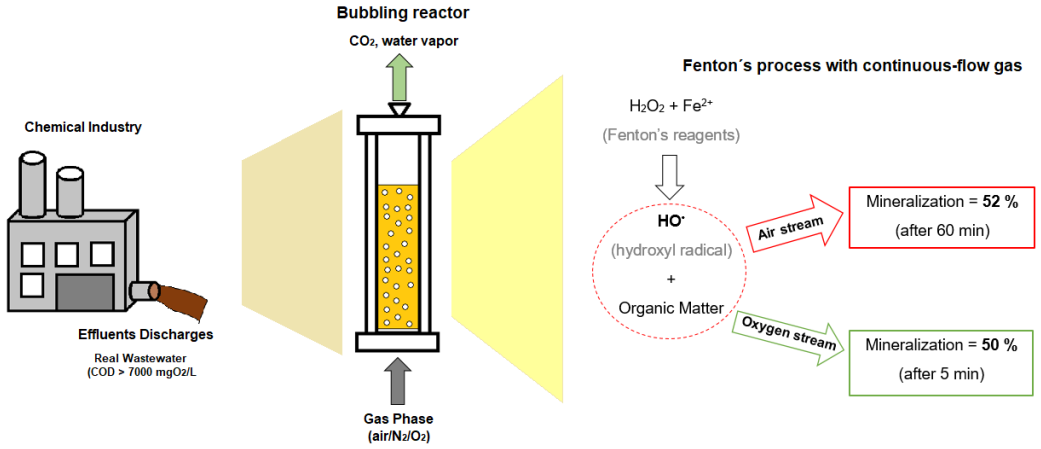

- Fenton's process in bubble reactors (BRs) was effective for real wastewater treatment;
- The treatment occurred with a continuous gas (air, O_2 or N_2) bubbling;
- The increase of the oxidant dose yielded a change in the temperature profile;
- The use of oxygen increased the efficiency of mineralization during the treatment;
- Temperature control in the BR was more effective than in a reactor with mechanical stirring.

The contents of this chapter were adapted from: Vanessa N. Lima, Carmen S. D. Rodrigues, Emanuel F. S. Sampaio, Luis M. Madeira (2020). *Insights into real industrial wastewater treatment by Fenton's oxidation in gas bubbling reactors*. **Journal of Environmental Management** (accepted).

Abstract: *In the present study, bubbling reactors (BRs) were chosen to design a new procedure for real industrial wastewater (WW) treatment by Fenton's oxidation. The process was carried out in BRs under batch mode for the treatment of a WW with a high organic load (chemical oxygen demand (COD) above 7000 mgO_2/L), being the efficient mixing of the liquid phase ensured by the gas bubbling. The parameters that influenced the WW treatment (i.e., H_2O_2 and Fe^{2+} concentration, and initial pH) were optimized in a smaller BR (0.5 L volumetric capacity); the maximum oxidation efficiency (dissolved organic carbon (DOC) removal = 52 % and COD removal = 83 % after 60 min) was reached under the following conditions: Q_{air} = 1.0 L/min (measured at room temperature and atmospheric pressure), [H_2O_2] = 22.5 g/L, [Fe^{2+}] = 0.75 g/L, and pH = 4.6 – original WW pH. It wasn't detected any significant effect in the process efficiency of the air flow rate and gas phase composition (i.e., N_2, and air), but when the process was performed with continuous O_2 bubbling an increase in the DOC removal (from 43 % to 53 %) was observed after 5 min of oxidation. Even so, the high costs discourage the use of pure oxygen streams in real WWTPs. To understand the dynamics of the process, the continuous air bubbling was compared to another mixing mode (mechanical stirring), and similar mineralization was achieved, proving the feasibility of Fenton's process in a BR. In addition, the gas bubbling proved to be more efficient in terms of heat dissipation during the treatment, decreasing temperature profiles along the oxidation of heavily charged real effluents. An effective scale-up with a bubble column reactor with a higher volumetric capacity by a factor of almost one order of magnitude was also proved, providing similar mineralization. The final effluent was non-toxic and more biodegradable; however it was still above the discharge limits of the local legislation, and so the original WW was treated by photo-Fenton's process, reaching almost 80 % mineralization.*

4.1. Introduction

Wastewaters (WW) discharge in water courses is environmentally damaging as long as they contain a significant organic load (Gulkaya *et al.* 2006; Poyatos *et al.* 2010; San Sebastián Martínez *et al.* 2003). WW characteristics are extremely diverse, presenting very often a high concentration of chemical pollutant species (Poyatos *et al.* 2010; Shon *et al.* 2006), mainly those resulting from industrial chemical processes. Such pollutants detrimentally affect the environment and the human health (Harold *et al.* 2014), particularly due to their toxicity (e.g., due to the presence of aromatic compounds) (US EPA 2014) and low-biodegradability that affects the microbiota and plants (Jing *et al.*, 2015). The risks associated have boost the environmental policies around the world, demanding effective treatment technologies to reduce these pollutants to levels framed in local legislation (European Council 2010).

The WW technologies implemented at wastewater treatment plants (WWTPs) focus on processes ranging from physical (e.g., filtration (Sincero and Sincero 2002)) to biological (e.g., activated sludge (Grady Jr. *et al.* 2011)). However, the potential of chemical processes stands out due to their efficiency in the full (or partial) destruction of many pollutants (Lima *et al.* 2018a). In this scenario, the advanced oxidation processes (AOPs) have been highlighted as environmentally friendly, clean and efficient technologies (Deng and Zhao 2015; Dewil *et al.* 2017; Muruganandham *et al.* 2014; Oller *et al.* 2011). The promising features of AOPs are the formation of extremely reactive oxidizing species (e.g., $HO^{\bullet}$ with an oxidation potential of 2.8 (Papadopoulos *et al.* 2007; Zhang *et al.* 2015)) that oxidize the pollutants as highlighted in Eqs. 4.1 and 4.2 for the case of $HO^{\bullet}$ (hydroxyl radical), promoting the oxidation of organic species (RH) into intermediate species that can ultimately be converted into carbon dioxide and water (Neyens and Baeyens 2003; Rodrigues *et al.* 2018a):

$$RH + HO^{\bullet} \rightarrow \text{Intermediate species} \quad (4.1)$$

$$\text{Intermediate species} + HO^{\bullet} \rightarrow CO_2 + H_2O \quad (4.2)$$

A well-known AOP is the Fenton process (Fenton 1894), which has advantages for WW treatment due to the low capital cost, high efficiency, uncomplicated control, and the application of environmentally friendly reagents (H_2O_2 and Fe^{2+}) (Lucas and Peres 2006). In the Fenton's process, the organic matter is oxidized by $HO^{\bullet}$ (Eq. 4.1), which is formed by the catalytic decomposition of H_2O_2 in the presence of Fe^{2+} (Eq. 4.3) (Barb *et*

al. 1949; Fenton 1894; Walling 1975), being the catalyst regenerated by reaction with hydrogen peroxide (Eq. 4.4) (Walling 1975).

$$H_2O_2 + Fe^{2+} \rightarrow HO^{\bullet} + HO^{-} + Fe^{3+} \quad (4.3)$$

$$Fe^{3+} + H_2O_2 \rightarrow Fe^{2+} + HO_2^{\bullet} + H^{+} \quad (4.4)$$

The Fenton's process has been reported extensively in the literature, being crucial to address the optimization of the main operation parameters (i.e., temperature, initial pH, and reagents concentrations) for the effective treatment of either model compounds or synthetic effluents, generally with low complexity (Bouasla *et al.* 2010; Oturan and Aaron 2014; Torrades and García-Montaño 2014; Xu *et al.* 2017), or even real WWs (Esteves *et al.* 2019; Guedes *et al.* 2003; San Sebastián Martínez *et al.* 2003), particularly those resulting from chemical industries.

The research about the application of Fenton's oxidation in multiphase reactors has increased as an alternative to the homogeneous batch or continuous stirred-tank reactors (CSTRs). In the recent years, significant results were reported for applications of Fenton's process in fluidized-bed (Qin *et al.*, 2018a, 2018b; Wei *et al.*, 2015) and bubbling reactor (Lima *et al.*, 2018b; Rodrigues *et al.*, 2018a) configurations. Particularly, the bubbling reactors (BRs) seem to be encouraging for Fenton's process implementation due their features, e.g. easy control, maintenance, and adaptation for large systems at WWTPs. In addition, for application in environmental (and other) engineering systems, the gas bubbling has high interest (Lyu *et al.*, 2019) due to the high mass and heat transfer rates (Deckwer, 1979; Kantarci *et al.*, 2005; Zehner and Kraume, 2000), which drives the application of BRs to pollutant treatment in two-phase systems (e.g., gas stream treatment in liquid phase (Tokumura *et al.*, 2008; Xie *et al.*, 2019; Yan *et al.*, 2016)). Nevertheless, the application of Fenton's oxidation (or others AOPs) to real WW treatment in BRs has not been reported yet.

So, aiming to implement an efficient strategy to perform the Fenton oxidation, BRs were chosen to evaluate the treatability of a real industrial WW. The treatment was performed by the homogeneous Fenton process using, as a mixing mode, continuous gas bubbling, a process only reported for simulated effluents treatment (Lima *et al.*, 2018b; Rodrigues *et al.*, 2018a). The primary operating conditions were optimized in a detailed parametric study in order to maximize process mineralization. The treatment efficiency (and heat management) was also evaluated comparing the continuous gas bubbling with the classic mechanical stirring. Still, the process was scaled-up to a bubble column reactor (BCR), processing almost one order of magnitude more volume than the BR. Finally, in

order to improve the mineralization, the WW was also treated by the photo-Fenton process.

4.2 Material and methods

4.2.1 Real industrial wastewater

The real industrial wastewater (WW) was collected in a chemical industry plant located in Portugal. The samples were stored in 4 L-capacity plastic bottles at -15 ºC. Before the WW treatment, they were defrosted at room temperature and homogenized to obtain an effluent with the same conditions for all runs.

4.2.2 Reactors configuration

Fenton's oxidation experiments were performed in a 900 mL-capacity acrylic jacketed bubbling batch reactor – BR. The temperature of the medium (T_{ref} = 25 ºC) was controlled by recirculating water in the reactor jacket with the help of a thermostatic bath (Polystat CC1). The gas bubbling inside the reactor was performed by continuous gas supply with an air pump (HAILEA, ACO-2202). The gas bubbling was reached with a cylindrical gas diffuser (coarse-grain inert stone – HxD = 2.5x1.4 cm) installed centrally and axially inside the reactor. The continuous bubbling was controlled using a flowmeter (Ohmega FL-2015) installed in the gas piping between the pump/gas system and the BR, in order to obtain a predetermined gas flow rate (Q_{gas}) following the procedure described elsewhere (Lima *et al.*, 2018b; Rodrigues *et al.*, 2018a).

The Fenton's oxidation run without gas bubbling was carried out under the same batch reactor without the presence of the gas diffuser. For this experiment, the mixing inside the reactor was performed by agitation with a mechanical stirring system at 250 rpm, for which a magnetic bar and stirrer plate (P-Selecta, model AGIMATIC-S) have been used.

The scale-up was carried out in a 9 L-capacity acrylic jacketed bubble column reactor (BCR); for more details about this device please refer to previous works (Lima *et al.*, 2018b; Rodrigues *et al.*, 2018a)). The temperature of the medium (T_{ref} = 25 ºC) was also controlled by recirculating water through the reactor jacket connected to a thermostatic bath (Polystat CC1), and the air bubbling (1.0 L/min, measured at room temperature and atmospheric pressure) was reached by feeding the gas phase through a dispersive plate (with nine holes of ø - 0.5 mm) placed in the bottom of the BCR.

The photo-Fenton's process was carried out in a 500 mL-capacity glass cylindrical reactor coupled with a TQ 150 mercury lamp, which has a power of 150 W (corresponding to a light intensity of 500 W/m^2 – 60 W/m^2 in the UV region and 440 W/m^2 in the visible region). As described elsewhere (Rodrigues *et al.*, 2018b), the lamp was placed axially centred in the reactor inside a quartz jacketed tube with temperature control using recirculating water from a thermostatic bath (Polystat CC1).

4.2.3 Experimental Procedure

4.2.3.1 Fenton's experiments

For the dark Fenton's oxidation runs, the BR was filled with 500 mL of WW; then, and if required, the pH of the effluent was adjusted with 1 M H_2SO_4 (99 %, VWR) or 3 M NaOH (99%, Vencilab) to the desired value. After the required mass of catalyst ($Fe_2SO_4.7H_2O$, 99%, Panreac) was added to the solution, the gas bubbling was turned on at the same time that the H_2O_2 (30 %, VWR) was injected (this instant coincides with the starting of the reaction – t = 0). For the reaction without bubbling, it was proceeded the same way, but replacing the gas bubbling by the mechanical stirring as described above.

For the scale-up runs, the BCR was filled with 4.0 L of WW at the natural pH, and the Fenton's oxidation was carried out at room temperature and atmospheric pressure following the same procedure as described above for the BR.

In all experiments, liquid samples were collected at pre-selected times for measuring, immediately, the pH (pH meter Level 2 from Inoar), the temperature and residual H_2O_2 concentration. Moreover, the dissolved organic carbon (DOC) and chemical oxygen demand (COD) were also determined in the samples after stopping the homogeneous reaction by adjusting the pH to 10 (which promotes the elimination of residual H_2O_2 (Zhang *et al.*, 2005)) using 5 M NaOH.

4.2.3.2 Processes assisted with radiation

For the runs with UV-vis radiation, the photo-reactor (described in section 2.2) was filled with 300 mL of WW at the natural pH and room temperature. For the photo-Fenton's trial, it was added the mass of catalyst ($Fe_2SO_4.7H_2O$) required, followed by H_2O_2 at the same time that the mercury lamp was turned on (this instant coincides with the starting of the reaction - t = 0). The sampling of the liquid along these runs was performed as described above for the Fenton's trials.

4.2.4 Analytical methods

For determination of the DOC, all samples were filtered through a 0.45 µm PTFE filter, and the measurement was performed according to method 5310 D (APHA, 1988) using a TOC-L analyzer from Shimadzu. For the COD analysis, it was performed according to method 5220 D in closed reflux (APHA, 1988). The biological oxygen demand (BOD_5) was measured according to method 5210 D (APHA, 1988); the incubation was performed at 20 ºC during five days in an OxiTOP Box (WTW) incubator. The total suspended solids (TSS) was quantified by gravimetry through method 2540 B (APHA, 1995). The turbidity was measured according to Method 2130 B (APHA, 1988), using a turbidimeter HI88703 from Hanna Instrument. The toxicity of the effluent was assessed by inhibition of *Vibrio fischeri* in accordance with the standard DIN/EN/ISO 11348-3 (Standardization 2005). For the latter, the neutralized samples were in contact at 15 ºC with the bacteria, and the bioluminescence was measured after 5, 15 and 30 min in a Microtox Model 500 analyzer (Modern Water). The residual H_2O_2 concentration along the oxidation experiments was measured according to the method developed by Sellers (Sellers, 1980); for that a HEλIOS γ spectrophotometer (from Thermo Electron Corporation) was used for measuring the absorbance at 400 nm of the yellow-orange complex formed after the reaction between the hydrogen peroxide with titanium oxalate (IV).

4.3 Results and discussion

Table 4.1 reports the characterization of the real industrial wastewater before treatment. The WW has a high organic load (COD above 7000 mgO_2/L)), and low biodegradability (represented by the low BOD_5:COD ratio - 0.007). The low biodegradability is associated with the presence of organic chemical toxic species (not identified in this study), which limits the application of biological treatments.

So, taking into account the features of this real WW, it was decided to evaluate the feasibility of the Fenton's treatment process using bubbling reactors. The results about the effects of the main operating parameters of the Fenton's oxidation in the WW treatment are reported and discussed in the following sections.

Table 4.1 Characteristics of the real industrial wastewater before and after the Fenton and photo-Fenton processes under optimal conditions (removal efficiencies are shown between brackets).

Parameters	Original WW	WW treated by Fenton's oxidation*	WW treated by photo-Fenton's oxidation**	Emission limit value[a]
pH	4.6	6.9[b]	7.1[b]	6.0-9.0
Turbidity (NTU)	8.90	0.05 (99 %)	0.03 (99 %)	---
TSS (mg/L)	52.4	250.3	248.2	60
BOD_5 (mg O_2/L)	47	60	n.d.[c]	40
COD (mg O_2/L)	7019	1193 (83 %)	772 (89 %)	150
DOC (mg C/L)	2482	1290 (52 %)	512 (79 %)	---
BOD_5:COD	0.007	0.04	---	---
Vibrio fischeri inhibition $_{30\ min.}$ (%)	0.00	0.00	0.00	---

* Treatment performed in the bubbling reactor using continuous bubbling of air at 1.0 L/min.
** Treatment performed in the photo-reactor with mechanical stirring (250 rpm).
[a] Portuguese legislation for discharge of wastewaters (ordinance no. 236 of August 1, 1998).
[b] pH after neutralization.
[c] n.d. - not determined.

4.3.1 Effect of reaction parameters

A parametric study was performed to evaluate the effect of primary reaction conditions of the Fenton's process, namely reagents (H_2O_2 and Fe^{2+}) concentration, and initial pH.

4.3.1.1 Effect of the oxidant dose

The H_2O_2 concentration is an essential parameter of the Fenton's process. The optimization of H_2O_2 dose is responsible for ensuring enough amount of oxidant for an efficient formation of $HO^{\bullet}$ species by Fenton's reaction (Eq. 4.3). Besides, its minimization represents a reduction of costs and reagents for processes in WWTPs, notably when the WW contains a high organic load.

The range of oxidant doses was calculated from the theoretical stoichiometry required based on the initial COD of the WW (Deng and Englehardt, 2008; Lucas and Peres, 2009). The stoichiometric H_2O_2 concentration obtained (14.9 g/L) represents the value needed to perform the complete removal of the COD present in the WW. Oxidant doses

in the range of 0.5 - 1.7 as compared to the stoichiometric one have been employed. The initial catalyst concentration was calculated to obtain a $[Fe^{2+}]$:$[H_2O_2]$ ratio (w/w) of 1:20 (value recommended by other authors (Pérez *et al.*, 2002; Torrades *et al.*, 2003)), yielding 0.75 g/L of Fe^{2+}. The initial pH of the liquid was the original of the WW (pH_0 ~ 4.6, cf. Table 4.1).

Figure 4.1 reports the influence of the hydrogen peroxide concentration, showing that when the oxidant dose was increased above 20 g/L, 43% of DOC removal was achieved after 5 min, regardless of the H_2O_2 dose (namely 22.5 or 25.0 g/L – Fig. 4.1a). For all the doses tested, the WW mineralization was initially fast, with a low increase until the end of the process. For doses below the stoichiometric one, the DOC removals decreased to 37 and 25 % at the end of the process when H_2O_2 concentrations of 12.5 and 7.5 g/L were dosed, as a consequence of the low formation of $HO^{\bullet}$ species along the treatment process. The maximum DOC removal was achieved when 22.5 g/L of H_2O_2 was dosed, being the mineralization reached 52 % at 60 min. Above this value, the difference of DOC removal was negligible, which could indicate the onset of scavenging reactions of the $HO^{\bullet}$ formed with excess H_2O_2 (Eq. 4.5) (Walling, 1975), reducing the amount of oxidizing species available for mineralization.

$$H_2O_2 + HO^{\bullet} \rightarrow HO_2^{\bullet} + H_2O \quad (4.5)$$

For all H_2O_2 doses tested, the pH decreased abruptly at 5 min of reaction, but the acidification was steeper when dosing above 15 g/L of oxidant (from pH 4.6 to 1.98 - Fig. 4.1b). A similar result was reported by Guerreiro *et al.* (2016) for the treatment of sugarcane vinasse when a range of 14.5 to 25 g/L of H_2O_2 was tested (in a batch reactor with mechanical stirring). The pH reduction along the reaction is commonly associated with the formation of intermediate species (Esteves *et al.*, 2019), probably organic acids (i.e., short-chain organic acids) that result from aromatic organic compounds degradation (Zazo *et al.*, 2005).

In spite of the high doses of oxidant, the H_2O_2 consumption was fast for all runs, being nearly entirely consumed (> 95%) at 30 min of the process (Fig. 4.1c); a similar trend was reported by Esteves *et al.* (2019), whom used 25 g/L of H_2O_2 for the treatment of high-strength olive mill wastewater. Without H_2O_2 available, the oxidation was considerably slowed down, as can be seen in the DOC removal and pH profiles, which show a plateau after ca. 15-30 min; for this reason, it was decided to stop the runs after 60 min. It is noteworthy that for the treatment of real WWs with high organic loads by Fenton's oxidation are usually required high H_2O_2 doses, as also reported by Gulkaya *et*

al. (2006) whom employed above 90 g/L of H_2O_2 for the treatment of a carpet dyeing WW with a similar DOC concentration (2400 mgC/L).

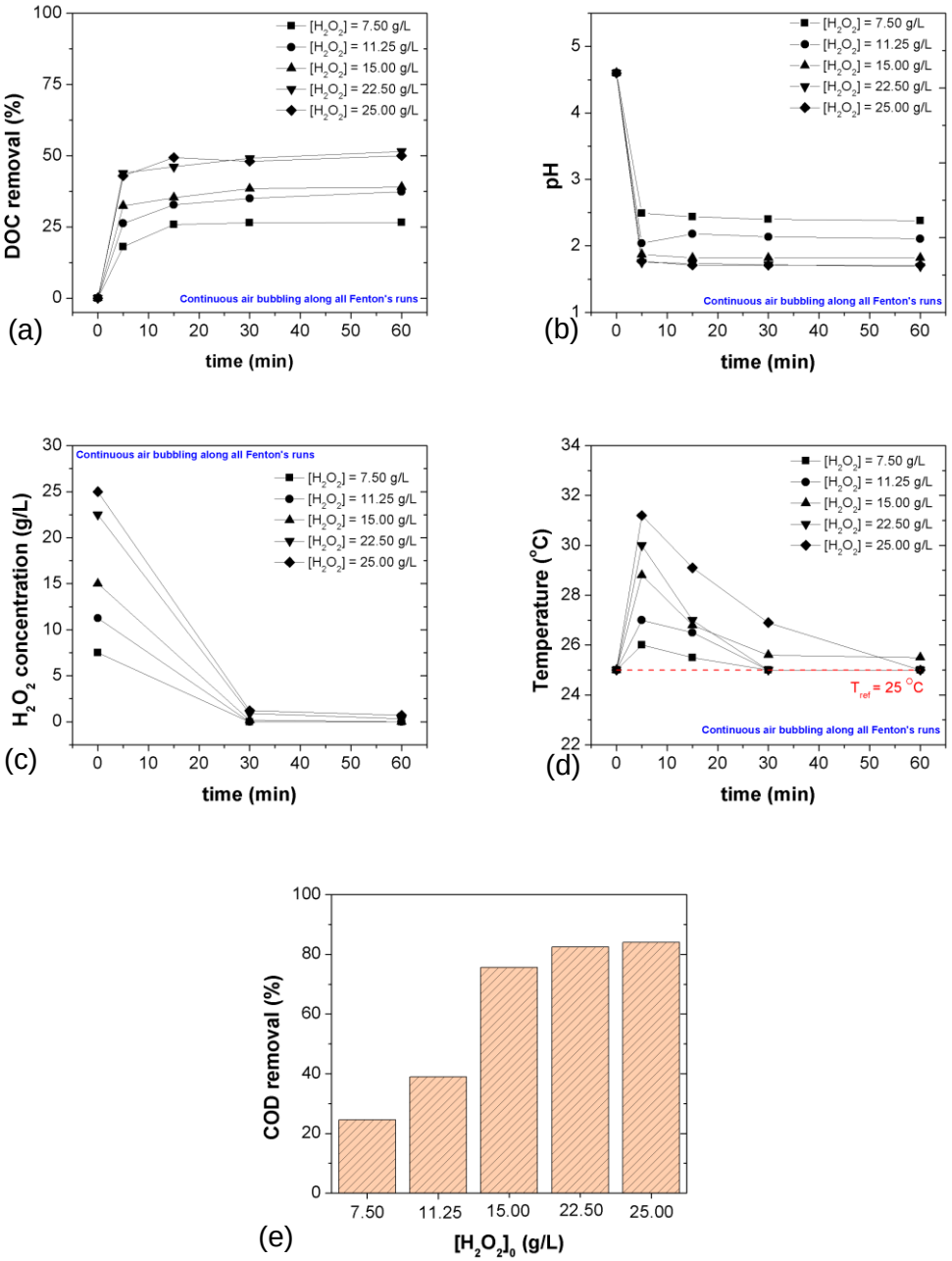

Figure 4.1 Influence of oxidant dose on the evolution of the DOC removal (a), reduction of pH (b), consumption of H_2O_2 (c), and temperature profile (d) along the oxidation process, and COD removal (e) after the WW treatment (t = 60 min) performed in the bubble reactor. Experimental conditions: $[Fe^{2+}]$ = 0.75 g/L, pH = 4.6, V = 0.5 L, $T_{ref.}$ = 25 ºC, and Q_{air} = 1.0 L/min.

Due to the range of H_2O_2 doses, a change in the temperature profile along the reactions was observed (Fig. 4.1d). Regardless of the oxidant dose, a fast increase in the temperature was observed. For the Fenton's process, the increase of temperature is

strongly associated with the following (exothermic) reactions: 1) $HO^{\bullet}$ formation (Eq. 4.3) and 2) oxidation of organic compounds by $HO^{\bullet}$ (Eqs. 4.1-4.2). So, the fast $HO^{\bullet}$ formation, summed to a significant mineralization of a complex and heavily charged WW, releases enough heat which increases the temperature of the liquid phase. For this study, this effect was most notorious in the runs with H_2O_2 doses above 20 g/L, which provided increases of temperature that reached 5-6 ºC above the reference temperature (T_{ref} = 25 ºC). Similar behaviour was reported by Martínez *et al.* (2003) for the treatment of an extremely polluted industrial wastewater by the Fenton's process (in a reactor with mechanical stirring), whom observed a "quick boiling" of the liquid phase due to the increase of the temperature when using a high H_2O_2 load (5 M, which corresponds to 170 g/L). Even though this AOP is known to be exothermic, the thermal profile is not usually reported in the literature, but can be an important issue to take into account in what concerns safety operation of chemical reactors in WWTPs, particularly during oxidation of effluents with a huge organic load, which might be considerably exothermic.

Regarding the COD removal in the overall treatment (i.e., after 60 min), Fig. 4.1e shows that it increases with the oxidant dose, but for 25 g/L of H_2O_2 the benefits are almost negligible. So, the dose of 22.5 g/L (providing 83% of COD removal) was selected as the optimal one for subsequent runs.

4.3.1.2 Effect of the catalyst dose

A series of experiments were carried out to determine the best catalyst concentration for the WW treatment. Data along process time are shown in the Appendix section (Fig. A. 2.1), while Fig. 4.2a) reports the influence of the catalyst concentration in the overall DOC and COD reduction.

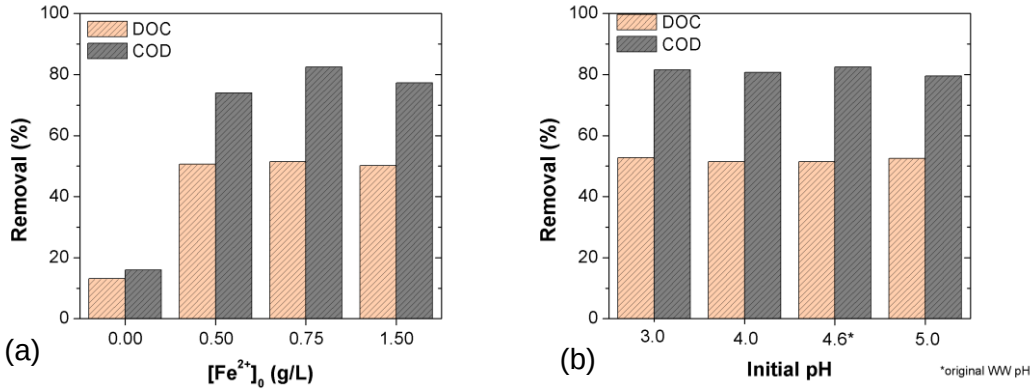

Figure 4.2 Effect of the catalyst dose (a) and initial pH (b) on the WW treatment (t = 60 min) performed in the bubble reactor. Experimental conditions: $[H_2O_2]_{a) \text{ and } b)}$ = 22.5 g/L, $[Fe^{2+}]_{b)}$ = 0.75 g/L, $pH_{a)}$ = 4.6, V = 0.5 L, $T_{ref.}$ = 25 ºC, and Q_{air} = 1.0 L/min.

For the process without catalyst ($[Fe^{2+}]$ = 0.00 g/L), more than 10 % of DOC was removed quickly within 5 min of treatment (Fig. 4.1a). After this time, the mineralization increased a little bit reaching 13 % after 60 min (Fig 4.2a), due to the low oxidation potential of the H_2O_2 (1.77 eV (Papadopoulos *et al.*, 2007)) and the absence of radicals being formed when H_2O_2 is used alone, without catalyst. The maximum DOC and COD removals after 60 min of treatment (52 and 83 %, respectively) were observed for the dose of 0.75 g/L of Fe^{2+}, in spite that minor differences were obtained for the other concentrations tested (cf. Fig A.2.1a and Fig 4.2a)). The reduction of the process efficiency observed for the highest catalyst dose may be associated with the parallel scavenging reaction between the Fe^{2+} in excess and the formed $HO^{\bullet}$ (Eq. 4.6) (Walling, 1975).

$$Fe^{2+} + HO^{\bullet} \rightarrow Fe^{3+} + HO^{-} \quad (4.6)$$

For the run with only H_2O_2, the pH reduced a little bit (Fig. A.2.1b in the Appendix section), while for all Fenton's experiments the medium acidification was similar regardless of the iron concentration (Fig. A.2.1b), which reflects the low influence of the catalyst dose under the range tested. It was found by complementary blank runs that the pH decrease is mostly due to the organics oxidation and not to the iron salt addition to the medium (data not shown).

Regarding the evolution of H_2O_2 along the processes, for the experiment without iron the oxidant concentration only slightly decreased, remaining more than 15 g/L at the end of the treatment (Fig. A.2.1c). On the other hand, for all Fenton's runs in the presence of iron the reduction of the H_2O_2 concentration was fast, being slightly steeper for the superior Fe^{2+} dose, in which the full nearly complete oxidation consumption was achieved after 30 min (Fig. A.2.1c).

Finally, the thermal profiles were also similar for all Fenton's runs (Fig. A.2.1d), due to the also similar mineralization histories, while for the experiment using only hydrogen peroxide, the temperature increase was negligible (Fig. A.2.1d).

4.3.1.3 Effect of the initial pH

Further experiments were carried out to evaluate the influence of the initial pH in the WW oxidation, which was adjusted in order to obtain a range between 3.0 to 5.0 (a pH range ideal for Fenton's oxidation (Bautista *et al.*, 2008)). However, the pH did not show any

significant effect on the overall DOC and COD removals, i.e., after 60 min of oxidation (Fig. 4.2b).

Data along process time are shown in the Appendix section (Fig. A.2.2). It was found again that the reduction of DOC reached to a similar removal (above 40 %) after 5 min, increasing slowly until 60 min of the process regardless of the initial pH (Fig. A.2.2a). Similar patterns were found in terms of pH reduction (Fig. A.2.2b) that was very quick at 5 min of process time, reaching values as low as 1.8, but remained nearly the same for longer reaction times, whatever the initial pH of the WW. The consumption of the oxidant (Fig. A.2.2c) was also similar, reaching almost full consumption after 60 min of treatment. Finally, the temperature profile (Fig. A.2.2d) along the runs followed the same overall trend.

For the following experiments, the pH was the original one of the wastewater (4.6), which decreases the costs with chemicals for the WW treatment process.

4.3.2 Influence of the reactor parameters

Some factors could affect the phenomena inside the BR along the treatment process, for example, the gas flow rate (and inherently the gas velocity), the composition of the gas phase, and the bubble size (Lima *et al.*, 2018a). Taking into account the technical restrictions of the BR configuration, only the effects of air flow rate and gas phase composition were evaluated, and the gathered results are reported in the next sections.

4.3.2.1 Influence of the air flow rate

For the WW treatment herein addressed, the gas bubbling will be the main parameter responsible for the mixing inside the reactor (Lima *et al.*, 2018b; Rodrigues *et al.*, 2018a). The mixing rate is a limiting factor for the $HO^{\bullet}$ formation, and it is strongly associated with the continuous production (and consumption) of $HO^{\bullet}$ along the oxidative process (Farshchi *et al.*, 2019). So, the determination of the appropriate air flow rate is essential to regulate the treatment process in a BR.

To evaluate the influence of the air flow rate, experiments were carried wherein this parameter was changed in the range between 1 to 5 L/min of air (see Fig. A.2.3 in the Appendix A.2.2 for data along time). For the DOC removal (Fig. A.2.3a), reduction of the pH (Fig. A.2.3b), and oxidant consumption (Fig. A.2.3c), almost no differences have been noticed when the air flow rate was changed. So, one can anticipate that the BR

had a similar performance showing an excellent mixing along the process, as reported in other similar previous studies (Lima *et al.*, 2018b; Rodrigues *et al.*, 2018a). On the other hand, it is known that the increase of the air flow rate promotes the rise of the gas velocity inside the liquid phase, increasing the turbulence inside the BR, thus affecting the heat transfer rate (Kantarci *et al.*, 2005). However, from the temperature profiles obtained (Fig. A.2.3d), one can conclude that in the range tested, the air bubbling did not affect heat dissipation.

4.3.2.2 Effect of the gas phase composition

The gas phase composition is a fundamental parameter of AOPs performed in BRs, as shown for ozonation (Lucas *et al.*, 2009) and electro-Fenton (Nidheesh and Gandhimathi, 2015) processes. For both cases, the gas supplied in the BR (O_3 or O_2) is responsible for contributing to the effluents oxidation (Deng and Zhao, 2015; Lima *et al.*, 2018a). So, the influence of the gas phase composition during the real WW treatment by Fenton's oxidation in the BR was evaluated. Oxygen (O_2) and nitrogen (N_2) pure streams were selected for this study because these constituents are present in the air stream previously tested.

Figure 4.3 reports the effect of the gas phase composition along the WW treatment by Fenton's oxidation with continuous gas bubbling under the previously identified best operating conditions. The DOC removal (~ 51 % - Fig. 4.3a) obtained using air bubbling was similar when the N_2 stream was bubbled (one should notice that nitrogen is the major constituent of air, ca. 79%). However, when air was replaced by a pure O_2 stream, the DOC removal increased achieving a reduction above 50 % after 5 min of reaction, with a slight increase along the treatment time (Fig. 4.3a), demonstrating the influence of O_2 for the degradation of organic matter under the conditions tested. It should be noted that pure oxygen feeding, under the same gas flow rate, favours oxygen solubility. The increase of DOC removal (reaching > 55 % after 60 min) could be associated with the: 1) oxidation of organic compounds by O_2 itself (oxidation potential – 1.23 eV (Legrini *et al.*, 1993)) and/or 2) formation of superoxide species ($O_2^{\bullet-}$) produced through the reaction between oxygen and Fe^{2+} (Eq. 4.7).

$$O_2 + Fe^{2+} \rightarrow Fe^{3+} + O_2^{\bullet-} \quad (4.7)$$

In addition, the intermediate species could interact with the oxygen to form peroxyl radicals ($RO_2^{\bullet}$) – Eq. 4.8 – an intermediate species that initiates organics degradation through oxidation (Zhang *et al.*, 2008) with $HO^{\bullet}$ up to complete mineralization (Eq. 4.2).

$$O_2 + R^{\bullet} \rightarrow RO_2^{\bullet} \quad (4.8)$$

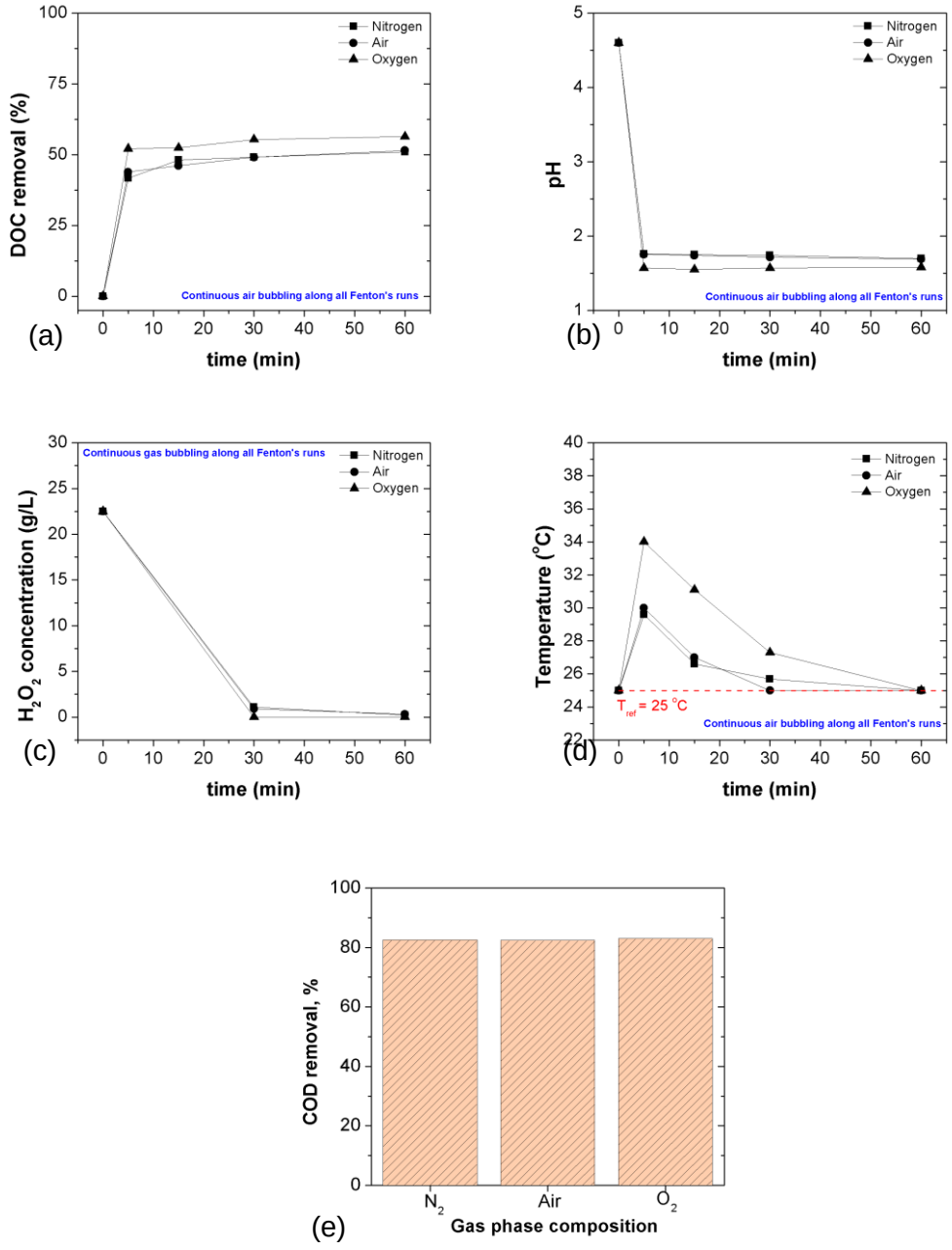

Figure 4.3 Influence of the gas phase composition (air, N_2 or O_2) on the evolution of the DOC removal (a), reduction of pH (b), consumption of H_2O_2 (c), and temperature profile (d) along the oxidation process, and COD removal (e) after the WW treatment (t = 60 min) performed in the bubble reactor. Experimental conditions: $[H_2O_2]$ = 22.50 g/L; $[Fe^{2+}]$ = 0.75 g/L, pH = 4.6, V = 0.5 L, $T_{ref.}$ = 25 ºC, and Q_{gas} = 1.0 L/min.

Thus, a slight increase in the acidification (Fig. 4.3b) for the WW treatment with O_2 was observed, and the consumption of H_2O_2 was nearly complete after 30 min of reaction (Fig. 4.3c), even if a slight increase of DOC removal until the end of process was

observed. Regarding the temperature profile, a steeper increase was observed (above 9 ºC) when O_2 was used, reaching ~ 35 ºC (Fig. 4.3d) under the same conditions of gas flow rate, probably due to the increase of the mineralization under these conditions. However, the COD removal after 60 min of treatment was similar (above 80%) regardless of the gas phase composition (Fig. 4.3e), which might be due to the formation of inorganic oxidation by-products.

Some effects on the Fenton process with O_2 and N_2 had already been reported by Du *et al.* (2006) and Du and Lei (2007); however, the continuous air bubbling for the treatment of real wastewaters by Fenton's oxidation was never reported. Even so, as demonstrated by these authors and our data, the best efficiency of Fenton's oxidation was reached when O_2 was present in the liquid medium. Nevertheless, aiming for the application at WWTPs, the use of gas bubbling using pure gas streams is more expensive. So, in the next sections, the Fenton process is employed with continuous air bubbling under the best conditions previously identified.

4.3.2.3 Influence of the mixing mode

The efficiency of the Fenton's process is promoted by a good mixing of the liquid phase (Farshchi *et al.*, 2019), which can be reached through different strategies. Usually, the Fenton's process is performed with continuous mechanical stirring. To assess the efficiency of the air bubbling along the Fenton's process, the BR was compared with another mixing mode, where air bubbling was replaced by mechanical stirring.

Figure 4.4 shows the influence of the reactor configuration (two mixing modes) in the WW treatment by Fenton's oxidation. It was observed that regardless of the mixing mode (bubbling or stirring), the DOC removal was similar (Fig. 4.4a). The mineralization was initially quite fast in both processes, and, for this reason, the reduction of the pH (Fig. 4.4b) and consumption of H_2O_2 (Fig. 4.4c) followed the same trends in both reactors. The results reinforce the usability of the BR to ensure an effective and efficient mixing along the Fenton process for the treatment of a real WW. Regarding the temperature profiles (Fig. 4.4d), the results showed that they are considerably affected by the reactor configuration employed. For the run with mechanical stirring, the temperature reached by the liquid as a consequence of the oxidative process was superior (although almost not affecting the mineralization – see Fig. 4.4a), reaching an increase of more than 17 ºC in only 5 min (Fig. 4.4d). After this time the temperature decreased slowly along the process, never reaching $T_{ref.}$ (25 ºC), even after 120 min. In opposition, for the run with air bubbling, the temperature increased only ~ 5 ºC and the T_{ref} was achieved after 30

min, allowing to conclude that the gas bubbling promoted an excellent heat transfer along the treatment (a primary advantage of bubbling processes (Rollbusch *et al.*, 2015; Shah *et al.*, 1982; Zehner and Kraume, 2000)), which is crucial in what concerns industrial processes safety.

To evaluate the effect of the reactor configuration on the heat released along the $HO^{\bullet}$ formation (i.e., exclude the organics oxidation), two blank runs using only Fenton's reagent in water (under the same conditions tested for WW treatment) were carried out; results are shown in Fig. A. 2.4. For both experiments, a change in the thermal profile was observed due to $HO^{\bullet}$ formation; however, a superior increase in temperature was again registered for the mechanical stirring process. Although temperature increased due to the exothermic Fenton reaction, degradation of organics is considerably much more exothermal (compare temperature profiles in Fig. A. 2.4 and Fig. 4.4d).

So, considering that it was obtained a similar DOC and COD reduction for both configurations (Figs. 4.4a and 4. 4e, respectively), the BR proved to be more efficient in terms of thermal control during highly exothermic reactions, and this further increases the interest in gas bubbling for WWTPs.

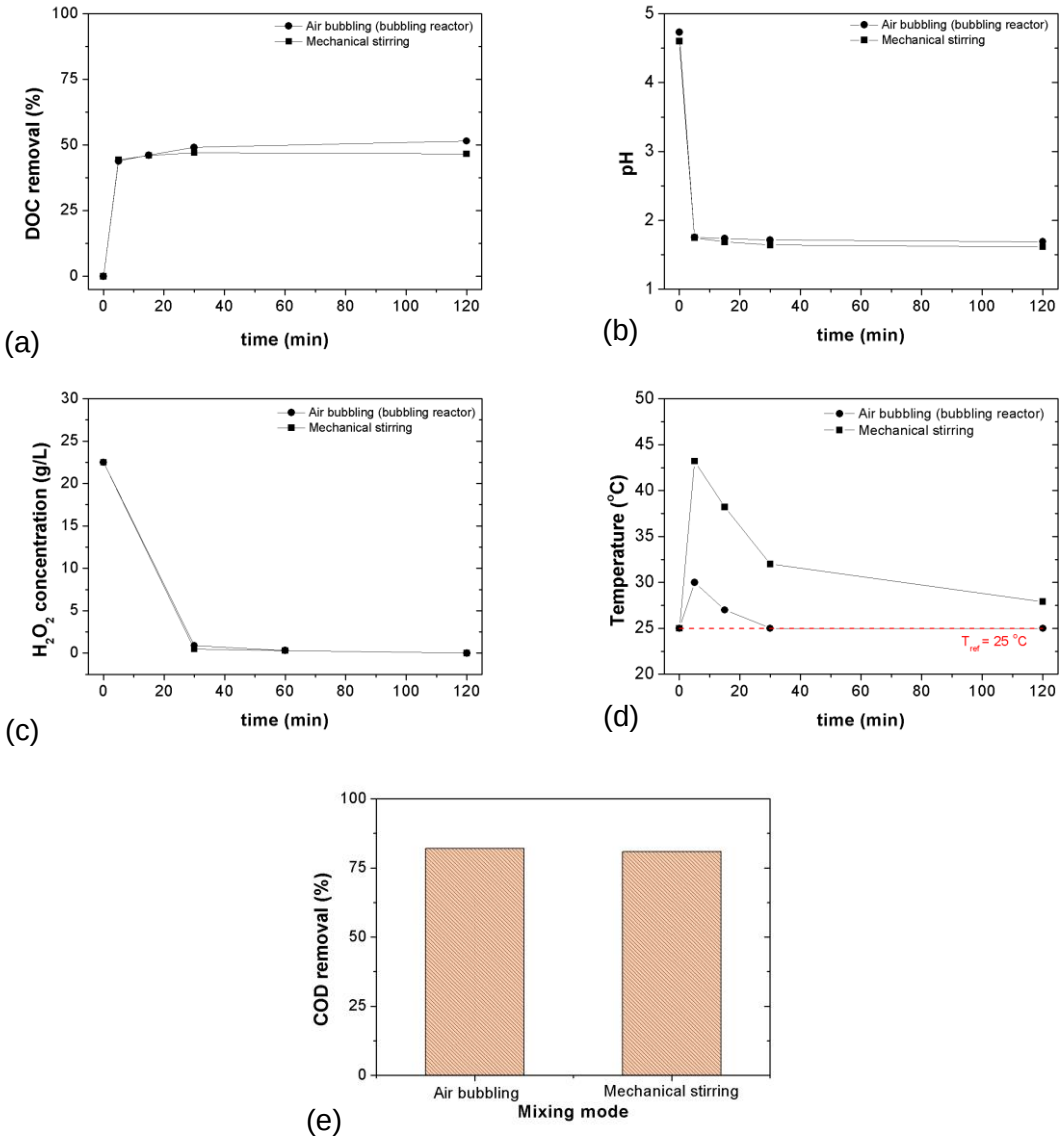

Figure 4.4 Influence of the reactor configuration mixing mode on the evolution of the DOC removal (a), reduction of pH (b), consumption of H_2O_2 (c), and temperature profile (d) along the oxidation process, and COD removal (e) after the WW treatment (t = 60 min) performed in the bubble reactor with and without air bubbling. Experimental conditions: $[H_2O_2]$ = 22.50 g/L; $[Fe^{2+}]$ = 0.75 g/L, pH = 4.6, V = 0.5 L, $T_{ref.}$ = 25 ºC, $Q_{air\ at\ BR}$ = 1.0 L/min or $V_{batch\ reactor}$ = 250 rpm.

4.3.3 Scale-up to a bubble column reactor (BCR)

Considering the possible future application of the Fenton's process with continuous air supply in WWTPs, a scale-up from the BR to a BCR (with a capacity ca. 1 order of magnitude higher) was performed. Due to experimental limitations, different air dispersers have been used (i.e., a cylindrical gas diffuser in the BR, and a dispersive plate with nine holes in the BCR), but with the same reactor diameter (9.8 cm).

Figure 4.5 shows the results obtained with the scale-up. A very slight increase of the mineralization was observed when the process was carried out in the BCR, being this effect noticed after 5 min of reaction (Fig. 4.5a). However, the reductions of the pH (Fig. 4.5b) and H_2O_2 (Fig. 4.5c) were similar for both reactors. The temperature increase was more pronounced in the BCR, being that after 5 min the temperature increased 9 ºC above $T_{ref.}$ (Fig. 4.5d), demonstrating an effect of the bubble size and reactor aspects ratios in the heat dissipation. The increase of the liquid volume in the BCR implied a less efficient contact between the gas and the liquid phase, thus affecting the dissipation of heat generated by the Fenton and oxidation reactions (both exothermic processes). In spite of the change in the thermal profile, the COD removal was similar in both bubbling reactors (above 80%) – Fig. 4.5e. So, it is concluded that the process was effectively scaled-up, although larger scales are still required for application in WWTPs. Besides, it is worth noting that this process has the advantage of being able to be applied in tanks already equipped with bubbling systems, as in dissolved air flotation (Rubio *et al.*, 2002) and air stripping (Fang and Lin, 1988) units present in WWTPs.

The presence of solids in suspension in the raw WW (TSS ~ 53 mg/L) was detected, which is possibly associated with the industrial process (cf. Table 4.1). The increase of the TSS content after the Fenton's process is related with the dosage of catalyst salt used, yielding an iron-containing sludge. Turbidity of the WW was considerably eliminated because coagulation occurs together with the Fenton's process with subsequent sedimentation of the flocs upon neutralization of the final effluent. Such final effluent was non-toxic (0.0% of *Vibrio fischeri* inhibition) and its biodegradability increased (BOD_5:COD raised from 0.007 to 0.04 – see Table 4.1). In spite of the high reduction of organic matter (52% in terms of DOC and 83% in terms of COD), the COD concentration at the end of this process (above 1000 mgO_2/L) was above the emission limit value imposed by the decree-law number 236/98 of the Portuguese Legislation (Portugal 1998)) for wastewater discharge, so another treatment process was required.

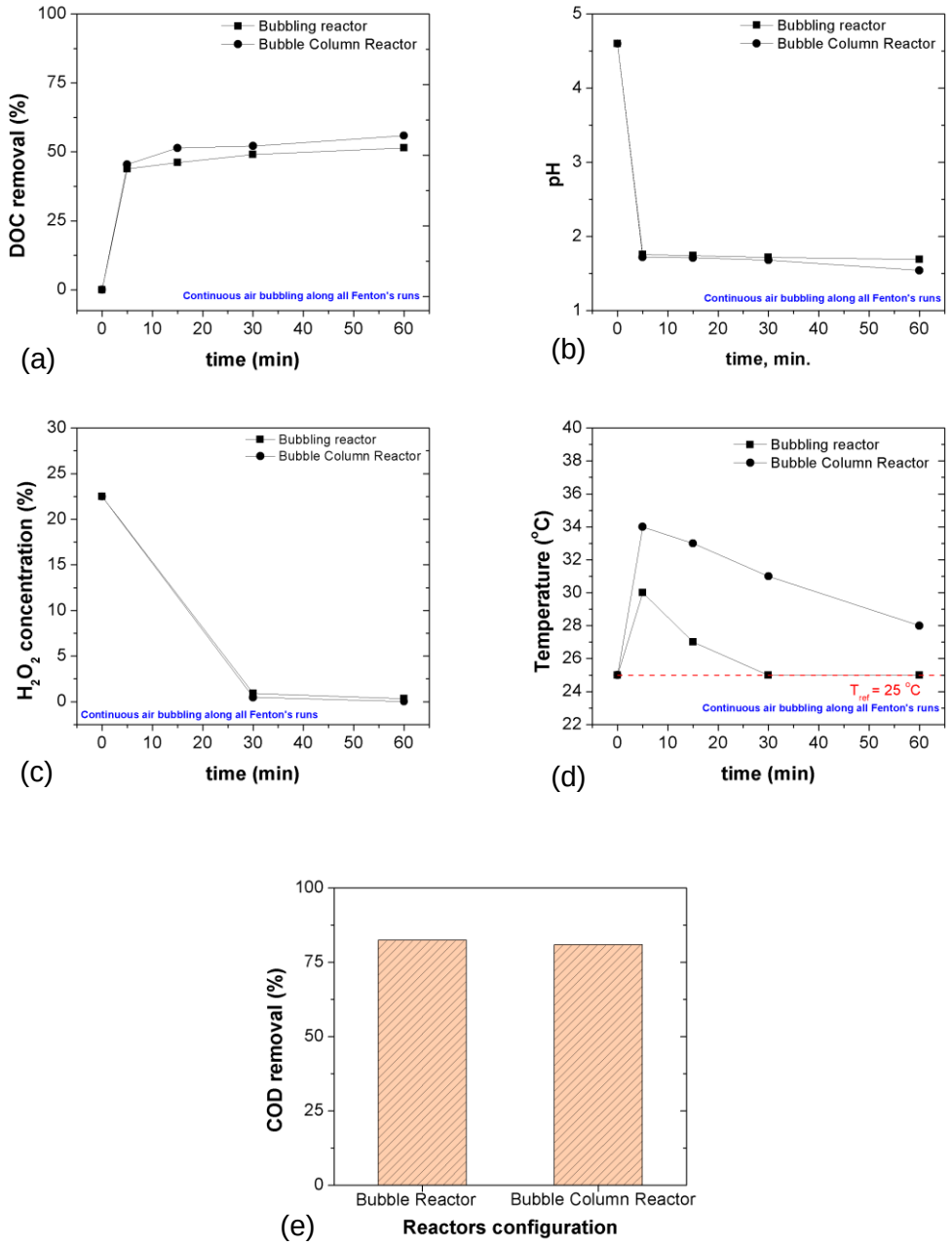

Figure 4.5 Evolution of the DOC removal (a), reduction of pH (b), consumption of H_2O_2 (c), and temperature profile (d) along the oxidation process, and COD removal (e) after the WW treatment (t = 60 min) performed in the bubble column and in the bubble column reactor. Experimental conditions: $[H_2O_2]$ = 22.50 g/L; $[Fe^{2+}]$ = 0.75 g/L, pH = 4.6, $V_{at\ BR}$ = 0.5 L, $V_{at\ BCR}$ = 4.0 L $T_{ref.}$ = 25 ºC, Q_{air} = 1.0 L/min.

4.3.4 WW oxidation with UV-vis assisted processes

In order to obtain an effective treatment of the WW, the photo-Fenton process was performed. Photo-Fenton's oxidation is a process based on the formation of HO$^{\bullet}$ species by interaction of the Fenton's reagents with UV-visible radiation (Eq. 4.9) (Gao *et al.*, 2013; Oturan and Aaron, 2014; Rodrigues *et al.*, 2013; Will *et al.*, 2004). Apart from that,

one should also consider the photolysis of H_2O_2 that also allows the formation of further $HO^{\bullet}$ species (Eq. 4.10) (Haber and Weiss, 1934).

$$Fe^{3+} + H_2O + h\nu \rightarrow Fe^{2+} + HO^{\bullet} + H^{+} \quad (4.9)$$

$$H_2O_2 + h\nu \rightarrow 2HO^{\bullet} \quad (4.10)$$

The UV-assisted processes were carried out in a photo-reactor without air supply, because the reactor configuration available did not allow an efficient gas bubbling, and, as shown above, there is no increase in the mineralization using air bubbling along Fenton's oxidation under the conditions tested (see section 3.3). So, the process was carried out with mechanical stirring at 250 rpm, and reagents concentrations used were the same optimized for the Fenton process.

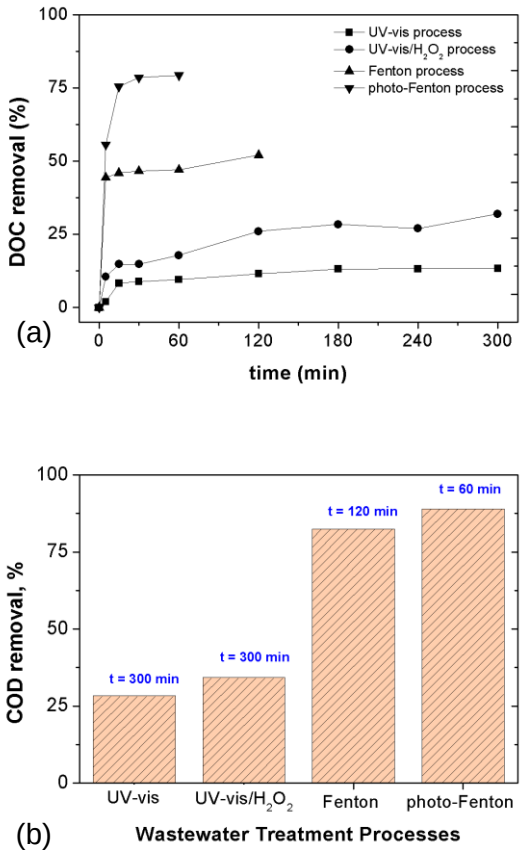

Figure 4.6 Evolution of the DOC removal (a) along the oxidation processes and COD removal (b) after the WW treatment (t = 60 min) performed using different AOPs (UV-vis, UV-vis/H_2O_2, Fenton, and photo-Fenton). Experimental conditions: [H_2O_2] = 22.50 g/L, [Fe^{2+}] = 0.75 g/L, I = 500 W/m^2, pH = 4.6, V = 0.5 L, $T_{ref.}$ = 25 ºC.

Figure 4.6 reports the influence of the different AOPs along the WW treatment. Mineralization increased when the WW was treated with the photo-Fenton process, reaching ~ 80% of DOC removal (Fig. 4.6a) and nearly 90 % of COD removal after 60 min (Fig. 4.6b). Regarding the treatment performed with the UV-vis radiation (without any reagents – direct photolysis), the DOC removal achieved only 10% after 5 h of treatment and increased to 30% when the treatment was realized with UV-vis/H_2O_2 (Fig. 4.6a). The COD removal also increased with the UV-vis/H_2O_2 process (Fig. 4.6b).

The photo-Fenton process under the conditions tested improved the characteristics of the WW to values closer to the emission limits imposed in the Portuguese Legislation (Portugal 1998) (cf. Table 4.1). However, the process must be optimized to further improve its performance and reduce the Fenton's reagents doses, thus inherently decreasing the cost associated with the treatment process, which will be the aim of future work.

4.4 Conclusions

Some insights about the treatment of real industrial wastewater using Fenton's oxidation in bubble reactors were presented in this study, being the main conclusions the following:

- In the parametric process study, it was verified that only the H_2O_2 concentration affected considerably the Fenton process efficiency in the BR (in the ranges tested), reaching, approximately, 50 and 80% of DOC and COD removal, respectively, under the best conditions found.
- The gas phase composition influenced the process, being that the maximum DOC removal (56% after 60 min) was obtained when the Fenton process was performed in the BR with continuous oxygen bubbling.
- The BR shows to be useful to perform the WW treatment by the Fenton process and better temperature control was reached when compared with a classic batch reactor with mechanical stirring.
- The scale-up for a bubble column reactor shows reproducibility and feasibility of the process;
- The treated wastewater was more biodegradable and non-toxic, however, the organic load, in terms of COD, exceeds the emission limits established in Portuguese Legislation, requiring further treatment.

- The photo-Fenton process under the same conditions improved considerably the mineralization and allowed to remove nearly 80% of DOC after 60 min of treatment.

4.5 References

APHA, A., 1995. Standard methods for the examination of water and wastewater.

APHA, W.A., 1988. Standard methods for the examination of water and wastewater, in: Association, A.P.H. (Ed.), Water Pollution Control Federation. American Water Works Association, Washington DC,.

Barb, W.G., Baxendale, J.H., George, P., Hargrave, K.R., 1949. Reactions of ferrous and ferric ions with hydrogen peroxide. *Nature* 163, 692–694.

Bautista, P., Mohedano, A.F., Casas, J.A., Zazo, J.A., Rodriguez, J.J., 2008. An overview of the application of Fenton oxidation to industrial wastewaters treatment. *J. Chem. Technol. Biotechnol.* 83, 1323–1338.

Bouasla, C., Samar, M.E.H., Ismail, F., 2010. Degradation of methyl violet 6B dye by the Fenton process. *Desalination* 254, 35–41.

Deckwer, W., 1979. On the mechanism of heat transfer in Bubble Column Reactors. *Chem. Eng. Sci.* 35, 1341–1346.

Deng, Y., Englehardt, J.D., 2008. Hydrogen peroxide-enhanced iron-mediated aeration for the treatment of mature landfill leachate. *J. Hazard. Mater.* 153, 293–299.

Deng, Y., Zhao, R., 2015. Advanced Oxidation Processes (AOPs) in Wastewater Treatment. *Curr. Pollut. Reports* 1, 167–176.

Dewil, R., Mantzavinos, D., Poulios, I., Rodrigo, M.A., 2017. New perspectives for Advanced Oxidation Processes. *J. Environ. Manage*. 195, 93–99.

Du, Y., Zhou, M., Lei, L., 2006. Role of the intermediates in the degradation of phenolic compounds by Fenton-like process. *J. Hazard. Mater.* 136 (3), 859-865.

Esteves, B.M., Rodrigues, C.S.D., Maldonado-Hódar, F.J., Madeira, L.M., 2019. Treatment of high-strength olive mill wastewater by combined Fenton-like oxidation and coagulation/flocculation. *J. Environ. Chem. Eng.* 7, 103252.

European Council, 2010. DIRECTIVE 2010/75/EU OF THE EUROPEAN PARLIAMENT AND OF THE COUNCIL of 24 November 2010 on industrial emissions (integrated pollution prevention and control). Off. J. Eur. Union L334, 17–119.

Fang, C.S., Lin, J.H., 1988. Air stripping for treatment of produced water. *Soc. Pet. Eng.* - SPE Calif. Reg. Meet. CRM 1987 40, 619–614.

Farshchi, M.E., Aghdasinia, H., Khataee, A., 2019. Heterogeneous Fenton reaction for elimination of Acid Yellow 36 in both fluidized-bed and stirred-tank reactors:

Computational fluid dynamics versus experiments. *Water Res.* 151, 203–214.

Fenton, H.J.H., 1894. LXXIII.—Oxidation of tartaric acid in presence of iron. *J. Chem. Soc. Trans.* 65, 899–910.

Gao, Y., Gan, H., Zhang, G., Guo, Y., 2013. Visible light assisted Fenton-like degradation of rhodamine B and 4-nitrophenol solutions with a stable poly-hydroxyl-iron/sepiolite catalyst. *Chem. Eng. J.* 217, 221–230.

Grady Jr., C.P.L., Daigger, G.T., Love, N.G., Filipe, C.D.M., 2011. Activated Sludge, in: Biological Wastewater Treatment. *CRC Press*, Boca Raton, pp. 381–470.

Guerreiro, L.F., Rodrigues, C.S.D., Duda, R.M., de Oliveira, R.A., Boaventura, R.A.R., Madeira, L.M., 2016. Treatment of sugarcane vinasse by combination of coagulation/flocculation and Fenton's oxidation. *J. Environ. Manage.* 181, 237–248.

Gulkaya, I., Surucu, G.A., Dilek, F.B., 2006. Importance of H_2O_2/Fe^{2+} ratio in Fenton's treatment of a carpet dyeing wastewater. *J. Hazard. Mater.* 136, 763–769.

Haber, F., Weiss, J., 1934. The catalytic decomposition of hydrogen peroxide by iron salts. *Proc. R. Soc. London. Ser. A - Math. Phys. Sci.* 147, 332–351.

Harold, P.D., de Souza, A.S., Louchart, P., Russell, D., Brunt, H., 2014. Development of a risk-based prioritisation methodology to inform public health emergency planning and preparedness in case of accidental spill at sea of hazardous and noxious substances (HNS). *Environ. Int.* 72, 157–163.

Jing, Z., Cao, S., Yu, T., Hu, J., 2015. Degradation Characteristics of Aniline with Ozonation and Subsequent Treatment Analysis. *J. Chem.* 2015, 1–6.

Kantarci, N., Borak, F., Ulgen, K.O., 2005. Bubble column reactors. *Process Biochem.* 40, 2263–2283.

Legrini, O., Oliveros, E., Braun, A.M., 1993. Photochemical processes for water treatment. *Chem. Rev.* 93, 671–698.

Lima, V.N., Rodrigues, C.S.D., Borges, R.A.C., Madeira, L.M., 2018a. Gaseous and liquid effluents treatment in bubble column reactors by advanced oxidation processes: A review. *Crit. Rev. Environ. Sci. Technol.* 48, 1–48.

Lima, V.N., Rodrigues, C.S.D., Madeira, L.M., 2018b. Application of the Fenton's process in a bubble column reactor for hydroquinone degradation. *Environ. Sci. Pollut. Res.* 25, 34851–34862.

Lucas, M., Peres, J., 2006. Decolorization of the azo dye Reactive Black 5 by Fenton and photo-Fenton oxidation. *Dye. Pigment.* 71, 236–244.

Lucas, M.S., Peres, A.J., 2009. Removal of COD from olive mill wastewater by Fenton's reagent: Kinetic study. *J. Hazard. Mater.* 168, 1253–1259.

Lucas, M.S., Peres, J.A., Lan, B.Y., Li Puma, G., 2009. Ozonation kinetics of winery wastewater in a pilot-scale bubble column reactor. *Water Res.* 43, 1523–1532.

Lyu, T., Wu, S., Mortimer, R.J.G., Pan, G., 2019. Nanobubble Technology in Environmental Engineering: Revolutionization Potential and Challenges. *Environ. Sci. Technol.* 53, 7175–7176.

Marco, A., Esplugas, S., Saum, G., 1997. How and why combine chemical and biological processes for wastewater treatment, *Water Science and Technology*, 35(4), 321-327.

Muruganandham, M., Suri, R.P.S., Jafari, S., Sillanpää, M., Lee, G.-J., Wu, J.J., Swaminathan, M., 2014. Recent Developments in Homogeneous Advanced Oxidation Processes for Water and Wastewater Treatment. *Int. J. Photoenergy* 2014, 1–21.

Neyens, E., Baeyens, J., 2003. A review of classic Fenton's peroxidation as an advanced oxidation technique. *J. Hazard. Mater.* 98, 33–50.

Nidheesh, P.V., Gandhimathi, R., 2015. Electro Fenton oxidation for the removal of Rhodamine B from aqueous solution in a bubble column reactor under continuous mode. *Desalin. Water Treat.* 55, 263–271.

Oller, I., Malato, S., Sánchez-Pérez, J.A., 2011. Combination of Advanced Oxidation Processes and biological treatments for wastewater decontamination-A review. *Sci. Total Environ.* 409, 4141–4166.

Oturan, M.A., Aaron, J.J., 2014. Advanced oxidation processes in water/wastewater treatment: Principles and applications. A review. *Crit. Rev. Environ. Sci. Technol.* 44, 2577–2641.

Papadopoulos, A.E., Fatta, D., Loizidou, M., 2007. Development and optimization of dark Fenton oxidation for the treatment of textile wastewaters with high organic load. *J. Hazard. Mater.* 146, 558–563.

Pérez, M., Torrades, F., Domènech, X., Peral, J., 2002. Fenton and photo-Fenton oxidation of textile effluents. *Water Res.* 36, 2703–2710.

Poyatos, J.M., Muñio, M.M., Almecija, M.C., Torres, J.C., Hontoria, E., Osorio, F., 2010. Advanced oxidation processes for wastewater treatment: state of the art. Water. *Air. Soil Pollut.* 205, 187–204.

Qin, Y., Geng, S., Jiao, W., Liu, Y., 2018a. Deep Oxidation Degradation of Aniline Wastewater by O_3/Fe(II) Process Enhanced Using High-Gravity Technology. *Chinese J. Energ. Mater.* 26, 448–454.

Qin, Y., Luo, S., Geng, S., Jiao, W., Liu, Y., 2018b. Degradation and mineralization of aniline by O_3/Fenton process enhanced using high-gravity technology. *Chinese J. Chem. Eng.* 26, 1444–1450.

Rodrigues, C.S.D., Borges, R.A.C., Lima, V.N., Madeira, L.M., 2018a. *p*-Nitrophenol degradation by Fenton's oxidation in a bubble column reactor. *J. Environ. Manage.* 206, 774–785.

Rodrigues, C.S.D., Madeira, L.M., Boaventura, R.A.R., 2013. Optimization and economic analysis of textile wastewater treatment by photo-fenton process under artificial and simulated solar radiation. *Ind. Eng. Chem. Res.* 52.

Rodrigues, C.S.D., Silva, R.M., Carabineiro, S.A.C., Maldonado-Hódar, F.J., Madeira, L.M., 2018b. Dye-containing wastewater treatment by photo-assisted wet peroxidation using Au nanosized catalysts. *J. Chem. Technol. Biotechnol.* 93, 3223–3232.

Rollbusch, P., Bothe, M., Becker, M., Ludwig, M., Grünewald, M., Schlüter, M., Franke, R., 2015. Bubble columns operated under industrially relevant conditions – Current understanding of design parameters. *Chem. Eng. Sci.* 126, 660–678.

Rubio, J., Souza, M.L., Smith, R.W., 2002. Overview of flotation as a wastewater treatment technique. *Miner. Eng.* 15, 139–155.

San Sebastián Martínez, N., Fernández, J.F., Segura, X.F., Ferrer, A.S., 2003. Pre-oxidation of an extremely polluted industrial wastewater by the Fenton's reagent. *J. Hazard. Mater.* 101, 315–322.

Sellers, R.M., 1980. Spectrophotometric determination of hydrogen peroxide using potassium titanium (IV) oxalate. *Analyst* 105, 950–954.

Shah, Y.T., Kelkar, B.G., Godbole, S.P., Deckwer, W.-D., 1982. Design parameters estimations for bubble column reactors. *AIChE J.* 353–379.

Shon, H.K., Shon, H.K., Vigneswaran, S., Snyder, S.A., 2006. Effluent Organic Matter (EfOM) in Wastewater: Constituents, Effects, and Treatment. *Crit. Rev. Environ. Sci. Technol.* 36, 327–374.

Sincero, A.P., Sincero, G.A., 2002. Conventional Filtration, in: Physical-Chemical Treatment of Water and Wastewater. *CRS Press*, Boca Raton, pp. 327–371.

Tokumura, M., Nakajima, R., Znad, H.T., Kawase, Y., 2008. Chemical absorption process for degradation of VOC gas using heterogeneous gas-liquid photocatalytic oxidation: Toluene degradation by photo-Fenton reaction. *Chemosphere* 73, 768–775.

Torrades, F., García-Montaño, J., 2014. Using central composite experimental design to optimize the degradation of real dye wastewater by Fenton and photo-Fenton reactions. *Dye. Pigment.* 100, 184–189.

Torrades, F., Pérez, M., Mansilla, H.D., Peral, J., 2003. Experimental design of Fenton and photo-Fenton reactions for the treatment of cellulose bleaching effluents. *Chemosphere* 53, 1211–1220.

US EPA, 2014. Priority Pollutant List. Effl. Guidel. 2.

Walling, C., 1975. Fenton's reagent revisited. *Acc. Chem. Res.* 8, 125–131.

Wei, Q., Qiao, S., Sun, B., Zou, H., Chen, J., Shao, L., 2015. Study on the treatment of simulated coking wastewater by O_3 and O_3/Fenton processes in a rotating packed bed. *RSC Adv.* 5, 93386–93393.

Will, I.B.S., Moraes, J.E.F., Teixeira, A.C.S.C., Guardani, R., Nascimento, C.A.O., 2004. Photo-Fenton degradation of wastewater containing organic compounds in solar reactors. *Sep. Purif. Technol.* 34, 51–57.

Xie, R., Ji, J., Guo, K., Lei, D., Fan, Q., Leung, D.Y.C., Huang, H., 2019. Wet scrubber coupled with UV/PMS process for efficient removal of gaseous VOCs: Roles of sulfate and hydroxyl radicals. *Chem. Eng. J.* 356, 632–640.

Xu, M., Wu, C., Zhou, Y., 2017. Advanced treatment of petrochemical secondary effluent by Fenton: Performance and organics removal characteristics. *Water Sci. Technol.* 75, 1431–1439.

Yan, L., Liu, J., Feng, Z., Zhao, P., 2016. Continuous degradation of BTEX in landfill gas by the UV-Fenton reaction. *RSC Adv.* 6, 1452–1459.

Yingxun Du, M.Z., Lei, L., 2007. Kinetic model of 4-CP degradation by Fenton/O_2 system. *Water Res.* 41, 1121–1133.

Zazo, J.A., Casas, J.A., Mohedano, A.F., Gilarranz, M.A., Rodríguez, J.J., 2005. Chemical pathway and kinetics of phenol oxidation by Fenton's reagent. *Environ. Sci. Technol.* 39, 9295–9302.

Zehner, P., Kraume, M., 2000. Bubble Columns, in: Ullmann's Encyclopedia of Industrial Chemistry. Wiley-VCH Verlag GmbH & Co. KGaA, Weinheim, Germany, p. 34.

Zhang, B.T., Zhang, Y., Teng, Y., Fan, M., 2015. Sulfate radical and its application in decontamination technologies. *Crit. Rev. Environ. Sci. Technol.* 45, 1756–1800.

Zhang, B.T., Zhao, L.X., Lin, J.M., 2008. Study on superoxide and hydroxyl radicals generated in indirect electrochemical oxidation by chemiluminescence and UV-Visible spectra. *J. Environ. Sci.* 20, 1006–1011.

Zhang, H., Heung, J.C., Huang, C.P., 2005. Optimization of Fenton process for the treatment of landfill leachate. *J. Hazard. Mater.* 125, 166–174.

Part III: Waste Gas Treatment

This part presents the experimental data relative to the treatment of a gas stream containing a model volatile organic compound (toluene) by Fenton's process in bubbling reactors, and a study concerning the treatment of toluene gaseous stream and a real wastewater simultaneously, by the Fenton's process, in a bubbling reactor.

Chapter 5. Sequential Gas-Liquid Treatment for Gaseous Toluene Degradation by Fenton's Oxidation in Bubble Reactors

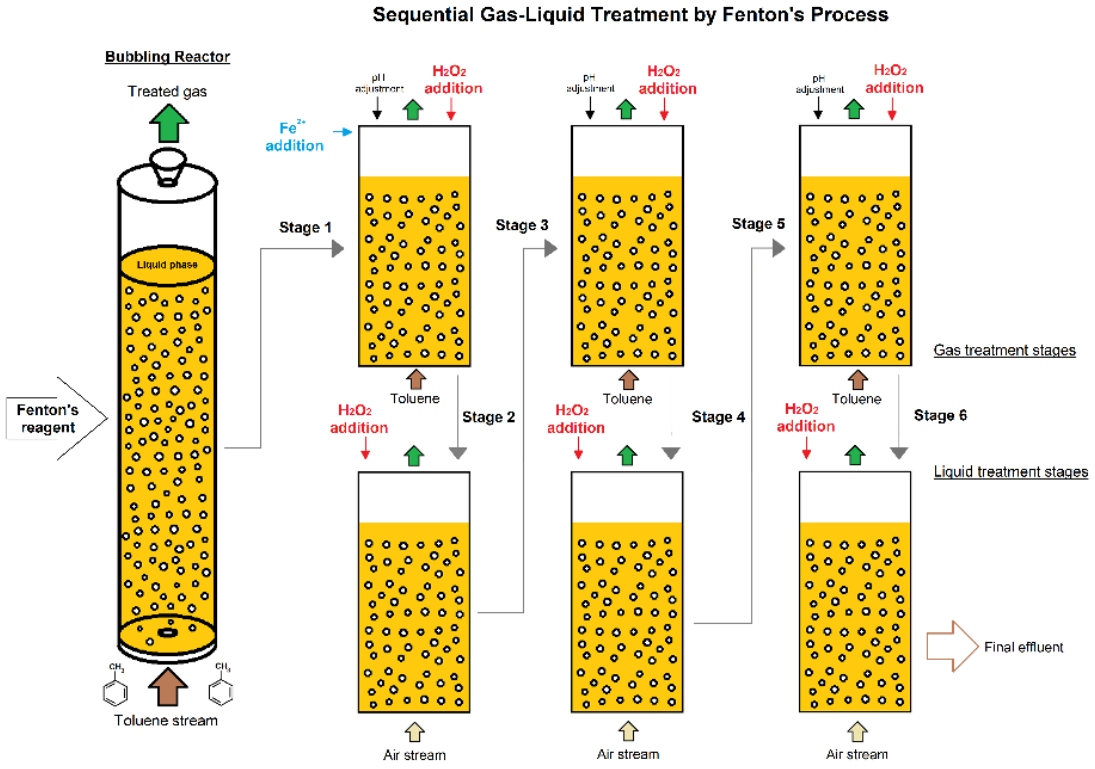

- The toluene treatment by Fenton's process was optimized;
- The absorption + oxidation process decreases when increased temperature;
- The liquid treatment stage increased the mineralization and biodegradability;
- Bubbling column reactor was selected to scale-up the process;
- The sequential gas-liquid treatment reached three gas treatment stages.

The contents of this chapter were adapted from: Lima, V. N., Rodrigues, C. S., and Madeira, L. M. *Sequential gas-liquid treatment for gaseous toluene degradation by Fenton's oxidation in bubble reactors*. (2020). **Journal of Environmental Chemical Engineering**, 8(3), 103796.

Abstract: *A lab scale bubble reactor (BR) configuration was employed to evaluate the degradation of gaseous toluene by Fenton's oxidation under semi-batch mode operation (i.e., with continuous gas bubbling in the liquid phase where organics oxidation is carried out). A parametric study was performed for evaluating the effect of Fenton's process operating parameters, such as temperature and concentration of* Fe^{2+} *and* H_2O_2*, in the removal of toluene from the gas stream. The maximum amount of toluene transferred (0.041 mol per liter of solution) was reached when the optimal conditions ([*Fe^{2+}*] = 2.5 mM, [*H_2O_2*] = 20 mM, and T = 25 ºC, at pH 3.0) were used after 120 minutes of reaction, yielding the highest average toluene absorption rate (5.78 x 10-6 mol/L.s). The treatment of the gas stream increased, however, the organic load in the aqueous phase, so a subsequent treatment stage of the liquid was performed. Additionally, a scale-up of the sequential gas-liquid treatment for a bubble column reactor (BCR) was carried out for several cycles, up to almost 20 h. This strategy, making use of the Fenton's process for treating the toluene gas stream, with intermediate liquid oxidation stages, allowed to reach more gas treatment stages, while providing a final effluent that is non-toxic (0.0% of inhibition of Vibrio Fischeri) and biodegradable.*

5.1 Introduction

The chemical industries discharge gaseous emissions containing volatile organic compounds (VOCs) into the atmosphere, and thus severe problems for the air quality are generated around the world (Lee *et al.* 2002; Cerqueira *et al.* 2003; Orlando *et al.* 2010). VOCs such as benzene, toluene, ethylbenzene, and xylene (BTEX) stand out as chemical species that present severe risks to the environment and human health (Durmusoglu, Taspinar, and Karademir 2010; Hinwood *et al.* 2007; Bolden *et al.* 2015; Correa *et al.* 2012). Some of these compounds, e.g., toluene, exhibit high toxicity levels (US EPA 2005), so they are sorted in the list of priority pollutants (US EPA 2014) that should be removed. Therefore, measures must be taken to reduce the levels of these pollutants in the atmosphere (Ciccioli 2011).

Regarding the technologies available for toluene (and all other BTEX compounds) removal from gas streams, the literature reports the application of non-destructive processes like adsorption (Daifullah and Girgis 2003; Štandeker *et al.* 2009), absorption, condensation, and filtration (Corsi and Seed 1995). Despite their proven efficiency on BTEX removal, these methods only transfer the pollutants from the gas to another phase, not providing an effective degradation; destructive processes are more interesting, potentially minimizing the risks.

There are several destructive processes, but the advanced oxidation processes (AOPs) have received increasing attention (Bekbolet 2011). The works presented in the open literature report excellent performance of different AOPs for the removal of these contaminants from liquid effluents (Oturan and Aaron 2014) by the action of oxidizing species like $HO^{\bullet}$ (hydroxyl radical). The Fenton reaction is one of the classic AOPs that makes use of $HO^{\bullet}$ (oxidation potential of 2.80 V (Legrini *et al.* 1993)) for pollutants mineralization/degradation (Gligorovski *et al.* 2015). In such a process, the radicals are formed through the catalytic decomposition of hydrogen peroxide (H_2O_2) by ferrous ion (Fe^{2+}) according to Eq. 5.1 (Barb *et al.* 1949; Walling 1975), which is regenerated according to Eq. 5.2:

$$H_2O_2+Fe^{2+}\rightarrow OH^{-}+HO^{\bullet}+Fe^{3+} \quad (5.1)$$

$$Fe^{3+}+H_2O_2\rightarrow Fe^{2+}+H^{+}+HOO^{\bullet} \quad (5.2)$$

Fenton's reaction has low risks since it makes use of environmental friendly reagents and operates under moderate conditions of temperature and pressure – close to room temperature and atmospheric pressure (Fenton 1894; Babuponnusami and Muthukumar 2014). The oxidation and mineralization of the organic polluting compounds (e.g., VOCs)

through the action of the hydroxyl radicals in a liquid medium yields oxidized products as intermediate species, which can be subsequently oxidized up to CO_2 and water – Eq. 5.3 (Ramirez *et al.* 2007).

$$\text{VOCs} \xrightarrow{HO^{\bullet}\ \text{(liquid phase)}} \text{products} \xrightarrow{HO^{\bullet}\ \text{(liquid phase)}} CO_2 + H_2O \qquad (5.3)$$

For these reasons, the Fenton process has been frequently applied to treat wastewaters produced from many chemical processes (Pliego *et al.* 2015). Nevertheless, to treat organic compounds present in the gas phase by the Fenton's process, firstly one needs to transfer the pollutants from the gas to the liquid. It is in the latter, which contains Fenton's reagents, that the degradation of the pollutants occurs; such a process can be carried out in a bubble reactor (Handa *et al.* 2013; Tokumura *et al.* 2013; Lima *et al.* 2018).

The bubble reactors (BR) that are commonly employed in the chemical industries for different processes (Kantarci *et al.* 2005) can be extremely efficient in gas streams treatment by Fenton's oxidation due to the good mass and heat transfer rates (Lima *et al.* 2018). In addition, the BRs have the advantage of flexibility with different modes operation, namely continuous (Rosales *et al.* 2009; Nidheesh and Gandhimathi 2015), wherein the liquid and gas phases are fed co-current or counter-currently, or semi-batch mode (Rodrigues *et al.* 2018), wherein the liquid phase is fed discontinuously and the gas stream continuously. Thus, various alternatives of gas treatment may be performed in BRs, ensuring new opportunities for AOPs and particularly for the Fenton process. The effectiveness of VOCs (namely toluene) treatment in BRs by different AOPs has already been reported for UV/peroxymonosulfate (Xie *et al.* 2019), UV/H_2O_2 (G. Liu, Ji, *et al.* 2017), and photo-Fenton (Tokumura, Shibusawa, and Kawase 2013). However, photo-reactors are required in such AOPs, which increases the cost of the treatment process by the required UV-assisted oxidation.

The research in the field of gas streams treatment by Fenton's oxidation has emerged in the last decade, but only a few works have been reported in the open scientific literature with focus on bubbling reactors (Zhao *et al.* 2014; Y. Liu *et al.* 2015; G. Liu, Huang, *et al.* 2017; Guo *et al.* 2011). Even so, the treatment of toluene from the gas phase by oxidation and the assessment of its implications, such as the formation of intermediate compounds and the increase of the organic load which remains in the liquid phase, has been only sparsely reported (Choi *et al.* 2014; Yan *et al.* 2016; G. Liu, Ji, *et al.* 2017; Xie *et al.* 2019). Still, the effect of several important process parameters like the reaction's temperature were disregarded in most of the previous studies that address the treatment of BTEX by Fenton (or photo-Fenton) processes in BRs.

So, in this study, two different BRs operating in semi-batch mode were chosen to evaluate the effects of the Fenton process on the treatment of a gas stream containing toluene. Firstly, the optimization of the process was carried out in a lab-scale BR to assess the influence of the main parameters of the Fenton reaction. Then, a scale-up into a bubble column reactor (BCR) with a 10 times superior volumetric capacity was performed, under the conditions optimized in the BR, to proof the concept at a larger scale and particularly to proceed, for a longer time, with a sequential treatment with intermediate stages of absorption + oxidation of toluene followed by the treatment of the liquid effluent produced. To the best of our knowledge, there are no studies reported that adopted this approach of sequential gas-liquid treatment in bubbling reactors.

5.2 Material and methods

5.2.1 Simulated toluene gas stream

The removal of the model compound (toluene) was evaluated using a simulated gas stream containing toluene in air. Such stream was produced by the stripping of toluene following the method described by other authors (Tokumura *et al.* 2008; G. Liu, Huang, *et al.* 2017); for that, a clean air stream was bubbled into a 500 mL washing bottle (Duran) containing pure liquid toluene (99 %, from JMGS) - see Fig. 5.1a. The temperature of the solution was kept at 25 ºC (using a Polystat CC1 thermostatic bath from Huber) and kept slightly above atmospheric pressure. The air stream was supplied continuously with an air pump (model air 550R plus from Sera Precision) at a flow rate (Q_{air}) of 0.5 L/min. Then, the concentrated toluene was taken to a mixing bottle where a new clean air stream was fed at the same flow rate to dilute the toluene-containing stream. The resulting gas that was fed to the bubbling reactors had a toluene concentration of 0.04 g/L, for a total gas flow rate (Q_{gas}) of 1.0 L/min. All gas flow rates were measured at room temperature and atmospheric pressure.

5.2.2 Bubbling reactors

Fenton's oxidation of the toluene-containing simulated gas stream was carried out in two distinct acrylic reactors that were operated under semi-batch mode, at atmospheric pressure: the first was a 0.9 L–capacity acrylic bubble reactor (BR) (Fig. 5.1b), and the second a 9.0 L-capacity bubble column reactor (BCR) (Fig. 5.1c). Both reactors were equipped with a temperature control system using water recycling through a thermal

jacket connected to a thermostatic bath (Polystat CC1 from Huber); this allowed keeping the temperature constant along the process (± 0.5 ºC).

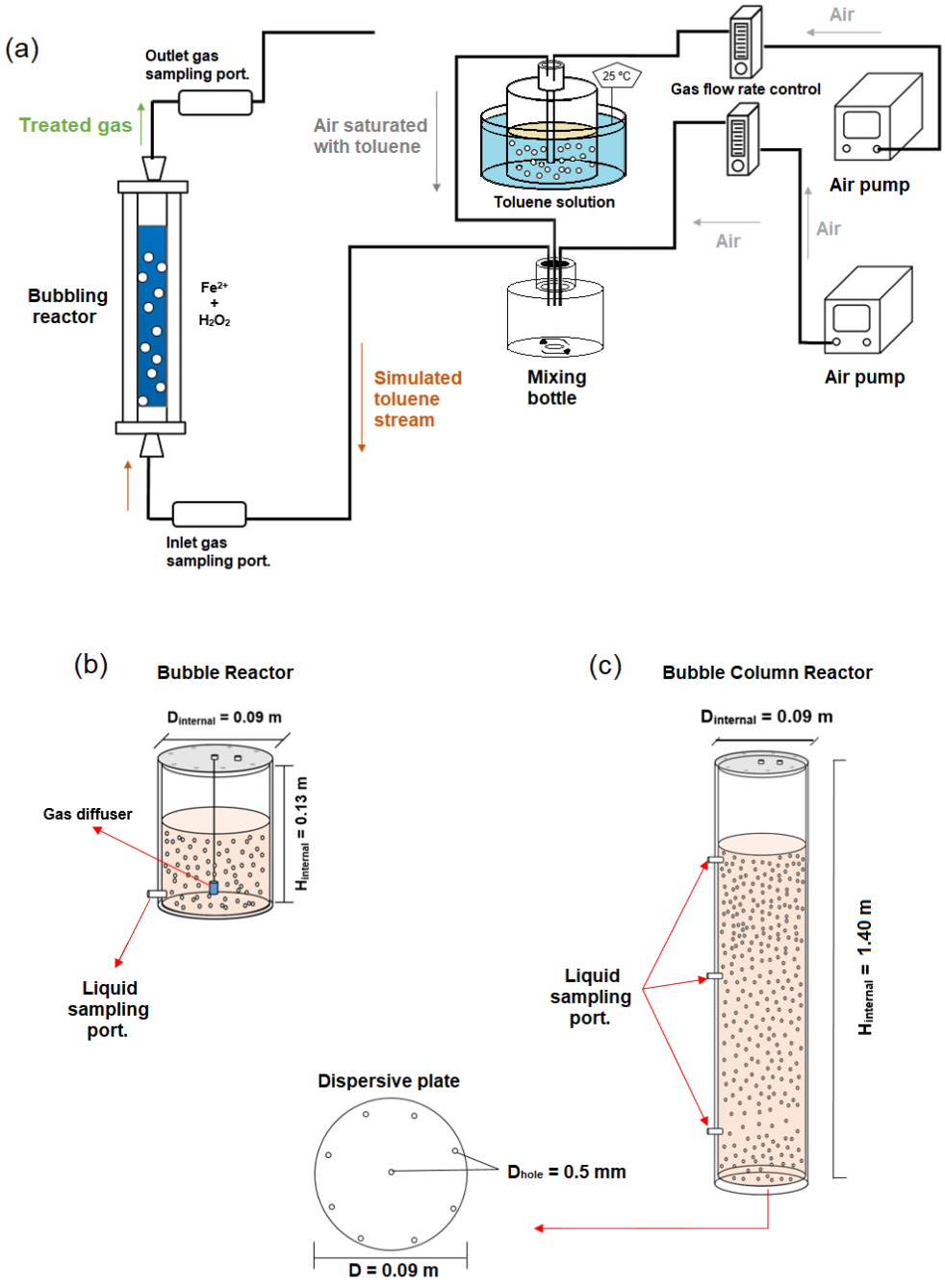

Figure 5.1 Scheme of the experimental set-up for the treatment of gaseous toluene by the Fenton's process (a), and details of the bubbling reactor (b) and bubble column reactor (c).

The bubbling of the gas stream, in both the BR and BCR, was performed by gas diffusers. In the BR, a cylindrical gas diffuser (coarse-grain inert stone with 2.5x1.4 cm,

HxD, respectively) was placed axially centred, while in the BCR a dispersive plate with holes of ø = 0.5 mm was located in the bottom of the reactor (for more details please refer to previous works (Rodrigues *et al.* 2018; Lima, Rodrigues, and Madeira 2018)). In all runs, the gas stream containing toluene was continuously bubbled inside the liquid phase. For the liquid phase treatment stages, a clean air stream was fed instead of toluene at the same gas flow rate. In all the experiments the bubbling of toluene or clean air promotes turbulence inside the reactor and has shown to be effective in liquid homogenization, so no mechanical stirring was required. In such stages, no stripping of organic oxidation products apart from toluene has been observed.

5.2.3 Fenton process procedure and process efficiency indicators

Initially, the reactors were filled with a volume (V_{liquid}) of 0.5 L or 5.0 L (for the BR and BCR, respectively) of distilled water (with a dissolved organic carbon – DOC – content less than 0.1 mgC/L) and the desired temperature to be reached set in the control system. Then, the pH was adjusted to 3.0 with 1 M H_2SO_4 (99 %, VWR), which was measured using a pH-meter (Inolab model pH level 2); this pH value was selected because it is commonly recognised to be the optimum for Fenton's reaction (Babuponnusami and Muthukumar 2014; Deng and Zhao 2015). After pH adjustment, the desired amount of ferrous sulfate ($FeSO_4.7H_2O$, 99%, Panreac) was added. Finally, the reactor was closed, and the desired volume of hydrogen peroxide (30 % w/v, VWR) introduced; at the same time, the feeding of the toluene stream was started (this instant corresponds to the initial reaction time - t = 0 min).

Along all runs, gas samples were periodically collected at the outlet of the reactors to assess the presence of volatile compounds (toluene and gaseous organic intermediates – e.g., benzene or ethylbenzene) in the gas phase. Apart from toluene, no other organic products have been detected by GC in the outlet stream. The average toluene absorption rate (N, in mol/L.s) by the liquid phase during a given time period of operation (t_{op}) was calculated following Eq. 5.4:

$$N = \frac{Q_{gas} \int_0^{t_{op}} (C_{in} - C_{out}) dt}{M_{toluene} V_{reactor} t_{op}} \quad (5.4)$$

where C_{in} and C_{out} represent the gas inlet and outlet toluene concentrations, in g/L, respectively, Q_{gas} represents the gas feed flow rate, in L/min, $M_{toluene}$ stands for the

molecular weight of toluene, $V_{reactor}$ represents the liquid phase volume inside the reactor, in L, and *t* means the process time, in s.

On the other hand, the overall amount of toluene transferred (η – mol/L) was calculated following Eq. 5.5:

$$\eta = \frac{Q_{gas} \int_0^{top} (C_{in} - C_{out}) dt}{M_{toluene} V_{reactor}} \quad (5.5)$$

The liquid phase was also sampled in pre-established reaction times. To measure the residual H_2O_2 concentration and the chemical oxygen demand (COD), samples were immediately analyzed after sampling. The residual dissolved organic carbon (DOC) was determined after stopping the homogeneous Fenton reaction in the sampling flasks with an excess of sodium sulfite (98%, Panreac), which instantaneously consumes any residual hydrogen peroxide.

The biodegradability and acute toxicity of the final liquid effluent were analyzed after pH increase up to 10 using 5 M NaOH (99 %, Vencilab) to stop the Fenton reaction because under such conditions H_2O_2 quickly decomposes (Rodrigues, Madeira, and Boaventura 2014).

5.2.4 Analytical Methods

Toluene concentrations in the gas streams were measured by gas chromatography (Agilent 7820A, column HP-5M S) with flame ionization detection (GC-FID). A sample of 50 µL of the gas was inserted into the GC injector using a manual gas-tight syringe (Agilent). The injector, detector, and oven column were operated at 220, 250, and 100 ºC, respectively. Helium was used as carrier gas at a flow rate of 25 mL/min.

DOC concentration (that represents the carbon fraction of the intermediate compounds formed and accumulated in the liquid phase) was measured according to method 5310 D (APHA 1988) using a TOC-L analyzer (Shimadzu); this method is not enough to determine the volatile carbon fraction in liquid samples.

COD was measured according to the closed reflux method (Method 5220 B (APHA 1988)) using a Nanocolor Vario 4 digester and a Nanocolor 500 D photometer (both apparatus from Macherey-Nagel). These analyses were performed immediately after collecting the samples, aiming to reduce the loss of volatile compounds that can remain in the liquid.

Residual H_2O_2 concentration in the liquid phase was determined by the potassium titanium (IV) oxalate spectrophotometry method, being that the absorbance of the complex formed at 400 nm (Sellers 1980) was measured in a Helios γ spectrophotometer (from Thermo Electron Corporation).

Biodegradability of the final effluent was quantified by the specific oxygen uptake rate (k' – $mgO_2/g_{VSS}h$), which was calculated from the ratio between the decline of the curve of dissolved oxygen vs. time and the volatile suspended solids (VSS) of the activated sludge (APHA 1988). For this procedure, biomass was collected from an activated sludge tank of a municipal wastewater treatment plant. A biological oxygen monitor (YSI Model 5300 B) was used to measure the consumption of dissolved oxygen in the degradation of the biodegradable organic matter by the biomass at 20 °C for 30 min.

Acute toxicity of the liquid phase was measured in samples collected at the end of the experiments, according to standard DIN/EN/ISO 11348-3 (ISO 2005), i.e., by inhibition of the bioluminescent bacterium *Vibrio fischeri*. In this quantification, the bacterium was put in contact with samples during 5, 15, and 30 min, at 15 °C, and after these periods, the bioluminescence was measured in a Microtox apparatus, model 500 (Modern Water).

All analytical methods were measured in duplicate, and the coefficient of variation was less than 2% for DOC determination and 4% for the other parameters.

5.3 Results and discussion

5.3.1. Parametric study in the lab-scale BR

The optimization of the Fenton's process for the treatment of a gas stream containing toluene was carried out in this study. For that, a parametric study was performed (operating the process in the lab scale BR), which aimed to evaluate the influence of the process parameters (reaction's temperature, Fe^{2+} and H_2O_2 concentrations) in the transfer of toluene (gas-to-liquid), with its simultaneous oxidation in the liquid phase (where Fenton's reactants have been previously introduced). For all runs, the initial pH was fixed at 3.0 because it was the optimum value for the oxidation of several pollutants by the Fenton process, as mentioned above, although any effect of this parameter on toluene mass transfer was noticed in the pH range of 3.0-5.0 (data not show).

5.3.1.1 Influence of the reaction's temperature

Two runs were carried out to evaluate the influence of the reaction's temperature, being chosen values of 25 and 40 ºC. These reaction temperatures were selected because they are in the optimal range (25 to 50 ºC) reported in the literature for Fenton's oxidation (Lima *et al.* 2018). While temperatures below 25 °C could slow down the reaction rate and the efficiency of the process (Wang 2008; Guedes *et al.* 2003), temperatures above 40 ºC could induce the presence of water vapor and organics in the gas outlet stream (compromising the GC analyses), and promote the self-decomposition of the hydrogen peroxide (Lucas and Peres 2009).

First of all, it was evaluated the effect of temperature in the transfer of toluene from the gas to the liquid phase; for that, blank runs (where the liquid phase was only water, without any of the Fenton's reagents) were performed. Figure 5.2 a) presents the results obtained in terms of the ratio between the toluene concentration in the gas phase at the outlet and inlet of the BR ($C_{out}(t)/C_{in}$) along process time. For both temperatures tested, just after 5 minutes of bubbling the presence of toluene in the outlet stream was observed. This concentration (C_{out}) continuously increased up to 32 and 45 min for 25 and 40 ºC, respectively. Saturation of the water is reached at this point, i.e. when the concentration at the outlet is equal to the inlet one. The mass transfer is associated with the solubility of toluene in water, which depends on the temperature. Sanemasa *et al.* (1982) reported solubilities of toluene in water of 0.516 g/L at 25 ºC, close to that obtained in this study under the same temperature (0.006 mol/L, equivalent to 0.59 g/L – cf. Table 5.1). However, the solubility of VOCs increases with the rise of the temperature. So, the time for saturation is higher for 40 ºC; inherently, the amount of toluene transferred per liter of solution (as well as the average absorption rate) increased from 25 to 40 ºC (Table 5.1), which is associated to the increase of the VOC concentration in liquid phase (Xie *et al.* 2019).

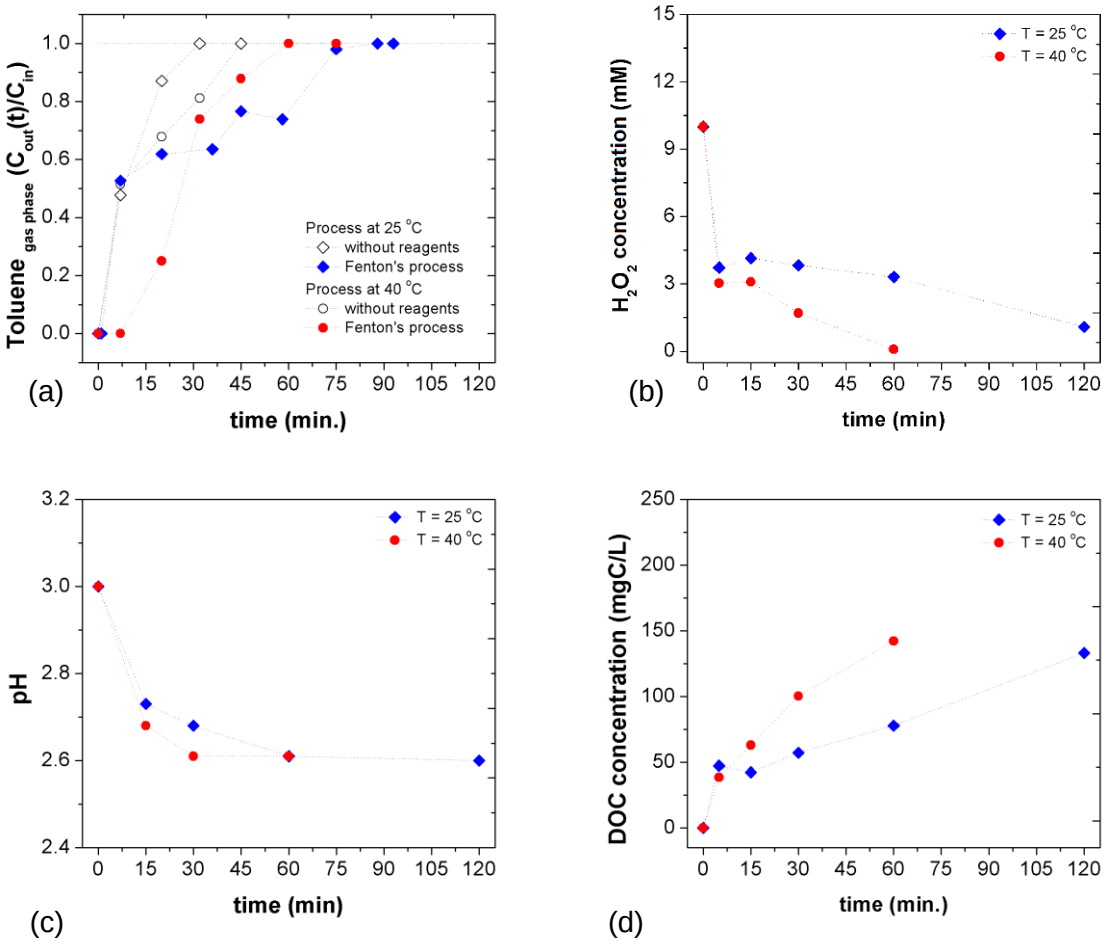

Figure 5.2 Influence of temperature in the toluene concentration at the outlet of the BR along the blank runs (without reagents) and Fenton's runs (a), and in the concentration of H_2O_2 (b), pH (c) and concentration of DOC (d) in the liquid phase along time. Experimental conditions: V = 0.5 L, pH_0 = 3.0, T = 25 ºC, and $Q_{toluene}$ = 1.0 L/min, $[H_2O_2]_{0\ when\ used}$ = 10 mM, and $[Fe^{2+}]_{0\ when\ used}$ = 2.5 mM.

The effect of temperature (25 and 40 ºC) in the simultaneous transfer and degradation of toluene (absorption + oxidation) by Fenton's reagent was assessed. In these two runs the concentrations of H_2O_2 and Fe^{2+} were fixed at 10 and 2.5 mM, respectively, yielding an Fe^{2+}:H_2O_2: molar ratio equal to 1:4, identical to that used in another study, where it was treated a gaseous effluent containing BTEX by the homogeneous Fenton process (Yan *et al.* 2016). While transferring toluene from the gas to the liquid, simultaneous oxidation occurs in the latter due to the action of the hydroxyl radicals (Eq. 5.3), increasing the driving force for further toluene transfer. In both experiments it was observed that the toluene outlet concentration increased gradually along time, reaching at 25 ºC $C_{out}(t)/C_{in}$ close to 1 at 75 min (against 60 min at 40 ºC) of treatment (see Fig. 5.2 a), which leads to more toluene transferred for the liquid phase. The average absorption rate for a fixed time increased almost two-fold when compared to the process

without reaction (e.g. from 6.51 x 10^{-6} to 1.01 x 10^{-5} mol/L.s after 30 min at 40 ºC, cf. Table 5.1). As expected, the average toluene absorption rate along the reactions decreased regardless of the temperature tested. Therefore, when $C_{out}(t)/C_{in}$ reached 1.0 (Fig. 5.2a), the average absorption rate reduced to 4.90 x 10^{-6} and 5.19 x 10^{-6} mol/L.s at 25 and 40 ºC, respectively – see Table 5.1. The overall amount of toluene transferred per liter of solution was lower at 40 ºC compared to the one reached at 25 ºC (0.019 *vs*. 0.022 mol/L) because the process lasted less time (cf. Table 5.1). This is related with the fact that the kinetics of the reactions are improved for higher temperatures (Guedes *et al.* 2003), which leads to a higher amount of $HO^{\bullet}$ radicals formed in a short time, and to the rapid oxidation of the toluene (that was transferred to the liquid phase). Consequently, an abrupt decrease in the concentration of hydrogen peroxide in the aqueous phase was observed (see Fig. 5.2b); so the oxidant was in solution less time. Some authors reported that at higher temperatures the decrease of H_2O_2 available is driven by the acceleration of the molecular decomposition into O_2 and water (Guedes *et al.* 2003; Lucas and Peres 2009). In addition, the reduction of the medium pH for the process at 40 ºC (Fig. 5.2c) was slightly faster, which proved the increase of the oxidation rate. Actually, the acidification is often associated with the formation of carboxylic acids, as described in other works (Qiu *et al.* 2014; Kavitha and Palanivelu 2005; Lima, Rodrigues, and Madeira 2018), which are among the most refractory species formed during oxidation of organic compounds (Martínez *et al.* 2007). This fact was corroborated by the higher amount of organic compounds formed, possibly benzoic acid (reported as intermediate of the toluene oxidation (Choi, Bae, and Lee 2014)) or short-chain organic acids, in shorter reaction times and that remained in solution for the run at 40 ºC, since the DOC for a reaction time of e.g. 60 min was higher at 40 ºC (150 mgC/L) than at 25 ºC (~ 70 mgC/L) – see Fig. 5.2d. As stated above, it was found that the Fenton process did not generate new organic pollutants in the gas phase, i.e., no gaseous intermediates commonly reported in the literature (e.g., benzene or ethylbenzene) have been identified in the outlet stream.

Table 5.1 Experimental conditions, process duration, average toluene absorption rate, and amount of toluene transferred after all experiments of the parametric study in the lab-scale bubbling reactor.

T (ºC)	$[Fe^{2+}]$ (mM)	$[H_2O_2]$ (mM)	Process duration (min)	Average absorption rate (mol/L.s)		Toluene transferred (mol/L)
				At 30 min	*Overall process*	
Gas treatment in the BR						
Blank runs						
25	0	0	32	4.99×10^{-6}	3.32×10^{-6}	0.006
40	0	0	45	6.51×10^{-6}	4.74×10^{-6}	0.012
Fenton's runs						
25	2.5	10	75	8.17×10^{-6}	4.90×10^{-6}	0.022
40	2.5	10	60	1.01×10^{-5}	5.19×10^{-6}	0.019
25	**0.0**	10	35	5.38×10^{-6}	5.38×10^{-6}	0.009
25	**1.0**	10	36	5.47×10^{-6}	4.56×10^{-6}	0.010
25	**2.5**	10	75	8.17×10^{-6}	4.90×10^{-6}	0.022
25	**5.0**	10	64	7.22×10^{-6}	3.69×10^{-6}	0.014
25	2.5	**5**	36	5.76×10^{-6}	3.87×10^{-6}	0.008
25	2.5	**10**	75	8.17×10^{-6}	4.90×10^{-6}	0.022
25	2.5	**20**	>120	1.21×10^{-5}	5.78×10^{-6}	0.041

5.3.1.2 Effect of the ferrous ion dose

Figure 5.3 reports the performance of the toluene treatment by Fenton's oxidation using different concentrations of iron (at 25 ºC). In this study, an experiment using only H_2O_2 (10 mM) was performed, for which C_{out} increases quickly along the process (Fig. 5.3a). The average absorption rate in the first 30 min and overall toluene transferred increased slightly as compared to the blank run (only water without reagents), being that after 35 min, liquid saturation occurred (see Table 5.1). A reduction in the oxidant concentration has been observed in the experiment without iron (Fig. 5.3b), which can be due to the hydrogen peroxide self-decomposition, stripping and consumption in the oxidation process. Actually, a very low accumulation of organic species occurred (represented by the DOC concentration that reached only ca. 10 mgC/L after 30 minutes (Fig. 5.3d)). This minor increase in the organics concentration in the liquid phase might be ascribed to the much smaller oxidation potential of the H_2O_2 (i.e., 1.78 V (Legrini *et al.* 1993)) as compared to the hydroxyl radical (i.e., 2.80 V (Legrini *et al.* 1993)). For that reason, the pH remained nearly constant during the process (Fig. 5.3b).

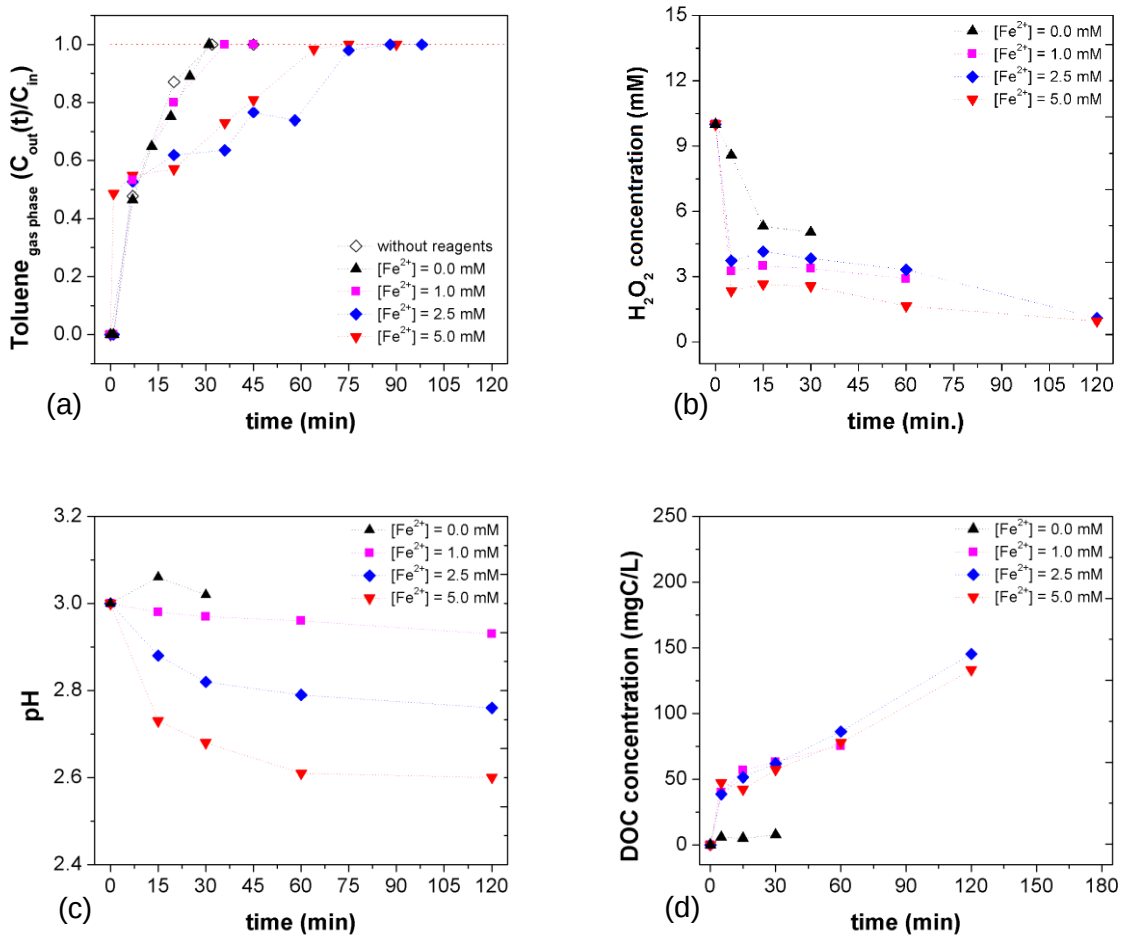

Figure 5.3 Effect of the catalyst dose in the toluene concentration at the outlet of the BR (a), and in the concentration of H_2O_2 (b), pH (c) and concentration of DOC (e) in the liquid phase along Fenton's reaction time. Experimental conditions: V = 0.5 L, pH_0 = 3.0, T = 25 ºC, $[H_2O_2]_0$ = 10 mM, and $Q_{toluene}$ = 1.0 L/min.

For all catalyst concentrations tested, C_{out} increased along reaction time until reaching the liquid's saturation. This time increases with the dose of iron up to 2.5 mM (t = 75 min) and then decreases for a higher catalyst dose (down to 64 min) – see Fig 5.3a, leading to a higher amount of toluene transferred per liter of solution for 2.5 mM (0.022 mol/L) against 1.0 (0.010 mol/L) and 5.0 mM (0.014 mol/L) of Fe^{2+} – see Table 5.1. As compared to the blank run (water without any reagents), when employing increasing iron doses the process time is enlarged because the driving force for toluene mass transfer is increasingly favoured by the higher amount of $HO^{\bullet}$ species formed in the liquid, inherently increasing the average absorption rate (Table 5.1). The inversion observed at 5 mM of ferrous ion may be explained by scavenging of the hydroxyl radicals by the excess of iron in solution (Eq. 5.6) (Walling 1975); this promotes the decrease of the oxidative species available to degrade the toluene transferred and consequently the

amount of oxidized compounds formed in the liquid phase decreases for 5 mM of Fe^{2+} – cf. Fig. 5.3d.

$$HO^{\bullet} + Fe^{2+} \rightarrow HO^{-} + Fe^{3+} \quad (5.6)$$

The concentration of H_2O_2 that remained in solution along the process was similar for both 1.0 and 2.5 mM of catalyst (Fig. 5.3b), being that more than 60% of the H_2O_2 dosed was consumed in the first minutes of reaction. However, the largest reduction in the H_2O_2 concentration was observed when using more catalyst ($[Fe^{2+}]$ = 5.0 mM), reaching a consumption above 75% in the first 5 min (Fig 5.3b).

During Fenton's reaction, the pH of the medium decreased up to 60 min and then remained nearly constant (see Fig. 5.3c). As previously mentioned, the acidification of the medium along the Fenton process is associated with carboxylic acids formations; for this reason, some authors report this parameter to be indicative of the oxidation stage along Fenton's reaction and a way to indirectly follow the process. Yet, the addition of the iron sulfate also promotes acidification of the medium. The highest reduction of pH observed for the highest iron dose may be associated with the increased amount of ferrous species added. Regarding the organic compounds formed along the process, the DOC was similar for all concentrations tested (Fig 5.3d), reaching values ranging from 90 to 120 mgC/L for 1.0 and 2.5 mM of Fe^{2+}, respectively, at 120 min of reaction. The optimum Fe^{2+} dose found corresponds to a $[Fe^{2+}]$:$[H_2O_2]$ molar ratio of 0.25, the same of the study by Liu *et al.* (G. Liu, Huang, *et al.* 2017) when treating a gas stream containing benzene by Fenton's oxidation.

5.3.1.3 Effect of the oxidant dose

Figure 5.4 reports the performance of Fenton's oxidation to degrade toluene using different H_2O_2 concentrations. An experiment using only $[Fe^{2+}]$ was not performed, taking into account that G. Liu, Huang *et al.* (2017) did not report any effect of it on the VOCs mass transfer to an aqueous $FeSO_4$ solution; still, no oxidation at all should occur without oxidant present in solution. When increasing the H_2O_2 dose, the time to reach the solution saturation increased (Fig 5.4a), reaching the highest amount of toluene transferred (and toluene absorption rate) for an H_2O_2 dose of 20 mM - Table 5.1; so, the performance of the overall treatment increased. Similar results were reported by G. Liu, Huang, *et al*. (2017), who observed an increase in the removal of benzene from the gas phase when more oxidant was dosed.

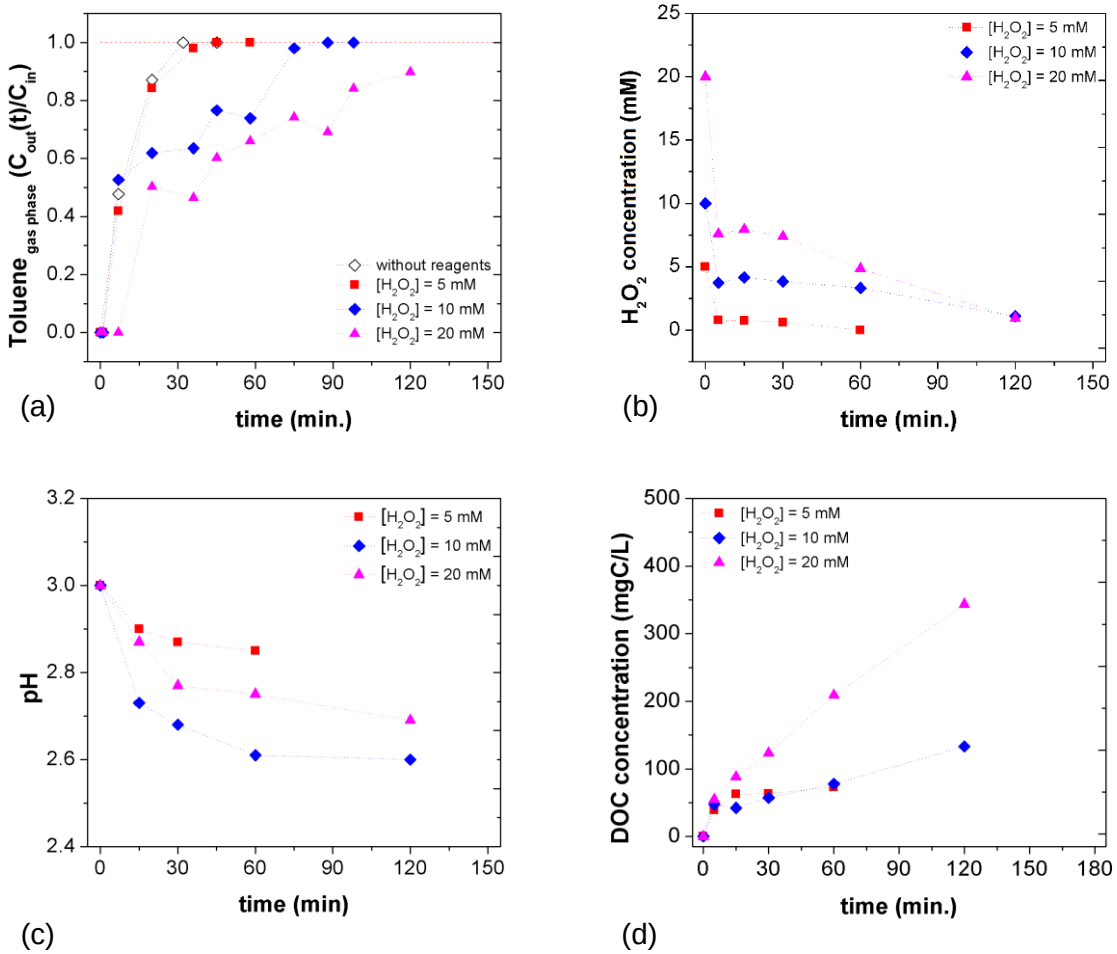

Figure 5.4 Effect of the oxidant dose in the toluene concentration at the outlet of the BR (a), and in the concentration H_2O_2 (b), pH (c) and concentration of DOC (d) in the liquid phase during Fenton's reaction time. Experimental conditions: V = 0.5 L, pH_0 = 3.0, T = 25 ºC, $[Fe^{2+}]_0$ = 2.5 mM, and $Q_{toluene}$ = 1.0 L/min.

Regardless of the oxidant concentration added, the reduction of the H_2O_2 available was fast in the first minutes of reaction (Fig 5.4b), being that in the experiment carried out with 5 mM of H_2O_2 it was completely consumed in only 30 min of reaction – approximately the same time that $C_{out}(t)/C_{in}$ = 1 was reached (see Fig 5.4a). Meanwhile, when increasing the concentration of H_2O_2 to 20 mM, more than 75% of the oxidant was consumed after 60 min of reaction, but its concentration was continuously reduced until 120 min. In this experiment, the process was interrupted at 120 min because it was observed a high formation of intermediate compounds, which increased the turbidity of the liquid phase and provoked the formation of a dense foam that compromised the GC analyses of the outlet gas stream. For this reason, $C_{out}(t)/C_{in}$ did not reach the maximum value of 1. The pH reduction in the liquid phase was more significant when the H_2O_2 dose was increased up to 10 mM (Fig 5.4c), so it is expectable that more carboxylic acids have been formed in such run. For 20 mM of H_2O_2, equivalent to an $[Fe^{2+}]$:$[H_2O_2]$

molar ratio of 0.125, it is expectable (according to other reports) that the oxidation rate and mechanism change, favouring the formation of intermediate compounds with higher molecular weight (as, for example, cresol and benzaldehyde (Long *et al.* 2014; Tokumura *et al.* 2013; Choi *et al.* 2014), and hydroquinone (Ardizzone *et al.* 2008)) that remain in the liquid phase along the treatment, and do not induce such a strong medium acidification. Consequently, the DOC concentration in the liquid phase increased along the treatment process, and for the experiment that was carried out with the highest concentration of H_2O_2 (20 mM), it was reached a DOC level of ~ 340 mgC/L after 120 min of Fenton's process (see Fig 5.4d).

It is worth noting that no H_2O_2 concentrations above 20 mM were tested because of the high amounts of organic compounds formed in the liquid phase under such conditions, which produced the problems reported above; moreover, it would increase the operating costs. Therefore, the H_2O_2 concentration was fixed at 20 mM for the next runs.

The partial (or incomplete) mineralization of the toluene along the Fenton process had already been reported, and some authors point out the accumulation of intermediate compounds in the liquid phase as a drawback of the discontinuous process (Moulis and Krýsa 2013), advising the use of a continuous operation system or recycling of the liquid phase. In our work, the organic load of the liquid effluent (COD > 850 mgO_2/L) was clearly above the maximum emission limit (COD = 30-100 mgO_2/L) required by the Commission Implementing Decision (EU) 2016/902 under Directive 2010/75/EU of the European Parliament and of the Council (Directive 2010; 2016). Therefore, we decided to perform intermediate stages of liquid treatment, as discussed in the following section. Decreasing the organic load of the aqueous phase would also provide the opportunity for new (subsequent) cycle(s) of toluene transfer, allowing for a continuous process operation in the same device – such possibility will be also addressed hereinbelow.

5.3.2 Sequential treatment of the gas stream containing toluene and liquid effluent produced

5.3.2.1 Sequential treatment in the lab-scale BR

In order to reduce the organic load that remains in the liquid effluent after treatment of the toluene-containing gas stream under the best conditions reported above (i.e., $[H_2O_2]_0$ = 20 mM, $[Fe^{2+}]_0$ = 2.5 mM, and T = 25 °C), a liquid phase (effluent) treatment was performed. In this new stage, i.e., after stopping the treatment of the gas containing

toluene, air bubbling was started to promote mixing. Afterwards, one more entire cycle was carried out – gas treatment stage with subsequent oxidation of the liquid.

Figure 5.5 reports the performance of Fenton's oxidation along the gas-liquid treatment stages (2 cycles, 4 stages in total). The first toluene treatment stage (stage 1) replicated efficiently the results obtained using the optimized conditions (see the previous section and results shown in Tables 5.1 and 5.2). Effectively, C_{out} increased until nearly 120 min (Fig 5.5a). During this time H_2O_2 had been fully consumed (Fig 5.5b), while the DOC accumulated in the liquid phase reached almost 350 mgC/L (Fig. 5.5c); then, the gas treatment was finished. Considering the COD concentration accumulated in the liquid (932 mgO_2/L – Table 5.2) and the full oxidant consumption on stage 1, more H_2O_2 (58 mM, calculated by the stoichiometric amount required for the complete oxidation up to CO_2 of the remaining organic matter (Lucas and Peres 2009)) was added to the effluent to proceed with the liquid treatment (stage 2). In the meantime, toluene bubbling has been replaced by air bubbling (at the same flow rate) that ensures efficient mixing, as reported before (Lima *et al.* 2018; Rodrigues *et al.* 2018). During the 2nd stage, the concentrations of H_2O_2 (Fig 5.5b), DOC (Fig 5.5c) and COD (see Table 5.2) were gradually reduced. The DOC and COD removals reached 25 % and 63 % at the end of stage 2, respectively; besides, the biodegradability of the effluent produced increased from 33.0 (end of stage 1, or beginning of stage 2) to 93.5 $mgO_2/g_{VSS}h$ (cf. Table 5.2).

Taking into account the characteristics of the effluent at the end of the 2nd stage, a new toluene treatment (stage 3) was started in order to evaluate also the performance of the overall process (toluene absorption and Fenton´s oxidation) in a liquid phase containing organics. For this, the same H_2O_2 concentration (58 mM) was added, and the toluene bubbling was initiated again. It is worth noting that, for the sequential process, no more catalyst was added, because the iron dissolved in the liquid phase ($FeSO_4$ was added at the beginning of stage 1) is regenerated. So, the application of a sequential treatment reduces the formation of iron sludge. The toluene bubbling lasted 30 min only, i.e., when C_{out} reached the feed concentration (Fig 5.5a); in this period, H_2O_2 was gradually consumed, remaining nearly 48 mM in solution at the end of this step (Fig 5.5b). The DOC concentration accumulated in the liquid phase reached 396 mgC/L (Fig 5.5c), while the COD concentration reached 477 mgO_2/L (Table 5.2) by the end of stage 3. So, the 2nd liquid treatment cycle (stage 4) was performed, but in this case, no further oxidant was introduced in the reactor, making use of the remaining one. During this last stage, a gradual reduction in the H_2O_2 concentration down to 10 mM after 2.5 h of treatment was observed (Fig 5.5b). Simultaneously, the DOC concentration was reduced to 224 mgC/L (Fig 5.5c), and the COD to 376 mgO_2/L (Table 5.2); the performances

reached during the 2nd liquid treatment stage represent a reduction of more than 21 % in terms of COD, and a mineralization of 43% (see Table 5.2). The treatment process was interrupted when the oxidant consumption was reduced to a very low rate. It is noteworthy that the final effluent produced was non-toxic and the biodegradability further increased, up to 103.3 $mgO_2/g_{VSS}h$ (Table 5.2).

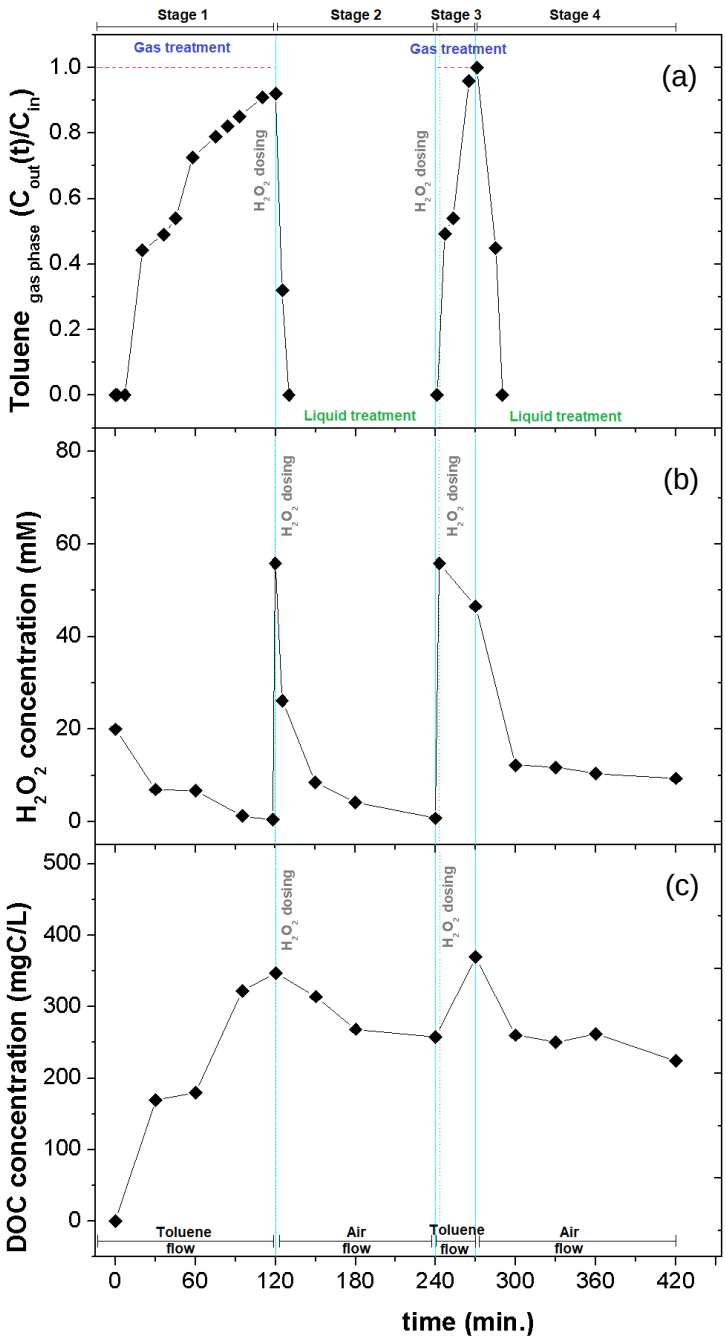

Figure 5.5 Performance of the sequential gas-liquid treatment in the BR in terms of the toluene concentration at the outlet of the BR (a), and concentration of H_2O_2 (b) and DOC (c) along the Fenton process. Experimental conditions: V = 0.5 L, T = 25 ºC, pH_0 = 3.0, $[Fe^{2+}]_0$ = 2.5 mM, $[H_2O_2]_0$ = 20 mM, and $Q_{toluene/air}$ = 1.0 L/min.

Table 5.2 Gas treatment stages indicators, and characterization of the liquid effluent (and its treatment efficiency) along the sequential gas-liquid treatment in the bubbling reactor.

Gas treatment stages indicators				
Stage	**Duration of the treatment stage (min)**	**Average absorption rate (mol/L.s)**		**Toluene transferred (mol/L)**
		At 30 min	*Overall process*	
1st toluene treatment stage (Stage 1)	120	1.24×10^{-5}	5.81×10^{-6}	0.041
2nd toluene treatment stage (Stage 3)	30	5.57×10^{-6}	3.71×10^{-6}	0.009

Liquid characteristics and its treatment efficiency				
Stage	**COD (mgO_2/L)[1]**	**DOC (mgC/L)[1]**	**Biodegradability ($mgO_2/g_{VSS}h$)**	**Acute toxicity[2] (%)**
Beginning of stage 2	932	346	33.0	0.0
End of stage 2	339 [63 %]	258 [25 %]	93.5	0.0
Beginning of stage 4	477	396	64.4	0.0
End of stage 4	376 [21 %]	224 [43 %]	103.3	0.0

[1] % removal values of the liquid treatment stages shown between square brackets.
[2] Value of % inhibition of *Vibrio Fischeri* at 30 min of contact time.

In what concerns the levels of toluene absorption rate and amount of toluene transferred to the liquid, both decreased from the 1st to the 2nd gas treatment stage – Table 5.2. These results indicate an adverse effect towards toluene absorption due to the presence of organic matter in the liquid phase after the 1st cycle of treatment. Even so, the proposed sequential treatment, i.e., a gas treatment stage followed by a liquid treatment stage, has shown to be effective in toluene treatment by Fenton's oxidation.

Upon the proof-of-concept of the sequential gas-liquid treatment, it was decided to work with a bubbling reactor with a higher volumetric capacity in order to extend the sequential treatment process for several cycles. So, a scale-up from the BR (0.5 L) to a BCR (5.0 L) was considered, i.e., using 10 times more of liquid volume. The sequential toluene-liquid treatment was carried in the BCR, also aiming to enable adequate liquid sampling throughout the treatment (therefore reducing possible effects associated to volume reduction), and the results obtained are described in the following section.

5.3.2.2 Sequential treatment in a BCR

Figure 5.6 reports the sequential gas-liquid treatment in the BCR. The gas-liquid treatment stages were sequentially numbered, so that after each gas (toluene) treatment stage (1, 3, and 5), a liquid treatment stage occurred (2, 4 and 6), as reported in section 3.2.1 for the BR. During the gas treatment stages, toluene bubbling was kept, while during each liquid treatment stage, the gas (toluene) was replaced by clean air at the same flow rate.

To start the 1st gas treatment stage the experimental conditions optimized in the parametric study (reported in section 5.3.1) were adopted – pH_0 = 3.0, T = 25 ºC, $[H_2O_2]_0$ = 20 mM and $[Fe^{2+}]_0$ = 2.5 mM.

Along the 1st toluene treatment stage (stage 1), C_{out} increased gradually (Fig 5.6a), while the H_2O_2 concentration (Fig 5.6b) and pH (Fig 5.6c) decreased along the process. Inherently, both DOC and COD accumulated in the liquid along this gas treatment stage, reaching values above 200 mgC/L and 700 mgO_2/L (Fig 5.6d), respectively. The treatment stage was stopped after 2 h, and at this time, the toluene transferred reached 0.008 mol/L (Table 5.3). At this point, the 1st liquid treatment step (stage 2) was initiated making use of the remaining H_2O_2 in the solution, and the treatment was extended for more 2 hours. Along the first 15 min of this 2nd stage, it was observed that C_{out} decreased quickly down to zero (Fig 5.6a) as a consequence of the air bubbling that promoted the stripping of the dissolved toluene not yet converted. Therefore, for the effective treatment of the toluene transferred, in future works one should consider other strategies to recover and oxidize such lost toluene (e.g., by gas recirculation). Even so, some oxidation of the organics present in the liquid should have occurred, as proved by the slight reduction of pH (from 2.60 to 2.53 – Fig 5.6c) and H_2O_2 concentration (which was fully consumed – Fig 5.6b), while the COD concentration decreased a little bit (Fig 5.6d); still, the biodegradability of the effluent increased from 77 to 111 $mgO_2/g_{VSS}h$ while exhibiting no toxicity (see Table 5.3).

For the 2nd gas treatment stage (stage 3), it was adopted the strategy of reusing the initial conditions of pH and oxidant concentration to achieve an efficient toluene treatment. So, the pH was adjusted to 3.0, and H_2O_2 (20 mM) was added to the effluent at the same time that the toluene bubbling was started. Along this gas treatment stage, the C_{out} increased quickly during the first 45 min of treatment (4.75 h of sequential treatment – Fig 5.6a), which might be due to the interference of existing organics in toluene absorption. However, it was observed a very fast reduction of the H_2O_2 concentration with almost full consumption (Fig 5.6b) while the pH was reduced from 3.0

to 2.6 (Fig 5.6c). For this reason, and in order to increase the toluene absorption, H_2O_2 was added again to the effluent, which extended the toluene treatment for more 40 min (corresponding to 5.4 h of sequential treatment – Fig 5.6). In the meantime, the COD increased substantially, achieving more than 1000 mgO_2/L at the end of stage 3 (Fig 5.6d), which promoted the increase of the turbidity and the formation of a dense foam (as previously reported). So, for this reason, this gas treatment stage was interrupted. At this instant, a hydrogen peroxide concentration of ca. 10 mM remained available in the liquid phase. In such 2nd gas treatment step (stage 3), the toluene transferred (as well as the average absorption rate) decreased as compared to stage 1 (see Table 5.3), which was attributed to the effect of the organics accumulation. The 2nd liquid treatment step (stage 4) was then performed, and during the first 2 h of oxidation, the existing H_2O_2 was gradually consumed (Fig. 5.6b); at this point, the concentrations of DOC and COD were above 300 mgC/L and 1000 mgO_2/L, respectively, and for this reason it was adopted the strategy of establishing again the initial conditions of pH (with adjustment to 3.0) and H_2O_2 (with addition of more oxidant) at 8 h of the sequential gas-liquid treatment (see Fig. 5.6). So, the 2nd liquid treatment stage was prolonged, and the COD and DOC concentrations decreased to nearly 750 mgO_2/L and 300 mgC/L (Fig. 5.6d), respectively, at ca. 8.5 h. However, because the H_2O_2 was fully consumed (Fig 5.6b), and in order to further promote the organic load oxidation, more oxidant was added again until the same concentration, thus being possible to extend the treatment (until 12 h). The new oxidant dose was enough to reach a DOC and a COD reduction down to ca. 280 and 520 mg/L, respectively. The mineralization of the organic load existent in the liquid phase during this stage of treatment was 12 %, and COD decreased 52% (Table 5.3). However, the biodegradability decreased (from 60 to 32 $mgO_2/g_{VSS}h$ – Table 5.3), although the effluent is still non-toxic (see Table 5.3).

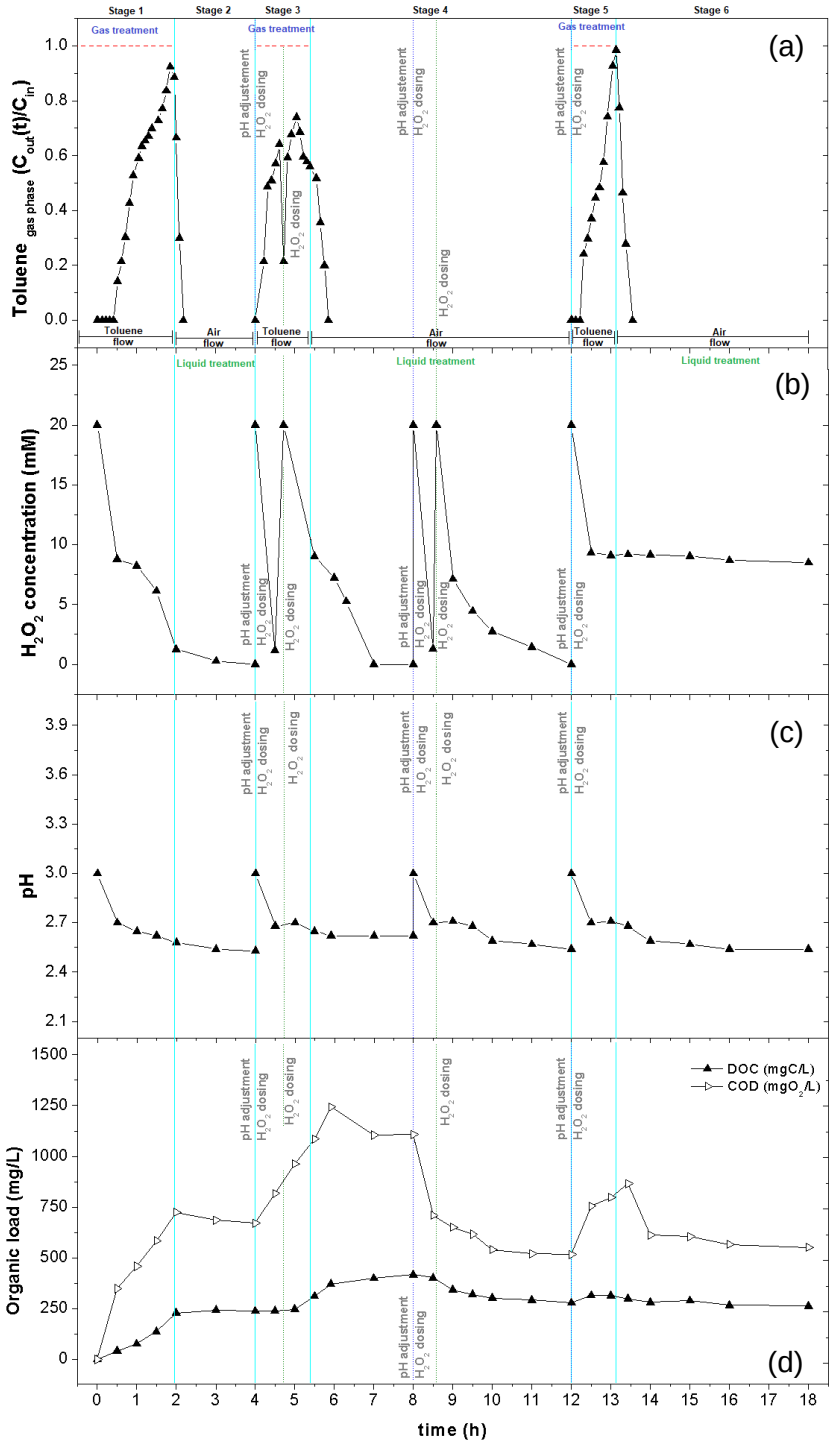

Figure 5.6 Performance of the sequential gas-liquid treatment in the BCR in terms of the toluene concentration at the outlet of the BCR (a), concentration of H_2O_2 (b), pH (c) and concentrations of DOC and COD (d) along the Fenton process time. Experimental conditions: V = 5.0 L, T = 25 ºC, $pH_{0,\ pH\ adjust\ steps}$ = 3.0, $[Fe^{2+}]_0$ = 2.5 mM, $[H_2O_2]_{0,\ oxidant\ dose\ steps}$ = 20 mM, and $Q_{toluene/air}$ = 1.0 L/min.

The 3rd toluene treatment stage (stage 5) was performed after re-establishing the initial conditions of pH and H_2O_2 concentration. The gas treatment was carried for almost 70

min (Fig. 5.6a), providing an increase in the toluene absorbed (Table 5.3). The H_2O_2 concentration was reduced to about 10 mM (Fig 5.6b), and the pH decreased to 2.7 (Fig 5.6c). The organic load increased, as expected, being reached more than 850 mgO_2/L of COD, with a negligible variation on the DOC (Fig. 5.6d). So, the 3rd and final liquid treatment step (stage 6) was implemented without adding further H_2O_2, and proceeded along 5 h; during the effluent oxidation the H_2O_2 concentration decreased only very slightly (from 10 to 7.5 mM – Fig. 5.6b), and the same occurred with the pH that hardly changed (Fig. 5.6c). Even so, the DOC and particularly the COD concentrations were reduced to nearly 260 mgC/L and 550 mgO_2/L (Fig 5.6d), respectively. The treatment was interrupted when the H_2O_2 concentration remained nearly constant, suggesting that it was no longer being efficiently used to oxidize the organic matter. The final effluent, after the last liquid treatment stage, was even more biodegradable than upon the previous stage, and still non-toxic (see Table 5.3).

Regarding the overall performance of the sequential gas-liquid treatment, it was observed that the proposed strategy was efficient, allowing to implement three consecutive gas absorption + oxidation stages with intermediate liquid oxidation, lasting in total almost 20 h. However, the final effluent has a COD level above the emission limit value (30-100 mgO_2/L) imposed by the European Parliament and the Council (Directive 2010; 2016). So, the liquid treatment steps still need to be optimized, for instance, through new additions of catalyst and/or oxidant; this will be the goal of future works. Alternatively, one may consider to couple downstream a biological unit for the liquid effluent management, because it is non-toxic and biodegradable.

One of the drawbacks of the process is the loss of some non-oxidized toluene during the liquid treatment stages (Fig. 5.6a). For this reason, for future work, it is suggested to promote the gas phase recycling, so that the untreated volatile pollutant is not dragged from the liquid to the gas phase by air stripping.

Table 5.3 Gas treatment stages indicators, and characterization of the liquid effluent (and its treatment efficiency) along the sequential gas-liquid treatment in the bubbling column reactor.

Gas treatment stages indicators				
Stage	**Duration of the treatment stage (min)**	**Average absorption rate (mol/L.s)** *At 30 min*	*Overall process*	**Toluene transferred (mol/L)**
1st toluene treatment stage (Stage 1)	120	1.01×10^{-6}	2.14×10^{-6}	0.008
2nd toluene treatment stage (Stage 3)	45	7.12×10^{-7}	9.86×10^{-7}	0.003
3rd toluene treatment stage (Stage 5)	68	1.96×10^{-6}	1.14×10^{-6}	0.006

Liquid characteristics and its treatment efficiency				
Stage	**COD (mgO_2/L)[1]**	**DOC (mgC/L)[1]**	**Biodegradability ($mgO_2/g_{VSS}h$)**	**Acute toxicity[2] (%)**
Beginning of stage 2	723	239	77	0.0
End of stage 2	676 [7 %]	228 [4 %]	111	0.0
Beginning of stage 4	1085	315	60	0.0
End of stage 4	516 [52 %]	278 [12 %]	32	0.0
Beginning of stage 6	865	298	18	0.0
End of stage 6	551 [36 %]	263 [11 %]	42	0.0

[1] % removal values of the liquid treatment stages shown between square brackets.
[2] Value of % inhibition of *Vibrio Fischeri* at 30 min of contact time.

5.4 Conclusions

The treatment of a gaseous effluent containing toluene by Fenton's oxidation in bubbling reactors has been evaluated in the present study, as well as the sequential gas-liquid treatment in the same reactor configurations; it was concluded that:

- The rise of the temperature of the reaction medium (an important operating parameter) promoted an increase of the toluene mass transfer and average toluene absorption rate from the gas to the liquid when there is no reaction. However, for Fenton's oxidation, the rise of the temperature (from 25 to 40 ºC) did not favor the overall process.
- Under optimized conditions ($[Fe^{2+}]$ = 2.5 mM, $[H_2O_2]$ = 20 mM, and T = 25 ºC), the average toluene absorption rate increased, and the toluene transferred from the gas to the liquid phase achieved 0.041 mol/L after 120 minutes of reaction;
- The gas treatment strategy proposed was responsible for the generation of an effluent with a high amount of organic compounds, and so a subsequent treatment of the liquid phase was required;
- In the preliminary sequential gas-liquid treatment carried out in the BR two toluene (and liquid) treatment stages were successfully implemented, being that during each of the two stages the liquid treatment was enough to mineralize 25 and 43 % of the effluent produced after each gas treatment stage;
- The process under optimized conditions was successfully implemented in a larger scale device (BCR), which allowed to extend the sequential gas-liquid treatment for almost 20 h, with three toluene treatment stages and subsequent steps of liquid oxidation; this yielded a final effluent that is non-toxic and biodegradable.

5.5 References

APHA, WEF A. 1988. 'Standard Methods for the Examination of Water and Wastewater'. In *Water Pollution Control Federation*, edited by American Public Health Association. Washington DC,: American Water Works Association.

Ardizzone, S., C. L. Bianchi, G. Cappelletti, A. Naldoni, and C. Pirola. 2008. 'Photocatalytic Degradation of Toluene in the Gas Phase: Relationship between Surface Species and Catalyst Features'. *Environmental Science and Technology* 42 (17): 6671–76.

Babuponnusami, A., and Karuppan Muthukumar. 2014. 'A Review on Fenton and Improvements to the Fenton Process for Wastewater Treatment'. *Journal of Environmental Chemical Engineering* 2 (1): 557–72.

Barb, W. G., J. H. Baxendale, P. G., and K. R. Hargrave. 1949. 'Reactions of Ferrous and Ferric Ions with Hydrogen Peroxide'. *Nature* 163 (4148): 692–94.

Bekbolet, M. 2011. 'Fundamentals of Advanced Oxidation Processes'. *Water, Wastewater and Soil Treatment by AOPs*, 13–22.

Bolden, A. L., C. F. Kwiatkowski, and T. Colborn. 2015. 'New Look at BTEX: Are Ambient Levels a Problem'. *Environmental Science and Technology* 49 (9): 5261–76.

Cerqueira, M. A., C. A. Pio, P. A. Gomes, J. S. Matos, and T. V. Nunes. 2003. 'Volatile Organic Compounds in Rural Atmospheres of Central Portugal'. *Science of the Total Environment* 313 (1–3): 49–60.

Choi, K., S. Bae, and W. Lee. 2014. 'Degradation of Off-Gas Toluene in Continuous Pyrite Fenton System'. *Journal of Hazardous Materials* 280: 31–37.

Ciccioli, P. 2011. 'VOCs and Air Pollution'. *Chemistry and Analysis of Volatile Organic Compounds in the Environment*, 92–174.

Correa, S. M., G. Arbilla, M.R.C. Marques, and K. M.P.G. Oliveira. 2012. 'The Impact of BTEX Emissions from Gas Stations into the Atmosphere'. *Atmospheric Pollution Research* 3 (2): 163–69.

Corsi, R.L., and L. Seed. 1995. 'Biofiltration of BTEX: Media, Substrate, and Loadings Effects'. *Environmental Progress* 14 (3): 151–58.

Daifullah, A. A.M., and B. S. Girgis. 2003. 'Impact of Surface Characteristics of Activated Carbon on Adsorption of BTEX'. *Colloids and Surfaces A: Physicochemical and Engineering Aspects* 214 (1–3): 181–93.

Deng, Y., and R. Zhao. 2015. 'Advanced Oxidation Processes (AOPs) in Wastewater Treatment'. *Current Pollution Reports* 1 (3): 167–76.

Directive, Council. 2010. 'Directive 2010/75/EU of the European Parliament and of the Council'. *Official Journal of the European Union* 334: 17–119.

Directive, Council. 2016. 'Commission Implementing Decision (EU) 2016/902'. *Official Journal of the European Union* 2001 (May): 20–30.

Durmusoglu, E., F. Taspinar, and A. Karademir. 2010. 'Health Risk Assessment of BTEX Emissions in the Landfill Environment'. *Journal of Hazardous Materials* 176 (1–3): 870–77. h

Fenton, H.J.H. 1894. 'LXXIII.—Oxidation of Tartaric Acid in Presence of Iron'. *Journal of the Chemical Society, Transactions* 65: 899–910.

Gligorovski, S., R. Strekowski, S. Barbati, and D. Vione. 2015. 'Environmental Implications of Hydroxyl Radicals (•OH)'. *Chemical Reviews* 115 (24): 13051–92.

Guedes, A. M.F.M., L. M.P. Madeira, R.A.R. Boaventura, and C. A.V. Costa. 2003. 'Fenton Oxidation of Cork Cooking Wastewater—Overall Kinetic Analysis'. *Water Research* 37 (13): 3061–69.

Guo, R. T., Wei Guo Pan, Xiao Bo Zhang, Jian Xing Ren, Qiang Jin, Hong Jian Xu, and Jiang Wu. 2011. 'Removal of NO by Using Fenton Reagent Solution in a Lab-Scale Bubbling Reactor'. *Fuel* 90 (11): 3295–98.

Handa, M., Y. Lee, M. Shibusawa, M. Tokumura, and Y. Kawase. 2013. 'Removal of VOCs in Waste Gas by the Photo-Fenton Reaction: Effects of Dosage of Fenton Reagents on Degradation of Toluene Gas in a Bubble Column'. *Journal of Chemical Technology and Biotechnology* 88 (1): 88–97.

Hinwood, A. L., C. Rodriguez, T. Runnion, D. Farrar, F. Murray, A. Horton, D. Glass, *et al.* 2007. 'Risk Factors for Increased BTEX Exposure in Four Australian Cities'. *Chemosphere* 66 (3): 533–41.

ISO. 2005. 'Water Quality - Determination of the Inhibitory Effect of Water Method, Samples on the Light Emission of Vibrio Fischeri (Luminescent Bacteria Test) - Part 3: Using Freeze-Dried Bacteria'. In . International Organization for Standardzation.

Kantarci, N., F. Borak, and K.O. Ulgen. 2005. 'Bubble Column Reactors'. *Process Biochemistry* 40 (7): 2263–83.

Kavitha, V., and K. Palanivelu. 2005. 'Degradation of Nitrophenols by Fenton and Photo-Fenton Processes'. *Journal of Photochemistry and Photobiology A: Chemistry* 170

(1): 83–95.

Lee, S. C., M. Y. Chiu, K. F. Ho, S. C. Zou, and Xinming Wang. 2002. 'Volatile Organic Compounds (VOCs) in Urban Atmosphere of Hong Kong'. *Chemosphere* 48 (3): 375–82.

Legrini, O., E. Oliveros, and A.M. Braun. 1993. 'Photochemical Processes for Water Treatment'. *Chemical Reviews* 93 (2): 671–98.

Lima, V. N., C. S. D. Rodrigues, R. A. C. Borges, and L. M. Madeira. 2018. 'Gaseous and Liquid Effluents Treatment in Bubble Column Reactors by Advanced Oxidation Processes: A Review'. *Critical Reviews in Environmental Science and Technology* 48 (16–18): 1–48.

Lima, V. N., C. S.D. Rodrigues, and L. M. Madeira. 2018. 'Application of the Fenton's Process in a Bubble Column Reactor for Hydroquinone Degradation'. *Environmental Science and Pollution Research* 25 (35): 34851–62.

Liu, G., H. Huang, R. Xie, Q. Feng, R. Fang, Y. Shu, Y. Zhan, X. Ye, and C. Zhong. 2017. 'Enhanced Degradation of Gaseous Benzene by a Fenton Reaction'. *RSC Adv.* 7 (1): 71–76.

Liu, G., J. Ji, H. Huang, R. Xie, Q. Feng, Y. Shu, Y. Zhan, *et al.* 2017. 'UV/H2O2: An Efficient Aqueous Advanced Oxidation Process for VOCs Removal'. *Chemical Engineering Journal* 324: 44–50.

Liu, Y., Y. Wang, Q. Wang, J. Pan, Y. Zhang, J. Zhou, and J. Zhang. 2015. 'A Study on Removal of Elemental Mercury in Flue Gas Using Fenton Solution'. *Journal of Hazardous Materials* 292 (July): 164–72.

Long, A., Y. Lei, and H. Zhang. 2014. 'Degradation of Toluene by a Selective Ferrous Ion Activated Persulfate Oxidation Process'. *Industrial and Engineering Chemistry Research* 53 (3): 1033–39.

Lucas, M.S., and A. J. Peres. 2009. 'Removal of COD from Olive Mill Wastewater by Fenton's Reagent: Kinetic Study'. *Journal of Hazardous Materials* 168 (2–3): 1253–59.

Martínez, F., G. Calleja, J. A. Melero, and R. Molina. 2007. 'Iron Species Incorporated over Different Silica Supports for the Heterogeneous Photo-Fenton Oxidation of Phenol'. *Applied Catalysis B: Environmental* 70 (1–4): 452–60.

Moulis, F., and J. Krýsa. 2013. 'Photocatalytic Degradation of Several VOCs (n-Hexane, n-Butyl Acetate and Toluene) on TiO 2 Layer in a Closed-Loop Reactor'. *Catalysis*

Today 209: 153–58.

Nidheesh, P.V., and R. Gandhimathi. 2015. 'Electro Fenton Oxidation for the Removal of Rhodamine B from Aqueous Solution in a Bubble Column Reactor under Continuous Mode'. *Desalination and Water Treatment* 55 (1): 263–71.

Orlando, J. P., D. S. Alvim, A. Yamazaki, S. M. Corrêa, and L. V. Gatti. 2010. 'Ozone Precursors for the São Paulo Metropolitan Area'. *Science of the Total Environment* 408 (7): 1612–20.

Oturan, M. A., and J.J. Aaron. 2014. 'Advanced Oxidation Processes in Water/Wastewater Treatment: Principles and Applications. A Review'. *Critical Reviews in Environmental Science and Technology* 44 (23): 2577–2641.

Pliego, G., J.A. Zazo, P. Garcia-Muñoz, M. Munoz, J.A. Casas, and J.J. Rodriguez. 2015. 'Trends in the Intensification of the Fenton Process for Wastewater Treatment: An Overview'. *Critical Reviews in Environmental Science and Technology* 45 (24): 2611–92.

Qiu, C., S. Yuan, X. Li, H. Wang, B. Bakheet, S. Komarneni, and Y. Wang. 2014. 'Investigation of the Synergistic Effects for *p*-Nitrophenol Mineralization by a Combined Process of Ozonation and Electrolysis Using a Boron-Doped Diamond Anode'. *Journal of Hazardous Materials* 280: 644–53.

Ramirez, J.H., F.J. Maldonado-Hódar, A.F. Pérez-Cadenas, C. Moreno-Castilla, C.A. Costa, and L.M. Madeira. 2007. 'Azo-Dye Orange II Degradation by Heterogeneous Fenton-like Reaction Using Carbon-Fe Catalysts'. *Applied Catalysis B: Environmental* 75 (3–4): 312–23.

Rodrigues, C. S.D., R. A.C. Borges, V. N. Lima, and L. M. Madeira. 2018. '*p*-Nitrophenol Degradation by Fenton's Oxidation in a Bubble Column Reactor'. *Journal of Environmental Management* 206: 774–85.

Rodrigues, C. S.D., L. M. Madeira, and R.A.R. Boaventura. 2014. 'Synthetic Textile Dyeing Wastewater Treatment by Integration of Advanced Oxidation and Biological Processes - Performance Analysis with Costs Reduction'. *Journal of Environmental Chemical Engineering* 2 (2): 1027–39.

Rosales, E., M. Pazos, M. A. Longo, and M. A. Sanromán. 2009. 'Electro-Fenton Decoloration of Dyes in a Continuous Reactor: A Promising Technology in Colored Wastewater Treatment'. *Chemical Engineering Journal* 155 (1–2): 62–67.

Sanemasa, I., M. Araki, T. Deguchi, and H. Nagai. 1982. 'Solubility Measurements of Benzene and the Alkylbenzenes in Water By Making Use of Solute Vapor.' *Bulletin*

of the Chemical Society of Japan 55 (4): 1054–62.

Sellers, R. M. 1980. 'Spectrophotometric Determination of Hydrogen Peroxide Using Potassium Titanium (IV) Oxalate'. *Analyst* 105 (1255): 950–54.

Štandeker, S., Z. Novak, and Ž. Knez. 2009. 'Removal of BTEX Vapours from Waste Gas Streams Using Silica Aerogels of Different Hydrophobicity'. *Journal of Hazardous Materials* 165 (1–3): 1114–18.

Tokumura, M., R. Nakajima, H. T. Znad, and Y. Kawase. 2008. 'Chemical Absorption Process for Degradation of VOC Gas Using Heterogeneous Gas-Liquid Photocatalytic Oxidation: Toluene Degradation by Photo-Fenton Reaction'. *Chemosphere* 73 (5): 768–75.

Tokumura, M., M. Shibusawa, and Y. Kawase. 2013. 'Dynamic Simulation of Degradation of Toluene in Waste Gas by the Photo-Fenton Reaction in a Bubble Column'. *Chemical Engineering Science* 100 (August): 212–24.

US EPA. 2005. 'Toxicological Review of Toluene'. *Washington (DC):US Environmental Protection Agency*.

US EPA. 2014. 'Priority Pollutant List'. *Effluent Guidelines*, 2. https://www.epa.gov/eg/toxic-and-priority-pollutants-under-clean-water-act.

Walling, C. 1975. 'Fenton's Reagent Revisited'. *Accounts of Chemical Research* 8 (4): 125–31.

Wang, S.. 2008. 'A Comparative Study of Fenton and Fenton-like Reaction Kinetics in Decolourisation of Wastewater'. *Dyes and Pigments* 76 (3): 714–20.

Xie, R., J. Ji, K. Guo, D. Lei, Q. Fan, D. Y.C. Leung, and H. Huang. 2019. 'Wet Scrubber Coupled with UV/PMS Process for Efficient Removal of Gaseous VOCs: Roles of Sulfate and Hydroxyl Radicals'. *Chemical Engineering Journal* 356: 632–40.

Yan, L., J. Liu, Z. Feng, and P. Zhao. 2016. 'Continuous Degradation of BTEX in Landfill Gas by the UV-Fenton Reaction'. *RSC Adv.* 6 (2): 1452–59.

Zhao, Y., X. Wen, T. Guo, and J. Zhou. 2014. 'Desulfurization and Denitrogenation from Flue Gas Using Fenton Reagent'. *Fuel Processing Technology* 128: 54–60.

Chapter 6. Simultaneous Treatment of Toluene-Containing Waste Gas and Industrial Wastewater by the Fenton Process

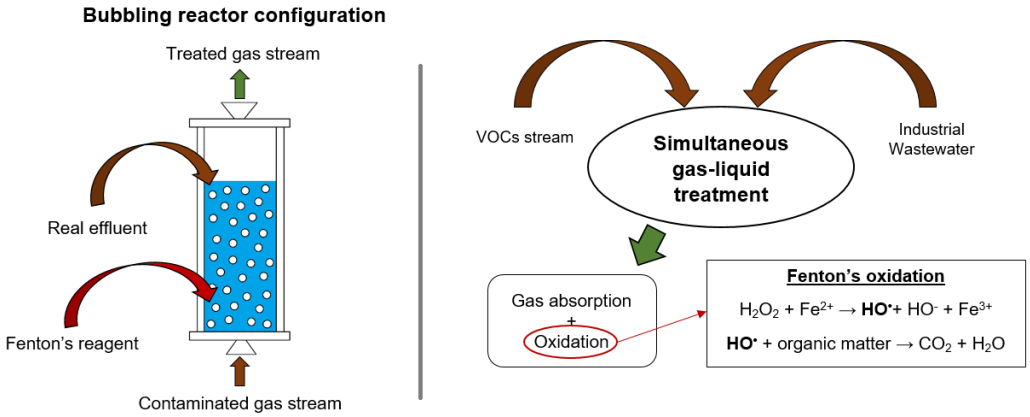

- First study concerning the simultaneous gas-liquid treatment using Fenton's reagent;
- The organic matter present in the wastewater affects the toluene absorption;
- A bubbling reactor proved to be useful to perform the simultaneous treatment;
- The partial toluene oxidation increases the organic matter content in the liquid phase.

The contents of this chapter were adapted from: Lima, V. N., Rodrigues, C. S. D., and Madeira, L. M. Simultaneous treatment of toluene-containing waste gas and industrial wastewater by the Fenton process (*submitted*).

Abstract: *This study reports a new perspective for the simultaneous oxidation of a volatile organic compound (VOC) – a toluene gas stream – and a real industrial liquid effluent by the Fenton's process; for that a lab-scale bubbling reactor, operating in semi-continuous mode, was used. A parametric study was carried out to evaluate the effect of the aqueous matrix (water vs. real effluent), catalyst species nature (Fe^{2+} vs. Fe^{3+}), concentration of organic matter in the liquid and inlet toluene concentration in both removal of toluene from the gas stream and wastewater mineralization. The presence of organic matter in the liquid phase decreased toluene absorption, but the simultaneous oxidation in the liquid phase extended the period of absorption until saturation (and inherently the amount of toluene transferred) while still oxidizing 25% of the organic matter present in the industrial effluent. The application of the Fenton-like ($H_2O_2 + Fe^{3+}$) process yielded a slightly reduced toluene transfer as compared to the Fenton one ($H_2O_2 + Fe^{2+}$) – ca. 10 %, although the overall mineralization has been similar. As expected, increasing the inlet toluene concentration reduces the process duration until liquid saturation, at the same time that higher accumulation of by-products in the liquid from oxidation was observed. Finally, a sequential treatment strategy was performed, wherein liquid oxidation follows the previous simultaneous gas-liquid treatment, representing a strategy for long term operation, providing opportunity for further VOC abatement in subsequent cycles. The main compounds resulting from oxidation remaining in the liquid phase after each stage were identified, allowing to close the carbon balance by ca. 80%.*

6.1 Introduction

The interest in advanced oxidation processes (AOPs) for the treatment of effluents has increased significantly in recent years, once these technologies are quite efficient from the environmental point of view, reducing significantly the risks associated with the pollutants emissions/discharges of organic toxic contaminants (Oturan and Aaron 2014; Deng and Zhao 2015; Lima *et al.* 2018a). This applies for the treatment of either liquid or gas pollutants, such as volatile organic compounds (VOCs) (G. Liu, Ji, *et al.* 2017; Mo *et al.* 2009; Xie *et al.* 2019; Moulis and Krýsa 2013; J. Zhao *et al.* 2020).

The AOPs involve the formation, *in situ*, of an oxidizing species (e.g., the hydroxyl radical - $HO^{\bullet}$ (Walling 1975; Gligorovski *et al.* 2015)) that are responsible to perform the total, or partial, degradation of organic pollutants (RH) through their oxidation with possible subsequent mineralization into CO_2 and water (Eq. 6.1).

$$RH + HO^{\bullet} \xrightarrow{\text{aqueous solution}} \text{by-products} \xrightarrow{HO^{\bullet}} CO_2 + H_2O \quad (6.1)$$

Among the numerous AOPs, the Fenton's process (Fenton 1894) stands out because it can be operated under moderate conditions of temperature and pressure (atmospheric pressure and room temperature), making use of environmentally friendly reagents. Such process is in short based on the reaction between hydrogen peroxide (H_2O_2) and a catalyst, typically iron (e.g., ferrous - Fe^{2+} or ferric - Fe^{3+} - salt), whose reaction produces the hydroxyl radical (Eq. 2) (Walling 1975; Barb *et al.* 1951a), which has an oxidation potential as high as 2.8 eV (Papadopoulos *et al.* 2007). Along the reaction, the regeneration of the catalyst also occurs as described in Eq. 6.3 for the ferric to ferrous iron conversion (Walling 1975; Barb *et al.* 1951b; 1951a)), although at a much smaller rate than Eq. 6.2 (Rivas *et al.* 2004; Beltran De Heredia *et al.* 2001; Walling and Goosen 1973):

$$Fe^{2+} + H_2O_2 \rightarrow HO^{-} + HO^{\bullet} + Fe^{3+}\ ,\ k_1 = 13.01\text{-}10^2\ M^{-1}.s^{-1} \quad (6.2)$$

$$Fe^{3+} + H_2O_2 \rightarrow Fe^{2+} + H^{+} + HO^{\bullet}{}_2\ ,\ k_2 = 0.01\ M^{-1}.s^{-1} \quad (6.3)$$

Apart from the advantages referred above, this process has shown to be suitable for the treatment of a wide range of effluents, from model compounds (Ma *et al.* 2000; Lima *et al.* 2018b; Rodrigues *et al.* 2018), with low complexity, till real effluents (Esteves *et al.* 2019; Lucas and Peres 2009), which are typically more difficult to remediate and far more complex.

Typically, when the Fenton's process is used the pollutants are in the same phase (liquid) where the treatment is processed. However, such AOP can also be used in the

remediation of gaseous effluents (e.g., gas streams containing VOCs), being firstly necessary to transfer the pollutant from the gas to the liquid phase where the Fenton's reagents are initially present and where oxidation occurs. The pollutant transfer from the gas to the liquid phase can be reached using bubbling reactors (BRs) (Hernández *et al.* 2011), which are multiphase devices with exceptional performance in terms of both mass and heat transfer (Kulkarni and Joshi 2011; Heijnen and Riet 1984). Therefore, for such kind of application, the process involves the absorption of the pollutant(s) in the liquid phase and a simultaneous oxidation by an oxidizing species (e.g., the $HO^{\bullet}$ species formed by the Fenton reaction (Eq. 6.2)), in an integrated process with simultaneous absorption and oxidation (Tokumura *et al.* 2008).

The application of the Fenton's process for gas treatment in BRs has already been reported in the literature, and includes the treatment of waste gas containing species like NO (Guo *et al.* 2011), NO_2 and SO_x (Y. Zhao *et al.* 2014), elemental mercury (Hg^0) (Y. X. Liu *et al.* 2015; Y. Liu *et al.* 2015), or hydrogen sulfide (H_2S) (Wang *et al.* 2019; Wang *et al.* 2019). On the other hand, for VOCs degradation other AOPs such as photo-Fenton (Tokumura *et al.* 2013; Tokumura *et al.* 2008; Handa *et al.* 2013), UV-Fenton (Chen *et al.* 2018) and UV/H_2O_2 (G. Liu, Ji, *et al.* 2017), UV/peroxymonosulfate (Xie *et al.* 2019) have been studied instead. Although these studies reveal that such configurations are in general extremely effective for diverse gas removals, when it comes to treating gas streams containing VOCs the incomplete oxidation yields the accumulation of organic intermediate compounds in the liquid phase (cf. Eq. 6.1), which has been poorly or scarcely addressed by other studies. Therefore, such issue must be clearly taken into account. If a solution is found, it opens the door for the simultaneous treatment of gas and liquid effluents in the same device, which is herein addressed, up to the authors' knowledge, for the first time.

The aim of this study is therefore to perform the proof-of-concept of the simultaneous treatment of a gas stream containing toluene (a model compound with high toxicity (US EPA 2005)), and a real industrial wastewater by Fenton's oxidation in the same device. The effects of the aqueous matrix nature (water *vs.* real effluent), iron species used as catalyst (ferrous *vs*. ferric salt), concentration of organic matter initially present in the liquid phase and the inlet toluene concentration were evaluated during the simultaneous gas-liquid treatment in terms of toluene removal (from the gas to the liquid) and organic load mineralization (in the liquid phase); still, the main compounds resulting from oxidation remaining in the liquid phase after each stage were identified.

6.2 Material and methods

6.2.1 Contaminated gas stream

The gas stream containing toluene has been simulated following the experimental set-up shown in Figure 6.1. For that, air (at a predetermined flow rate) is fed continuously into a 0.5 L glass washing bottle (Duran) containing 0.4 L liquid toluene (C_7H_8, 99 wt.%, from JMGS) submerged in water at 25 ºC using a Polystat CC1 thermostatic bath (Huber) to yield a saturated toluene gas stream. This saturated stream is fed to a second bottle where it is mixed (and inherently diluted) with a clean air stream at a predetermined flow rate. The inlet toluene concentration - C_{in} (measured using a GC following the procedure described in section 6.2.4.2) - was determined in sampling point no. 5 in Fig. 6.1. The air flow rate was pumped using an air pump (model air 550R plus from Sera Precision), and the gas flow rate in each line controlled using two direct-reading flowmeters (Cole Parmer) coupled with non-return valves (Swagelok). For all experiments, the gas flow rate fed into the reactor was maintained at 1.0 L/min (measured at room temperature and atmospheric pressure), which ensured perfect mixing inside the reactor without resorting to any mechanical stirring device (Lima *et al.* 2018b; Rodrigues *et al.* 2018). The inlet toluene concentration range (from 0.016 to 0.060 g/L) has been changed by dilution of the saturated toluene stream with air, keeping constant the total gas flow rate at 1.0 L/min.

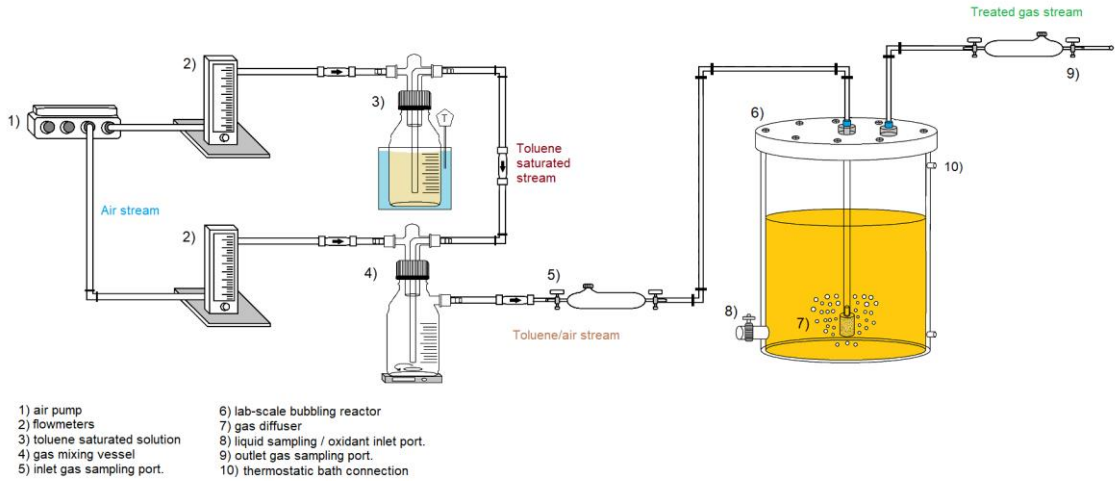

Figure 6.1 Experimental set-up used for the simultaneous gas-liquid treatment in the bubbling reactor.

6.2.2 Real industrial effluent

The real liquid effluent was collected in a chemical industry located in Portugal, in 4.5 L-capacity plastic bottles that were frozen at -15 ºC till use. For all experiments, after being defrosted (at room temperature), samples were homogenized, and diluted with distilled water (dissolved organic carbon - DOC < 1.0 mg C/L), if necessary, in a range of dilution factor (DF_{WW}) between 0.25-1.0; a value of DF_{ww} = 1 means a non-diluted effluent.

6.2.3 Bubbling reactor and experimental procedure

In this study, an acrylic bubble reactor (BR) with a 900 mL-capacity was used – Fig. 6.1. The BR was equipped with a recirculated water jacket connected to a thermostatic bath (Hubber, model Polystat CC1) to control the temperature inside it at 25.0 ± 1.0 ºC.

In a typical simultaneous gas-liquid treatment experiment, 500 mL of the industrial effluent (or water) was introduced in the reactor and, after the desired temperature has been reached, a predetermined mass of ferrous sulfate ($FeSO_4.7H_2O$, 99% from Panreac), or ferric chloride ($FeCl_3.6H_2O$, 98% from Labchem), was added into the reactor, which was then closed. Subsequently, a predetermined volume of H_2O_2 (30 % w/v from VWR) was added into the liquid phase through the liquid sampling port located at the bottom of the reactor and, at the same time, the toluene gas flow started bubbling into the aqueous solution; this corresponds to the time zero of the simultaneous gas-liquid treatment process. The bubbling of the gas phase was reached by using a cylindrical gas diffuser (coarse-grain inert stone of H = 2.5 cm and D = 1.4 cm) located centrally inside the reactor (cf. Fig. 6.1).

Along the experiments, gas samples were collected through the gas sampling port of the reactor to determine the toluene concentration in the outlet (C_{out}) stream. Moreover, liquid samples were also collected, through the sampling liquid port located at the bottom of the reactor, to measure immediately the pH and the residual concentration of hydrogen peroxide, as well as the DOC, COD, BOD_5, acute toxicity and biodegradability of the effluent after stopping the homogenous reaction in the sampling flasks by increasing the pH to 10 (which promotes the decomposition of residual H_2O_2 and precipitation of the dissolved iron (Rodrigues, Boaventura, and Madeira 2014)); this was followed by effluent neutralization for the biological analyses described in the following section.

In stages of the process in which only the treatment of the liquid effluent was carried out, the same procedure described above for the simultaneous gas-liquid treatment was adopted but replacing the bubbling of gas phase containing toluene by air.

6.2.4 Analytical methods

6.2.4.1 Gas phase analysis

The concentrations of toluene (C_{in} and C_{out}), and the presence of other gaseous aromatic by-product (i.e., benzene (99 %, JMGS) (Mo *et al.* 2009; Huang *et al.* 2011)), were determined by gas chromatography with flame ionization detection (GC-FID) with a GC from Agilent (model 7820A) coupled with a HP-5ms column (30 m, Ø = 0.320 mm, film 0.25 µm, from Agilent) whose oven was operated at 100 ºC. The carrier gas was helium at a flow rate of 25 mL/min, and the injector and FID detector were operated at 220 and 250 ºC, respectively. For these determination gas samples (50 µL) were manually sampled and injected using a manual gas-tight syringe (Agilent). No gas by-products were found along the experiments.

The average toluene absorption rate (*N*, in moles/L.s) from the simulated gas stream to the aqueous solution was calculated following Eq. 6.4:

$$N = \frac{Q \int_0^{t_{op}} (C_{in}-C_{out})dt}{M*V_{reactor}*t_{op}} \quad (6.4)$$

where *Q* represents the gas feed flow rate, in L/min, C_{in} and C_{out} represent the gas inlet and outlet toluene concentrations, in g/L, respectively, *M* stands for the molecular weight of toluene, $V_{reactor}$ represents the volume of the liquid phase inside the bubble reactor, in L, *t* is the process time and t_{op} means the overall operation time, in s.

The overall amount of toluene transferred per volume of liquid phase (η – mmol/L) was calculated following Eq. 6.5:

$$\eta = \frac{Q \int_0^{t_{op}} (C_{in}-C_{out})dt}{M*V_{reactor}} \times 1000 \quad (6.5)$$

6.2.4.2 Liquid effluent analysis

The residual concentration of H_2O_2 was measured according to the method developed by Sellers (1980). In this quantification, the absorbance at 400 nm was measured in a Helios γ spectrophotometer (Thermo Electron Corporation).

For the DOC determination, after filtrating the samples with a syringe filter of PTFE (0.45 µm, from VWR), it was proceeded according to the method 5310 D (APHA 1988) using a TOC-L analyzer (Shimadzu) – it should however be noted that this method not is adequate to determine the volatile organic fraction in liquid samples. The COD determination was performed in closed reflux (Method 5220 B (APHA 1988)). CBO_5 was determined according with the procedure described in method 5210 D (APHA 1988) using an OxiTOP Box apparatus (WTW) for samples incubation at 20 ºC during 5 days.

Acute toxicity was determined by inhibition of the bioluminescence of *Vibrio fischeri* bacterium, according to standard DIN/EN/ISO 11348-3 (ISO 2005) in a Microtox apparatus, model 500 (Modern Water). The biodegradability (k') was determined according to the method reported in Standard Methods (APHA 1998); for that, it was used a biological oxygen monitor (YSI Model 5300 B). More details about these methodologies can be found elsewhere (Rodrigues, Boaventura, and Madeira 2014).

By-products formed in the liquid phase were identified using a high-performance liquid chromatography apparatus (from Hitachi Elite LaChrom) equipped with a diode array detector (HPLC/DAD) also from Hitachi (model Elite LaChrom). Columns Purospher STAR RP-18 (5 mm, 250 × 4.0 mm) from Merck, and Rezex ROA-Organic Acid H+ (8%) (250 × 46 mm) from Phenomenex, were used for the identification of hydroquinone and *p*-benzoquinone (common toluene oxidation products), and carboxylic acids (i.e., oxalic, maleic, fumaric, succinic, formic, acetic, and pyruvic acid), respectively, according with the method described elsewhere (Lima *et al*. 2018b). All standard solutions were prepared using reagent grade with 99 % of purity, purchased from Sigma-Aldrich.

All analytical methods were measured in duplicate, and the coefficient of variation was less than 2% for DOC and 4% for the other parameters.

6.3. Results and discussion

Table 6.1 reports the main characteristics of the raw wastewater and after dilutions to ca. ½ and ¼ - DF_{ww} of 0.50 and 0.25, respectively). Regardless the dilution factor used, the chemical oxygen demand (COD) is clearly above the maximum limit for effluents discharge reported by the Portuguese Legislation (150 mg O_2/L – Decree-Law nº 236/98 (Portugal 1998)), indicating that this effluent requires a treatment. The samples also have low biodegradability (as inferred from the BOD_5/COD ratio < 0.4 (Chamarro, Marco, and Esplugas 2001)), indicating the possible inhibition of a biological process. So, an AOP is the more suitable option for their treatment.

Table 6.1 Characterization of the real effluent and after dilution to ca. ½ (dilution factor, DF_{ww}, of 0.50) and ¼ (dilution factor, DF_{ww}, of 0.25).

Parameters	**DF_{ww} = 1.00** [1]	**DF_{ww} = 0.50**	**DF_{ww} = 0.25**
pH	4.6 ± 0.1	4.4 ± 0.1	4.3 ± 0.2
DOC (mg C/L)	2600 ± 20	1300 ± 20	650 ± 10
COD (mg O_2/L)	8000 ± 50	4450 ± 50	2200 ± 20
BOD_5 (mg O_2/L)	7	14	21
BOD_5/COD	0.0009	0.0031	0.0175
Biodegradability (mg $O_2/g_{VSS}h$)	< 0.005	< 0.005	< 0.005
Toxicity[2] (%)	0.0	0.0	0.0

[1] Original wastewater, which was not diluted.
[2] Determined by *Vibrio Fischieri* inhibition after 30 min of contact time.

For the proof-of-concept of the simultaneous gas-liquid effluent treatment by the Fenton process, the effects of some parameters, i.e., aqueous matrix, catalyst species nature, concentration of organic matter and toluene concentration in the gas phase in the efficiency of the process were assessed and are discussed in the following sections.

6.3.1 Influence of the aqueous solution in the toluene absorption and oxidation

Firstly, the toluene mass transfer from the waste gas to the liquid was determined using two different aqueous matrices: industrial effluent and distilled water; this was carried out for experiments without (blank run) and with oxidation (Fenton's process). The blank experiments aim to determine the toluene absorption by the liquid phase. For all runs, the pH was fixed at 4.6 (original pH of the effluent, cf. Table 6.1), and the inlet toluene concentration was C_{in} = 0.04 g/L. For the Fenton experiments, i.e., in which absorption occurs at the same time that oxidation occurs in the liquid phase, the concentrations of the reagents were fixed for maintaining the COD:H_2O_2 and Fe^{2+}:H_2O_2 concentration ratios of 0.04 and 0.033, respectively (values previously optimized for the maximum DOC removal of the same effluent using Fenton's oxidation, without toluene bubbling (Lima *et al.*, 2020a)).

Figure 6.2 reports the ratio between the outlet and inlet concentration of toluene ($C_{out}(t)/C_{in}$) and the organic matter evolution (in terms of DOC) for the experiments performed using both aqueous matrices. For both blank runs it can be seen, in early process times, a gradual increase in the toluene outlet concentration regardless of the

aqueous solution nature (Fig. 6.2a) until $C_{out}(t)/C_{in}$ = 1.0, corresponding to the instant at which the process was stopped because the liquid was saturated and the absorption of toluene finished. An effect of the aqueous matrix was observed, being that the amount of toluene transferred (as well as the average absorption rate – Table 6.2) reduced from 9.58 mmol/L to 5.21 mmol/L when the absorption occurs with water and wastewater, respectively (Fig. 6.2b); it is worth mentioning that the fist value (~ 540 mg/L of toluene) is close to its reported solubility in water – 516 mg/L at 25 ºC (Sanemasa *et al.* 1982). Characteristics of real effluents, e.g., their diverse chemical species composition, and factors such as density, viscosity and surface tension regulate the gas-liquid mass transfer (Akita and Yoshida 1973). Even so, the bubbling system proved to be feasible for the toluene transfer for both aqueous matrices under the conditions tested.

The application of the Fenton's process increased the amount of toluene absorbed per liter of solution during the simultaneous gas-liquid wastewater treatment when compared with the blank run (Fig. 6.2b) due to positive effect of the process of absorption + oxidation as also reported by other authors (Tokumura, Shibusawa, and Kawase 2013); similarly, the average absorption rate along the whole process raised from 3.78 x 10^{-6} to 4.49 x 10^{-6} mol/L.s – Table 6.2. During the process, the continuous bubbling of toluene promotes the mass transfer at the same time that the pollutant is oxidized by the $HO^{\bullet}$ species (Eq. 6.1), reducing its concentration in the liquid phase (G. Liu, Ji, *et al.* 2017; Tokumura *et al.* 2013; G. Liu, Huang, *et al.* 2017), and consequently the driving force for mass transfer is increased in the direction of improving the toluene absorption. This occurs until the formation of hydroxyl radicals was stopped once the oxidant has been completely consumed. At this time, $C_{out}(t)/C_{in}$ reached 1.0, and the gas treatment was interrupted. However, the presence of organic matter in the liquid effluent can lead to a competition with the absorbed toluene for the formed hydroxyl radicals that are non-selective (Lee and von Gunten 2010). So the $HO^{\bullet}$ radicals produced by Fenton's reaction (Eq. 6.2) promote the oxidation of the organic matter (including the toluene transferred), yielding a final DOC removal of 25 % after 60 min of the process (Fig. 6.2c). For this experiment, the toluene transferred accounts to 17.3 mmol/L (~ 1.45 g C/L), which is considerable as compared to the DOC of the industrial effluent (2.6 g C/L – Table 6.1).

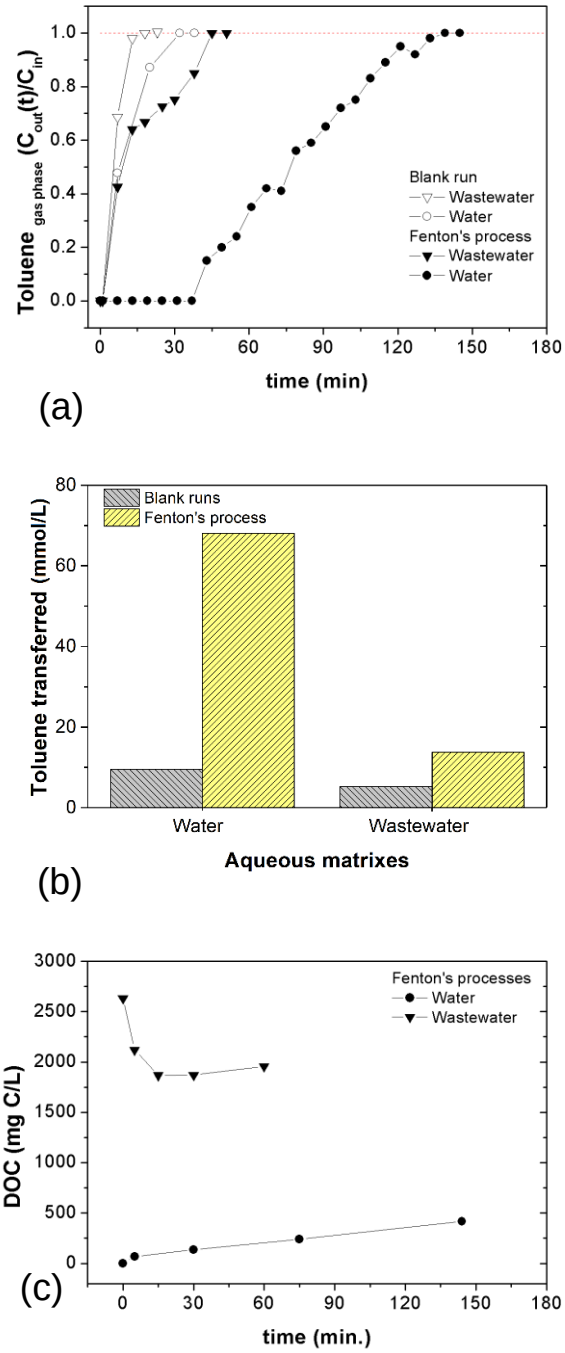

Figure 6.2 Effect of the aqueous matrices (water vs. real effluent) in the toluene removal (a), toluene transferred (b), and DOC removal (c) along the blank (without Fenton's reagents) and Fenton's experiments carried out in the bubbling reactor. Experimental conditions: $V_{water\ or\ WW}$ = 0.5 L, pH_0 = 4.6, T = 25 ºC, $Q_{toluene}$ = 1.0 L/min, C_{in} = 0.040 g/L, $[Fe^{2+}]$ = 0.75 g/L, $[H_2O_2]$ = 22.5 g/L (Fe^{2+}:H_2O_2 = 0.033).

Table 6.2 Average absorption rate after overall process for each experiment processed using water and the effluent.

Aqueous matrix	Experimental runs	Inlet toluene concentration (g/L)	Process duration (min)	Average absorption rate (mol/L.s)
Water	Blank run	0.040	32	4.99×10^{-6}
	Fenton process	0.040	139	8.17×10^{-6}
Wastewater (DF_{ww} = 1.00)	Blank run	0.040	23	3.78×10^{-6}
	Fenton process	0.040	51	4.49×10^{-6}
	Fenton-like process	0.040	49	4.14×10^{-6}
	Only H_2O_2	0.040	33	4.87×10^{-6}
	Only Fe^{2+}	0.040	19	4.41×10^{-6}
	Only Fe^{3+}	0.040	23	4.54×10^{-6}
DF_{ww} = 0.50	Blank run	0.040	28	5.23×10^{-6}
	Fenton process	0.040	77	6.04×10^{-6}
DF_{ww} = 0.25	Blank run	0.040	35	6.04×10^{-6}
	Fenton process	0.040	57	5.56×10^{-6}
DF_{ww} = 0.50	Blank run	0.016	56	1.62×10^{-6}
	Fenton process	0.016	152	2.01×10^{-6}
	Blank run	0.060	26	9.19×10^{-6}
	Fenton process	0.060	31	8.38×10^{-6}

On the other hand, in water (where there are almost no organic species initially present to compete with toluene for its oxidation), the amount of toluene transferred during the Fenton process increased quite significantly as compared to the simple absorption – blank run (from 9.58 to 68.12 mmol/L - cf. Fig. 6.2b). This results from the fact that the process was extended enormously, until 144 min (Fig. 6.2a), boosted by the high concentration of H_2O_2 dosed (> 20 g/L) and the high oxidation kinetics of Fenton's reaction (Ramirez *et al.* 2009). Under such conditions, the accumulation of by-products during oxidation leads to a DOC concentration increase, reaching >400 mg C/L at the end of the process (Fig. 6.2c). Such increase is associated with the formation of intermediate compounds from toluene oxidation (Eq. 6.1), e.g., cresols (Ardizzone *et al.* 2008), benzaldehyde (Xie *et al.* 2019), benzyl alcohol and benzoic acid (Huling *et al.* 2011).

6.3.2 Influence of catalyst nature: Fenton's vs. Fenton-like's process

Figure 6.3 reports a series of experiments that have been conducted to evaluate the effect of the catalyst species nature, i.e. Fe(II) vs. Fe(III), in the toluene abatement and organic matter oxidation. Experiments were carried, as in the previous section, with toluene absorption only (i.e., without the presence of any of the reagents in the liquid phase) or with the presence of: i) H_2O_2 only (without catalyst), ii) Fe^{2+} or Fe^{3+} (without H_2O_2) and iii) both H_2O_2 and Fe^{2+} or Fe^{3+} (Fenton or Fenton-like process, respectively). The concentrations of those reagents and the inlet toluene concentration were the same as applied in the previous section (Fe^{3+}:H_2O_2 = 0.033, wt.%) and C_{in} = 0.04 g/L, respectively.

For all experiments, an increase in the toluene absorption against the blank run (effluent without reagents) was observed (Fig. 6.3a), and the overall toluene transferred from the waste gas to the liquid effluent in each experiment increased following the order: Fenton > Fenton-like > only H_2O_2 > only Fe^{2+} ≈ only Fe^{3+} > blank run (Fig. 6.3b).

In the experiments wherein only iron salts were initially loaded in the liquid effluent, the toluene absorption was similar for both iron species, although a slight increase in the overall amount transferred in both runs against the blank run has been observed (from 5.21 to 5.30 mmol/L – Fig. 6.3b). Other authors have reported a negligible effect of the single Fe^{2+} application for VOCs removal in water (G. Liu, Huang, *et al.* 2017; Choi *et al.* 2014). The slight effect observed in our work can be associated with the high concentrations of Fe(II) and Fe(III) dosed (above > 0.50 g/L), which can originate oxidizing actives species (e.g., generation of H_2O_2 *in situ* (Santana-Casiano *et al.* 2006; Stumm and Lee 1961)) upon interaction with the oxygen dissolved in the aqueous solution (that increases with the continuous toluene-air stream bubbling (Yan *et al.* 2016)), performing some oxidation and therefore increasing the driving force for further toluene absorption. However, no effect on the organic matter removal (data not shown) was observed, and so one can infer that the presence of the iron salts on the simultaneous gas-liquid treatment was negligible.

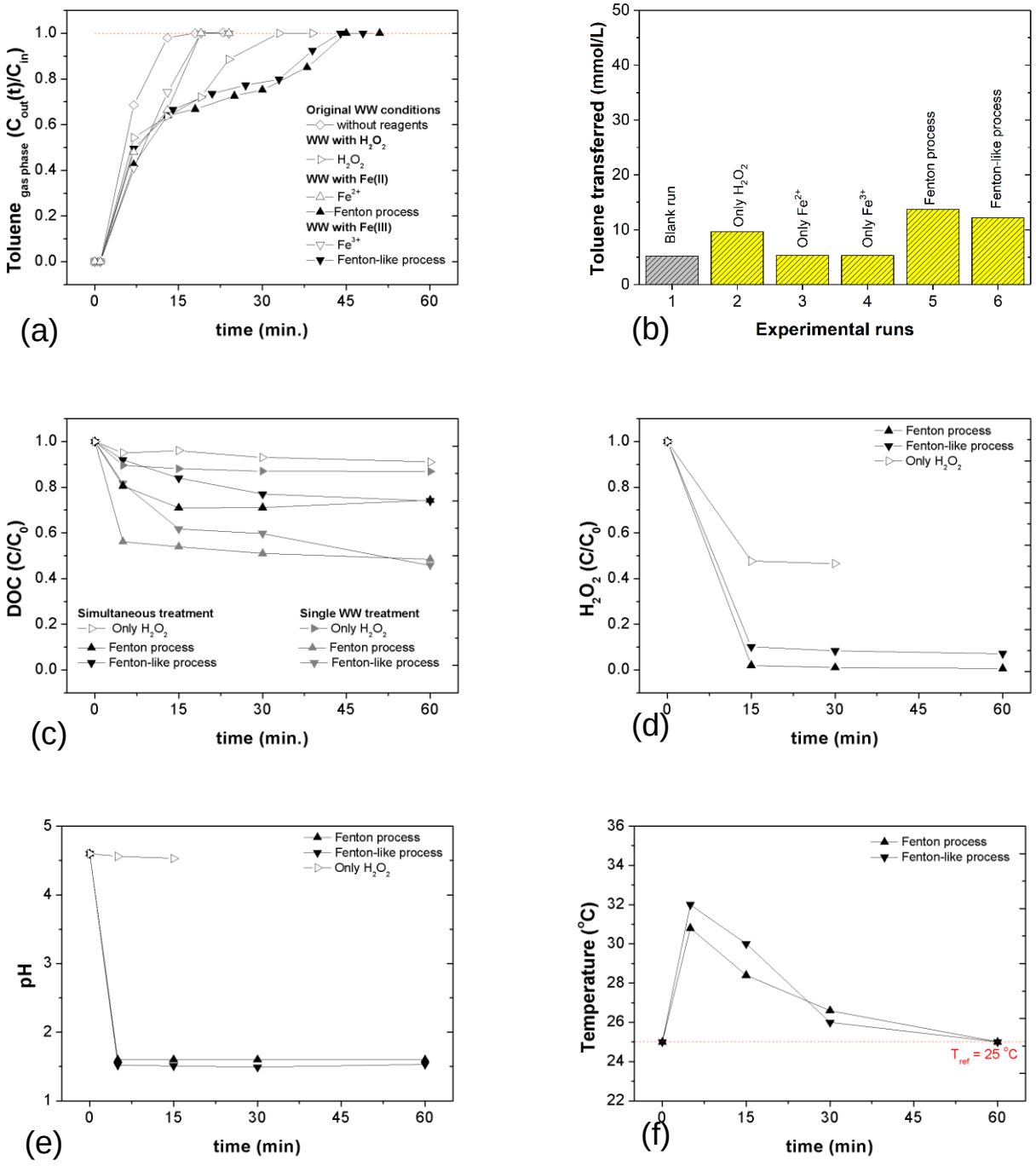

Figure 6.3 Effect of the catalysts nature in the toluene removal (a), toluene transferred (b), DOC removal (c), H_2O_2 consumption (d), pH reduction (e) and temperature profile (f) along the experiments performed for the simultaneous gas-liquid treatment. Experimental conditions: V = 0.5 L, pH_0 = 4.6, T = 25 ºC, $Q_{toluene}$ = 1.0 L/min, C_{in} = 0.040 g/L, $Fe^{2+ \text{ or } 3+}$:H_2O_2 = 0.033.

On the other hand, using only H_2O_2 (without catalyst), the toluene removal extended for more time (Fig. 6.3a), ca. 30 min, so that the overall toluene transferred reached ~ 9.60 mmol per liter (Fig 6.3b); this behaviour is related with the fact that H_2O_2 is an oxidizing species (although with a small oxidation potential – 1.77 eV (Papadopoulos, Fatta, and

Loizidou 2007)). This can be confirmed by the oxidation of some of the organic matter of the effluent initially present in the reactor that reached about 10% (Fig. 6.3c). To assess the effect of the toluene treatment in the liquid phase, an experiment was carried out in which the effluent oxidation was carried out with hydrogen peroxide alone but without toluene bubbling (called "Single WW treatment" in Fig. 6.3c). It was observed that the DOC removal was superior in the run without toluene bubbling, which can be associated with the effect of the partial oxidation of toluene that was oxidized into by-products, decreasing the apparent mineralization. In this experiment where simultaneous toluene absorption and wastewater oxidation was carried out in the presence of hydrogen peroxide alone, the H_2O_2 concentration decreased until ca. 50 % of the initial concentration (Fig. 6.3d), which reinforces the argument that it has been used for the toluene + effluent oxidation. However, one cannot rule out some stripping of the oxidant under the used bubbling conditions (Lima *et al*. 2018b), as well as the possible H_2O_2 self-decomposition (Eq. 6.6).

$$H_2O_2 \rightarrow {}^{1}/_{2}\, O_2 + H_2O \qquad (6.6)$$

Applying only H_2O_2, in the simultaneous treatment of gas-liquid effluent, the pH of the solution hardly changed (cf. Fig. 6.3e), which can indicate that the by-products formed and accumulated had not yet reached an advanced state of oxidation that is typically reported as being responsible by medium acidification, namely short-chain organic acids (Guerreiro *et al.* 2016; Zazo *et al.* 2005), or benzoic acid from toluene oxidation (Choi, *et al.* 2014).

The VOC abatement profile for both Fenton's reactions was similar (Fig. 6.3a), however the application of the classic Fenton's process (with Fe^{2+}) permits reaching a slightly increase in the overall amount of toluene transferred (13.73 mmol/L *vs*. 12.18 mmol/L as compared to the Fenton-like process (with Fe^{3+}) – Fig. 6.3b. For both processes, the toluene removal increased, boosted by the $HO^{\bullet}$ radicals formed. However, the initial oxidation rate decreased when the process was catalysed by Fe(III), as can be observed in the slower DOC removal for short process times (Fig. 6.3c). This is related with the rate constants reported above (cf. Eqs. 6.2-3), which are much higher for the ferrous to ferric ion conversion than the reverse. Even so, the final DOC removal reached similar values for both experiments (ca. 25 % after 60 min – Fig. 6.3c).

Again, the apparent mineralization decreased for both experiments (from 50 to 25 %) against the effluent treatment without toluene bubbling (single WW treatment – cf. Fig. 6.3c), which is due to the accumulation of by-products from toluene oxidation.

In what concerns the H_2O_2 consumption, it was accentuated for both processes, however using Fe^{3+} a slightly less reduction rate was observed (for the reasons described above – Fig. 6.3d. At the same time, the pH decreased abruptly from 4.6 until less than 2.0 in only 5 min for either the Fenton or Fenton-like process, remaining practically unchanged until the end of the reaction (Fig. 6.3e) for both experiments (it is worth noting that the slightly higher acidification of the Fenton-like process is also a consequence of the iron salt used, chloride vs. sulphate). Regarding the temperature, it changed along the reaction (Fig. 6.3f), reflecting a release of heat, in agreement to what was previously reported for this effluent treatment without toluene bubbling (Lima *et al.*, 2020b). Such behaviour is related with the fact that the organics oxidation are highly exothermic reactions (San Sebastián Martínez *et al.* 2003; Esteves *et al.* 2019), but the exothermicity of the Fenton and particularly of the Fenton-like process should not be ruled out (data not shown). Even so, such heat release is only noticed for short process times, coincident with medium acidification, hydrogen peroxide consumption and organics mineralization (Fig. 6.3).

6.3.3 Effect of the organic matter load in the liquid phase

The organic matter load present in the liquid phase is a limiting factor for the VOC mass transfer (absorption). Therefore, to better evaluate its effect in the simultaneous toluene and effluent treatment by Fenton's oxidation, a series of experiments was performed wherein the aqueous solution was the raw effluent, or diluted (see Table 6.1). This way, one is also able to simulate the effect of treating similar effluents, from the same industry, but with different organic loads. The Fenton reagents doses were adapted to keep the same Fe^{2+}:H_2O_2 ratio previously tested (0.033, wt.%), and the H_2O_2 concentrations in each run were adjusted to keep the COD:H_2O_2 ratio of 0.40 in all experiments.

Figure 6.4 reports the influence of the concentration of organic matter in the wastewater. It can be observed that, in the blank experiments, toluene absorption increased with the extended dilution, i.e. the more diluted the effluent was (going from DF_{WW} = 1.00 – undiluted – till DF_{WW} = 0.25 – diluted by a factor of 4), more time was required to reach solution saturation (Fig. 6.4a), whereas the amount of toluene transferred varied from 5.21 to 12.69 mmol/L (Fig. 6.4b).

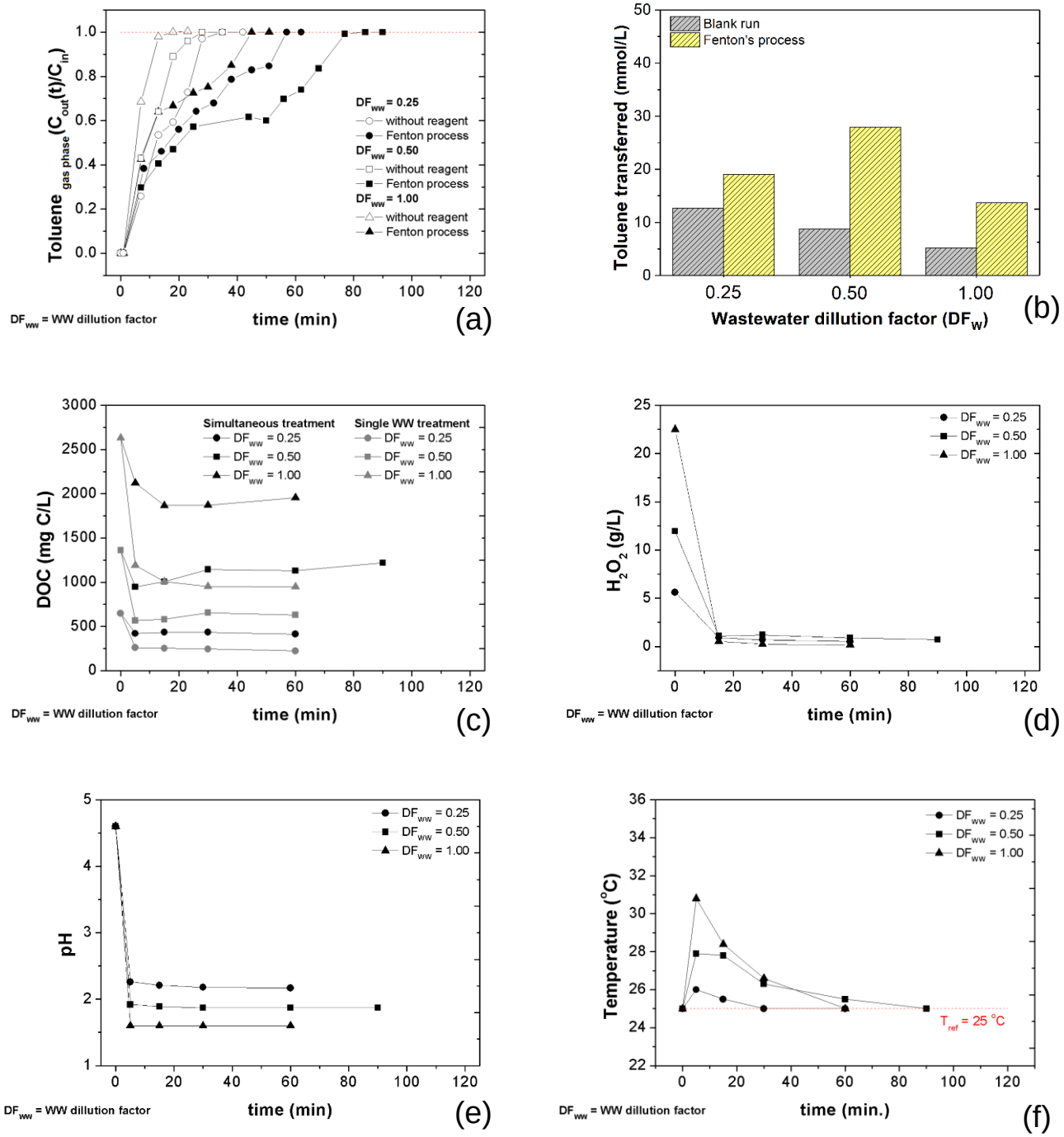

Figure 6.4 Influence of the organic matter concentration in liquid phase in the toluene removal (a), toluene transferred (b), DOC removal (c), H_2O_2 consumption (d), pH reduction (e) and temperature profile (f) along the experiments performed for the simultaneous gas-liquid treatment by the Fenton process. Experimental conditions: V = 0.5 L, T = 25 ºC, $Q_{toluene}$ = 1.0 L/min, C_{in} = 0.040 g/L, COD_0:H_2O_2 = 0.40 and Fe^{2+}:H_2O_2 = 0.033.

In the Fenton's experiments, the toluene transferred for all dilutions tested was increased as compared to the blank experiments (Figs. 6.4a and 6.4b), although for the intermediate dilution factor (DF_{WW} = 0.50) the efficiency of the gas treatment was the highest; in this experiment, the toluene transferred reached 27.91 mmol per liter of

solution (Fig. 6.4b), whereas the process extended for almost three times as compared to the run without reagents (from 28 to 77 min, Fig. 6.4a and Table 6.2). Regardless of the initial organic matter concentration, DOC removals reported the same tendency (Fig. 6.4c), proving the high oxidation rate. The most pronounced DOC removals have been observed for the treatment using higher concentrations of organic matter, suggesting that under such conditions the reaction accelerated the oxidation of the existing organic matter to less oxidizable compounds (e.g., short-chain organic acids (Zazo *et al.* 2005)). For all experiments, the apparent mineralization also decreased as compared to the runs without toluene bubbling (cf. "simultaneous treatment" *vs*. "single treatment" – Fig. 6.4c) once the by-products from toluene oxidation accumulated along the process.

Regarding the H_2O_2 evolution, for all experiments its reduction was extremely accentuated in short process times (Fig. 6.4d), which reinforces the high oxidation rate even for liquid effluents with less organic matter content. At the same time, the acidification and the temperature profile also followed the tendency of the reduction of organic matter content. Thus, the pH decreased more significantly in the experiment that provided the highest DOC removal (Fig. 6.4e), i.e., the undiluted effluent, probably due to short-chain organic acids formation, whereas the increase of temperature was also most pronounced in such conditions (Fig. 6.4f). Even so, it does not exceeds ca. 5 ºC, much smaller to what has been observed in a conventional stirred reactor (~20 ºC) for the same effluent (Lima *et al.*, 2020a), due to the excellent heat (apart from mass) transfer/management in these bubbling devices.

6.3.4 Effect of the inlet concentration of toluene

The concentration of pollutant in the gas phase has a relationship with the VOC mass transfer to the liquid phase, regulating the increased (or reduced) absorption (Tokumura *et al.* 2008).

Figure 6.5 reports the effect of the inlet toluene concentration on its transfer/removal from the gas stream to the liquid and on the organic matter load in the effluent. It can be observed that upon increasing the toluene concentration in the gas phase, the saturation of the effluent (without reagents) turns out to be faster (Fig. 6.5a). Even so, the overall toluene transfer increased once the higher feed concentration (0.060 g/L) ends up ensuring more toluene in solution (Fig. 6.5b, blank runs).

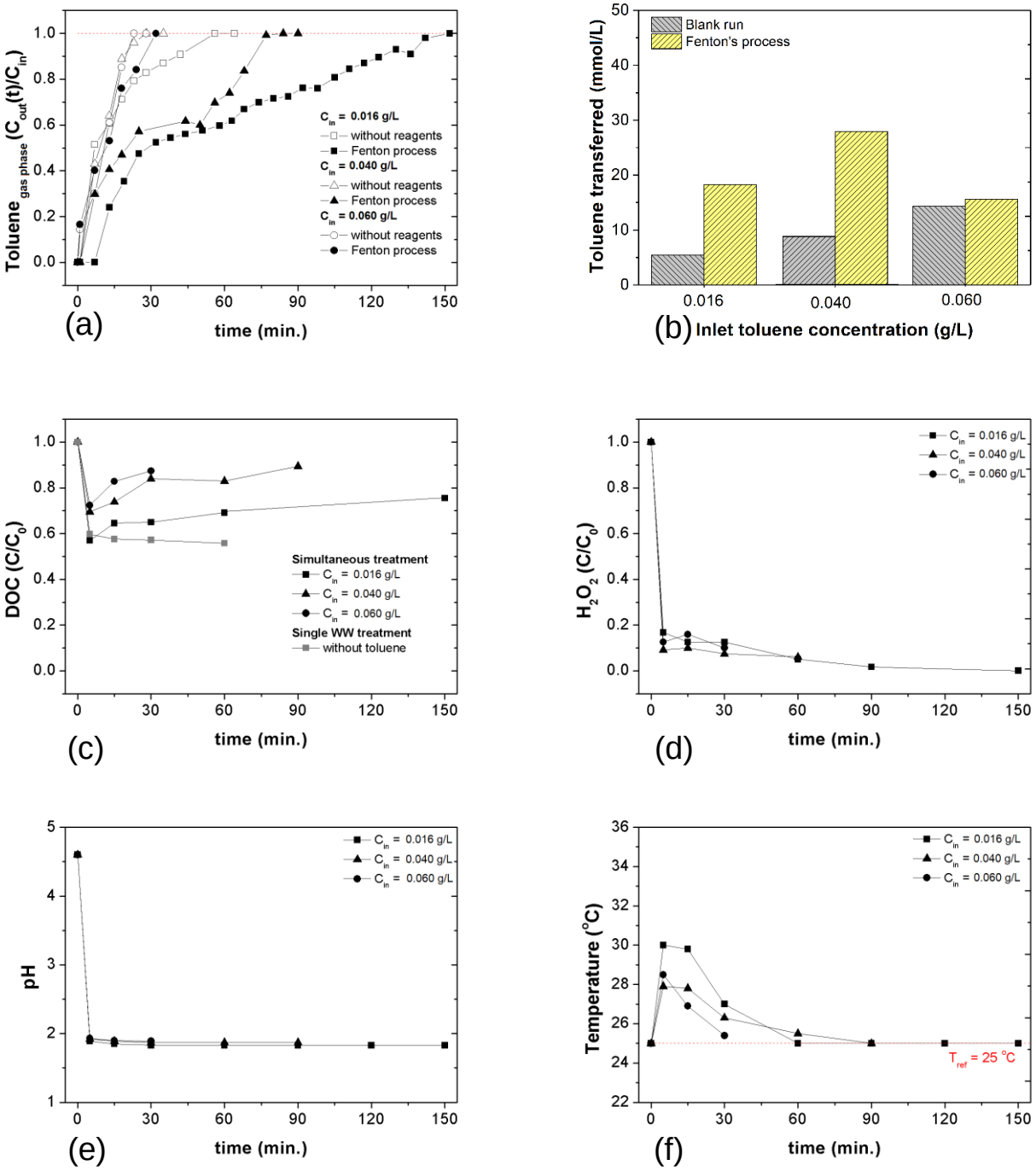

Figure 6.5 Effect of the inlet toluene concentration in the toluene removal (a), toluene transferred (b), DOC removal (c), H_2O_2 consumption (d), pH reduction (e) and temperature profile (f) along the experiments performed for the simultaneous gas-liquid treatment by the Fenton process. Experimental conditions: V = 0.5 L, T = 25 ºC, $Q_{toluene}$ = 1.0 L/min, COD_0:H_2O_2 = 0.40 and Fe^{2+}:H_2O_2 = 0.033.

For the simultaneous absorption and Fenton's oxidation, when the more concentrated toluene feed stream (0.060 g/L) was used, a similar overall toluene transfer, as compared to the process without Fenton's reagents, has been observed (Fig. 6.5b), at the same time that the accumulation of by-products increased considerably in short

process times (Fig. 6.5c). Therefore, to carry out the treatment under these extreme conditions, an increase in the oxidant/iron dosing or changes in the parameters that regulate the gas-liquid mass transfer (e.g., gas flow rate or bubble size) are required to improve and extend the treatment. On the other hand, when bubbling the less concentrated toluene stream, the process extended for more time, ca. 2.5 h (Fig. 6.5a), although the overall toluene transferred was not as high as that obtained using the intermediate feed toluene concentration of 0.040 g/L (Fig. 6.5b).

The H_2O_2 reduction also was again fast within the first 5 min of reaction (Fig. 6.5d), demonstrating that the highest oxidant consumption occurs mostly to oxidize the organic compounds already present in the effluent. At the same time, the pH decreased early in the reaction, and no major changes were observed afterwards over time (Fig. 6.5e). In parallel, the temperature profile of the liquid phase shows again the typical increase is short reaction times (Fig. 6.5f).

Taking into account that after the simultaneous gas-liquid treatment under semi-batch mode the liquid effluent still contains a significant organic load, it was decided to find a strategy to increase the mineralization; this will be addressed in the next section.

6.3.5 Strategy to increase the toluene removal and the mineralization

The simultaneous treatment of the gas-liquid effluent has been efficient in toluene abatement, but the undesirable accumulation of by-products remains a problem to be solved. Therefore, it was necessary to implement a new treatment stage that improves the removal of organic compounds.

Figure 6.6 reports the strategy attempted to improve the removal of toluene and organic matter from the liquid effluent. The strategy considers firstly the simultaneous gas-liquid treatment (stage 1), followed by a liquid treatment stage (stage 2). After stage 1, the pH of the aqueous phase was adjusted to 3.0 (an optimal value for Fenton's oxidation (Lima *et al.* 2018b; Yan *et al.* 2016)), and further H_2O_2 was added (determined by the stoichiometry of the reaction to oxidize the existing organic matter); in this stage, toluene bubbling has been replaced by air (at the same flow rate), which ensures an efficient mixing in the liquid phase. An important issue of this strategy is that in stage 2 no further catalyst is required, as it remains dissolved along the process.

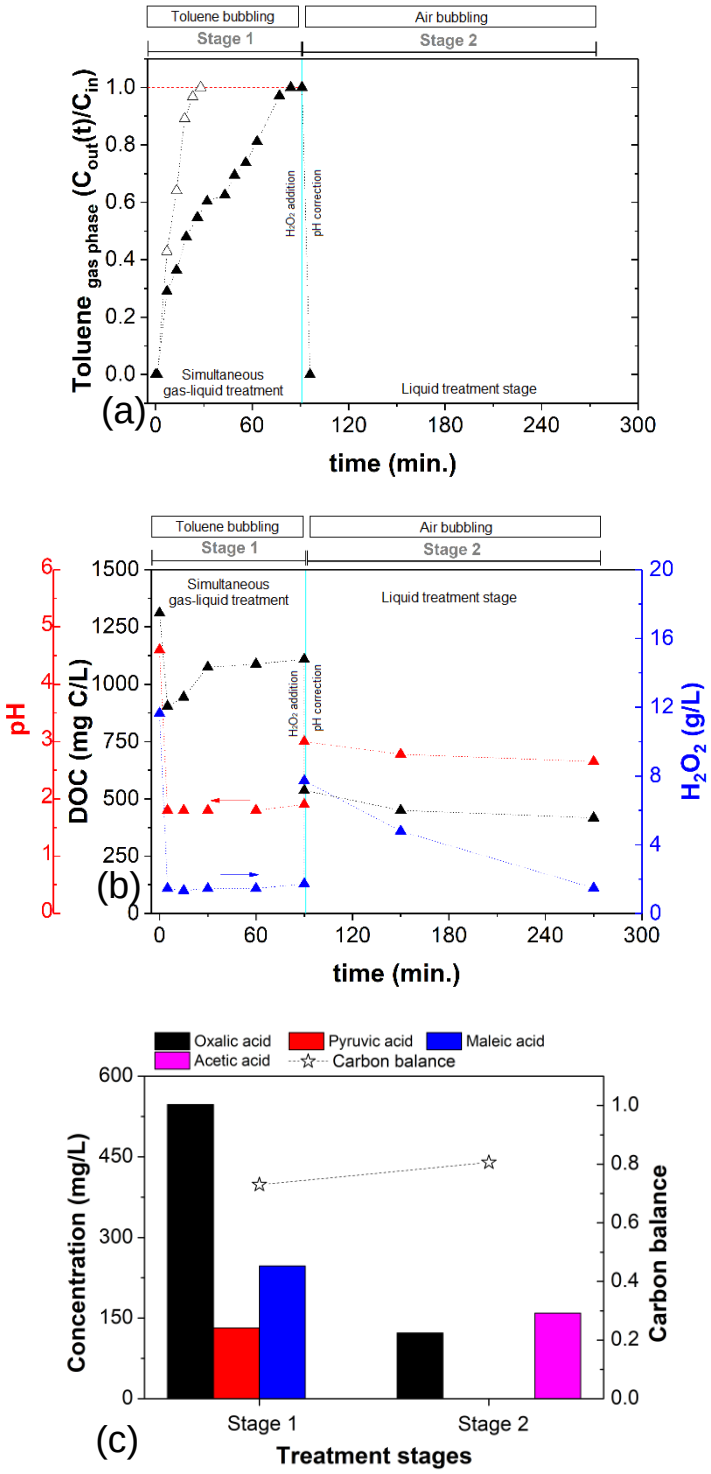

Figure 6.6 Effect of the sequential treatment by Fenton's oxidation in the toluene removal (a), H_2O_2 consumption, DOC and pH reduction (b) in the gas and liquid treatment stages, and by-products concentrations and carbon balance at the end of each treatment stage (c). Experimental conditions: *Stage 1* – V = 0.5 L, DF_{WW} = 0.50, pH_0 = 4.4, T = 25 ºC, $Q_{toluene}$ = 1.0 L/min, C_{in} = 0.040 g/L, COD_0:H_2O_2 = 0.40 and Fe^{2+}:H_2O_2 = 0.033; *Stage 2* – pH_0 = 3.0 and H_2O_2 = 6.0 g/L.

The process was implemented using the above-mentioned average concentrations of toluene and organic matter - since maximum toluene removal was reached under this

conditions. The results obtained in phase 1 (Fig. 6.6a) replicated efficiently the profile of toluene abatement previously reported (cf. Fig. 6.5a-b, ca. 30 mmol of toluene transferred per liter). In general, the trends reported for the hydrogen peroxide concentration, pH and residual DOC in Fig. 6.6 for stage 1 are similar to those described before, being noteworthy that during stage 2, i.e. along the liquid treatment step (wherein toluene has been replaced by air bubbling) that extended for 3 h, over 60 % of the organic matter was mineralized (Fig 6.6b). Therefore, subsequent cycles of gas absorption can be implemented, and the process operated continuously with several cycles, as demonstrated to be feasible elsewhere (Lima *et al.*, 2020b).

Apart from toluene, during the process the real industrial effluent has also been oxidized in the bubble reactor. Due to its extreme complexity, it is nearly impossible to look for all possible intermediates/oxidation products. Even so, oxidation products resulting from toluene oxidation (like hydroquinone, and benzoquinone) and common short-chain organic acids (oxalic, maleic, fumaric, succinic, formic, acetic, and pyruvic acid) have been analyzed at the end of both stages (Fig. 6.6c). At the end of stage 1 short-chain organic acids were identified in the liquid phase (i.e., oxalic, pyruvic and maleic acids), although other peaks of unidentified compounds also appeared in the chromatograms. At the end of stage 2 oxalic and acetic acids were found. The concentration of oxalic acid decreased during stage 2, at the same time that the acetic acid was formed (Fig. 6.6c), corroborating the oxidation of several organics into this last oxidation product, including possibly the conversion of both pyruvic and maleic acid. In addition, the organics identified represented above 70 % of the residual carbon at the end of the stage 1 (carbon balance represented if Fig. 6.6c, calculated by the ratio between the sum of the total carbon of the intermediate compounds quantified and the DOC after each stage). Such carbon balance increased to above 80 % after stage 2 – Fig. 6.6c.

6.4 Conclusions

This work reports a novel process for the simultaneous gas-liquid treatment using Fenton's reagent in a bubbling reactor. In particular, it was proved the concept of treating a toluene-containing gas stream while the liquid phase was composed by a real and complex industrial wastewater. It was concluded that:

- Toluene absorption by a real industrial effluent was effectively achieved, even though against a clean matrix (water) the overall toluene transferred decreased due to the presence of the organic compounds;

- The application of the Fenton process improved the toluene removal from the gas stream at the same time that mineralization of the organic matter present in the effluent was promoted;
- Both Fenton and Fenton-like processes proved to be viable for the simultaneous treatment, although for the latter the overall toluene transferred has slightly decreased;
- The reduction of organic matter in liquid phase increased the toluene absorption, although with the simultaneous oxidation a maximum toluene removal has been reached under average organic matter contents of the liquid effluent;
- The increase of the inlet toluene concentration to high levels proved to be disadvantageous for the simultaneous gas-liquid treatment since saturation of the liquid phase can occur very quickly;
- The application of the simultaneous gas-liquid treatment allowed the toluene abatement although with an accumulation of by-products, which can be effectively mineralized in a subsequent liquid treatment stage.

6.5 References

Akita, K., and F. Yoshida. 1973. 'Gas Holdup and Volumetric Mass Transfer Coefficient in Bubble Columns'. *Ind Eng Chem Process Des Dev* 12: 76–80.

APHA, WEF A. 1988. 'Standard Methods for the Examination of Water and Wastewater'. In *Water Pollution Control Federation*, edited by American Public Health Association. Washington DC,: American Water Works Association.

Ardizzone, S., C. L. Bianchi, G. Cappelletti, A. Naldoni, and C. Pirola. 2008. 'Photocatalytic Degradation of Toluene in the Gas Phase: Relationship between Surface Species and Catalyst Features'. *Environmental Science and Technology* 42 (17): 6671–76.

Barb, W. G., J. H. Baxendale, P. George, and K. R. Hargrave. 1951a. 'Reactions of Ferrous and Ferric Ions with Hydrogen Peroxide. Part I.—The Ferrous Ion Reaction'. *Trans. Faraday Soc.* 47 (0): 462–500.

Barb, W. G., J. H. Baxendale, P. George, and K. R. Hargrave. 1951b. 'Reactions of Ferrous and Ferric Ions with Hydrogen Peroxide. Part II. - The Ferric Ion Reaction'. *Transactions of the Faraday Society* 47 (0): 591–616.

Beltran D. H., Jesus, J. Torregrosa, J. R. Dominguez, and J. A. Peres. 2001. 'Kinetic Model for Phenolic Compound Oxidation by Fenton's Reagent'. *Chemosphere* 45 (1): 85–90.

Chamarro, E., A. Marco, and S. Esplugas. 2001. 'Use of Fenton Reagent to Improve Organic Chemical Biodegradability'. *Water Research* 35 (4): 1047–51.

Chen, H., J. Liu, Y. Pei, P. Zhao, Y. Zhang, L. Yan, T. Zhang, W. Li, Chuandong Wu, and M. Hussain. 2018. 'Study on the Synergistic Effect of UV/Fenton Oxidation and Mass Transfer Enhancement with Addition of Activated Carbon in the Bubble Column Reactor'. *Chemical Engineering Journal* 336: 82–91.

Choi, K., S. Bae, and W. Lee. 2014. 'Degradation of Off-Gas Toluene in Continuous Pyrite Fenton System'. *Journal of Hazardous Materials* 280: 31–37.

Deng, Y., and R. Zhao. 2015. 'Advanced Oxidation Processes (AOPs) in Wastewater Treatment'. *Current Pollution Reports* 1 (3): 167–76.

Esteves, B. M., C. S.D. Rodrigues, F.J. Maldonado-Hódar, and L. M. Madeira. 2019. 'Treatment of High-Strength Olive Mill Wastewater by Combined Fenton-like Oxidation and Coagulation/Flocculation'. *Journal of Environmental Chemical Engineering* 7 (4): 103252.

Fenton, H.J.H. 1894. 'LXXIII.—Oxidation of Tartaric Acid in Presence of Iron'. *Journal of the Chemical Society, Transactions* 65: 899–910.

Gligorovski, S., R. Strekowski, S. Barbati, and D. Vione. 2015. 'Environmental Implications of Hydroxyl Radicals (•OH)'. *Chemical Reviews* 115 (24): 13051–92.

Guerreiro, L. F., C. S.D. Rodrigues, R. M. Duda, R. A. de Oliveira, R. A.R. Boaventura, and L. M. Madeira. 2016. 'Treatment of Sugarcane Vinasse by Combination of Coagulation/Flocculation and Fenton's Oxidation'. *Journal of Environmental Management* 181 (October): 237–48.

Guo, R. T., W. G. Pan, X. B. Zhang, J. X. Ren, Q. Jin, H. J. Xu, and J. Wu. 2011. 'Removal of NO by Using Fenton Reagent Solution in a Lab-Scale Bubbling Reactor'. *Fuel* 90 (11): 3295–98.

Handa, M., Y. Lee, M. Shibusawa, M. Tokumura, and Y. Kawase. 2013. 'Removal of VOCs in Waste Gas by the Photo-Fenton Reaction: Effects of Dosage of Fenton Reagents on Degradation of Toluene Gas in a Bubble Column'. *Journal of Chemical Technology and Biotechnology* 88 (1): 88–97.

Heijnen, J. J., and K. Van't Riet. 1984. 'Mass Transfer, Mixing and Heat Transfer Phenomena in Low Viscosity Bubble Column Reactors' 28: B21–B42.

Hernández, M., G. Quijano, R. Muñoz, and S. Bordel. 2011. 'Modeling of VOC Mass Transfer in Two-Liquid Phase Stirred Tank, Biotrickling Filter and Airlift Reactors'. *Chemical Engineering Journal* 172 (2–3): 961–69.

Huang, H., D. Ye, D. Y.C. Leung, F. Feng, and X. Guan. 2011. 'Byproducts and Pathways of Toluene Destruction via Plasma-Catalysis'. *Journal of Molecular Catalysis A: Chemical* 336 (1–2): 87–93.

Huling, S. G., S. Hwang, D. Fine, and S. Ko. 2011. 'Fenton-like Initiation of a Toluene Transformation Mechanism'. *Water Research* 45 (16): 5334–42.

ISO. 2005. 'Water Quality - Determination of the Inhibitory Effect of Water Method, Samples on the Light Emission of Vibrio Fischeri (Luminescent Bacteria Test) - Part 3: Using Freeze-Dried Bacteria'. In . International Organization for Standardzation.

Kováts, P., D. Thévenin, and K. Zähringer. 2017. 'Investigation of Mass Transfer and Hydrodynamics in a Model Bubble Column'. *Chemical Engineering and Technology* 40 (8): 1434–44.

Kulkarni, A. V., and J. B. Joshi. 2011. 'Design and Selection of Sparger for Bubble Column Reactor. Part I: Performance of Different Spargers'. *Chemical Engineering*

Research and Design 89 (10): 1972–85.

Lee, Y., and U. von Gunten. 2010. 'Oxidative Transformation of Micropollutants during Municipal Wastewater Treatment: Comparison of Kinetic Aspects of Selective (Chlorine, Chlorine Dioxide, FerrateVI, and Ozone) and Non-Selective Oxidants (Hydroxyl Radical)'. *Water Research* 44 (2): 555–66.

Lima, V. N., C. S. D. Rodrigues, R. A. C. Borges, and L. M. Madeira. 2018a. 'Gaseous and Liquid Effluents Treatment in Bubble Column Reactors by Advanced Oxidation Processes: A Review'. *Critical Reviews in Environmental Science and Technology* 48 (16–18): 1–48.

Lima, V. N., C. S.D. Rodrigues, and L. M. Madeira. 2018b. 'Application of the Fenton's Process in a Bubble Column Reactor for Hydroquinone Degradation'. *Environmental Science and Pollution Research* 25 (35): 34851–62.

Lima, V. N., C. S.D. Rodrigues, E. F. S. Sampaio and L. M. Madeira. 2020a. 'Sequential gas-liquid treatment for gaseous toluene degradation by Fenton's oxidation in bubble reactors. *Journal of Environmental Chemical Engineering*, 8(3), 103796.

Lima, V. N., C. S.D. Rodrigues, and L. M. Madeira. 2020b. "Insights into real industrial wastewater treatment by Fenton's oxidation in gas bubbling reactors". *Journal of Environmental Management* (accepted).

Liu, G., H. Huang, R. Xie, Q. Feng, R. Fang, Y. Shu, Y. Zhan, X. Ye, and C. Zhong. 2017. 'Enhanced Degradation of Gaseous Benzene by a Fenton Reaction'. *RSC Adv.* 7 (1): 71–76.

Liu, G., J. Ji, H. Huang, R. Xie, Q. Feng, Y. Shu, Y. Zhan, *et al.* 2017. 'UV/H_2O_2: An Efficient Aqueous Advanced Oxidation Process for VOCs Removal'. *Chemical Engineering Journal* 324: 44–50.

Liu, Y. X., J. Zhang, and Y. Yin. 2015. 'Removal of Hg^0 from Flue Gas Using Two Homogeneous Photo-Fenton-like Reactions'. *AIChE Journal* 61 (4): 1322–33.

Liu, Y., Y. Wang, Q. Wang, J. Pan, Y. Zhang, J. Zhou, and J. Zhang. 2015. 'A Study on Removal of Elemental Mercury in Flue Gas Using Fenton Solution'. *Journal of Hazardous Materials* 292 (July): 164–72.

Lucas, M.S., and A. J. Peres. 2009. 'Removal of COD from Olive Mill Wastewater by Fenton's Reagent: Kinetic Study'. *Journal of Hazardous Materials* 168 (2–3): 1253–59.

Ma, Y. S., S. T. Huang, and J. G. Lin. 2000. 'Degradation of 4-Nitrophenol Using the

Fenton Process'. *Water Science and Technology* 42 (3–4): 155–60.

Mo, J., Y. Zhang, Q. Xu, Y. Zhu, J. J. Lamson, and R. Zhao. 2009. 'Determination and Risk Assessment of By-Products Resulting from Photocatalytic Oxidation of Toluene'. *Applied Catalysis B: Environmental* 89 (3–4): 570–76.

Moulis, F., and J. Krýsa. 2013. 'Photocatalytic Degradation of Several VOCs (n-Hexane, n-Butyl Acetate and Toluene) on TiO_2 Layer in a Closed-Loop Reactor'. *Catalysis Today* 209: 153–58.

Oturan, M. A., and J. J. Aaron. 2014. 'Advanced Oxidation Processes in Water/Wastewater Treatment: Principles and Applications. A Review'. *Critical Reviews in Environmental Science and Technology* 44 (23): 2577–2641.

Papadopoulos, A. E., D. Fatta, and M. Loizidou. 2007. 'Development and Optimization of Dark Fenton Oxidation for the Treatment of Textile Wastewaters with High Organic Load'. *Journal of Hazardous Materials* 146 (3): 558–63.

Portugal. 1998. *Decreto-Lei Nº 236/98*. Edited by Ministério do Ambiente. Portugal: Diário da República I Série A.

Rivas, F. J., V. Navarrete, F. J. Beltrán, and J. F. García-Araya. 2004. 'Simazine Fenton's Oxidation in a Continuous Reactor'. *Applied Catalysis B: Environmental* 48 (4): 249–58.

Rodrigues, C. S.D., R. A.R. Boaventura, and L. M. Madeira. 2014. 'Technical and Economic Feasibility of Polyester Dyeing Wastewater Treatment by Coagulation/Flocculation and Fenton's Oxidation'. *Environmental Technology (United Kingdom)* 35 (10): 1307–19.

Rodrigues, C. S.D., R. A.C. Borges, V. N. Lima, and L. M. Madeira. 2018. '*p*-Nitrophenol Degradation by Fenton's Oxidation in a Bubble Column Reactor'. *Journal of Environmental Management* 206: 774–85.

San Sebastián Martínez, N., J. F. Fernández, X. F. Segura, and A. S. Ferrer. 2003. 'Pre-Oxidation of an Extremely Polluted Industrial Wastewater by the Fenton's Reagent'. *Journal of Hazardous Materials* 101 (3): 315–22.

Sanemasa, I., M. Araki, T. Deguchi, and H. Nagai. 1982. 'Solubility Measurements of Benzene and the Alkylbenzenes in Water By Making Use of Solute Vapor.' *Bulletin of the Chemical Society of Japan* 55 (4): 1054–62.

Santana-Casiano, J. M., M. González-Dávila, and F. J. Millero. 2006. 'The Role of Fe(II) Species on the Oxidation of Fe(II) in Natural Waters in the Presence of O_2 and

H_2O_2'. *Marine Chemistry* 99 (1–4): 70–82.

Sellers, R. M. 1980. 'Spectrophotometric Determination of Hydrogen Peroxide Using Potassium Titanium (IV) Oxalate'. *Analyst* 105 (1255): 950–54.

Stumm, W., and G. F. Lee. 1961. 'Oxygenation of Ferrous Iron'. *Industrial & Engineering Chemistry* 53 (2): 143–46.

Tokumura, M., R. Nakajima, H. T. Znad, and Y. Kawase. 2008. 'Chemical Absorption Process for Degradation of VOC Gas Using Heterogeneous Gas-Liquid Photocatalytic Oxidation: Toluene Degradation by Photo-Fenton Reaction'. *Chemosphere* 73 (5): 768–75.

Tokumura, M., M. Shibusawa, and Y. Kawase. 2013. 'Dynamic Simulation of Degradation of Toluene in Waste Gas by the Photo-Fenton Reaction in a Bubble Column'. *Chemical Engineering Science* 100: 212–24.

US EPA. 2005. 'Toxicological Review of Toluene'. *Washington (DC):US Environmental Protection Agency*.

Walling, C.. 1975. 'Fenton's Reagent Revisited'. *Accounts of Chemical Research* 8 (4): 125–31.

Walling, C., and A. Goosen. 1973. 'Mechanism of the Ferric Ion Catalyzed Decomposition of Hydrogen Peroxide. Effect of Organic Substrates'. *Journal of the American Chemical Society* 95 (9): 2987–91.

Wang, Y., Y. Liu, and J. Xu. 2019. 'Separation of Hydrogen Sulfide from Gas Phase Using Ce^{3+}/Mn^{2+}-Enhanced Fenton-like Oxidation System'. *Chemical Engineering Journal* 359: 1486–92.

Wang, Y., Z. Wang, J. Pan, and Y. Liu. 2019. 'Removal of Gaseous Hydrogen Sulfide Using Fenton Reagent in a Spraying Reactor'. *Fuel*, 70–75.

Xie, R., J. Ji, K. Guo, D. Lei, Q. Fan, D. Y.C. Leung, and H. Huang. 2019. 'Wet Scrubber Coupled with UV/PMS Process for Efficient Removal of Gaseous VOCs: Roles of Sulfate and Hydroxyl Radicals'. *Chemical Engineering Journal* 356: 632–40.

Yan, L., J. Liu, Z. Feng, and P. Zhao. 2016. 'Continuous Degradation of BTEX in Landfill Gas by the UV-Fenton Reaction'. *RSC Adv.* 6 (2): 1452–59.

Zazo, J. A., J. A. Casas, A. F. Mohedano, M. A. Gilarranz, and J. J. Rodríguez. 2005. 'Chemical Pathway and Kinetics of Phenol Oxidation by Fenton's Reagent'. *Environmental Science and Technology* 39 (23): 9295–9302.

Zhao, J., W. Xi, C. Tu, Q. Dai, and X. Wang. 2020. 'Catalytic Oxidation of Chlorinated

VOCs over Ru/TixSn1-x Catalysts'. *Applied Catalysis B: Environmental* 263: 118237.

Zhao, Y., X. Wen, T. Guo, and J. Zhou. 2014. 'Desulfurization and Denitrogenation from Flue Gas Using Fenton Reagent'. *Fuel Processing Technology* 128: 54–60.

Part IV: Conclusions & Future Perspectives

Chapter 7. Final Conclusions and Future Work

7.1 Final conclusions

This thesis focused on the proof-of-concept of a novel process for the simultaneous treatment of gaseous and liquid organic effluents by Fenton's oxidation in one multiphase reactor, namely a bubbling reactor. In this sense, the applicability of this reactor configuration was firstly and separately evaluated in the degradation of a model volatile organic pollutant (toluene) present in a gas stream and in the mineralization of organic compounds present in liquid effluents. Firstly, the oxidation of a liquid solution containing hydroquinone (selected model compound) and the treatability of an industrial wastewater were assessed. Afterwards, the abatement of a gaseous stream containing toluene was studied; finally, the simultaneous treatment of gas and liquid effluents was proved. The reactors selected (bubbling reactor - BR, and bubbling column reactor - BCR) showed to be adequate to perform the Fenton's oxidation, being the following the most relevant conclusions:

- For the hydroquinone treatment in the liquid phase within the BCR, the air flow rate, as well as the liquid height, did not influenced the model compound removal and mineralization, under the ranges tested. It was proved that the mixing inside the BCR was efficient using only a continuous air supply during the reactions. The main parameters of the process, i.e., Fenton's reagent concentrations, temperature, and initial pH, were optimized. The hydroquinone was completely degraded, and total organic carbon (TOC) removal reached 55 % after the treatment, resulting in a final non-toxic effluent. Besides, the mechanism of hydroquinone degradation was proposed, based on intermediate compounds identification.
- The treatment of a real (industrial) wastewater with high organic load was firstly evaluated within the BR, and the optimization of key reaction parameters allowed to reach dissolved organic carbon (DOC) and chemical oxygen demand (COD) removals above 50 % and 80 %, respectively. Additionally, it was observed that the composition of the gas phase influenced the organic matter removal, especially when using a pure oxygen (O_2) stream, which yielded a slight increase in the mineralization (from 50 to 56 % after 60 min of treatment, as compared to air or nitrogen). The wastewater treatment within the BR proved to be

advantageous for the temperature control along this exothermic process when compared with conventional stirring (commonly used). The scale-up to BCR provided similar mineralizations, which leads to the conclusion that both reactors could perform the treatment of real effluents under optimized conditions.

- The toluene treatment was optimized within the BR, and the effect of some operating conditions (temperature, and Fenton's reagent concentration) were evaluated. It was observed that the increase in process temperature (from 25 to 40 ºC) promoted a positive effect in the toluene transfer from the gas phase to the water for the run without reaction; however, when the simultaneous oxidation was carried out, it decreased the efficiency of the toluene absorption, as a consequence of the effect of the Fenton process kinetics on the gas treatment. In what concerns Fenton's reagents dosing, an optimal value was determined for the Fe^{2+} concentration. On the other hand, the increase of the H_2O_2 concentration improved the toluene mass transfer to the water in a process of absorption + oxidation. The partial toluene oxidation represented an accumulation of intermediate oxidation compounds in the liquid phase, so a sequential gas-liquid treatment was carried out which demonstrated to be satisfactory in both toluene and organic compounds removal. The scale-up to a BCR promoted the extension of the toluene abatement stages, while it was observed an effective removal of the organic matter in the intermediate liquid phase treatment stages. Also, there was an increase in the biodegradability of the treated effluent after each gas-liquid treatment cycle.
- Finally, the simultaneous gas-liquid treatment was performed under semi-continuous mode within the BR. The toluene-containing gas stream was treated together with an industrial wastewater. An effect of the aqueous matrix was observed when the toluene stream was bubbled inside the effluent, which provided a reduction of the VOC absorption (without reaction) when compared with water. Even so, the application of the Fenton reagent increased the toluene mass transfer in the absorption + oxidation process, proving the applicability of the simultaneous gas-liquid treatment in bubbling reactors. Some parameters were evaluated in this study, i.e., nature of employed catalyst species, organic matter concentration in the liquid phase, and toluene concentration in the inlet gas stream. The effects of the Fenton and Fenton-like processes were similar for the organic matter oxidation in the liquid phase (~ 25 % of mineralization after the treatment), although for the overall amount of toluene transferred, a slight decreased has been observed using the Fenton-like's reagent (Fe^{3+} + H_2O_2). The reduction of the organic matter concentration in the aqueous solution increased

the toluene absorption in the run without reaction; however, during the oxidation process, the results were not linear, showing the necessity to optimize the process depending on the liquid phase organic load. The increase of the inlet toluene concentration led to a reduction in the treatment duration, and an increase in the by-products accumulation, which decreased the apparent mineralization of the treated wastewater. Again, an optimization of the treatment is required depending on the gas phase composition. Finally, the sequential gas-liquid treatment was implemented, leading to an organic matter oxidation degree of more than 60 % in the final treated effluent. The identification of the oxidation by-products showed high concentrations of short-chain organic acids, which were reduced effectively with the liquid treatment stage.

7.2 Future work

This thesis dealt with treatment processes for gaseous and liquids streams contaminated with organic compounds within bubbling reactors operating under the semi-batch mode. Given that it was possible to prove the concept and promote the treatment of both liquid and gaseous streams simultaneously in the same device by Fenton's oxidation, some future work is suggested, namely:

- Study the treatment with continuous gas recycling in order to allow the treatment of the residual gas in the same operating system, which would lead to the promotion of the VOC concentration reduction in the residual waste gas during the liquid treatment stages;
- From the industrial application perspective, the simultaneous gas-liquid treatment should be carried out in a reactor operating under continuous mode, i.e., with gas and liquid streams fed continuously, in counter-current mode. For an efficient treatment, the Fenton reagents dosing (i.e., hydrogen peroxide and iron) should be done continuously along the oxidation process, and the effect of operating conditions (e.g., initial pH, temperature, flow rates, etc.) should be evaluated and optimized;
- Additionally, the treatment should be performed by a heterogeneous Fenton process using supported catalysts in order to allow the catalyst recovery after the treatment process, besides reducing the possible formation of iron sludge - a limitation of the homogeneous Fenton process. For this process, it should be considered the textural and chemical surface properties of the catalysts in the

VOC absorption and reaction, and it would be necessary to optimize the conditions. The use of monolithic structures could be considered;

- Finally, we should look into the application of oxidants with better stability, e.g., sodium persulfate, as an alternative to hydrogen peroxide, as a way to prevent possible oxidant losses during the oxidation.

Appendixes

A1 Appendix for Chapter 3

This appendix shows some experimental results obtained in the evaluation of the hydroquinone degradation using Fenton's oxidation in a bubbling column reactor (BCR).

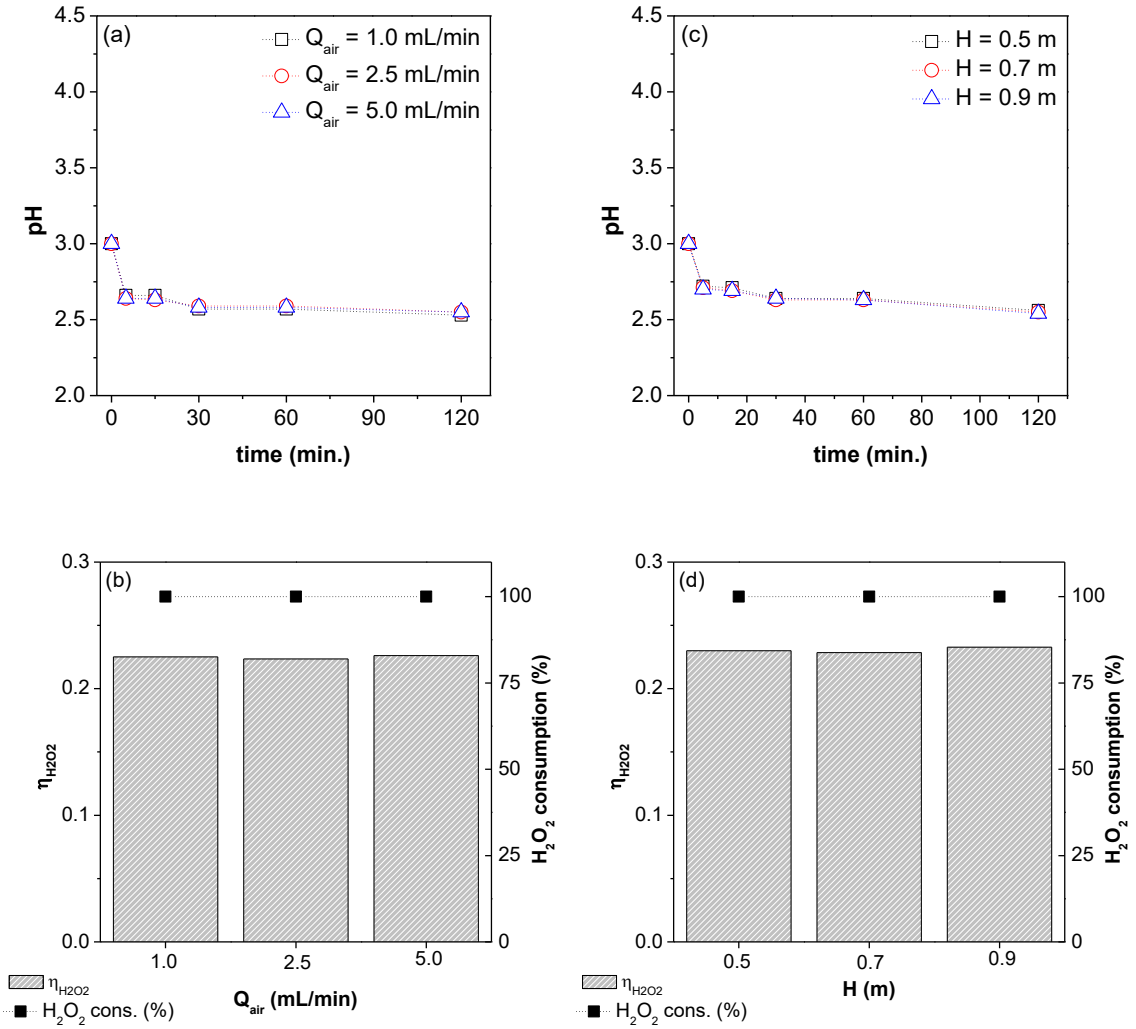

Figure A.1.1 Evolution of pH along reaction time (a) and H_2O_2 consumption and efficiency of its use at 120 minutes of reaction (b) for different air flow rates ($[H_2O_2]$ = 500 mg/L; $[Fe^{2+}]$ = 45 mg/L; T = 24 ºC; pH = 3.0; $V_{effluent}$ = 7 L; H_3 = 0.5 m); evolution of pH along reaction time (c) and H_2O_2 consumption and efficiency of its use at 120 minutes of reaction (d) for different sampling heights ($[H_2O_2]$ = 500 mg/L; $[Fe^{2+}]$ = 45 mg/L; T = 24 ºC; pH = 3.0; $V_{effluent}$ = 7 L; Q_{air} = 2.5 mL/min).

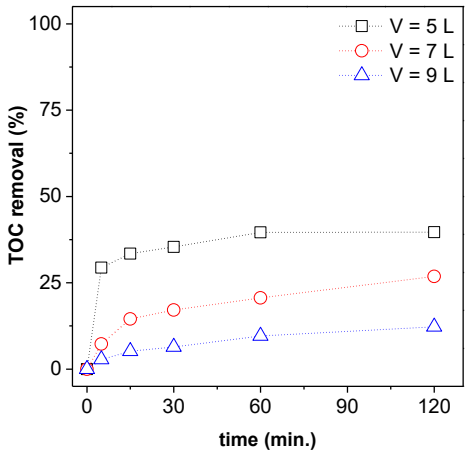

Figure A.1.2 TOC removal along reaction time for different volumes of effluent ([H_2O_2] = 500 mg/L; [Fe^{2+}] = 45 mg/L; T = 24 ºC; pH = 3.0; Q_{air} = 2.5 mL/min).

The gas holdup (ε_g) was calculated through Eq. A.1.1 by measuring the internal clear liquid (distilled water) height (H_{CL}) and the aerated liquid height (H_{AL}) for different air flow rates and volumes of liquid initially present in the column. Data obtained are reported in Table A.1.1.

$$\varepsilon_g = \frac{H_{AL} - H_{CL}}{H_{AL}} \qquad \text{(A.1.1)}$$

Table A.1.1 Level of the liquid and liquid aerated in the BCR used.

		Gas flow rate (mL/min)		
Volume into		1.0	2.5	5.0
the BCR (L)	H_{CL} (cm)	H_{AL} (cm)	H_{AL} (cm)	H_{AL} (cm)
5.0	55.0	55.8	56.5	58.0
7.0	99.0	99.7	100.8	103.0
9.0	112.0	112.6	113.9	116.3

A2 Appendix for Chapter 4

This appendix shows some experimental results obtained in the evaluation of the wastewater treatment in bubbling reactors by Fenton's oxidation.

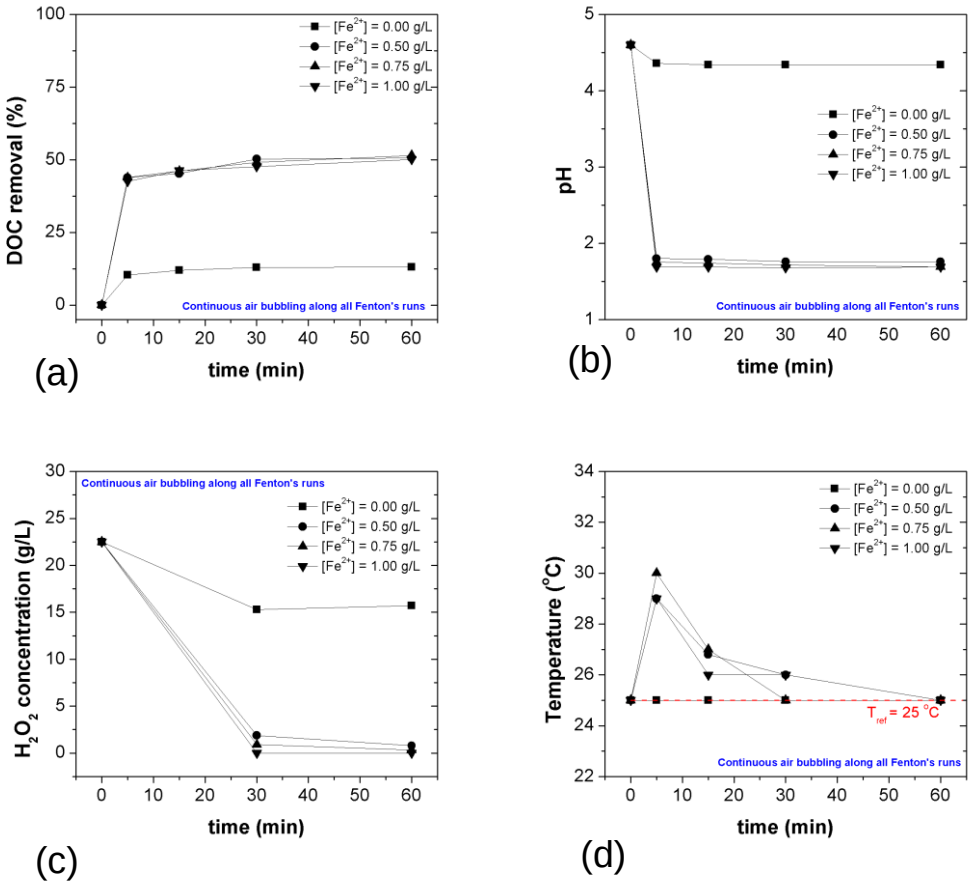

Figure A.2.1 Effect of the catalyst dose in the DOC removal (a), reduction of the pH (b), consumption of H_2O_2 (c) and temperature profile (d) along Fenton oxidation in a bubbling reactor. Experimental conditions: $[H_2O_2]$ = 22.50 g/L, pH = 4.6, V = 0.5 L, $T_{ref.}$ = 25 ºC, Q_{air} = 1.0 L/min.

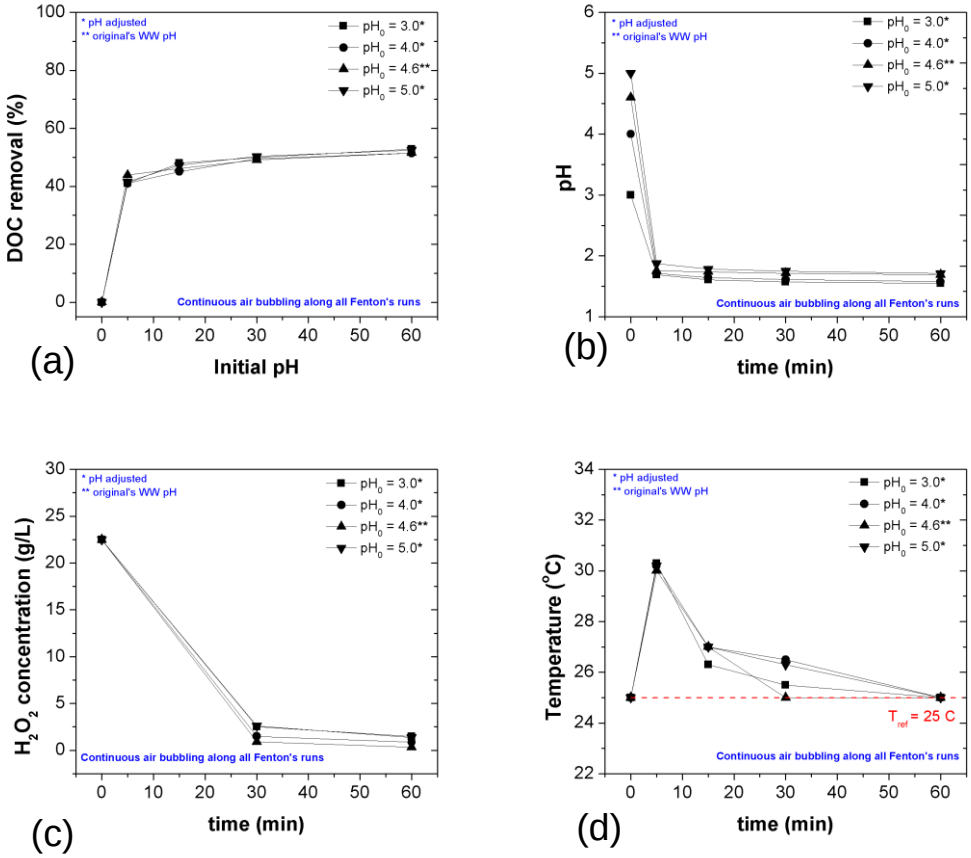

Figure A.2.2 Effect of the initial pH in the DOC removal (a), reduction of the pH (b), consumption of H_2O_2 (c) and temperature profile (d) along Fenton oxidation in a bubbling reactor. Experimental conditions: $[H_2O_2]$ = 22.50 g/L; $[Fe^{2+}]$ = 0.75 g/L, V = 0.5 L, $T_{ref.}$ = 25 ºC, Q_{air} = 1.0 L/min.

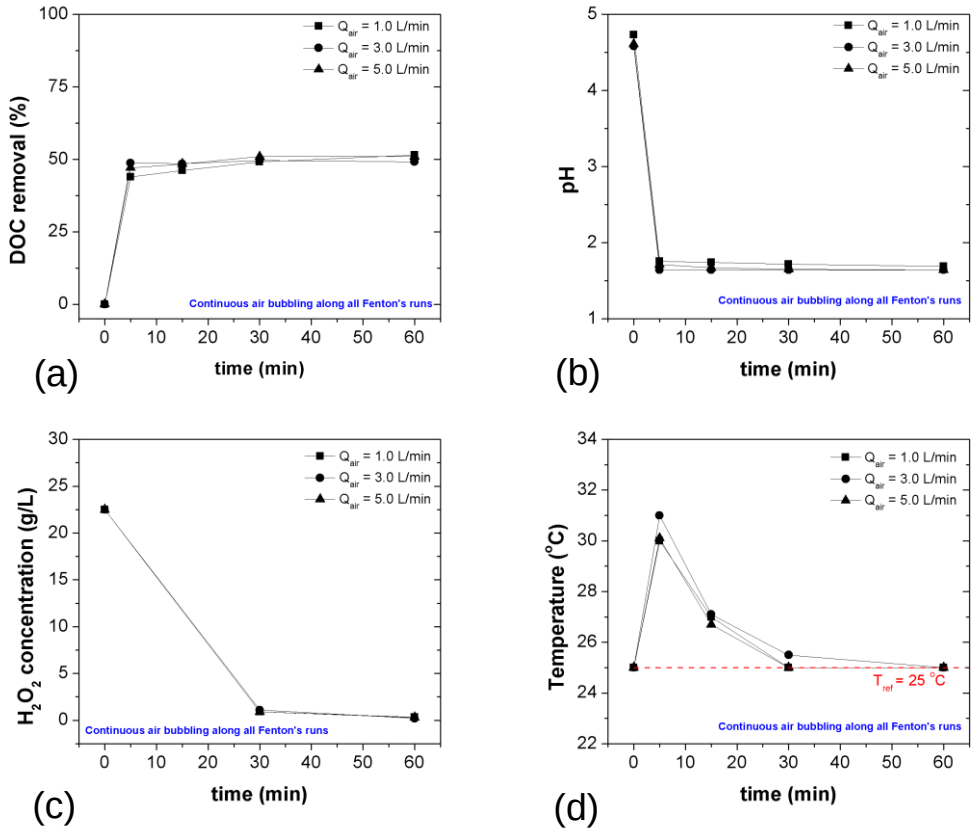

Figure A.2.3 Influence of the air flow rate in the DOC removal (a), reduction of the pH (b), consumption of H_2O_2 (c) and temperature profile (d) along Fenton oxidation in a bubbling reactor. Experimental conditions: $[H_2O_2]$ = 22.50 g/L; $[Fe^{2+}]$ = 0.75 g/L, pH = 4.6, V = 0.5 L, $T_{ref.}$ = 25 ºC, Q_{air} = 1.0 L/min.

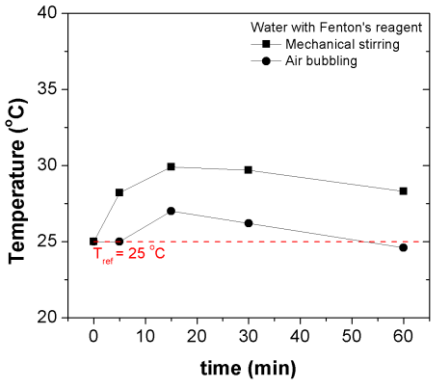

Figure A.2.4 Influence of the mixing mode on the temperature profile along Fenton's process blank runs (only water) performed with and without gas bubbling. Experimental conditions: $[H_2O_2]$ = 22.50 g/L; $[Fe^{2+}]$ = 0.75 g/L, pH = 4.6 (adjusted), V_{water} = 0.5 L, Tref. = 25 ºC, $Q_{air\ at\ BR}$ = 1.0 L/min or $V_{batch\ reactor}$= 250 rpm.